5-2023

Polymeric Biomaterials Approaches for Engineering the in Vitro Cellular Microenvironment for MSCs

Mahsa Letter-Mahsa Haseli
University of Arkansas-Fayetteville

Polymeric Biomaterials Approaches for Engineering the in Vitro Cellular Microenvironment for MSCs

A dissertation submitted in partial fulfillment
of the requirements for the degree of
Doctor of Philosophy in Engineering

by

Mahsa Haseli
University of Zanjan
Bachelor of Science in Chemical Engineering, 2013
University of Iran Islamic Azad University
Master of Science in Chemical Engineering, 2017

May 2023
University of Arkansas

This dissertation is approved for recommendation to the Graduate Council.

Jorge Almodovar, Ph.D.
Thesis Director

Shannon Servoss, Ph.D.
Committee Member

Audie Thompson, Ph.D.
Committee Member

Raj Raghavendra Rao, Ph.D.
Committee Member

Rebekah Margaret Samsonraj, Ph.D.
Committee Member

Abstract

Cell therapy is a technology that relies on replacing diseased or dysfunctional cells with healthy functioning ones. One of the cells used for such advanced therapies are stem cells, owing to their ability to differentiate into specific cells required for repairing damaged or defective tissues or cells. The majority of cell-based products are intended to transiently persist in the patient, secreting factors which then allow the patient's body to heal; in these products, the cells are subsequently eliminated from the body. Furthermore, unique manufacturing platforms, in addition to novel commercialization strategies, will be required to create a successful, sustainable cell therapy industry. Currently in cell manufacturing companies, need to produce adherent cells, that bind to a solid surface such as tissue culture- treated plastic. In some cases, the growth surface needs to be treated or coated with a matrix (such as natural proteins) to facilitate cell adhesion. Cells can be grown on large flat surfaces or on spherical microcarriers for suspension-based culture in bioreactors. However, those proteins leading to batch-to-batch variability and concerns regarding contamination and affects the cell therapeutic potency. This thesis aims to develop techniques based on the merger of novel materials approaches to manipulate cell microenvironments in culture. For controlling cell-cell interaction and cell-soluble factor interactions, layer-by-layer deposition of ionic biopolymers were developed (Heparin as a negative charge polymer, collagen and Poly-L-Lysin are used as positive charge polymers). In addition, techniques were developed to control the viability of cells under hypoxic conditions within collagen hydrogels by controlling the three-dimensional properties of hydrogels and oxygen delivery (Perfluorocarbon-based oxygen carriers). In addition, to control cell-soluble factor interactions, Metal-Organic-Frameworks (MOFs) nanocarriers application was discussed as a carrier for delivering interferon-gamma (IFN-γ) to cells.

Acknowledgements

As I reach the final steppingstone toward obtaining my graduate degree from University of Arkansas (UofA) I wish to acknowledge the countless people who, in one way or another, were vital in this achievement.

First of all, I would like to thank to Dr. Jorge Almodovar for his continued support and encouragement throughout my Ph.D. journey; without whose support, I would never have the passion for doing a Ph.D. His patient, motivating leadership, and continuous mentorship empowered me to thrive throughout my graduate studies. Also, I would like to thank my other committee members: Dr. Shannon Servoss, Dr. Audie Thompson, Dr. Raj Raghavendra Rao, and Dr. Rebekah Margaret Samsonraj. I would also like to thank Dr. Tammy Lutz-Rechtin for her mentorship and support through my research work and life. She was the best mentors ever, whose mentorship and presence around the lab made this research possible. I would like to thank all my mentors who are always supporting me patiently. I truly appreciate everything you have done for me so far and hope to continue learning from you

Finally, I am thankful to all students who helped me in my project: David A. Castilla-Casadiego, Luis Pinzon-Herrera, Alexander Hillsley, Katherine A. Miranda-Muñoz, Srikanth Sivaraman, and Josh Phipps. It was a fulfilling experience working alongside all of you. To all my friends that I have made while in graduate school, thank you for the many memories that we made together.

I would like to express my gratitude to my parents for their never-ending encouragement and support. Thank you to my younger brother, Sina Haseli, for his moral support and love throughout my studies.

Finally, I would like to thank the kind boy that has been my biggest supporter, my husband, Hossein. I believe he deserves a doctorate by association, as he has been the rock to my graduate studies. Thank you for taking extra duties being along with me in the lab during Covid-19 pandemic. You were a constant reminder to stay positive through the tough times, and with that I will forever love and support you.

Table of Contents

List of Publications

- **Chapter Two :**

Published:

M. Haseli *et al.*, "Immunomodulatory functions of human mesenchymal stromal cells are enhanced when cultured on HEP/COL multilayers supplemented with interferon-gamma," *Mater. Today Bio*, vol. 13, no. November 2021, p. 100194, 2022, doi: 10.1016/j.mtbio.2021.100194.

- **Chapter Three :**

Published:

M. Haseli, L. Pinzon-Herrera, and J. Almodovar, "Crosslinked Layered Surfaces of Heparin and Poly(L-Lysine) Enhance Mesenchymal Stromal Cell Behavior in the Presence of Soluble Interferon Gamma," *Cells Tissues Organs*, pp. 1–13, 2021, doi: 10.1159/000521609.

- **Chapter Four:**

Published:

J. Phipps *et al.*, "Delivery of Immobilized IFN-γWith PCN-333 and Its Effect on Human Mesenchymal Stem Cells," *ACS Biomater. Sci. Eng.*, 2022, doi: 10.1021/acsbiomaterials.2c01038

Introduction

Cell-based therapy aims to repair and regenerate organs and tissues [1]. Existing organ and tissue replacement strategies suffer from poor survival cells and immunological rejection limitations [2]. Mesenchymal stromal cells (MSCs) are of particular interest for cellular therapy programs to overcome these limitations. MSCs contribute to the repair of damaged tissues and possess remarkable immunomodulatory activity by producing anti-inflammatory and immunosuppressive factors [3][4]. Therefore, MSCs have become a promising implement for new medical applications and therapies to treat diverse diseases and disorders such as graft-versus-host disease, inflammatory diseases, and autoimmune disorders. However, the inflammatory cytokine milieu plays a critical role in stimulating MSCs immunomodulatory activity. In particular, It has been shown that the immunosuppressive properties of MSCs rely on the existence of IFN-γ in the microenvironment [5]. However, IFN-γ has shown a significant anti-proliferative effect [6][7]. In addition, cells behavior is affected by the surrounding microenvironment in culture, including growth factors, the extracellular matrix (ECM), and contact with other cells [8][9]. Therefore, there is a need to have a better cells microenvironment engineer. In most cell culture, cells are placed within an artificial microenvironment which lacks complexity and affects cells behavior. To overcome these limitations, polymeric biomaterials will help increase the cell survival and immunomodulatory activity of MSCs. Also, polymeric biomaterials will tackle mimicking the microenvironment ECM limitations in cell-based therapy and manufacturing process. Therefore, polymeric biomaterials approaches could be used to control a cell's environment and then analyze the cell's response with respect to dynamics and the level of expression of multiple genes. This contribution will advance the translation of engineered constructs from the lab bench to patient care.

1.1. Cell Microenvironment

In vivo, cells are surrounded by a complex microenvironment characterized by growth factors, the extracellular matrix (ECM), and contact with other cells [8][9]. Mimicking a cell's microenvironment helps us analyze and understand the role of the microenvironment on cell responses via biophysical, biochemical, or other routes. Also, cell microenvironment has many aspects that affects the cells behavior such as dedifferentiation and subsequent tumor growth [10]. Cell microenvironment for a single cell is composed of ECM, cell-cell contact working in collaboration with the secretion of paracrine factors (e.g., cytokines, chemokines, and growth factors), extracellular vehicles (EVs), physical and mechanical properties of adjuvant cells, ECM, and movement of organism or the movement of the physiological fluids such as blood [11][12].

In vivo, cells are surrounded by ECM that is a three dimensional complex and dynamic structure filled with the matrix containing glycosaminoglycans [13] and proteins [14], which are known as proteoglycans [9] and growth factors [15][16]. In the cell microenvironment, cells receive signals from the ECM which modulates cell attachment, shape, morphology, migration, orientation, and proliferation. The ECM contains of many molecules that are in constant contact with both growth factors and neighboring cells [17][18]. Also, paracrine mediators (e.g., cytokines, chemokines, and growth factors) modulate the cells microenvironment and influence the activity of resident cells [19]. Therefore, having better understanding of cells microenvironment is important to control cells functions. Mimicking cells microenvironment give rise to understand not only control the interaction of cells with ECM, but also to test various ECM combinations in order to control cell functions in culture. Cell-cell contact also affect cells behaviors, functions and signaling between the two cell types [20].

Cytokines and growth factors are essential regulators of the tissue microenvironment. They are produced by cells and/or their neighboring cells in an autocrine or paracrine manner [21] and often combine with other microenvironmental components to elicit non-linear responses (i.e., threshold-based [22] or synergistic responses). Another important factor is the interaction of a cell with its surrounding matrix. In vivo, cells are typically in direct contact with surrounding cells and ECM. ECM is produced by cells and consists of collagens, proteoglycans, adhesive glycoproteins, glycosaminoglycans, and associated bound protein modulators of cell function [13][14].

ECM modulates cell's behavior such as attachment, shape, morphology, migration, orientation, and proliferation. ECMs based on their components and structures are capable of transmitting specific signals on biochemical levels that satisfy the role of cells in the tissue repair process. For example, stem cells can interpret biomaterial instructions through cell– matrix interactions and then modulate their fate determination [23]. Several studies showed that biomaterial's properties such as surface topography and chemical composition can regulate cell adhesion, differentiation, migration, and proliferation [24][25]. Further insight into understanding such signals will facilitate the design of culture technologies that mimic critical aspects of the in vivo microenvironment and facilitate better control over cell responses in vitro. Therefore, it is important to not only control the interaction of cells with ECM, but also to test various ECM combinations in order to control cell behavior in culture. Currently, biomaterials have driven substantial advances to improve therapeutics at the clinical level, and at the same time, provide a favorable platform for the establishment of artificial niches to cells' behavior [26][27].

1.2. Biomaterials

For over 100 years, researchers have employed in vitro cell culture methods; however, the artificial substrates and matrices typically used to maintain cell survival and differentiation provide a relatively poor approximation of biological tissue. Artificial polymer coatings are relatively inexpensive, stable, and straightforward to prepare yet typically provide a poor approximation of real soft and wet biological tissue and thus often perform sub optimally. A bare polystyrene plastic surface, for example, generally will not support living cells, and most thin polymer coatings, which are similarly hydrophobic and brittle, will not significantly extend cell viability [28]. While biomaterials that incorporate natural biopolymers have been developed, these are typically not stable over weeks, and are difficult to work with, or are prohibitively expensive to purchase or manufacture in bulk.

1.2.1. Polyelectrolyte Multilayers

Biomaterials such as polyelectrolytes' layer-by-layer (LbL) coating, in principle, possess the key characteristic of a tunable modulus Figure 2-1. Layer by Layer Assembly process [33].LbL coating can be readily deposited or assembled from aqueous solution becomes adhered, stable, and insoluble while retaining soft gel-like properties that resemble those of a real ECM, to a controllable extent [28]. LbL deposition has been a simple method for biologically relevant surfaces by creating nanoscale thin films. It provides compositional uniqueness of natural or synthetic polymers, such as stimulating a specific signal to cells and enhancing cellular behavior [29]. LbL involves the alternative absorption of polycations and polyanions to produce films with specific and controlled physical-chemical characteristics by adapting the experimental parameters, such as pH, ionic strength, and polyelectrolyte concentration [30][31][32].

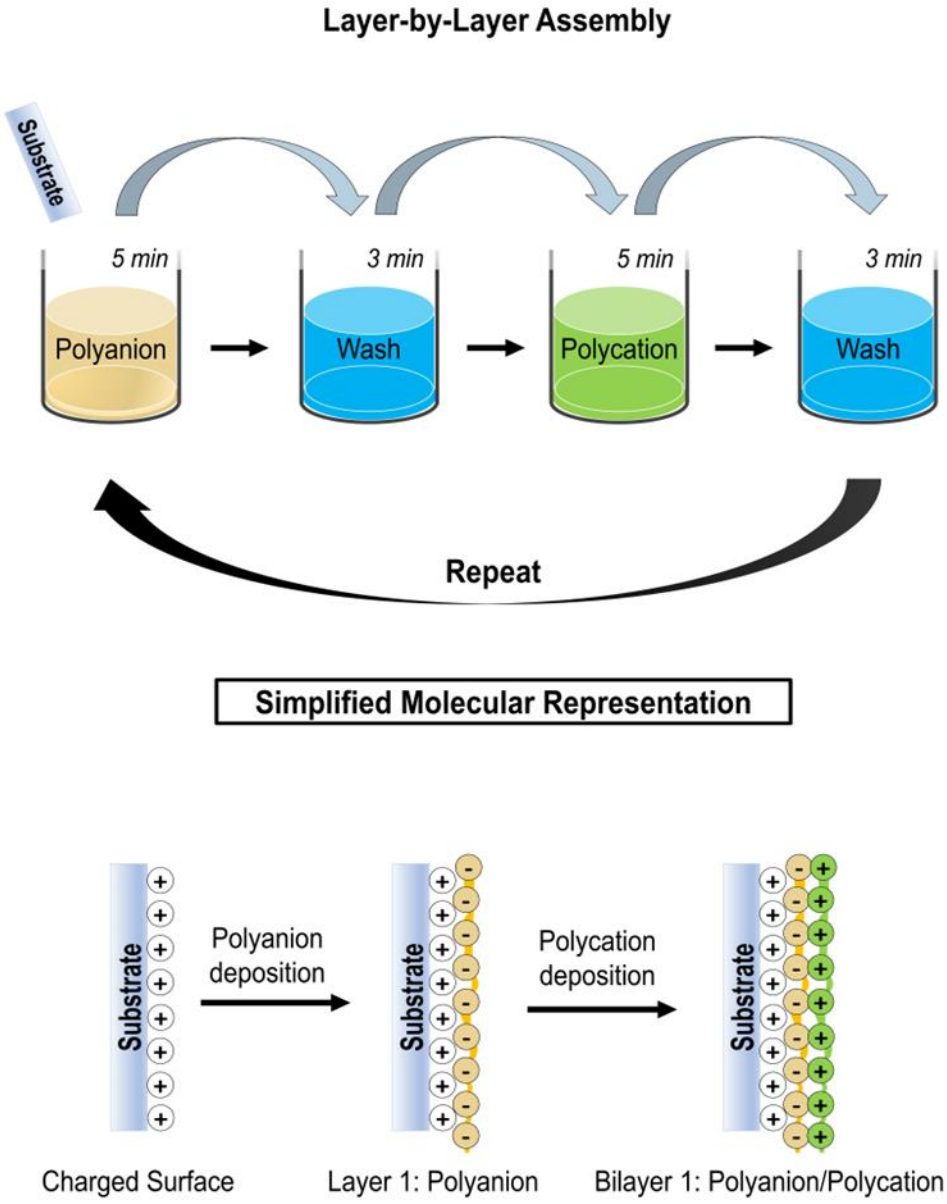

Figure 2-1. Layer by Layer Assembly process [33].

Synthetic polyelectrolytes such as poly- (styrene sulfonate) (PSS, a strong polyelectrolyte), poly(acrylic acid) (PAA), or poly(allylamine hydrochloride) (PAH) have been widely used in cell/film studies. The main advantage of using synthetic polymers is the possibility of adjusting certain parameters, including ionic strength and pH of assembly, to a considerable degree, and

easy to modify chemically. The most frequently studied synthetic PEM is, by far, linearly growing and dense (PSS/PAH) film. For example, in one study human MSCs were cultured on (PSS/PAH) films on conductive indium tin oxide (ITO) electrodes as a platform for growing viable cell sheets [34]. In this study, films made of 9-layer pairs ending with PSS and of ~20 nm in thickness were used. The resulting stem cell sheets retained their phenotypic profile and mesodermal differentiation potency. The authors showed that both an electrochemically induced local pH lowering and a global decrease in the environmental pH resulted in a rapid detachment of intact stem cell sheets. Furthermore, they evidenced that the recovered stem cells sheets maintained their capacity to differentiate toward the adipogenic and osteogenic lineages. Natural biopolymers, such as collagen (COL), gelatin, hyaluronan (HA), chondroitine sulfate (CS), or heparin (HEP) can be used as building blocks for PEM films. In the study done by Chen at al. [35] showed that (COL/HEP) films have been employed as titanium coatings to study endothelial progenitor cell (EPC) attachment and proliferation. In vitro, the (COL/HEP) greatly increased EPC attachment and proliferation. Furthermore, platelet adhesion was found to be reduced on such coatings.

1.2.2. Biopolymers

Biopolymers are produced by the cells of a living organism [36]. They include polysaccharides (chitosan and cellulose) and proteins (laminin, collagen, fibronectin) that have been used as scaffold materials for tissue engineering and biomedical applications [37][38]. We engineered an array of biomaterials using heparin, collagen, and poly-l-lysine (PLL) in this work.

Heparin is a highly sulfated glycosaminoglycan that contains negatively charged carboxylate or sulfate groups, which are present in the extracellular matrix (ECM) and the surface of cells [39][40]. Due to the electrostatic interactions and binding with amino acids, heparin plays a role

in cellular functions such as cell adhesion, proliferation, differentiation, migration, and inflammation [41][42]. Furthermore, heparin is well known for its anticoagulant properties. Still, apart from this ability, heparin has the ability to bind ECM proteins, such as collagen, and thus plays an essential role in organizing the structure and composition of the ECM. Many studies showed that heparin could prevent the proteolytic cleavage of and improve IFN-γ signaling [39][43].

Collagen is a fibrous protein in the ECM of connective tissues, which is the most abundant protein in mammalian tissues and other ECM molecules to generate and maintain tissue form and function [44][45]. Although collagen has excellent biocompatibility and strongly promotes proliferation, differentiation, and migration of cells, its low immunogenicity has been limited for clinical applications.

Poly-L-lysine is a biocompatible polycation with a large number of active amino groups. PLL can adopt different secondary structures (e.g., random coil, b-sheet, or a-helix) depending on the pH of the solution. PLL has been used for many different purposes, such as the study of DNA-Protein interactions, drug delivery, and coating material to improve cell attachment to plastic and glass surfaces [46].

1.3. Isolated Mesenchymal Stem cells (MSCs): History and Present

Mesenchymal stem cells (MSCs) were first identified along with haemopoietic stem cells in the bone marrow [47]. MSCs originally were distinguished from hemopoietic stem cells, because MSCs adhere to a culture dish, unlike the hemopoietic cells that stay in suspension [47]. Arnold Caplan coined the term “mesenchymal stem cell” in the late 1980s, with early work published by Friedenstein and collaborators in the 1960s that didn’t use the MSCs nomenclature [48][49]. Ease in isolation and expansion of colonies of individual MSCs make them favorable for stem

cell research [49]. Initially, MSCs were thought to be located only in the bone marrow, but more recently they have been isolated from adipose tissue [50], dental pulp [51], endometrium [52], human breast milk [53], placenta amniotic fluid [54], umbilical cord blood [55], Whar-ton's jelly and many others [56][57]. In order to ensure that the results obtained by different scientific groups could be compared, they stated that the cells considered MSCs should:

- adhere to plastic wares in standard culture conditions using tissue culture flasks.
- exhibit specific surface marker expression; >95% cells must be positive for CD105 (endoglin), CD73 (5'-nucleotidase) and CD90 (Thy-1); besides, these cells must not express CD45 (protein tyrosine phosphatase, receptor type, CD34, CD14, CD11b, CD79a (MB-1 membrane glycoprotein), CD19 (B lymphocyte surface antigen B4) and HLA-II (human leukocyte antigen class II).
- be able to differentiate into osteoblasts, adipocytes and chondroblasts in vitro [58].

They additionally suggested, that differentiation towards osteoblasts should be confirmed with Alizarin Red or von Kossa staining, adipocytic differentiation with Oil Red O staining, while chondroblast differentiation with Alcian Blue or immunohistology-chemical staining [58]. However, it is important to remember that these criteria would apply only to human MSCs, since the surface antigen expression profile may be different in other species.

1.3.1. Mesenchymal Stromal Cells

Human mesenchymal stromal cells (hMSCs) are of particular interest for cellular therapy programs [59]. They can differentiate into mesodermal lineage cells, including adipocytes, osteoblasts, and chondrocytes [2][3]. During tissue damage, hMSCs also have the ability to secrete paracrine and anti-inflammatory factors to repair tissue [18][19][20]. In addition, hMSCs contribute to the repair of damaged tissues and possess remarkable immunomodulatory activity

by producing anti-inflammatory and immunosuppressive factors [3][4],[65]–[68]. With regard to the latter, hMSCs inhibit the activation, proliferation, and function of both adaptive immune and innate immune cells, such as B cells and T cells for the former and dendritic cells (DCs), natural killer (NK) cells, and neutrophils for the latter [3][69][70]. Immunology will contribute to the design of cells or cell transplant systems that are not rejected by the immune system [71]. In regard to human mesenchymal stromal cells (hMSCs), they are treated with soluble interferon-gamma (IFN-γ) to enhance their immunosuppressive properties.

Immune suppression by hMSCs appears as a multifactorial process that relies on cell-cell contact working in collaboration with the secretion of soluble immune factors [11][12]. These specific immune factors, including interferon gamma (IFN-γ), tumor necrosis factor alpha (TNF-α), or interleukin 1 beta (IL-1β) that initiate the hMSCs immunosuppression program, which induces synthesis of protein factors, in particular indolamine-2,3-dioxygenase (IDO) and inducible nitric oxide synthase (iNOS) [72][73][74]. Therefore, hMSCs have become a promising implement for new medical applications and therapies to treat diverse diseases and disorders such as graft-versus-host disease, inflammatory diseases, and autoimmune disorders [75][7]. Although several pathways have been involved in this process, the ability of immunosuppression of hMSCs has not been fully clarified.

It has been shown that the immunosuppressive properties of hMSCs relies on the existence of IFN-γ in the microenvironment [5]. Interferon IFN-γ is a potent pro-inflammatory cytokine produced by CD4+ lymphocytes, NK cells, and macrophages. It plays essential and complex roles in innate and adaptive immune responses against viral infections, bacteria, protozoa, and graft-versus-host disease (GVHD) [76][77]. A study showed that IFN-γ has the ability to modulate the immune properties and differentiation potential of hMSCs, which has a significant

anti-proliferative effect [6]. There is a need to reduce the anti-proliferative effect of IFN-γ on hMSCs. In addition, there is a need to learn from cell biology, such as what controls cellular differentiation and growth and how ECM components affect cell function [78].

1.4. Metal-organic frameworks (MOFs)

The pretreatment of hMSCs with IFN-γ enhances the immunomodulation of cells. However, pretreatment of hMSCs may limit the potential of hMSCs to modulate immune responses for more than a few days in environments due to transient effects [47]. To address the transient effects of pretreatment, IFN-γ encapsulated in delivery particle may provide sustaining presentation of bioactive IFN-γ to potentiate hMSCs immunomodulatory activity. Metal-organic frameworks (MOFs) are porous crystalline materials synthesized with metal-containing nodes and organic ligands [48][49]. Recent years have seen a significant increase in the study of metal-organic frameworks (MOFs) since their foundational introduction by Omar Yagi and coworkers [79][80][81][82][83][84][85]. These porous crystalline particles are often produced on the nanoscale and due to their interchangeable parts, are vastly customizable [86]. This ability to selectively choose components and synthesize tailor-made MOFs allows these particles to be functionalized as well as have their three-dimensional size and shape manipulated [81][87]. This is further promoted by the open pores and large surface areas of MOFs which allow materials to move into the particles providing a high loading capacity and surface area [87]. This trait has also been exploited to encapsulate or trap objects, which can be as big as proteins or as small as gas particles making MOFs promising devices for gas storage, drug delivery, and protein immobilization and/or encapsulation [86]. MOFs have many advantages, such as tunable but uniform pore sizes, ultrahigh surface area, and easy modification, that make for the immobilization of many molecules, such as metal complexes, nanoparticles, and enzymes. The

study done by Phipps and coworkers shows that MOFs-PCN333(Fe) containing IFN-γ are not cytotoxic to hMSCs, can promote the expression of proteins that play a role in immune response, and are capable of inducing indoleamine 2,3-dioxygenase (IDO) production similar to that of soluble IFN-γ at lower concentrations [88].

1.5. Research Rationale

This dissertation is focused on improving human mesenchymal stromal cell's behavior via HEP/COL LbL fabrication (Chapter 2), HEP/PLL LbL fabrication (Chapter 3), MOFs delivery in cell media (Chapter 4), MOFs delivery capability coated in LbL fabrication as a three-dimensional substrate (Chapter 5), collagen hydrogel as an oxygen-releasing material (Chapter 6), and commercialization (Chapter 7). It supports work done by Mahsa Haseli and Dr. Jorge Almodovar to assemble a novel, three-dimensional HEP/COL multilayers substrate for cell manufacturing applications. The (HEP/COL) multilayers can be applied to any surface including bioreactors or microcarriers which can be used to cell culture meant for cell-based therapies aimed at treating several immune diseases.

1.6. References

[1] A. Khademhosseini, Y. Du, B. Rajalingam, J. P. Vacanti, and R. S. Langer, "Microscale technologies for tissue engineering," *Adv. Tissue Eng.*, vol. 103, no. 8, pp. 349–369, 2008, doi: 10.1142/9781848161832_0017.

[2] T. Cordonnier, J. Sohier, P. Rosset, and P. Layrolle, "Biomimetic materials for bone tissue engineering - State of the art and future trends," *Adv. Eng. Mater.*, vol. 13, no. 5, pp. 135–150, 2011, doi: 10.1002/adem.201080098.

[3] A. Uccelli, L. Moretta, and V. Pistoia, "Mesenchymal stem cells in health and disease," *Nat. Rev. Immunol.*, vol. 8, no. 9, pp. 726–736, 2008, doi: 10.1038/nri2395.

[4] F. Gao *et al.*, "Mesenchymal stem cells and immunomodulation: Current status and future prospects," *Cell Death Dis.*, vol. 7, no. 1, 2016, doi: 10.1038/cddis.2015.327.

[5] M. W. Klinker, R. A. Marklein, J. L. Lo Surdo, C. H. Wei, and S. R. Bauer, "Morphological features of IFN-γ-stimulated mesenchymal stromal cells predict overall immunosuppressive capacity," *Proc. Natl. Acad. Sci. U. S. A.*, vol. 114, no. 13, pp. E2598–E2607, 2017, doi: 10.1073/pnas.1617933114.

[6] J. Croitoru-Lamoury *et al.*, "Interferon-γ regulates the proliferation and differentiation of mesenchymal stem cells via activation of indoleamine 2,3 dioxygenase (IDO)," *PLoS One*, vol. 6, no. 2, 2011, doi: 10.1371/journal.pone.0014698.

[7] D. A. Castilla-Casadiego, J. R. García, A. J. García, and J. Almodovar, "Heparin/Collagen Coatings Improve Human Mesenchymal Stromal Cell Response to Interferon Gamma," *ACS Biomater. Sci. Eng.*, vol. 5, no. 6, pp. 2793–2803, 2019, doi: 10.1021/acsbiomaterials.9b00008.

[8] F. M. Watt and W. T. S. Huck, "Role of the extracellular matrix in regulating stem cell fate," *Nat. Rev. Mol. Cell Biol.*, vol. 14, no. 8, pp. 467–473, 2013, doi: 10.1038/nrm3620.

[9] R. O. Hynes, "The extracellular matrix: not just pretty fibrils," *Science (80-.).*, vol. 326, no. 5957, pp. 1216–1219, 2009, doi: 10.1126/science.1176009.

[10] H. Ozcelik *et al.*, "Cell Microenvironment Engineering and Monitoring for Tissue Engineering and Regenerative Medicine : The Citation Accessed Citable Link Cell Microenvironment Engineering and Monitoring for Tissue Engineering and Regenerative Medicine : The Recent Advances," *Biomed Res. Int.*, vol. 2014, no. i, pp. 1–18, 2014.

[11] J. Cuerquis *et al.*, "Human mesenchymal stromal cells transiently increase cytokine production by activated T cells before suppressing T-cell proliferation: Effect of interferon-γ and tumor necrosis factor-α stimulation," *Cytotherapy*, vol. 16, no. 2, pp. 191–202, 2014, doi: 10.1016/j.jcyt.2013.11.008.

[12] T. J. Kean, P. Lin, A. I. Caplan, and J. E. Dennis, "MSCs: Delivery routes and engraftment, cell-targeting strategies, and immune modulation," *Stem Cells Int.*, vol. 2013, 2013, doi: 10.1155/2013/732742.

[13] H. Lortat-Jacob, "The molecular basis and functional implications of chemokine interactions with heparan sulphate," *Curr. Opin. Struct. Biol.*, vol. 19, no. 5, pp. 543–548, 2009, doi: 10.1016/j.sbi.2009.09.003.

[14] M. F. Brizzi, G. Tarone, and P. Defilippi, "Extracellular matrix, integrins, and growth factors as tailors of the stem cell niche," *Curr. Opin. Cell Biol.*, vol. 24, no. 5, pp. 645–651, 2012, doi: 10.1016/j.ceb.2012.07.001.

[15] E. Fuchs, T. Tumbar, and G. Guasch, "Socializing with the neighbors: Stem cells and their niche," *Cell*, vol. 116, no. 6, pp. 769–778, 2004, doi: 10.1016/S0092-8674(04)00255-7.

[16] K. A. Moore and I. R. Lemischka, "Stem cells and their niches," *Science (80-.).*, vol. 311, no. 5769, pp. 1880–1885, 2006, doi: 10.1126/science.1110542.

[17] T. A. Wilgus, “Growth Factor–Extracellular Matrix Interactions Regulate Wound Repair,” *Adv. Wound Care*, vol. 1, no. 6, pp. 249–254, 2012, doi: 10.1089/wound.2011.0344.

[18] O. Saksela and M. Laiho, “Growth factors and the extracellular matrix,” *Duodecim.*, vol. 106, no. 3, pp. 297–306, 1990, doi: 10.1096/fasebj.11.1.9034166.

[19] M. Khan, “Human mesenchymal stem cells,” *Hum. Mesenchymal Stem Cells*, vol. 1416, no. Cmc, pp. 1–127, 2021, doi: 10.1016/s0141-0229(97)83511-9.

[20] V. Poltavets, M. Kochetkova, S. M. Pitson, and M. S. Samuel, “The role of the extracellular matrix and its molecular and cellular regulators in cancer cell plasticity,” *Front. Oncol.*, vol. 8, no. OCT, pp. 1–19, 2018, doi: 10.3389/fonc.2018.00431.

[21] A. R. Shelke Roscoe, J. A. , Morrow, G. R. , Colman, L. K. , Banerjee, T. K. , & Kirshner, J. J., “Paracrine and autocrine signals induce and maintain mesenchymal and stem cell states in the breast,” *Bone*, vol. 23, no. 1, pp. 1–7, 2008, doi: 10.1016/j.cell.2011.04.029.Paracrine.

[22] P. Zandstra, E. Jervis, D. Kilburn, C. Eaves, and J. Pirel, “Concentration-dependent internalization of a cytokine/cytokine receptor complex in human hematopoietic cells,” *Exp. Hematol.*, vol. 26, no. 8, p. 720, 1998, doi: 10.1002/(sici)1097-0290(19990520)63:4<493::aid-bit13>3.3.co;2-s.

[23] X. Zhao, Q. Li, Z. Guo, and Z. Li, “Constructing a cell microenvironment with biomaterial scaffolds for stem cell therapy,” *Stem Cell Res. Ther.*, vol. 12, no. 1, pp. 1–13, 2021, doi: 10.1186/s13287-021-02650-w.

[24] A. Kumari, S. K. Yadav, and S. C. Yadav, “Biodegradable polymeric nanoparticles based drug delivery systems,” *Colloids Surfaces B Biointerfaces*, vol. 75, no. 1, pp. 1–18, 2010, doi: 10.1016/j.colsurfb.2009.09.001.

[25] S. Martino, F. D’Angelo, I. Armentano, J. M. Kenny, and A. Orlacchio, “Stem cell-biomaterial interactions for regenerative medicine,” *Biotechnol. Adv.*, vol. 30, no. 1, pp. 338–351, 2012, doi: 10.1016/j.biotechadv.2011.06.015.

[26] X. Zhao, K. Cui, and Z. Li, “The role of biomaterials in stem cell-based regenerative medicine,” *Future Med. Chem.*, vol. 11, no. 14, pp. 1779–1792, 2019, doi: 10.4155/fmc-2018-0347.

[27] E. For, “Enabling Technologies for Cell-Based Clinical Translation E NABLING T ECHNOLOGIES FOR C ELL -B ASED C LINICAL T RANSLATION Increased Survival and Function of Mesenchymal Stem Cell Spheroids Entrapped in Instructive Alginate Hydrogels,” pp. 1–9, 2016.

[28] M. J. Landry, F. G. Rollet, T. E. Kennedy, and C. J. Barrett, “Layers and Multilayers of Self-Assembled Polymers: Tunable Engineered Extracellular Matrix Coatings for Neural Cell Growth,” *Langmuir*, vol. 34, no. 30, pp. 8709–8730, 2018, doi: 10.1021/acs.langmuir.7b04108.

[29] V. Gribova, R. Auzely-Velty, and C. Picart, “Polyelectrolyte multilayer assemblies on materials surfaces: From cell adhesion to tissue engineering,” *Chem. Mater.*, vol. 24, no. 5, pp. 854–869, 2012, doi: 10.1021/cm2032459.

[30] C. Picart *et al.*, “Primary cell adhesion on RGD-functionalized and covalently crosslinked thin polyelectrolyte multilayer films,” *Adv. Funct. Mater.*, vol. 15, no. 1, pp. 83–94, 2005, doi: 10.1002/adfm.200400106.

[31] C. Picart, “Polyelectrolyte Multilayer Films: From Physico-Chemical Properties to the Control of Cellular Processes,” *Curr. Med. Chem.*, vol. 15, no. 7, pp. 685–697, 2008, doi: 10.2174/092986708783885219.

[32] P. Gentile, I. Carmagnola, T. Nardo, and V. Chiono, “Layer-by-layer assembly for biomedical applications in the last decade,” *Nanotechnology*, vol. 26, no. 42, p. 422001, 2015, doi: 10.1088/0957-4484/26/42/422001.

[33] D. A. Castilla-Casadiego *et al.*, “Methods for the Assembly and Characterization of Polyelectrolyte Multilayers as Microenvironments to Modulate Human Mesenchymal Stromal Cell Response,” *ACS Biomater. Sci. Eng.*, vol. 6, no. 12, pp. 6626–6651, 2020, doi: 10.1021/acsbiomaterials.0c01397.

[34] O. Guillaume-Gentil, O. V. Semenov, A. H. Zisch, R. Zimmermann, J. Vörös, and M. Ehrbar, “PH-controlled recovery of placenta-derived mesenchymal stem cell sheets,” *Biomaterials*, vol. 32, no. 19, pp. 4376–4384, 2011, doi: 10.1016/j.biomaterials.2011.02.058.

[35] J. Chen, C. Chen, Z. Chen, J. Chen, Q. Li, and N. Huang, “Collagen/heparin coating on titanium surface improves the biocompatibility of titanium applied as a blood-contacting biomaterial,” *J. Biomed. Mater. Res. - Part A*, vol. 95 A, no. 2, pp. 341–349, 2010, doi: 10.1002/jbm.a.32847.

[36] A. Tchobanian, H. Van Oosterwyck, and P. Fardim, “Polysaccharides for tissue engineering: Current landscape and future prospects,” *Carbohydr. Polym.*, vol. 205, pp. 601–625, 2019, doi: 10.1016/j.carbpol.2018.10.039.

[37] B. W. Kim, *Clinical regenerative medicine in urology*. 2017.

[38] A. K. Nayak, S. A. Ahmed, M. Tabish, and M. S. Hasnain, *Natural polysaccharides in tissue engineering applications*. Elsevier Inc., 2019.

[39] M. S. Douglas, D. A. Rix, J. H. Dark, D. Talbot, and J. A. Kirby, “Examination of the mechanism by which heparin antagonizes activation of a model endothelium by interferon-gamma (IPN-γ),” *Clin. Exp. Immunol.*, vol. 107, no. 3, pp. 578–584, 1997, doi: 10.1046/j.1365-2249.1997.3141206.x.

[40] S. Sarrazin, D. Bonnaffé, A. Lubineau, and H. Lortat-Jacob, “Heparan sulfate mimicry: A synthetic glycoconjugate that recognizes the heparin domain of interferon-γ inhibits the cytokine activity,” *J. Biol. Chem.*, vol. 280, no. 45, pp. 37558–37564, 2005, doi:

10.1074/jbc.M507729200.

[41] S. J. Paluck, T. H. Nguyen, and H. D. Maynard, “Heparin-Mimicking Polymers: Synthesis and Biological Applications,” *Biomacromolecules*, vol. 17, no. 11, pp. 3417–3440, 2016, doi: 10.1021/acs.biomac.6b01147.

[42] J. Dinoro *et al.*, “Sulfated polysaccharide-based scaffolds for orthopaedic tissue engineering,” *Biomaterials*, vol. 214, no. December 2018, p. 119214, 2019, doi: 10.1016/j.biomaterials.2019.05.025.

[43] H. Lortat-Jacob, F. Baltzer, and J. A. Grimaud, “Heparin decreases the blood clearance of interferon-γ and increases its activity by limiting the processing of its carboxyl-terminal sequence,” *J. Biol. Chem.*, vol. 271, no. 27, pp. 16139–16143, 1996, doi: 10.1074/jbc.271.27.16139.

[44] D. L. Kusindarta and H. Wihadmadyatami, “The Role of Extracellular Matrix in Tissue Regeneration,” *Tissue Regen.*, 2018, doi: 10.5772/intechopen.75728.

[45] G. A. Di Lullo, S. M. Sweeney, J. Körkkö, L. Ala-Kokko, and J. D. San Antonio, “Mapping the ligand-binding sites and disease-associated mutations on the most abundant protein in the human, type I collagen,” *J. Biol. Chem.*, vol. 277, no. 6, pp. 4223–4231, 2002, doi: 10.1074/jbc.M110709200.

[46] S. C. Shukla, A. Singh, A. K. Pandey, and A. Mishra, “Review on production and medical applications of e-polylysine,” *Biochem. Eng. J.*, vol. 65, pp. 70–81, 2012, doi: 10.1016/j.bej.2012.04.001.

[47] O. F. Blood and C. T. O. Connective, “PHYSIOLOGICAL REVIEWS,” vol. IV, no. 4, pp. 533–563, 1924.

[48] A. I. Caplan and The, “Mesenchymal Stem Cells,” *Chem. Phys. Lett.*, vol. 7, no. 6, pp. 581–582, 1970, doi: 10.1016/0009-2614(70)87009-9.

[49] R. K. C. A. K. S. L. A. J. FRIEDENSTEIN, “THE DEVELOPMENT OF FIBROBLAST COLONIES IN MONOLAYER CULTURES OF GUINEA-PIG BONE MARROW AND SPLEEN CELLS,” *Development*, pp. 1–6, 1897.

[50] A. J. Katz, A. Tholpady, S. S. Tholpady, H. Shang, and R. C. Ogle, “Cell Surface and Transcriptional Characterization of Human Adipose-Derived Adherent Stromal (hADAS) Cells,” *Stem Cells*, vol. 23, no. 3, pp. 412–423, 2005, doi: 10.1634/stemcells.2004-0021.

[51] B. M. Seo *et al.*, “Investigation of multipotent postnatal stem cells from human periodontal ligament,” *Lancet*, vol. 364, no. 9429, pp. 149–155, 2004, doi: 10.1016/S0140-6736(04)16627-0.

[52] X. Meng *et al.*, “Endometrial regenerative cells: A novel stem cell population,” *J. Transl. Med.*, vol. 5, pp. 1–10, 2007, doi: 10.1186/1479-5876-5-57.

[53] S. Patki, S. Kadam, V. Chandra, and R. Bhonde, “Human breast milk is a rich source of multipotent mesenchymal stem cells,” *Hum. Cell*, vol. 23, no. 2, pp. 35–40, 2010, doi: 10.1111/j.1749-0774.2010.00083.x.

[54] P. S. in ’t Anker *et al.*, “Isolation of Mesenchymal Stem Cells of Fetal or Maternal Origin from Human Placenta,” *Stem Cells*, vol. 22, no. 7, pp. 1338–1345, 2004, doi: 10.1634/stemcells.2004-0058.

[55] P. S. In ’t Anker *et al.*, “Amniotic fluid as a novel source of mesenchymal stem cells for therapeutic transplantation [1],” *Blood*, vol. 102, no. 4, pp. 1548–1549, 2003, doi: 10.1182/blood-2003-04-1291.

[56] B. M. Deasy *et al.*, “High harvest yield, high expansion, and phenotype stability of CD146 mesenchymal stromal cells from whole primitive human umbilical cord tissue,” *J. Biomed. Biotechnol.*, vol. 2009, 2009, doi: 10.1155/2009/789526.

[57] H. Wang *et al.*, “Mesenchymal Stem Cells in the Wharton’s Jelly of the Human Umbilical Cord,” *Stem Cells*, vol. 22, no. 7, pp. 1330–1337, 2004, doi: 10.1634/stemcells.2004-0013.

[58] M. Dominici *et al.*, “Minimal criteria for defining multipotent mesenchymal stromal cells. The International Society for Cellular Therapy position statement,” *Cytotherapy*, vol. 8, no. 4, pp. 315–317, 2006, doi: 10.1080/14653240600855905.

[59] T. L. Ramos *et al.*, “MSC surface markers (CD44, CD73, and CD90) can identify human MSC-derived extracellular vesicles by conventional flow cytometry,” *Cell Commun. Signal.*, vol. 14, no. 1, pp. 1–14, 2016, doi: 10.1186/s12964-015-0124-8.

[60] G. Brooke *et al.*, “Therapeutic applications of mesenchymal stromal cells,” *Semin. Cell Dev. Biol.*, vol. 18, no. 6, pp. 846–858, 2007, doi: 10.1016/j.semcdb.2007.09.012.

[61] M. F. Pittenger, D. E. Discher, B. M. Péault, D. G. Phinney, J. M. Hare, and A. I. Caplan, “Mesenchymal stem cell perspective: cell biology to clinical progress,” *npj Regen. Med.*, vol. 4, no. 1, 2019, doi: 10.1038/s41536-019-0083-6.

[62] E. H. Javazon, K. J. Beggs, and A. W. Flake, “Парадоксы Пассажирования.Pdf,” vol. 32, pp. 414–425, 2004.

[63] Y. P. Rubtsov, Y. G. Suzdaltseva, K. V. Goryunov, N. I. Kalinina, V. Y. Sysoeva, and V. A. Tkachuk, “Regulation of Immunity via Multipotent Mesenchymal Stromal Cells,” *Acta Naturae*, vol. 4, no. 1, pp. 23–31, 2012, doi: 10.32607/20758251-2012-4-1-23-31.

[64] K. Suzuki, N. Chosa, S. Sawada, N. Takizawa, T. Yaegashi, and A. Ishisaki, “Enhancement of Anti-Inflammatory and Osteogenic Abilities of Mesenchymal Stem Cells via Cell-to-Cell Adhesion to Periodontal Ligament-Derived Fibroblasts,” *Stem Cells Int.*, vol. 2017, 2017, doi: 10.1155/2017/3296498.

[65] R. E. Newman, D. Yoo, M. A. LeRoux, and A. Danilkovitch-Miagkova, “Treatment of

inflammatory diseases with mesenchymal stem cells," *Inflamm. Allergy - Drug Targets*, vol. 8, no. 2, pp. 110–123, 2009, doi: 10.2174/187152809788462635.

[66] P. S. Frenette, S. Pinho, D. Lucas, and C. Scheiermann, *Mesenchymal stem cell: Keystone of the hematopoietic stem cell niche and a stepping-stone for regenerative medicine*, vol. 31. 2013.

[67] Y. Wang, X. Chen, W. Cao, and Y. Shi, "Plasticity of mesenchymal stem cells in immunomodulation: Pathological and therapeutic implications," *Nat. Immunol.*, vol. 15, no. 11, pp. 1009–1016, 2014, doi: 10.1038/ni.3002.

[68] J. A. Ankrum, J. F. Ong, and J. M. Karp, "Mesenchymal stem cells: Immune evasive, not immune privileged," *Nat. Biotechnol.*, vol. 32, no. 3, pp. 252–260, 2014, doi: 10.1038/nbt.2816.

[69] A. J. Nauta and W. E. Fibbe, "Immunomodulatory properties of mesenchymal stromal cells," *Blood*, vol. 110, no. 10, pp. 3499–3506, 2007, doi: 10.1182/blood-2007-02-069716.

[70] K. English, "Mechanisms of mesenchymal stromal cell immunomodulation," *Immunol. Cell Biol.*, vol. 91, no. 1, pp. 19–26, 2013, doi: 10.1038/icb.2012.56.

[71] P. H. . J. B. M. . S. C. T. et al Gary, "The New England Journal of Medicine Downloaded from nejm.org on April 1, 2015. For personal use only. No other uses without permission. Copyright © 1990 Massachusetts Medical Society. All rights reserved.," *New English J. Med.*, vol. 323, no. 16, pp. 1120–1123, 1990.

[72] A. Gebler, O. Zabel, and B. Seliger, "The immunomodulatory capacity of mesenchymal stem cells," *Trends Mol. Med.*, vol. 18, no. 2, pp. 128–134, 2012, doi: 10.1016/j.molmed.2011.10.004.

[73] G. Ren *et al.*, "Mesenchymal Stem Cell-Mediated Immunosuppression Occurs via Concerted Action of Chemokines and Nitric Oxide," *Cell Stem Cell*, vol. 2, no. 2, pp. 141–150, 2008, doi: 10.1016/j.stem.2007.11.014.

[74] M. Krampera *et al.*, "Role for Interferon-γ in the Immunomodulatory Activity of Human Bone Marrow Mesenchymal Stem Cells," *Stem Cells*, vol. 24, no. 2, pp. 386–398, 2006, doi: 10.1634/stemcells.2005-0008.

[75] R. R. Sharma, K. Pollock, A. Hubel, and D. McKenna, "Mesenchymal stem or stromal cells: A review of clinical applications and manufacturing practices," *Transfusion*, vol. 54, no. 5, pp. 1418–1437, 2014, doi: 10.1111/trf.12421.

[76] J. N. M. Ijzermans and R. L. Marquet, "Interferon-gamma: A Review," *Immunobiology*, vol. 179, no. 4–5, pp. 456–473, 1989, doi: 10.1016/S0171-2985(89)80049-X.

[77] Y. Liu *et al.*, "Mesenchymal stem cell-based tissue regeneration is governed by recipient T lymphocytes via IFN-γ and TNF-α," *Nat. Med.*, vol. 17, no. 12, pp. 1594–1601, 2011, doi: 10.1038/nm.2542.

[78] N. P. Group, “The Otogeny of the Neural Crest in Avian.”

[79] M. Eddaoudi, H. Li, and O. M. Yaghi, “Highly porous and stable metal-organic frameworks: Structure design and sorption properties,” *J. Am. Chem. Soc.*, vol. 122, no. 7, pp. 1391–1397, 2000, doi: 10.1021/ja9933386.

[80] J. Kim *et al.*, “Assembly of metal-organic frameworks from large organic and inorganic secondary building units: New examples and simplifying principles for complex structures,” *J. Am. Chem. Soc.*, vol. 123, no. 34, pp. 8239–8247, 2001, doi: 10.1021/ja010825o.

[81] M. Eddaoudi *et al.*, “Modular chemistry: Secondary building units as a basis for the design of highly porous and robust metal-organic carboxylate frameworks,” *Acc. Chem. Res.*, vol. 34, no. 4, pp. 319–330, 2001, doi: 10.1021/ar000034b.

[82] H. Kim *et al.*, “Hydrogen Storage in Microporous Metal-Organic Frameworks,” *Science (80-.).*, vol. 73, no. 1973, pp. 12–15, 2002.

[83] D. J. Tranchemontagne, J. L. Tranchemontagne, M. O’keeffe, and O. M. Yaghi, “Secondary building units, nets and bonding in the chemistry of metal–organic frameworks,” *Chem. Soc. Rev.*, vol. 38, no. 5, pp. 1257–1283, 2009, doi: 10.1039/b817735j.

[84] M. Karagianni *et al.*, “A comparative analysis of the adipogenic potential in human mesenchymal stromal cells from cord blood and other sources,” *Cytotherapy*, vol. 15, no. 1, pp. 76-88.e2, 2013, doi: 10.1016/j.jcyt.2012.11.001.

[85] J. R. Long and O. M. Yaghi, “The pervasive chemistry of metal-organic frameworks,” *Chem. Soc. Rev.*, vol. 38, no. 5, pp. 1213–1214, 2009, doi: 10.1039/b903811f.

[86] H. Furukawa, K. E. Cordova, M. O’Keeffe, and O. M. Yaghi, “The chemistry and applications of metal-organic frameworks,” *Science (80-.).*, vol. 341, no. 6149, 2013, doi: 10.1126/science.1230444.

[87] M. Eddaoudi *et al.*, “Systematic design of pore size and functionality in isoreticular MOFs and their application in methane storage,” *Science (80-.).*, vol. 295, no. 5554, pp. 469–472, 2002, doi: 10.1126/science.1067208.

[88] J. Phipps *et al.*, “Josh Phipps, Mahsa Haseli, Luis Pinzon-Herrera, Ben Wilson, Joshua Corbitt, Shannon Servoss, and Jorge Almodovar *,” 2022, doi: 10.1021/acsbiomaterials.2c01038.

2. Immunomodulatory Functions of Human Mesenchymal Stromal Cells Are Enhanced When Cultured on HEP/COL Multilayers Supplemented with Interferon-Gamma

Mahsa Haseli[1,d], David A. Castilla-Casadiego[1,2,d], Luis Pinzon-Herrera[1], Alexander Hillsley[2], Katherine A. Miranda-Muñoz[3], Srikanth Sivaraman[3], Adrianne M. Rosales[2], Raj Rghavendra-Rao[3], and Jorge Almodovar[1*]

[1]Ralph E. Martin Department of Chemical Engineering, University of Arkansas, 3202 Bell Engineering Center, Fayetteville, AR 72701, USA

[2]Mcketta Department of Chemical Engineering, the University of Texas at Austin, Austin, TX, 78712, USA

[3]Department of Biomedical Engineering, College of Engineering, University of Arkansas, Fayetteville, AR 72701, USA

[d] M.H. and D. A. C-C. contributed equally.

* The chapter was published and used with permission.

Abstract

Human mesenchymal stromal cells (hMSCs) are multipotent cells that have been proposed for cell therapies due to their immunosuppressive capacity that can be enhanced in the presence of interferon-gamma (IFN-γ). In this study, multilayers of heparin (HEP) and collagen (COL) (HEP/COL) were used as a bioactive surface to enhance the immunomodulatory activity of hMSCs using soluble IFN-γ. Multilayers were formed, via layer-by-layer assembly, varying the final layer between COL and HEP and supplemented with IFN-γ in the culture medium. We evaluated the viability, adhesion, real-time growth, differentiation, and immunomodulatory activity of hMSCs on (HEP/COL) multilayers. HMSCs viability, adhesion, and growth were

superior when cultured on (HEP/COL) multilayers compared to tissue culture plastic. We also confirmed that hMSCs osteogenic and adipogenic differentiation remained unaffected when cultured in (HEP/COL) multilayers in the presence of IFN-γ. We measured the immunomodulatory activity of hMSCs by measuring the level of indoleamine 2,3-dioxygenase (IDO) expression. IDO expression was higher on (HEP/COL) multilayers treated with IFN-γ. Lastly, we evaluated the suppression of peripheral blood mononuclear cell (PBMC) proliferation when co-cultured with hMSCs on (HEP/COL) multilayers with IFN-γ. hMSCs cultured in (HEP/COL) multilayers in the presence of soluble IFN-γ have a greater capacity to suppress PBMC proliferation. Altogether, (HEP/COL) multilayers with IFN-γ in culture medium provides a potent means of enhancing and sustaining immunomodulatory activity to control hMSCs immunomodulation.

Keywords: Layer-by-Layer, Human mesenchymal stromal cells, Collagen, Heparin, Interferon gamma.

2.1. Introduction

Human mesenchymal stromal cells (hMSCs) are of particular interest for cellular therapy programs [59]. During tissue damage, hMSCs have the ability to secrete paracrine and anti-inflammatory factors to repair tissue [62][63][64]. In addition, hMSCs contribute not only to the repair of damaged tissues but also possess remarkable immunomodulatory activity by producing anti-inflammatory and immunosuppressive factors [65][3][4][66][67][68]. Therefore, hMSCs have become apparent as a promising implement for new medical applications and therapies for the treatment of diverse diseases and disorders, such as graft-versus-host disease, inflammatory diseases, and autoimmune disorders [75][7]. Immunosuppression by hMSCs appears as a multifactorial process that relies on cell-cell contact working in collaboration with the secretion

of paracrine factors and extracellular vesicles (EVs) [11][12]. However, some studies showed that the immunosuppressive properties of hMSCs are more affected by paracrine mediators rather than cell-cell contact [88] [89]. Paracrine mediators (e.g., cytokines, chemokines, and growth factors) modulate the hMSCs microenvironment and influence the activity of resident cells [19]. These specific immune factors, including, interferon-gamma (IFN-γ), tumor necrosis factor-alpha (TNF-α), and interleukin 1 beta (IL-1β), initiate the hMSCs immunosuppression program by inducing the synthesis of protein factors, in particular indolamine-2,3-dioxygenase (IDO) and inducible nitric oxide synthase [72][73][74]. It has been shown that the immunosuppressive properties of hMSCs relies on the existence of IFN-γ in the microenvironment [5]. IFN-γ is a potent pro-inflammatory cytokine produced by $CD4^+$ lymphocytes, natural killer cells, and macrophages. It plays essential and complex roles in innate and adaptive immune responses against viral infections, bacteria, protozoa, and graft-versus-host disease (GVHD) [76][77]. However, our group and others have shown that IFN-γ has a significant anti-proliferative effect on hMSCs [6][7].

To overcome these limitations, polymeric biomaterials are engineered to enhance the survival, manufacturing efficiency, and delivery of hMSCs [90][91]. However, the function of polymeric biomaterials is correlated to the donor-donor variability of hMSCs [92][93]. In our previous work done by D. Castilla-Casadiego et al., bone-marrow-derived hMSCs were used to evaluate cell adhesion, proliferation, and cytokine expression on polyelectrolyte multilayers composed of heparin and collagen (HEP/COL) terminating in COL (12 layers HEP/COL) or HEP (13 layers HEP/COL) with IFN-γ supplementation in the culture medium [7]. We demonstrated that the use of (HEP/COL) multilayers is likely to improve the anti-proliferative effect of IFN-γ [7]. In addition, in the work of Cifuentes et al., we evaluated the impact of HEP/COL multilayers on the

growth, morphology, and secretome of bone marrow and adipose derived hMSCs [94]. The results of study by Cifuentes et al. suggested that HEP terminated layers are likely to increase hMSC potency under reduced serum conditions. While our previous work suggests that the immunosuppressive properties of hMSCs cultured on HEP/COL multilayers are enhanced in the presence of soluble IFN-γ, we have yet confirmed this. Thus, this manuscript directly evaluate the immunosuppressive properties of hMSCs cultured on HEP/COL multilayers both by measuring IDO function and suppression of peripheral blood mononuclear cell (PBMC) proliferation using hMSCs from different donors.

The layer-by-layer (LbL) deposition of polyelectrolytes provides compositional uniqueness of natural or synthetic polymers, such as stimulating a specific signal to cells and enhancing cellular behavior [29]. LbL involves the alternative absorption of polycations and polyanions to produce films with specific and controlled physical−chemical characteristics by adapting the experimental parameters, such as pH, ionic strength, and polyelectrolyte concentration [30][31][32]. Type I collagen is a major fibrous protein in the extracellular matrix (ECM) of connective tissues which interact with cells and other ECM molecules to generate and maintain tissue form and function [44][45]. Furthermore, heparin is a highly sulfated glycosaminoglycan that contains negatively charged carboxylate or sulfate groups present in the ECM and surface of cells [39][40]. Heparin has the ability to bind ECM proteins, such as collagen and thus plays an important role in organizing the structure and composition of the ECM.

Here, we continued our previous work to evaluate the immunomodulatory of two different donors of hMSCs-derived from bone marrow on polymeric multilayers composed of collagen (COL) and heparin (HEP) that are either terminated in COL (12 layers of HEP/COL) or HEP (13 layers of HEP/COL). The reason that we evaluated 12 and 13 layers of HEP/COL is related to

our previous work where we showed that there is no differences on cell function as a function of number of layers after 12 layers [94]. We also have previously demonstrated that 12 layers is the minimum number of layers to provide complete surface coverage [95]. These heparin/collagen arrangements will be noted as COL-ending and HEP-ending, respectively. The experiments were conducted for cases with and without IFN-γ as a supplement in the culture medium. The ability of polymeric multilayers, supplemented IFN-γ to induce sustained immunomodulatory activity, was evaluated by measuring IDO expression and PBMC proliferation suppression. In this study, hMSCs growth, viability, differentiation, immunophenotype, and suppression of PBMC proliferation were evaluated as a function of polymeric multilayer composition in the presence or absence of soluble IFN-γ. This study demonstrates that the LbL coating did not negatively influence the viability, adhesion, and differentiation of hMSCs. Moreover, this study shows that hMSCs cultured on (HEP/COL) multilayers supplemented with IFN-γ have a greater capacity to suppress PBMC proliferation. Altogether, this study shows that (HEP/COL) multilayers can modulate a hMSCs response to soluble factors, which may lead to manufacturing and hMSCs-based therapies.

2.2. Materials and Methods

2.2.1. (HEP/COL) multilayers fabrication

(HEP/COL) multilayers were constructed as described in our previous works [7][96][33][94]. Heparin sodium (HEP) purchased from Celsus Laboratories, Inc. (Cat. #PH3005) and lyophilized type I collagen sponges (COL) derived from bovine tendon (generously donated by Integra Lifesciences Holdings Corporation, Añasco, PR) were used to construct thin polymeric multilayers by the LbL technique on sterile tissue culture-treated plates from Corning Costar (Cat. #07-200- 740). Poly(ethylenimine) (PEI) (50% solution in Water, Mw ≈ 750 000) from

Sigma-Aldrich (Cat. #P3143) was used to produce a strong anchoring layer prior to (HEP/COL) multilayers fabrication. All polymer solutions were prepared at a concentration of 1.0 mg/mL in sodium acetate buffer (0.1 M sodium acetate anhydrous, 0.1 M acetic acid, at pH 5 for HEP and PEI, and pH 4 for COL). Sodium acetate buffer at pH 5 was used as washing solution. Ultrapure water at 18 MΩ·cm used to prepare polymeric and wash solutions was obtained from a Millipore-Sigma^{TM} Direct-Q^{TM} 3 (Cat. #ZRQSVP3US). Briefly, the process consisted of creating an anchoring layer by depositing PEI solution for 15 minutes to each well of a sterile tissue culture-treated plate and following with a washing step of 3 minutes. After this initial step, HEP and COL were added for 5 minutes alternating with an intermediate wash of 3 minutes. This process was followed until building a total of 12 polymeric layers of (HEP/COL) (layers ending with COL) and 13 polymeric layers of (HEP/COL) (layers ending with HEP). After preparing the multilayers, a final wash was done using Dulbecco's phosphate-buffered saline (DPBS)1X without Ca^{2+} and Mg^{2+}. Substrates were sterilized using ultraviolet (UV) for 10 min to eliminate any contaminations before cell culture.

2.2.2. Experimental design

In this work, the effects of the type of surface and the presence or absence of IFN-γ recombinant human protein (ThermoFisher, Cat. #PHC4031) in the culture medium were studied on the cellular response of hMSCs. Three surfaces were assessed; they consisted of a control surface of tissue culture plastic labeled as TCP, a bioactive surface of 12 polymeric layers of (HEP/COL) (layers ending with COL), and 13 layers of (HEP/COL) (layers ending with HEP). IFN-γ supplemented in cell medium, which was added in the cells medium immediately after cell seeding, was evaluated at a concentration of 50 ng/mL, and conditions with and without IFN-γ were designated as +IFN-γ and −IFN-γ, respectively. A 50 ng/mL concentration for soluble IFN-

γ was selected based on our previous study [25][26]. Time points and the initial number of cells were selected according to the nature of the specific method used [33].

2.2.3. Physical characterizations of (HEP/COL) multilayers

Atomic Force Microscope (AFM) images were taken using an Agilent Asylum MFP-3D AFM in contact mode, using a PPP-CONTR-10 (NanoAndMore, Resonance frequency 6-12 kHz, Force Constant 0.02-0.77 N/m) probe. 80 x 80 μm images were first taken of the dry substrate. The probe was then raised, and phosphate-buffered saline (PBS) was carefully added using a micropipette until both the probe and the substrate were completely submerged. The sample was then hydrated for 5 minutes to obtain "wet" images.

2.2.4. In-situ deposition of (HEP/COL) multilayers

The multilayer growth and IFN-γ interaction with the (HEP/COL) were followed by quartz crystal microbalance (QCM-D) with dissipation measurements. QCM-D measurements were performed on quartz crystal microbalance with dissipation from Biolin Scientific, Sweden. The multilayers build-up process was described in our previous work [33]. Briefly, the quartz crystal was immersed in 5:1:1 (volume parts) at 75 °C of water, 25% ammonia, and 30% hydrogen peroxide. The clean quartz crystal was placed in the QCM-D chamber. Then the PEI solution was injected at a flow rate of 100 mL/min continuously for 15 minutes. After PEI, and sodium acetate buffer at pH 5 was performed for 3 minutes at the same flow rate. The HEP solution was injected at the same rate for 5 minutes, followed by the same sodium acetate buffer at pH 5 injection. After that, the COL solution was injected for 5 minutes at the same rate, followed by the same sodium acetate buffer at pH 5 injection. HEP and COL were then alternately injected into the chamber (followed by the same sodium acetate buffer at pH 5 buffer injection after each injection). After 12 and 13 multilayers was build up on quartz crystal microbalance, the IFN-γ in

PBS at pH 7.4 was injected into the chamber for 1 hour. The frequency shift (Δf) and dissipation (ΔD) vs. time curves were recorded.

2.2.5. Chemical composition of HEP/COL multilayers

The elemental and chemical composition of the multilayers was confirmed by X-ray Photoelectron Spectroscopy (XPS) (Versaprobe XPS from Physical electronics). XPS experiments were performed at a photoelectron takeoff angle of 458 on dry glass substrate, and binding energy scales were referenced to the C1s peak (284.7eV).

2.2.6. Cell culture

Human bone marrow-derived Mesenchymal stem cells purchased from RoosterBio (Cat. #MSC-003), were used between passages 4−6. Donor#1 is a healthy 25-year-old male (Lot. 00174), and donor#2 is a healthy 22-year-old male (Lot. 00178). The product specification sheet provided by the vendor shows that these cells were positive for CD90 and CD166 hMSCs identity markers (as tested by flow cytometry), negative for CD45 and CD34 (as tested by flow cytometry) and could differentiate into fat and bone cells. hMSCs were grown in alpha-minimum essential media MEM Alpha (1×) from Gibco (supplemented with L-glutamine, ribonucleosides, and deoxyribonucleosides) (Cat. #12561-056) containing 20% fetal bovine serum from Gibco (Cat. #12662029), 1.2% penicillin-streptomycin from Corning (Cat. #30002CI), and 1.2% L-glutamine from Corning (Cat. #25005CI).

2.2.7. HMSC viability on (HEP/COL) multilayers

For hMSCs viability, the PrestoBlue^{TM} cell viability assay from Invitrogen (Cat. #A13261) was used. hMSCs (10000 cells/cm^2) were seeded on each surface prepared on a 96 well-plate, and cell viability was measured after 3 days of culture as described in our previous works [97] [98][94]. Briefly, the cell culture medium was removed after 3 days, and 100 µL per well

containing 90% fresh cell medium and 10% PrestoBlue reagent were added. The plate was incubated for 3 h, and the fluorescence intensity measurement was determined using a BioTek Multi-Mode Microplate Reader (Model Synergy^{TM} 2) with excitation/emission of 560/590 nm.

2.2.8. Real-time monitoring of hMSCs behavior on (HEP/COL) multilayers

A Real-Time Cell Analyzer (RTCA) xCELLigence instrument from ACEA Biosciences Inc. (Cat. #380601000) was used to measure real-time cell behavior. (HEP/COL) multilayers were constructed on the wells of an ACEA^{TM} E-Plate L8 (Cat. #300600840, cell growth area of 0.64 cm^2 per well), which are composed of tissue culture plastic, but they also contain sensors to measure impedance, and hMSCs at a concentration of 20000 cells/cm^2 were seeded on each condition evaluated; uncoated sensors, multilayers ending in HEP, and ending in COL with and without IFN-γ supplemented in the culture medium. xCELLigence instrument was configured as described in our previous works [97] [98]. Briefly, the xCELLigence RTCA S16 was placed inside the incubator to allow the S16 device to warm up for at least 2 hours before use. This step is to avoid any condensation on the station after starting the measurement stage. The RTCA was set up to monitor perform readings every 10 minutes for a period of 48 hours of cell culture.

2.2.9. Immunomodulatory factor expression of hMSCs on (HEP/COL) multilayers

hMSCs (5000 cells/cm^2) with and without IFN-γ treatment were seeded on each surface prepared on a 24 well-plate. IDO activity was measured after 6 days of culture (changing the cells medium every 2 days) as described in our previous works [97]. Briefly, cell supernatant 100 µL was mixed with 100 µL standard assay mixture consists of (potassium phosphate buffer (50 mM, pH 6.5), ascorbic acid (40 mM, neutralized with NaOH), catalase (200 µg/ml), methylene blue (20 µ M), and L-tryptophan (400 µM)). The mixture was kept at 37°C in a humidified incubator with 5% CO_2 for 30 minutes (in a dark environment to protect solutions from light) to allow IDO to

convert L-tryptophan to N-formyl-kynurenine. After that, the reaction was stopped by adding 100 µL trichloroacetic acid 30% (wt/vol) and incubated for 30 minutes at 58 °C. After hydrolysis of N-formyl-kynurenine to kynurenine, 100 µL of mixed cell supernatant/standard transfer into a well of a 96-well microplate, followed by adding 100 µL per well of 2% (w/v) p-dimethylaminobenzaldehyde in acetic acid on each well. Absorbance was read at 490 nm at the endpoint using a BioTek Synergy 2 spectrophotometer (Synergy LX Multi-Mode Reader from BioTek® Model SLXFA). Absorbance readings were converted to concentration of kynurenine using an equation obtained from a calibration curve (plot the absorbance vs. concentration of standard solutions). Amounts of kynurenine were normalized by number of cells per well.

2.2.10. Peripheral blood mononuclear cells co-culture

For the hMSCs immunosuppressive capacity, human primary peripheral blood mononuclear (PBMC), normal, human were purchased from ATCC (ATCC® PCS¬800¬011™ Part number: 302213). Briefly, 62,500 hMSCs (cells/cm^2) with and without IFN-γ treatment were seeded on each surface prepared on a 24 well-plate for 3 days. PBMCs were labeled using a Cell Trace Yellow Cell Proliferation Kit (Invitrogen) at a final dye concentration of 5 mM. Before being added to each well for co-culture, the PBMCs were incubated for 15 minutes with Human T Activator CD3/CD28 Dynabeads (Invitrogen) and Recombinant human IL-2 (30 U/mL). After this time, the PBMCs and Dynabeads were added to each well to achieve a 1:4 ratio of hMSCs to PBMCs. Based on the study done by Cuerquis et al. the reduction in the percentages of T cells was less significant at an MSC:PBMC ratio of 1:9 compared with 1:3 [11]. In other study, the results showed that a higher ratio of PBMCS/MSC is more efficient than a lower ratio [99]. In addition, other studies used the ratio 1:4 for MSCs/PBMCs for the co-culture experiment [100][101]. In this study, we used the ratio 1:4 to have a better comparison of results with others

studies. hMSCs: PBMCs co-cultures were maintained in alpha-minimum essential medium MEM Alpha (1×) from Gibco, supplemented with L-glutamine, ribonucleosides, and deoxyribonucleosides containing 20% fetal bovine serum from Gibco, 1.2% penicillin-streptomycin from Corning, and 1.2% L-glutamine from Corning for 3 days. After 3 days, the medium from the wells (containing the suspended PBMCs /Dynabeads) was collected into a 1.5 mL tube and protected from light. The tubes were placed in DynaMag magnets from Thermofisher (Cat. #12301D) to remove the Dynabeads. Then, PBMCs were resuspended in MEM Alpha followed by analysis on a BD FACSCanto II flow cytometer to investigate PBMCs proliferation in the presence and absence of hMSCs and/or IFN-γ onto multilayers and TCP. The data were normalized by using forward scatter (FSC) and side scatter (SSC) parameters to exclude cell debris and aggregates.

2.2.11. HMSC differentiation stains

hMSCs (5000 cells/cm^2) were seeded on each surface prepared on 24 well-plates and grown for 6 days in expansion medium (MEM Alpha (1×) from Gibco (supplemented with L-glutamine, ribonucleosides, and deoxyribonucleosides) containing 20% fetal bovine serum from Gibco, 1.2% penicillin-streptomycin from Corning, and 1.2% L-glutamine from Corning) at 37 °C in a humidified atmosphere of 5% CO_2. After the cells reached at least 50% confluency, they were exposed to osteogenic differentiation medium (DMEM low glucose, 10% fetal bovine serum from Gibco, 1% penicillin, 1% L-Glutamine, 50 μM ascorbic acid (Sigma, Cas Number: 50-81-7) (50 mg/10ml), 10 mM β-glycerophosphate (e.g., Sigma, CAS Number: 154804-51-0, G9422), 100 nM dexamethasone (e.g., Sigma, CAS Number 50-02-2)), and the medium was replaced every 2-3 days. Due to maintain the consistency of all experimental design, we seeded the cells with the regular expansion medium for 6days. After that we added the differentiation medium for

7-10 days. After culture for one week, cells were fixed with 10% formaldehyde. Alizarin Red S (Sigma, CAS Number 130-22-3) staining solution was prepared by dissolving 2 g of Alizarin Red S in 90 mL distilled water and adjusting the pH to 4.1–4.3 with ammonium hydroxide. Alizarin Red S solution was added, then rinsed with PBS. The sample was analyzed immediately under the microscope to detect calcium deposits. For adipogenic differentiation, an induction medium composed of complete DMEM high glucose supplemented with 10% fetal bovine serum from Gibco, 1% penicillin, 1% L-glutamine, 1 µM dexamethasone (e.g., Sigma, CAS Number 50-02-2), 0.01 mg/mL insulin (Sigma-Aldrich, Catalog No. I2643), 0.5 mM 3-isobutyl-1-methylxanthine (IBMX) (e.g., Sigma, CAS Number: 28822-58-4, I5879) , and 100µM indomethacin (Sigma, CAS Number: 53-86-1) was used. The medium was replaced every 2-3 days. After culture for a week, cells were fixed with 10% formaldehyde, stained with 0.5% (w/v) Oil Red O (Sigma-Aldrich, Catalog Number: O0625) in isopropanol and incubated at room temperature for 10-30 minutes in the dark, then washed twice with PBS. The sample was observed under a light microscope to determine the number of hMSCs-derived adipocytes.

2.2.12. Alkaline phosphatase (ALP) assay

To confirm osteogenic differentiation and to determine the level of activity of the differentiated hMSCs, two assays were performed: alkaline phosphatase (ALP) activity and total protein content (micro-BCA assay). Alkaline phosphatase activity was assessed using the Alkaline Phosphatase Colorimetric Assay Kit (Abcam ab83369). According to standard protocols, after the cell's exposure to osteogenic differentiation medium for periods of 3 days, cells were washed twice with PBS. Then, 50 µL of the cell lysate with assay buffer was added to a 96 well- plate and 50 µL p-nitrophenyl phosphate (pNPP). The samples were incubated at 25°C for 60 minutes and protected from light. In the last step, 20 µL stop solution was added to the wells, then; the

plate was read at 405 nm in a microplate reader (Synergy LX Multi-Mode Reader from BioTek® (Model SLXFA). Alkaline phosphatase (ALP) activity was normalized by total protein content (micro-BCA assay). The total protein content was determined according to the protocol of the manufacture 150 μL of sample was placed in a 96 well-plate with 150 μL of working reagent made from a micro-BCA protein assay kit (Thermo Scientific). The well plate was covered with foil and incubated at 37 °C for 2 hours. Absorbance was read at 562 nm using a BioTek Multi-Mode Microplate Reader (Model Synergy™ 2).

2.2.13. Flow cytometry analysis

Osteogenic and adipogenic cell markers of differentiated hMSCs were analyzed using flow cytometry. hMSCs (25000 cells/cm^2), with and without IFN-γ treatment, were seeded on each surface prepared on a 12 well-plate and expanded using growth medium at 37 °C in a humidified atmosphere 5% CO_2 for 6 days. After the cells reached at least 50% confluency, they were exposed to osteogenic and adipogenic differentiation medium, and the medium was replaced every 2-3 days. Undifferentiated cells grown in expansion media (MEM Alpha) were maintain as control. After 3 days, the cells were detached by trypsinization and washed twice with PBS (centrifuged at 300 g for 10 minutes). Aliquots were prepared containing 1 x 10^5 cells in PBS with 2% FBS for staining conjugated primary antibody were incubated against CD105 (PE Mouse anti-Human CD105, BD Biosciences), CD10 (PE Mouse anti-Human CD10, BD Biosciences), and CD92 (Alexa Fluor® 647 Mouse Anti-Human CD92, BD Biosciences). The samples were covered with aluminum foil during the process and incubated at 4 °C for 30 minutes in the dark. For each type of antibody used, an additional sample with a non-specific isotype control antibody was added. Isotype matched control antibodies PE labeled Mouse IgG1 (BD Pharmingen), and Alexa Fluor® 647 Mouse IgG1 κ Isotype Control (BD Pharmingen) were

used for assessment of background fluorescence. The Flow Cytometry analysis was performed using a BD FACS Canto II flow cytometer, using FlowJo software (Tree Star, Oregon, USA) for analysis. At least 10,000 gated events per acquisition were acquired. The median relative fluorescence unit was used for statistical analyses.

2.2.14. Statistical analysis

The results were presented as mean ± standard deviation. Comparisons among multiple groups were performed by one-way analysis of variance (ANOVA) using Minitab 17 for Windows. A p-value < 0.05 was considered statistically significant.

2.3. Results and Discussion

2.3.1. Surface characterization

The in-situ assembly deposition of (HEP/COL) multilayers was monitored by QCM-D. QCM-D detects the adsorbed mass of polyelectrolytes (ΔF) and measures the viscoelastic properties of the surface (ΔD) [102]. QCM-D was used here to investigate physical structures within the multilayer of heparin and collagen. Figure 2-1 shows the frequency shift (ΔF) and dissipation (ΔD) for the third, fifth, and seventh overtones for COL-ending and HEP-ending multilayers. The alternating 3 minutes of rinsing and 5 minutes of adsorption steps can be observed. The first 15 minutes correspond to a PEI step, followed by a 3 minutes rinsing step in Figure 2-1, each physical polyelectrolyte adsorption step is followed by 3 minutes of rinsing. The increase in -ΔF and ΔD of every (HEP/COL) sequential deposition shows that the polyelectrolytes gradually deposit onto the quartz crystal. This increase can be considered a linear increase of thickness for the multilayers. It is demonstrated that by increasing -ΔF the mass added to the layers increases, whereas the growth of ΔD is due to the enhanced viscoelastic structure of the deposited film [103]. Therefore, adding rough layers on quartz crystal has a shorter -ΔF, whereas a dense layer

has a large ΔD value. When collagen is deposited, -ΔF and ΔD have a sharp rise with great dispersion between different overtones in both COL and HEP-ending multilayers [104]. This indicates that the collagen is a loose and swollen layer [104]. In contrast, the heparin deposited shows a slight increase in -ΔF and a decrease in ΔD. These indicated that a rough layer was obtained after the heparin deposition [104]. Our previous study showed that HEP-ending multilayers have higher thickness and roughness than the COL-ending multilayers at both 25 ℃ and 37 ℃ [7]. In addition, the frequency shifts do not overlap for the different overtones not only in the rinse steps but also during the adsorption steps. Consequently, this indicates that the Sauerbrey relation is not valid for determining the film mass during rinse and adsorption steps, which indicates the film is more viscoelastic. Besides, the ratio of the change during rinse and the adsorption steps in the dissipation factor to the change in frequency (ΔD/(-ΔF/n)) remain higher than 4×10^{-7} $Hz^{-}1$; therefore, the film can be considered soft [105]. After adsorption of the IFN-γ, the frequency shifts no longer overlap. This indicates that adsorbed films are viscoelastic and that the mass does not follow the Sauerbrey relationship, so a more complex model might be used to determine the adsorbed mass from the frequency shift and dissipation data [106]. Figure 2-1(A) shows significant frequency shifts following the adsorption of the IFN-γ on the COL-ending multilayers surface for the 3 overtones, indicating that the IFN-γ is strongly adsorbed.

In contrast, Figure 2-1 (B) shows the decrease of the frequency shifts following the adsorption of the IFN-γ on the HEP-ending multilayers surface, resulting in negligible adsorption of the IFN-γ. Following adsorption of the IFN-γ, a quick decrease of the frequency shifts are found for both COL-ending and HEP-ending multilayers, which is due to the buffer effect, and the trend levels

[107]. These results indicate that the (HEP/ COL) multilayers present good stability in presence of the IFN-γ.

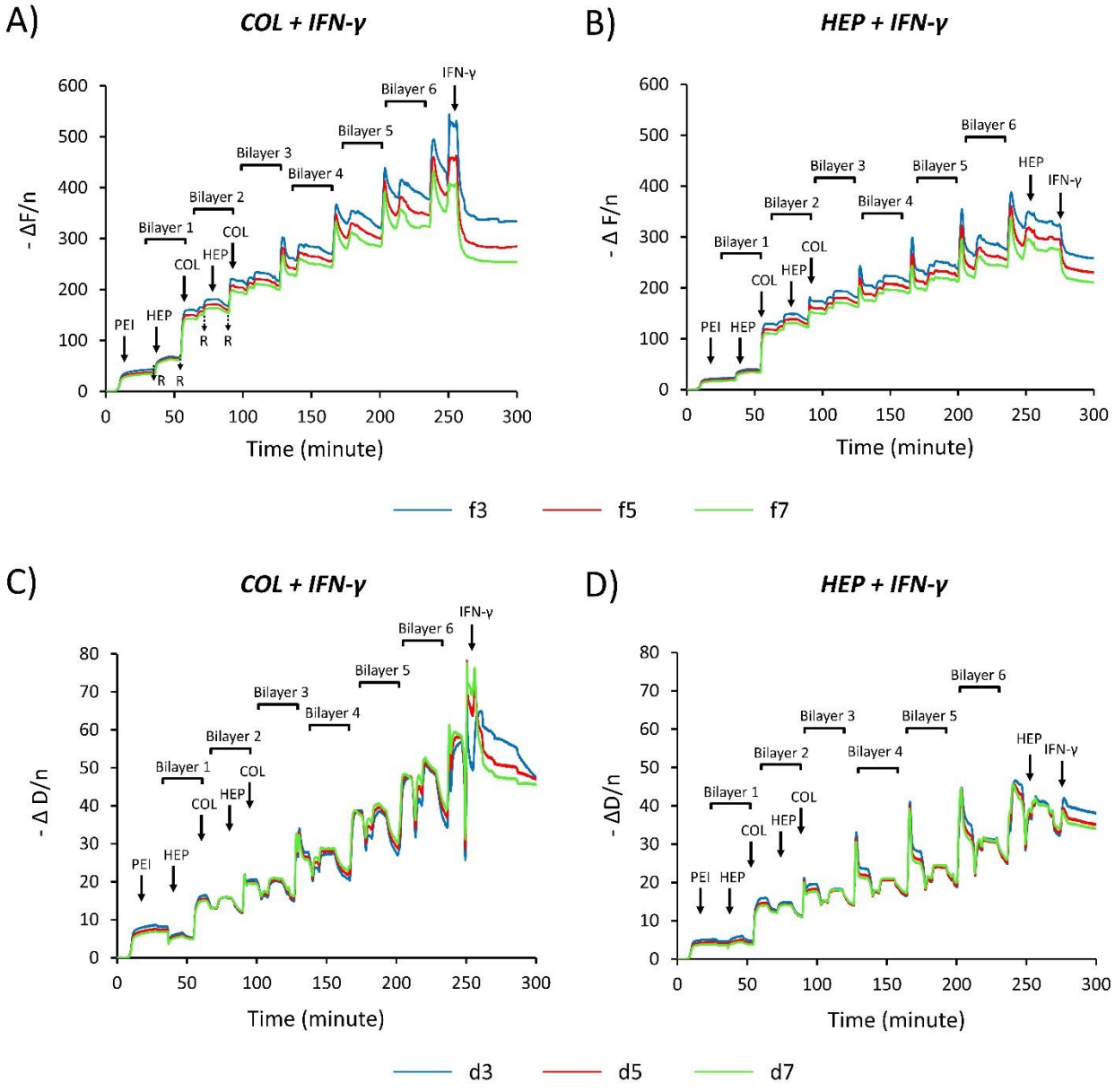

Figure 2-1. QCM-D data showing the normalized frequency shift & dissipation shift as a function of time for the 3rd, 5th, and 7th overtones during the construction of the COL ending and HEP ending multilayers with IFN-γ, with alternating 3-minute rinse and 5 minutes adsorption intervals. (A&B): shows the normalized frequency shift. (C&D): shows the normalized dissipation shift.

The topography of dried and wet (HEP/COL) multilayers was investigated by AFM for COL-ending and HEP-ending multilayers. Analyzing the topographic images in Figure 2-2 (A) shows HEP-ending multilayers has a larger cluster on the surface, which demonstrate considerable accumulation associated with surface deposition [106]. Also, the deposition of HEP-ending multilayers on dry condition leads to a rougher surface than the COL-ending multilayers. Regarding the wet condition, Figure 2-2 (B) shows that the surface has a greater number of smaller clusters on COL-ending than in HEP-ending, demonstrating that the HEP successfully attached to the surface and deposition of HEP may increase roughness of surfaces. These results confirm the conclusions drawn from the QCM-D results in which a rough layer was obtained after HEP deposition in wet conditions. Also, Figure 2-2 (A&B) show that the multilayers on dry condition are rougher. However, the multilayers have a smooth surfaces in wet condition which may improve cell adhesion as suggested by Salloum et al. who investigated the combined effects of increasing surface charge and hydrophobicity on vascular smooth muscle cell adhesion [108]. The XPS broad spectra and high-resolution spectra of COL-ending and HEP-ending multilayers are shown in Figure 2-2 (C&D). In our previous study, we demonstrated that the thickness of COL-ending multilayers was approximately 129 nm [7]. The XPS could only detect about 10 nm depth of nanometer surface; also, only the outmost layer can be examined from XPS. The XPS spectrum of COL-ending and HEP-ending multilayers contained five peaks corresponding to C1s (283.4 eV), N1s (398.4 eV), O1s (529.8 eV), Na KL1, Na2P, Na2S, and S2P (168.3 eV). Na and S were mainly the characteristic elements of heparin polysaccharide structure possessing $-COO^-$, $-SO_4^{-2}$ and -OH, while collagen contains a large number of various amino acids with $-NH_2$ and -COOH [109]. The presence of more sulfur was detected on the HEP-ending multilayers and revealed the presence of heparin [110]. According to the study of Dan Li et al. [111], collagen

has the characteristic sulfur element, but with low content, further demonstrated the successful assembly process. High-resolution spectra of S2p suggested that the surface presented more of S element on HEP-ending multilayers, indicating heparin's presence in the last layer. The increase of sulfur peak due to increasing the number of layers shows a successful deposition of heparin. This finding complies with a previous study by Almodovar et al. [112]. Moreover, oxygen and nitrogen intensity content decrease in HEP-ending multilayers compared to 12 multilayers, indicating that most surfaces of COL-ending multilayers were coated by collagen. In addition, COL-ending multilayers have a higher C1s peak compared to HEP-ending multilayers, including C-C (283.4 eV), C-O, and C–N (286.4 eV) groups. Consequently, a higher carbon, oxygen, and nitrogen content confirm the accumulation of collagen, while heparin deposition shows higher sulfur peaks.

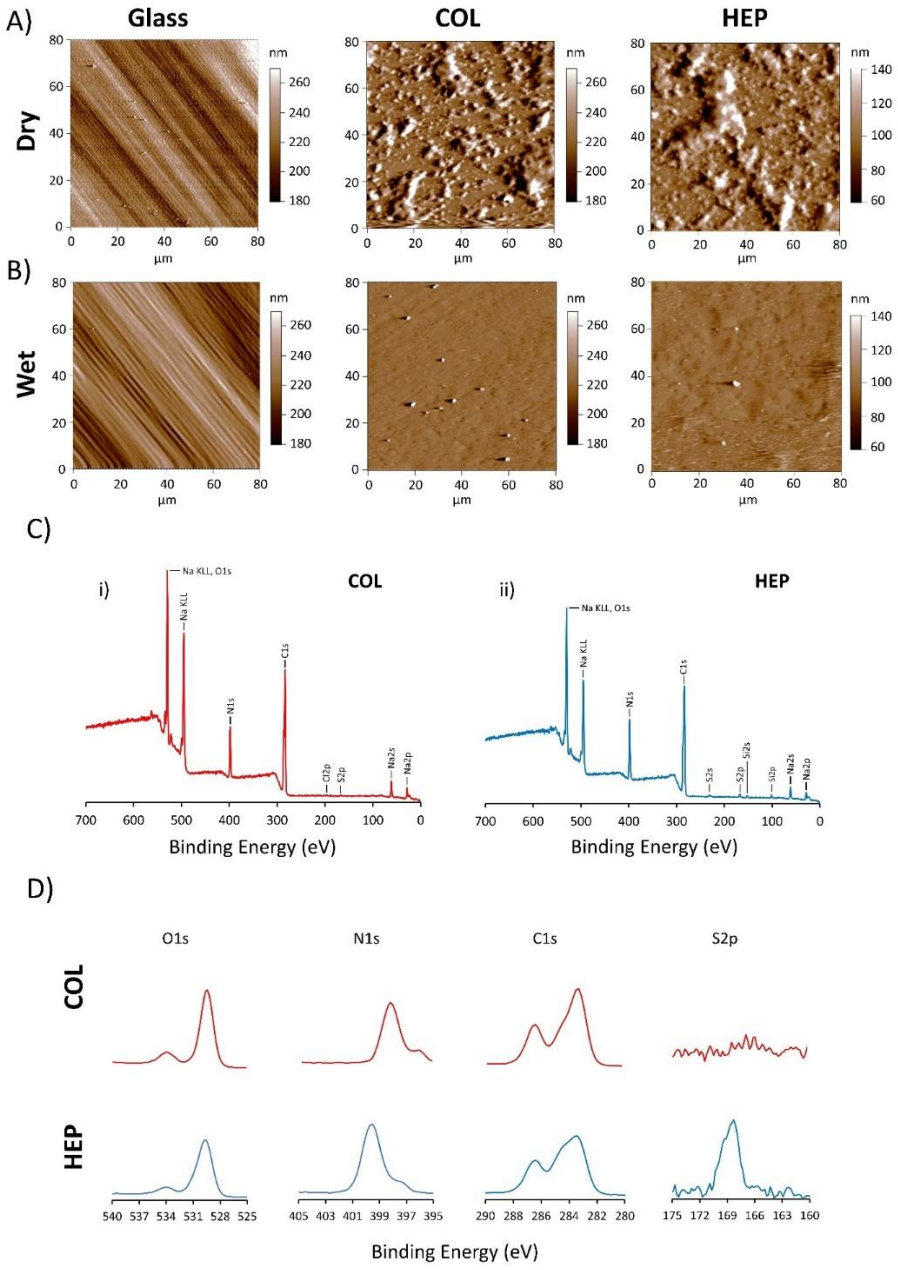

Figure 2-2. (A&B) Surface morphology as measured by AFM of uncoated glass, COL-ending, and HEP-ending multilayers on dry and wet conditions. Chemical properties of (HEP/COL) multilayers as measured by XPS broad spectra and high-resolution XPS. (C): XPS survey scan spectrum of COL-ending, and HEP-ending multilayers. (D): the corresponding specific spectrum of elemental COL-ending, and HEP-ending multilayers.

2.3.2. HMSC viability on (HEP/COL) multilayers

Fluorescence microscopy analysis of cells attached to the different surfaces after 72 h (Figure 2-3(A&A')) reveals that donor#1 and donor#2 hMSCs were well spread, showed a complete confluence and adopted a polygonal morphology on different surfaces. These results indicate that the conditions with (HEP/COL) multilayers with and without IFN-γ do not directly influence cellular phenotype via the organization of cytoskeleton.

The PrestoBlue reagent was used for measuring cell viability after 3 days of culturing cells. A cell density of 15000 cells/cm^2 was used in 96-well plates (working volume of 200 µL). hMSCs were seeded on TCP, COL-ending and HEP-ending multilayers with and without (50 ng/mL) IFN-γ supplemented in the cell culture medium. We selected a concentration of 50 ng/mL for soluble IFN-γ based on our previous study done by D. Castilla-Casadiego et al. [7] and H. Wobma et al. [113]. In the absence of the IFN-γ in culture medium, TCP surfaces were selected as the positive control, and its fluorescence intensity was normalized to 100%. All other conditions were assessed in relation to the positive control. Figure 2-3 (B) shows significant differences in the cell viability of donor#1 on COL-ending and HEP-ending multilayers without the IFN-γ compared to the control substrate ($p < 0.05$ and $p < 0.001$, respectively) after 72 h of incubation. However, donor#2 shows that cell viability is not significantly different for substrates containing (HEP/COL) multilayers compared to the control substrate (Figure 2-3 (B')). Also, Figure 2-3 (B) indicates that cell viability for donor#1 compared with the TCP surface has an increasing trend. In this regard, there is an approximately 24% increase in cell viability on COL-ending and about a 26% increase in cell viability on HEP-ending in absence of the IFN-γ in culture media. Similarly, donor#2 shows the same result (Figure 2-3 (B')). Therefore, it shows that the use of (HEP/ COL) multilayers can increase hMSCs viability. These results can indicate

that there is a synergistic action of (HEP/ COL) multilayers which leads to an increase in cell viability. These results are in line with the results shown in the next section using the real-time cell monitoring system. We observed and increase in cell adhesion and proliferation in the conditions where cells were cultured on (HEP/ COL) multilayers (Figure 2-3 (C & C').

In addition, regarding donor#1, despite following the increasing trend of cell viability compared to control substrate (TCP), the cell viability on HEP-ending multilayers with the IFN-γ is less than that of the HEP-ending multilayers without the IFN-γ. However, donor#2 shows that the surfaces with IFN-γ have a higher cell viability than the surfaces without IFN-γ. In particular, HEP-ending multilayers show the highest cell viability (Figure 2-3 (B')). Based on our previous study done by D. Castilla-Casadiego et al. [7], hMSCs showed an increase in their proliferation and protein expression when they were grown in multilayers of (HEP/COL) supplemented with IFN-γ. Moreover, Jingchun Du et al. [114] studied the effects of the IFN-γ on the antitumor activity of human amniotic fluid-derived mesenchymal stem cells and revealed that IFN-γ can enhance cell viability. The reason for the superior performance of heparin can be attributed to the fact that heparin has a large binding capacity for several proteins such as tumor necrosis factor-alpha (TNF-a), IFN-γ, and basic fibroblast growth factor (FGF-2), which can modulate cell adhesion and proliferation [115][116][117]. In fact, in our previous work by D. Castilla-Casadiego we observed an upregulation of FGF-2 expression when hMSCs were cultured on HEP-ending coatings [7]. Thus, (HEP/COL) multilayers even with and without the IFN-γ, have the ability to improve cell viability.

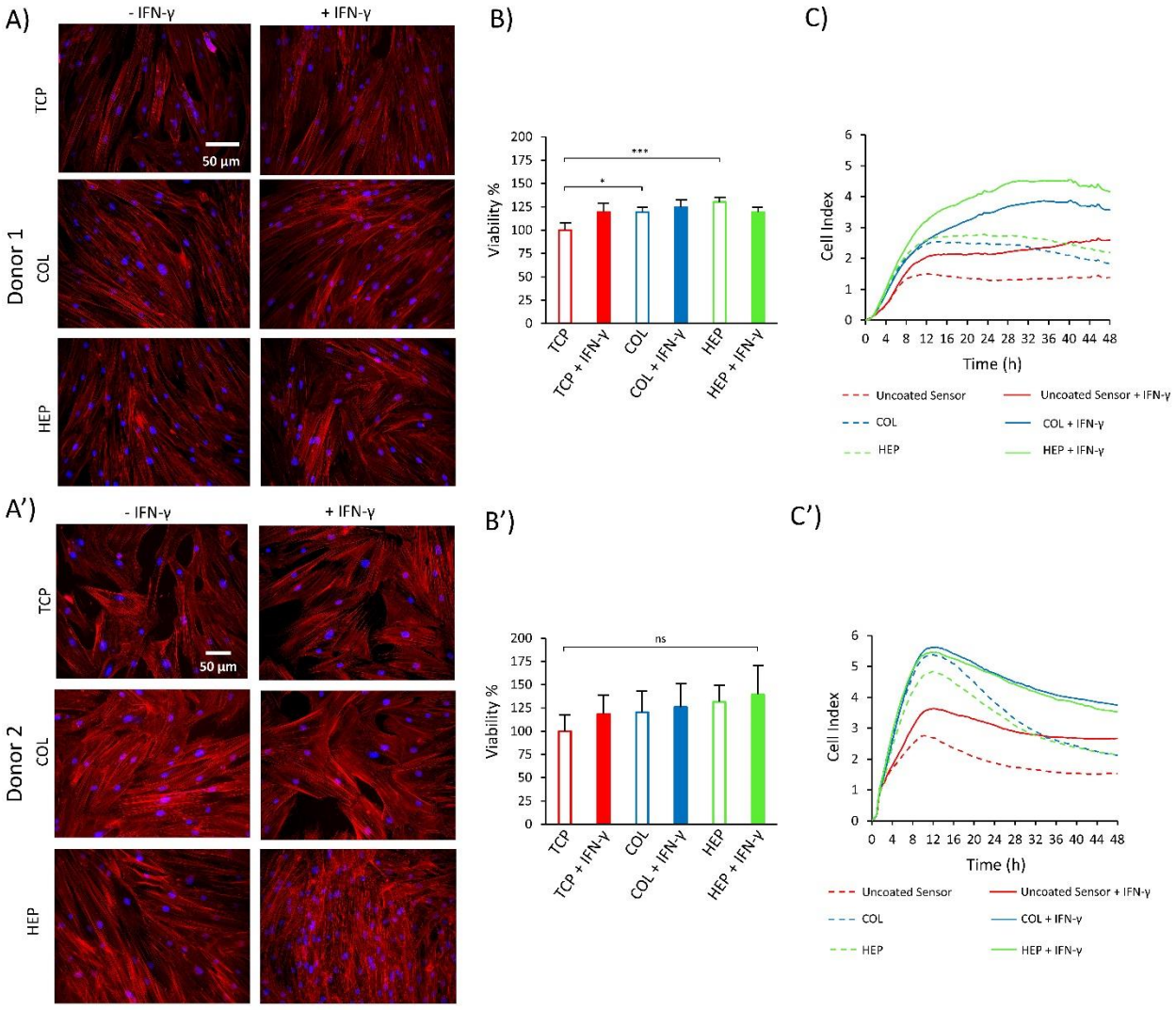

Figure 2-3. Fluorescence microscopy images of hMSCs nuclei and actin labeled with Hoechst and Actin Red, respectively, after 3 days of culture for donor#1 (A) and for donor#2 (A'). (B): PrestoBlue Viability assay for hMSCs cultured on TCP, COL-ending, and HEP-ending multilayers with and without IFN-γ for donor#1 (B) and for donor#2 (B'). Real-time monitoring of hMSCs grown on COL-ending, and HEP-ending multilayers during 48 hours of culture donor#1 (C) and for donor#2 (C'). Cell cultures were done on multilayers with and without IFN-γ and uncoated sensor was used as control. Data are presented as the mean ± standard deviation

of n = 4 samples. The p-values < 0.05 are represented by *, p-values < 0. 01 by **, p-values < 0. 001 by *** and p-values < 0.0001 by ****.

2.3.3. Real-time monitoring of cell behavior and proliferation

In this study, we cultured hMSCs at 25000 cells/cm^2 on COL-ending and HEP-ending multilayers to evaluate the real-time behavior of the cells during the first 48 hours of culture. The action of IFN-γ in the cell medium was also evaluated. As a control surface, hMSCs cultured on uncoated biosensors was evaluated. The Real-Time Cell Analyzer (RTCA) xCELLigence biosensor system was used, which allows cell proliferation and growth measurement. RTCA xCELLigence constantly measures the impedance difference caused by cells attached to microsensors present in culture plates (E-plates). The schematic of the xCELLigence instrument is shown in Figure 2-4. Impedance measurements are translated into a parameter known as the Cell Index (CI). CI is defined as the difference between the background electric resistance (measured using only cell medium) Z0, and the resistance measured at time t in the point i, Zi. The CI value is taken at a frequency of 15Ω. CI values are given by equation 1 [118].

$$CI = \frac{(Zi - Z0)}{15\Omega}$$

Equation 1

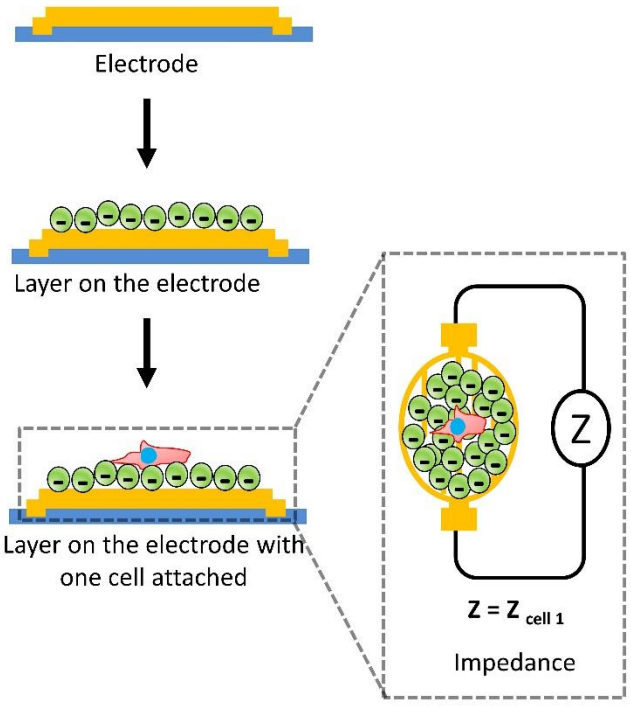

Figure 2-4. Schematic of layer deposition on Cell Analyzer (RTCA) xCELLigence instrument.

Therefore, the higher the CI, the greater the number of cells adhered to the bottom of the well [96].Figure 2-3 (C) shows the CI values as a function of the first 48 hours of culture for the 6 experimental conditions for donor#1.The results show a minor but continuous proliferation until 30 hours, followed by a period of stability where the decrease in the curves is very low. It is possible to identify a phase of CI increase that is attributed to the initial stage of cell adhesion. Donor#1 shows a slow cell adhesion stage in the evaluated period, reaching a maximum peak of around 30 hours. donor#2 shows a negative slope due to cell detachment that occurs after initial adhesion. This behavior is normal for most adherent cells. For donor#2, the cell adhesion stage reached a maximum at 12 hours (Figure 2-3 (C')). The addition of IFN-γ (at 50 ng/ml) led to a higher CI value for all conditions, with a significant increase on (HEP/COL) multilayers compared to the uncoated sensor. The presence of IFN-γ may increase hMSCs adhesion, which

is further amplified in the presence of (HEP/COL) multilayers [119]. This finding once again confirms that the multilayers improve the response of hMSCs to IFN-γ. In addition, the cultures on (HEP/COL) multilayers (without IFN-γ) also showed better results compared to the controls on uncoated surfaces.

2.3.4. IDO function

Indoleamine 2,3-dioxygenase (IDO) is a cytosolic heme protein that is vital for cell growth [120]. It can be determined by measuring the amino acid kynurenine in the culture supernatant after 6 days [121]. A cell density of 5000 cells/cm^2 was used in 24-well plates (working volume 600 µL). The ability of IFN-γ to induce IDO function in hMSCs was compared on TCP, COL-ending, and HEP-ending multilayers after 6 days post-stimulation with or without the IFN-γ supplemented in the cell culture medium. The level of IDO is determined by the amount of kynurenine measured (pg/cell), since IDO is known to be a catalyzer to convert L-tryptophan to kynurenine [120]. Results for IDO activity are summarized in Figure 2-5 (A), which shows that for donor#1, all surfaces with IFN-γ (including TCP, COL, and HEP) have two times higher levels of the IDO compared to surfaces without IFN-γ (60 pg/cell). Regarding the surfaces with IFN-γ, donor#2 shows significant differences for COL-ending and HEP-ending multilayers compared to the TCP (p-value< 0.05); in particular, the HEP-ending multilayers with IFN-γ have a higher level of the IDO expression. However, donor#1 shows the same level of the IDO expression for all surfaces containing the IFN-γ. These findings may indicate that IDO expression is related to donor behavior and different donors have different responses [122][123][124]. In addition, results for both donors show that using the (HEP/ COL) multilayers does not decrease the level of IDO activity in reference to the same amount of the IDO expression for the TCP and (HEP/ COL) multilayers without IFN-γ. These in vitro studies

indicate that the level of IDO depends on not only the different donor's response but also the presence of IFN-γ and the presence of the multilayers. These results are in line with the study done by Cifuentes et al. [94] that showed the IFN-γ is a key regulator of IDO activity. Moreover, pre-treatment of hMSCs with IFN-γ is frequently used to enhance the cells' immunomodulatory and differentiation activity by activating the expression of IDO [6][125]. However, we have demonstrated that the expression of IDO by hMSCs was higher when cultured on HEP-ending multilayers supplemented with IFN-γ for donor#2. These comply with our previous study, which indicated that HEP-ending multilayers supplemented with IFN-γ can promote the production of cells with pro-inflammatory and immunoregulatory capacities [7]. Therefore, using (HEP/COL) multilayers supplemented with IFN-γ in a culture medium can improve the cell's immunomodulatory activity which may vary donor-to-donor.

2.3.5. PBMC/hMSC co-culture

The ability of hMSCs to regulate the proliferation of peripheral blood mononuclear cells (PBMCs) was determined by direct-contact co-culture investigations of hMSCs and stimulated PBMCs. The investigation was conducted for TCP, COL-ending, and HEP-ending multilayers after 3 days post-stimulation with or without IFN-γ supplemented in the cell culture media. In addition, control conditions of PBMCs alone were evaluated on TCP, COL-ending, and HEP-ending with and without IFN-γ. PBMCs with Human T Activator CD3/CD28 Dynabeads (CDs) suspended in hMSCs attached to the surfaces are shown in Supplementary Figure S2.1. The proliferation of PBMCs alone (PBMCs seeded in the surface without hMSCs) was not negatively affected by multilayers with or without the IFN-γ supplemented in the cell culture medium, shows in Figure 2-5 (C&C')). This investigation indicates that the proliferation of PBMCs depends neither on the IFN-γ nor the multilayers. Regarding the proliferation of PBMCs co-

cultured with hMSCs from donor#1, the proliferation of PBMCs shows a slight reduction on TCP without IFN-γ compared to TCP with IFN-γ, which is not significant (Figure 2-5(C)). Also, hMSCs from donor #1 do not suppress PBMCs proliferation and has the same level of proliferation on TCP without IFN-γ, COL-ending, and HEP-ending multilayers with and without IFN-γ. HMSCs from donor #2 treated with IFN-γ are capable of reducing PBMCs proliferation, particularly when cultured on COL-ending multilayers. donor#2 shows a higher reduction on PBMCs proliferation when hMSCs cultured with IFN-γ on TCP than the without IFN-γ. In addition, donor#2 shows a higher reduction of PBMCs when cultured on HEP-ending. Also, the Division Index (total number of divisions / the number of cells at the start of culture) has the same trend as the number of PBMCs. Interestingly, peak fit analysis of PBMCs proliferation shows that hMSCs (both donor#1 & donor#2) allowed more generations of PBMCs to proliferate Figure 2-5 (E&E'). The results for donor#2 indicate that the presence of IFN-γ in COL-ending multilayers may increase hMSCs suppression capacity of PBMCs proliferation compared to surfaces without IFN-γ which also is related with the donor's behavior. In addition, HEP-ending multilayers may have the ability to suppress PBMCs proliferation for different donors without preactivated with IFN-γ.

Since IDO expression increases in the presence of IFN-γ in culture medium and the response is enhanced by the presence of the multilayers, we confirm that IFN-γ enhances the immunosuppressive potency of hMSCs cultured on HEP/COL coatings. Kwee et al. observed a similar behavior by studying the response to soluble IFN-γ of hMSCs cultured on collagen or fibrin biomaterials [126]. These findings for donor#2 are consistent with the results of [127] [128][126], which confirm the enhancement of hMSCs immunosuppressive potency due to the presence of IFN-γ on COL-ending multilayers. In addition, these results comply with our

previous study done by D. Castilla-Casadiego et al. [7] on cytokine expressions on the same multilayers, which suggested the (HEP/COL) multilayers are enhancing the activity of IFN-γ for producing pre-activated hMSCs with a higher immunosuppressive capability than those cultured in TCP with soluble IFN-γ. Therefore, we identified that (HEP/ COL) multilayers can promote not only immunoregulatory capacities but also the immunosuppression capacities. Kwee et al. suggests that the enhancement in immunosuppressive properties of hMSCs cultured on collagen biomaterials and exposed to soluble IFN-γ may be due to integrin engagement, however the response in strongly dependent on the donors [66]. There is a need to have a better understanding on different donor's behavior on (HEP/ COL) multilayers.

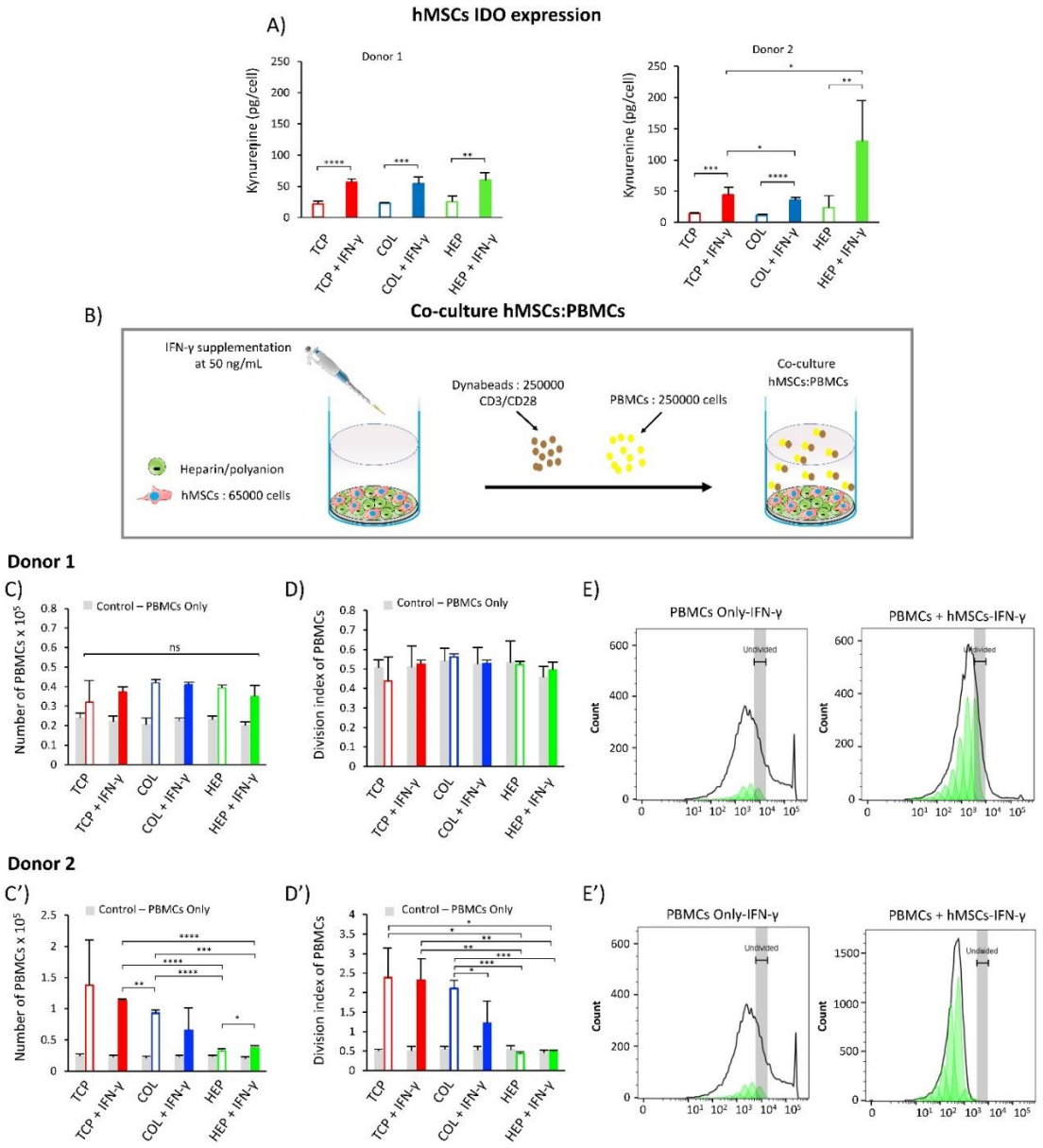

Figure 2-5. (A): Cells immunomodulatory potential by IDO activity for hMSCs from two different donors as cultured on TCP, COL-ending, and HEP-ending multilayers with and without IFN-γ. (B): direct-contact co-culture investigations of hMSCs and stimulated PBMCs. (C): The proliferation of PBMCs:hMSCs from donor#1. (D): The division index of PBMCs:hMSCs from donor#1 (E): peak fit analysis of PBMCs proliferation for donor#1. (C'): The proliferation of PBMCs:hMSCs from donor#2. (D'): The division index of PBMCs:hMSCs from donor#2 (E'): peak fit analysis of PBMCs proliferation for donor#2. The gray bars reflected the proliferation of

only PBMCs cultured in cells medium. Data are presented as the mean ± standard deviation of n = 4 samples. The p-values < 0.05 are represented by *, p-values < 0. 01 by **, p-values < 0. 001 by *** and p-values < 0.0001 by ****.

2.3.6. HMSC differentiation

After 6 days culture, the ability of hMSCs to differentiate into osteogenic and adipogenic lineages cells was induced by supplementing the growth media with differentiation media to confirm the multipotentiality of hMSCs after IFN-γ exposure and culture on (HEP/COL) multilayers. After about one week of incubation, cell functions associated with osteoblast differentiation (ALP activity, calcium deposition) and adipogenic differentiation were evaluated. To maintain the consistency of all experimental design, we seeded the cells with the regular expansion medium for six days. After that we added the differentiation medium for 7-10 days. Mineralization was also characterized from microscope images. Cell morphologies for long-term culture in normal, osteogenic, and adipogenic medium were evaluated on TCP, COL-ending, and HEP-ending multilayers with and without IFN-γ. Notably, in Figure 2-6 (A&B), treatment with IFN-γ had no inhibitory effect on both the osteogenic and adipogenic differentiation of hMSCs. There are large areas visible with red (Alizarin Red staining) and purple (Oil Red staining), indicating the formation of the calcified regions and adipocyte-like cells, respectively.
No staining was observed on cells cultured in regular expansion medium, as shown in Supplementary Figure S2.2&2.3. Control cells keep their polygonal morphology, which was followed by the loss of contact inhibition to multilayer growth. Figure 2-6 (A) shows that cells on TCP expressed only weak staining. However, hMSCs cultured on COL-ending and HEP-ending multilayers showed an increase in the size of calcium deposits formed by the clustering of cells due to the strong staining with Alizarin red, which indicates osteogenic differentiation of

cells. The same results were found for donor#2, as shown in Figure 2-6 (A'). Increasing the size of red color mineral nodules is a typical feature during osteogenic differentiation of hMSCs found in many other studies [129]. ALP is an enzyme present in bone-related cells and is considered key to mineralization [130]. Its activity is related to the level of inorganic phosphate, a component of the bone mineral phase [131]. Therefore, ALP activity has been considered as an early indicator of osteoblast differentiation. Results for ALP activity are summarized in Figure 2-6 (C&C').

Regarding donor#1, multilayers showed enhanced intracellular levels of ALP upon stimulation with IFN-γ as compared to TCP. Also, the TCP, COL-ending, and HEP-ending multilayer surfaces with IFN-γ have higher ALP activity than the surfaces without IFN-γ. In addition, Figure 2-6 (C)**.** shows that HEP-ending multilayers have a slightly better cell osteogenic differentiation than COL-ending multilayers, particularly with IFN-γ in culture medium. Similarly, donor#2 shows the same result Figure 2-6 (C'). Sabino et al. [132] suggested that this can be attributed to the fact that heparin has the ability to prompt osteogenic differentiation of hMSCs. These in vitro studies indicate that IFN-γ can improve the intercellular level of ALP activity. Also, a study done by C. Lamoury et al. indicated that IFN-γ influences the osteocytic differentiation of both mouse and human MSCs [6]. These findings show that the differentiation of hMSCs treatment with IFN-γ need more studies.

When cells were incubated in the basal adipogenic differentiation medium for seven days, the hMSCs changed from long spindle-shaped to flattened round, or polygonal cells Figure 2-6 (B&B'). The undifferentiated hMSCs controls (cultured in hMSCs growth medium) displayed no staining Figure S2.2&2.3. However, cells show good differentiation on TCP, COL-ending and

HEP-ending multilayers not only without IFN-γ but also with IFN-γ. These can indicate that IFN-γ does not suppress cells differentiation.

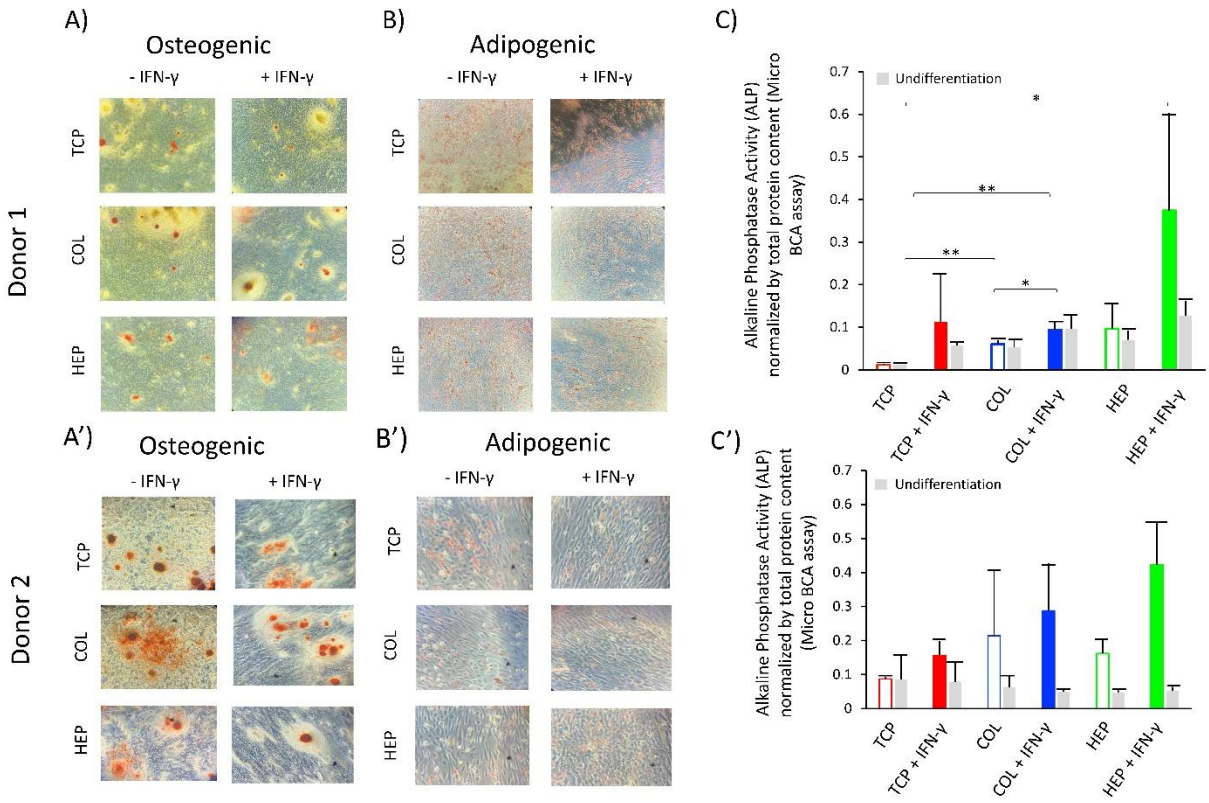

Figure 2-6. hMSCs differentiation. (A): Osteogenic differentiations were stained by Alizarin Red for donor#1. (B): Adipogenic differentiation were stained by Oil Red for donor#1. (C): Alkaline phosphatase (ALP) assays were performed after of induced osteogenesis on TCP, COL-ending, and HEP-ending multilayers donor#1. (A'): Osteogenic differentiations were stained by Alizarin Red for donor#2. (B'): Adipogenic differentiation were stained by Oil Red for donor#2. (C'): Alkaline phosphatase (ALP) assays were performed after of induced osteogenesis on TCP, COL-ending, and HEP-ending multilayers donor#2. Data are presented as the mean ± standard deviation of n = 4 samples. The p-values < 0.05 are represented by *, p-values < 0. 01 by **, p-values < 0. 001 by *** and p-values < 0.0001 by ****.

2.3.7. Immunophenotype assay

For the differentiation of hMSCs, three differentially expressed CD markers were selected for confirmation by flow cytometry. Expression of CD10, CD92, and CD105 in hMSCs from two individual donors on TCP, COL-ending, and HEP-ending with and without IFN-γ was analyzed. The study done by C. Granéli et al. suggested that CD10 and CD 92 are surface markers of the osteogenic and adipogenic differentiation [133]. In addition, the expression of the hMSCs-associated CD marker, CD105, was analyzed to evaluate changes in the hMSCs phenotype of the cells during the differentiation process. The expression of CD10 and CD92 were chosen to evaluate the osteogenic and adipogenic differentiation. The median fluorescence intensity MFI ratios (differentiated/undifferentiated) hMSCs for donor#1 and donor#2 are presented in Figure 2-7&Figure 2-8.

Regarding donor#1 osteogenic and adipogenic differentiation, the MFI of differentiated cells for CD10 is higher than that of the undifferentiated cells for all surfaces (containing TCP, COL-ending, and HEP-ending multilayers surface with and without IFN-γ) Figure 2-7. However, the MFI of differentiated cells for CD92 is slightly less than that of the undifferentiated cells (except for TCP with IFN-γ and HEP-ending multilayers without IFN-γ) Figure 2-7. Moreover, the expression of hMSCs marker CD105 was higher in the undifferentiated cells at all surfaces, which means that cells do not differentiate. Regarding donor#2, the same trend for CD10 and CD105 is observed, although the MFI of differentiated cells for CD92 was significantly increased compared with undifferentiated cells. Histograms of CD105, CD10, and CD92 are shown in Figure 2-8. CD10 is a cell surface that has been described as a surface marker present on hMSCs isolated from both bone marrow and adipose tissue [134][135][136]. As a result, an increase in the expression of CD10 shows that more cells differentiate between the osteogenic

and adipogenic cells. Also, CD92 is increased in adipogenic hMSCs. Consequently, CD10 and CD92 displayed a higher expression in both osteogenically and adipogenically differentiated hMSCs on all surfaces (TCP, COL-ending, and HEP-ending multilayers surface with and without IFN-γ) compared with an undifferentiated control. These results can indicate that both (HEP/COL) multilayers and IFN-γ do not affect the differentiation and phenotype of the cells.

Osteogenic

A)

MFI Ratio (Osteogenic differentiated /undifferentiated)						
	Conditions	- IFN-γ			+ IFN-γ	
CD Markers	TCP	COL	HEP	TCP	COL	HEP
CD 105	0.56	0.54	0.62	0.4	0.52	0.41
CD 10	1.76	1.95	2.18	1.04	2.03	0.95
CD 92	0.82	1	0.95	0.69	1.31	0.86

B)

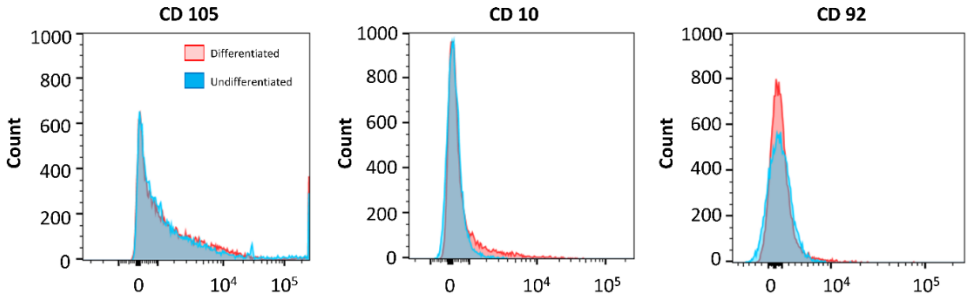

Adipogenic

A)

MFI Ratio (Adipogenic differentiated /undifferentiated)						
	Conditions	- IFN-γ			+ IFN-γ	
CD Markers	TCP	COL	HEP	TCP	COL	HEP
CD 105	0.72	0.54	0.007	0.16	0.58	0.4
CD 10	1.47	1.34	0.38	0.11	1.9	1.27
CD 92	0.88	1.27	0.28	0.11	1.83	1.09

B)

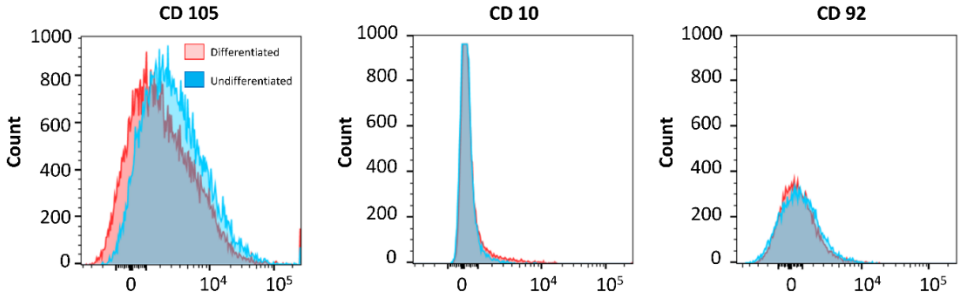

Figure 2-7. Flow cytometry donor#1 (A): MFI ratios between osteogenically differentiated and undifferentiated hMSCs donor#1. (B): Histograms of CD 105, CD10 and CD92. Adipogenic, (A): MFI ratios between adipogenically differentiated and undifferentiated hMSCs donor#1. (B): Histograms of CD 105, CD10, and CD92.

Osteogenic

A)

MFI Ratio (Osteogenic differentiated /undifferentiated)						
	Conditions	- IFN-γ			+ IFN-γ	
CD Markers		TCP	COL	HEP	TCP	COL	HEP
	CD 105	1.08	0.71	3.3	1.4	1.105	1.25
	CD 10	8.89	12.06	3.76	8.54	14.05	3.42
	CD 92	21.4	3.01	1.95	15.12	17.88	13.9

B)

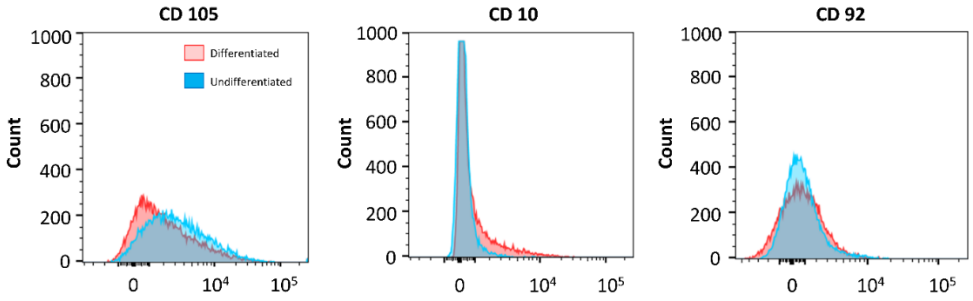

Adipogenic

A)

MFI Ratio (Adipogenic differentiated /undifferentiated)						
	Conditions	- IFN-γ			+ IFN-γ	
CD Markers		TCP	COL	HEP	TCP	COL	HEP
	CD 105	0.48	0.44	1.61	0.98	0.7	0.74
	CD 10	6.85	7.81	2.75	7.66	9.42	2.49
	CD 92	15.35	3.01	2.003	11.79	13.09	14.48

B)

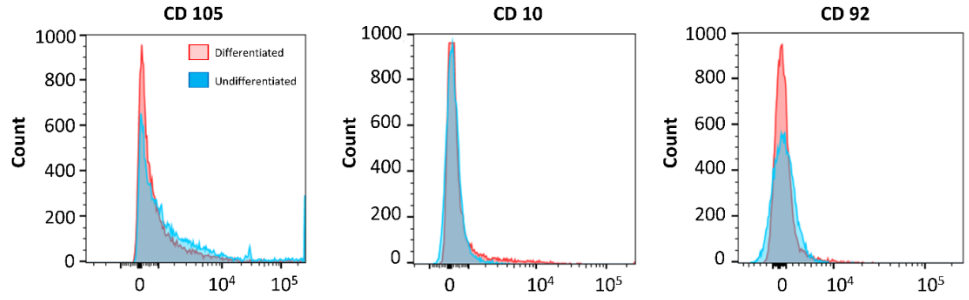

Figure 2-8. Flow cytometry donor#2 (A): MFI ratios between osteogenically differentiated and undifferentiated hMSCs donor#2. (B): Histograms of CD 105, CD10 and CD92. Adipogenic, (A): MFI ratios between adipogenically differentiated and undifferentiated hMSCs donor#2. (B): Histograms of CD 105, CD10, and CD92.

2.4. Conclusions

This study demonstrates that polyelectrolyte layers made of heparin and collagen were successfully built up using the layer-by-layer assembly method. QCM-D results demonstrate that the (HEP/COL) multilayers are soft and viscoelastic, and that IFN-g adsorption depends on the composition of the final layer. Also, (HEP/ COL) multilayers present good stability in presence of the IFN-γ. We observed that (HEP/COL) multilayers did not negatively influence the viability, adhesion, proliferation, and differentiation of hMSCs in the presence of soluble IFN-γ. Also, multilayers may lead to improve the anti-proliferation effect of IFN-γ on hMSCs. When CD3/CD28-activated peripheral blood mononuclear cells are co-cultured with hMSCs cultured on (HEP/COL) multilayers, a reduction in PBMC proliferation is observed compared to culture on TCP . In compliance with the present study, other studies demonstrated that the immunosuppression capacity of hMSCs on biomaterials between different donors are corelated to the IDO activity [126]. Our study shows that HEP-ending multilayers was the surface that offered a greater stimulation on the IDO expression, and PBMCs suppression. Though different responses were observed for the two donors evaluated. This study shows that (HEP/COL) multilayers can modulate hMSCs response to soluble factors, improving the immunosuppressive potential of hMSCs which may lead to more efficient cell manufacturing without additional expenses in the manufacturing process and produce a better-quality cell product. (HEP/COL) multilayers can be applied to any surface including bioreactors or microcarriers which can be used to culture hMSCs meant for cell-based therapies aimed at treating several immune diseases.

■ ASSOCIATED CONTENT

Supporting Information

Sample information of hMSCs control cells inducing by normal expansion medium, PBMCs with Human T Activator CD3/CD28 Dynabeads (CDs) suspended in hMSCs attached to the surfaces.

■ AUTHOR INFORMATION

Corresponding Author

*E-mail: jlalmodo@uark.edu

ORCID

Jorge Almodovar: 0000-0002-1151-3878

Present Address

§M.H., D.A.C.-C., J.A.: Ralph E. Martin Department of Chemical Engineering, University of Arkansas, 3202 Bell Engineering Center, Fayetteville, AR 72701, Phone: +1 479-575-3924, Fax: +1 479-575-7926.

Notes

The authors declare no competing financial interest.

2.5. Acknowledgement

This work was financially supported in part by the National Science Foundation under grant no. 2051582, by the Arkansas Bioscience Institute, and by the "Programa de Apoyo Institucional Para la Formación en Estudios de Posgrados en Maestrías y Doctorados de La Universidad del Atlántico, Colombia" by providing DCC a scholarship. The authors greatly appreciate the Arkansas Nano & Biomaterials Characterization Facility for help with the use of the XPS. Additionally, the authors thank Integra Life Sciences for their generous donation of lyophilized Type I Collagen. The authors greatly appreciate Dr. Greenlee and Sergio Ivan Perez

Bakovic from the University of Arkansas for equipment access and help during quartz crystal microbalance (QCM) measurements. The authors declare no financial interest.

AUTHOR CONTRIBUTIONS

Mahsa Haseli: The LbL multilayers, Cell viability, Proliferation, Differentiation, Flow cytometry, Co-Culture, QCM experiments, Data analyses, Data curation and writing-original draft preparation.

David A. Castilla-Casadiego: AFM, XPS, Co-Culture, Cell viability, Figures preparation, data curation, writing-original draft preparation, writing-reviewing and editing resources

Luis Pinzon-Herrera: xCELLigence RTCA, Fluorescence microscopy images, Data analyses and data curation.

Alexander Hillsley, Katherine A. Miranda-Muñoz and Srikanth Sivaraman: Data curation.

Adrianne M. Rosales and Raj Rghavendra-Rao: Writing-reviewing and editing resources.

Jorge Almodovar: Conceptualization, supervision, writing-reviewing and editing, resources, funding acquisition, project administration.

2.6. References

[1] A. Khademhosseini, Y. Du, B. Rajalingam, J. P. Vacanti, and R. S. Langer, "Microscale technologies for tissue engineering," *Adv. Tissue Eng.*, vol. 103, no. 8, pp. 349–369, 2008, doi: 10.1142/9781848161832_0017.

[2] T. Cordonnier, J. Sohier, P. Rosset, and P. Layrolle, "Biomimetic materials for bone tissue engineering - State of the art and future trends," *Adv. Eng. Mater.*, vol. 13, no. 5, pp. 135–150, 2011, doi: 10.1002/adem.201080098.

[3] A. Uccelli, L. Moretta, and V. Pistoia, "Mesenchymal stem cells in health and disease," *Nat. Rev. Immunol.*, vol. 8, no. 9, pp. 726–736, 2008, doi: 10.1038/nri2395.

[4] F. Gao *et al.*, "Mesenchymal stem cells and immunomodulation: Current status and future prospects," *Cell Death Dis.*, vol. 7, no. 1, 2016, doi: 10.1038/cddis.2015.327.

[5] M. W. Klinker, R. A. Marklein, J. L. Lo Surdo, C. H. Wei, and S. R. Bauer, "Morphological features of IFN-γ-stimulated mesenchymal stromal cells predict overall immunosuppressive capacity," *Proc. Natl. Acad. Sci. U. S. A.*, vol. 114, no. 13, pp.

E2598–E2607, 2017, doi: 10.1073/pnas.1617933114.

[6] J. Croitoru-Lamoury *et al.*, “Interferon-γ regulates the proliferation and differentiation of mesenchymal stem cells via activation of indoleamine 2,3 dioxygenase (IDO),” *PLoS One*, vol. 6, no. 2, 2011, doi: 10.1371/journal.pone.0014698.

[7] D. A. Castilla-Casadiego, J. R. García, A. J. García, and J. Almodovar, “Heparin/Collagen Coatings Improve Human Mesenchymal Stromal Cell Response to Interferon Gamma,” *ACS Biomater. Sci. Eng.*, vol. 5, no. 6, pp. 2793–2803, 2019, doi: 10.1021/acsbiomaterials.9b00008.

[8] F. M. Watt and W. T. S. Huck, “Role of the extracellular matrix in regulating stem cell fate,” *Nat. Rev. Mol. Cell Biol.*, vol. 14, no. 8, pp. 467–473, 2013, doi: 10.1038/nrm3620.

[9] R. O. Hynes, “The extracellular matrix: not just pretty fibrils,” *Science (80-.).*, vol. 326, no. 5957, pp. 1216–1219, 2009, doi: 10.1126/science.1176009.

[10] H. Ozcelik *et al.*, “Cell Microenvironment Engineering and Monitoring for Tissue Engineering and Regenerative Medicine : The Citation Accessed Citable Link Cell Microenvironment Engineering and Monitoring for Tissue Engineering and Regenerative Medicine : The Recent Advances,” *Biomed Res. Int.*, vol. 2014, no. i, pp. 1–18, 2014.

[11] J. Cuerquis *et al.*, “Human mesenchymal stromal cells transiently increase cytokine production by activated T cells before suppressing T-cell proliferation: Effect of interferon-γ and tumor necrosis factor-α stimulation,” *Cytotherapy*, vol. 16, no. 2, pp. 191–202, 2014, doi: 10.1016/j.jcyt.2013.11.008.

[12] T. J. Kean, P. Lin, A. I. Caplan, and J. E. Dennis, “MSCs: Delivery routes and engraftment, cell-targeting strategies, and immune modulation,” *Stem Cells Int.*, vol. 2013, 2013, doi: 10.1155/2013/732742.

[13] H. Lortat-Jacob, “The molecular basis and functional implications of chemokine interactions with heparan sulphate,” *Curr. Opin. Struct. Biol.*, vol. 19, no. 5, pp. 543–548, 2009, doi: 10.1016/j.sbi.2009.09.003.

[14] M. F. Brizzi, G. Tarone, and P. Defilippi, “Extracellular matrix, integrins, and growth factors as tailors of the stem cell niche,” *Curr. Opin. Cell Biol.*, vol. 24, no. 5, pp. 645–651, 2012, doi: 10.1016/j.ceb.2012.07.001.

[15] E. Fuchs, T. Tumbar, and G. Guasch, “Socializing with the neighbors: Stem cells and their niche,” *Cell*, vol. 116, no. 6, pp. 769–778, 2004, doi: 10.1016/S0092-8674(04)00255-7.

[16] K. A. Moore and I. R. Lemischka, “Stem cells and their niches,” *Science (80-.).*, vol. 311, no. 5769, pp. 1880–1885, 2006, doi: 10.1126/science.1110542.

[17] T. A. Wilgus, “Growth Factor–Extracellular Matrix Interactions Regulate Wound Repair,” *Adv. Wound Care*, vol. 1, no. 6, pp. 249–254, 2012, doi: 10.1089/wound.2011.0344.

[18] O. Saksela and M. Laiho, “Growth factors and the extracellular matrix,” *Duodecim.*, vol. 106, no. 3, pp. 297–306, 1990, doi: 10.1096/fasebj.11.1.9034166.

[19] M. Khan, “Human mesenchymal stem cells,” *Hum. Mesenchymal Stem Cells*, vol. 1416,

no. Cmc, pp. 1–127, 2021, doi: 10.1016/s0141-0229(97)83511-9.

[20] V. Poltavets, M. Kochetkova, S. M. Pitson, and M. S. Samuel, “The role of the extracellular matrix and its molecular and cellular regulators in cancer cell plasticity,” *Front. Oncol.*, vol. 8, no. OCT, pp. 1–19, 2018, doi: 10.3389/fonc.2018.00431.

[21] A. R. Shelke Roscoe, J. A. , Morrow, G. R. , Colman, L. K. , Banerjee, T. K. , & Kirshner, J. J., “Paracrine and autocrine signals induce and maintain mesenchymal and stem cell states in the breast,” *Bone*, vol. 23, no. 1, pp. 1–7, 2008, doi: 10.1016/j.cell.2011.04.029.Paracrine.

[22] P. Zandstra, E. Jervis, D. Kilburn, C. Eaves, and J. Pirel, “Concentration-dependent internalization of a cytokine/cytokine receptor complex in human hematopoietic cells,” *Exp. Hematol.*, vol. 26, no. 8, p. 720, 1998, doi: 10.1002/(sici)1097-0290(19990520)63:4<493::aid-bit13>3.3.co;2-s.

[23] X. Zhao, Q. Li, Z. Guo, and Z. Li, “Constructing a cell microenvironment with biomaterial scaffolds for stem cell therapy,” *Stem Cell Res. Ther.*, vol. 12, no. 1, pp. 1–13, 2021, doi: 10.1186/s13287-021-02650-w.

[24] A. Kumari, S. K. Yadav, and S. C. Yadav, “Biodegradable polymeric nanoparticles based drug delivery systems,” *Colloids Surfaces B Biointerfaces*, vol. 75, no. 1, pp. 1–18, 2010, doi: 10.1016/j.colsurfb.2009.09.001.

[25] S. Martino, F. D’Angelo, I. Armentano, J. M. Kenny, and A. Orlacchio, “Stem cell-biomaterial interactions for regenerative medicine,” *Biotechnol. Adv.*, vol. 30, no. 1, pp. 338–351, 2012, doi: 10.1016/j.biotechadv.2011.06.015.

[26] X. Zhao, K. Cui, and Z. Li, “The role of biomaterials in stem cell-based regenerative medicine,” *Future Med. Chem.*, vol. 11, no. 14, pp. 1779–1792, 2019, doi: 10.4155/fmc-2018-0347.

[27] E. For, “Enabling Technologies for Cell-Based Clinical Translation E NABLING T ECHNOLOGIES FOR C ELL -B ASED C LINICAL T RANSLATION Increased Survival and Function of Mesenchymal Stem Cell Spheroids Entrapped in Instructive Alginate Hydrogels,” pp. 1–9, 2016.

[28] M. J. Landry, F. G. Rollet, T. E. Kennedy, and C. J. Barrett, “Layers and Multilayers of Self-Assembled Polymers: Tunable Engineered Extracellular Matrix Coatings for Neural Cell Growth,” *Langmuir*, vol. 34, no. 30, pp. 8709–8730, 2018, doi: 10.1021/acs.langmuir.7b04108.

[29] V. Gribova, R. Auzely-Velty, and C. Picart, “Polyelectrolyte multilayer assemblies on materials surfaces: From cell adhesion to tissue engineering,” *Chem. Mater.*, vol. 24, no. 5, pp. 854–869, 2012, doi: 10.1021/cm2032459.

[30] C. Picart *et al.*, “Primary cell adhesion on RGD-functionalized and covalently crosslinked thin polyelectrolyte multilayer films,” *Adv. Funct. Mater.*, vol. 15, no. 1, pp. 83–94, 2005, doi: 10.1002/adfm.200400106.

[31] C. Picart, “Polyelectrolyte Multilayer Films: From Physico-Chemical Properties to the Control of Cellular Processes,” *Curr. Med. Chem.*, vol. 15, no. 7, pp. 685–697, 2008, doi:

10.2174/092986708783885219.

[32] P. Gentile, I. Carmagnola, T. Nardo, and V. Chiono, “Layer-by-layer assembly for biomedical applications in the last decade,” *Nanotechnology*, vol. 26, no. 42, p. 422001, 2015, doi: 10.1088/0957-4484/26/42/422001.

[33] D. A. Castilla-Casadiego *et al.*, “Methods for the Assembly and Characterization of Polyelectrolyte Multilayers as Microenvironments to Modulate Human Mesenchymal Stromal Cell Response,” *ACS Biomater. Sci. Eng.*, vol. 6, no. 12, pp. 6626–6651, 2020, doi: 10.1021/acsbiomaterials.0c01397.

[34] O. Guillaume-Gentil, O. V. Semenov, A. H. Zisch, R. Zimmermann, J. Vörös, and M. Ehrbar, “PH-controlled recovery of placenta-derived mesenchymal stem cell sheets,” *Biomaterials*, vol. 32, no. 19, pp. 4376–4384, 2011, doi: 10.1016/j.biomaterials.2011.02.058.

[35] J. Chen, C. Chen, Z. Chen, J. Chen, Q. Li, and N. Huang, “Collagen/heparin coating on titanium surface improves the biocompatibility of titanium applied as a blood-contacting biomaterial,” *J. Biomed. Mater. Res. - Part A*, vol. 95 A, no. 2, pp. 341–349, 2010, doi: 10.1002/jbm.a.32847.

[36] A. Tchobanian, H. Van Oosterwyck, and P. Fardim, “Polysaccharides for tissue engineering: Current landscape and future prospects,” *Carbohydr. Polym.*, vol. 205, pp. 601–625, 2019, doi: 10.1016/j.carbpol.2018.10.039.

[37] B. W. Kim, *Clinical regenerative medicine in urology*. 2017.

[38] A. K. Nayak, S. A. Ahmed, M. Tabish, and M. S. Hasnain, *Natural polysaccharides in tissue engineering applications*. Elsevier Inc., 2019.

[39] M. S. Douglas, D. A. Rix, J. H. Dark, D. Talbot, and J. A. Kirby, “Examination of the mechanism by which heparin antagonizes activation of a model endothelium by interferon-gamma (IPN-γ),” *Clin. Exp. Immunol.*, vol. 107, no. 3, pp. 578–584, 1997, doi: 10.1046/j.1365-2249.1997.3141206.x.

[40] S. Sarrazin, D. Bonnaffé, A. Lubineau, and H. Lortat-Jacob, “Heparan sulfate mimicry: A synthetic glycoconjugate that recognizes the heparin domain of interferon-γ inhibits the cytokine activity,” *J. Biol. Chem.*, vol. 280, no. 45, pp. 37558–37564, 2005, doi: 10.1074/jbc.M507729200.

[41] S. J. Paluck, T. H. Nguyen, and H. D. Maynard, “Heparin-Mimicking Polymers: Synthesis and Biological Applications,” *Biomacromolecules*, vol. 17, no. 11, pp. 3417–3440, 2016, doi: 10.1021/acs.biomac.6b01147.

[42] J. Dinoro *et al.*, “Sulfated polysaccharide-based scaffolds for orthopaedic tissue engineering,” *Biomaterials*, vol. 214, no. December 2018, p. 119214, 2019, doi: 10.1016/j.biomaterials.2019.05.025.

[43] H. Lortat-Jacob, F. Baltzer, and J. A. Grimaud, “Heparin decreases the blood clearance of interferon-γ and increases its activity by limiting the processing of its carboxyl-terminal sequence,” *J. Biol. Chem.*, vol. 271, no. 27, pp. 16139–16143, 1996, doi: 10.1074/jbc.271.27.16139.

[44] D. L. Kusindarta and H. Wihadmadyatami, “The Role of Extracellular Matrix in Tissue Regeneration,” *Tissue Regen.*, 2018, doi: 10.5772/intechopen.75728.

[45] G. A. Di Lullo, S. M. Sweeney, J. Körkkö, L. Ala-Kokko, and J. D. San Antonio, “Mapping the ligand-binding sites and disease-associated mutations on the most abundant protein in the human, type I collagen,” *J. Biol. Chem.*, vol. 277, no. 6, pp. 4223–4231, 2002, doi: 10.1074/jbc.M110709200.

[46] S. C. Shukla, A. Singh, A. K. Pandey, and A. Mishra, “Review on production and medical applications of e-polylysine,” *Biochem. Eng. J.*, vol. 65, pp. 70–81, 2012, doi: 10.1016/j.bej.2012.04.001.

[47] O. F. Blood and C. T. O. Connective, “PHYSIOLOGICAL REVIEWS,” vol. IV, no. 4, pp. 533–563, 1924.

[48] A. I. Caplan and The, “Mesenchymal Stem Cells,” *Chem. Phys. Lett.*, vol. 7, no. 6, pp. 581–582, 1970, doi: 10.1016/0009-2614(70)87009-9.

[49] R. K. C. A. K. S. L. A. J. FRIEDENSTEIN, “THE DEVELOPMENT OF FIBROBLAST COLONIES IN MONOLAYER CULTURES OF GUINEA-PIG BONE MARROW AND SPLEEN CELLS,” *Development*, pp. 1–6, 1897.

[50] A. J. Katz, A. Tholpady, S. S. Tholpady, H. Shang, and R. C. Ogle, “Cell Surface and Transcriptional Characterization of Human Adipose-Derived Adherent Stromal (hADAS) Cells,” *Stem Cells*, vol. 23, no. 3, pp. 412–423, 2005, doi: 10.1634/stemcells.2004-0021.

[51] B. M. Seo *et al.*, “Investigation of multipotent postnatal stem cells from human periodontal ligament,” *Lancet*, vol. 364, no. 9429, pp. 149–155, 2004, doi: 10.1016/S0140-6736(04)16627-0.

[52] X. Meng *et al.*, “Endometrial regenerative cells: A novel stem cell population,” *J. Transl. Med.*, vol. 5, pp. 1–10, 2007, doi: 10.1186/1479-5876-5-57.

[53] S. Patki, S. Kadam, V. Chandra, and R. Bhonde, “Human breast milk is a rich source of multipotent mesenchymal stem cells,” *Hum. Cell*, vol. 23, no. 2, pp. 35–40, 2010, doi: 10.1111/j.1749-0774.2010.00083.x.

[54] P. S. in ’t Anker *et al.*, “Isolation of Mesenchymal Stem Cells of Fetal or Maternal Origin from Human Placenta,” *Stem Cells*, vol. 22, no. 7, pp. 1338–1345, 2004, doi: 10.1634/stemcells.2004-0058.

[55] P. S. In ’t Anker *et al.*, “Amniotic fluid as a novel source of mesenchymal stem cells for therapeutic transplantation [1],” *Blood*, vol. 102, no. 4, pp. 1548–1549, 2003, doi: 10.1182/blood-2003-04-1291.

[56] B. M. Deasy *et al.*, “High harvest yield, high expansion, and phenotype stability of CD146 mesenchymal stromal cells from whole primitive human umbilical cord tissue,” *J. Biomed. Biotechnol.*, vol. 2009, 2009, doi: 10.1155/2009/789526.

[57] H. Wang *et al.*, “Mesenchymal Stem Cells in the Wharton’s Jelly of the Human Umbilical Cord,” *Stem Cells*, vol. 22, no. 7, pp. 1330–1337, 2004, doi: 10.1634/stemcells.2004-0013.

[58] M. Dominici *et al.*, “Minimal criteria for defining multipotent mesenchymal stromal cells. The International Society for Cellular Therapy position statement,” *Cytotherapy*, vol. 8, no. 4, pp. 315–317, 2006, doi: 10.1080/14653240600855905.

[59] T. L. Ramos *et al.*, “MSC surface markers (CD44, CD73, and CD90) can identify human MSC-derived extracellular vesicles by conventional flow cytometry,” *Cell Commun. Signal.*, vol. 14, no. 1, pp. 1–14, 2016, doi: 10.1186/s12964-015-0124-8.

[60] G. Brooke *et al.*, “Therapeutic applications of mesenchymal stromal cells,” *Semin. Cell Dev. Biol.*, vol. 18, no. 6, pp. 846–858, 2007, doi: 10.1016/j.semcdb.2007.09.012.

[61] M. F. Pittenger, D. E. Discher, B. M. Péault, D. G. Phinney, J. M. Hare, and A. I. Caplan, “Mesenchymal stem cell perspective: cell biology to clinical progress,” *npj Regen. Med.*, vol. 4, no. 1, 2019, doi: 10.1038/s41536-019-0083-6.

[62] E. H. Javazon, K. J. Beggs, and A. W. Flake, “Парадоксы Пассажирования.Pdf,” vol. 32, pp. 414–425, 2004.

[63] Y. P. Rubtsov, Y. G. Suzdaltseva, K. V. Goryunov, N. I. Kalinina, V. Y. Sysoeva, and V. A. Tkachuk, “Regulation of Immunity via Multipotent Mesenchymal Stromal Cells,” *Acta Naturae*, vol. 4, no. 1, pp. 23–31, 2012, doi: 10.32607/20758251-2012-4-1-23-31.

[64] K. Suzuki, N. Chosa, S. Sawada, N. Takizawa, T. Yaegashi, and A. Ishisaki, “Enhancement of Anti-Inflammatory and Osteogenic Abilities of Mesenchymal Stem Cells via Cell-to-Cell Adhesion to Periodontal Ligament-Derived Fibroblasts,” *Stem Cells Int.*, vol. 2017, 2017, doi: 10.1155/2017/3296498.

[65] R. E. Newman, D. Yoo, M. A. LeRoux, and A. Danilkovitch-Miagkova, “Treatment of inflammatory diseases with mesenchymal stem cells,” *Inflamm. Allergy - Drug Targets*, vol. 8, no. 2, pp. 110–123, 2009, doi: 10.2174/187152809788462635.

[66] P. S. Frenette, S. Pinho, D. Lucas, and C. Scheiermann, *Mesenchymal stem cell: Keystone of the hematopoietic stem cell niche and a stepping-stone for regenerative medicine*, vol. 31. 2013.

[67] Y. Wang, X. Chen, W. Cao, and Y. Shi, “Plasticity of mesenchymal stem cells in immunomodulation: Pathological and therapeutic implications,” *Nat. Immunol.*, vol. 15, no. 11, pp. 1009–1016, 2014, doi: 10.1038/ni.3002.

[68] J. A. Ankrum, J. F. Ong, and J. M. Karp, “Mesenchymal stem cells: Immune evasive, not immune privileged,” *Nat. Biotechnol.*, vol. 32, no. 3, pp. 252–260, 2014, doi: 10.1038/nbt.2816.

[69] A. J. Nauta and W. E. Fibbe, “Immunomodulatory properties of mesenchymal stromal cells,” *Blood*, vol. 110, no. 10, pp. 3499–3506, 2007, doi: 10.1182/blood-2007-02-069716.

[70] K. English, “Mechanisms of mesenchymal stromal cell immunomodulation,” *Immunol. Cell Biol.*, vol. 91, no. 1, pp. 19–26, 2013, doi: 10.1038/icb.2012.56.

[71] P. H. . J. B. M. . S. C. T. et al Gary, “The New England Journal of Medicine Downloaded from nejm.org on April 1, 2015. For personal use only. No other uses without permission. Copyright © 1990 Massachusetts Medical Society. All rights reserved.,” *New English J.*

Med., vol. 323, no. 16, pp. 1120–1123, 1990.

[72] A. Gebler, O. Zabel, and B. Seliger, "The immunomodulatory capacity of mesenchymal stem cells," *Trends Mol. Med.*, vol. 18, no. 2, pp. 128–134, 2012, doi: 10.1016/j.molmed.2011.10.004.

[73] G. Ren *et al.*, "Mesenchymal Stem Cell-Mediated Immunosuppression Occurs via Concerted Action of Chemokines and Nitric Oxide," *Cell Stem Cell*, vol. 2, no. 2, pp. 141–150, 2008, doi: 10.1016/j.stem.2007.11.014.

[74] M. Krampera *et al.*, "Role for Interferon-γ in the Immunomodulatory Activity of Human Bone Marrow Mesenchymal Stem Cells," *Stem Cells*, vol. 24, no. 2, pp. 386–398, 2006, doi: 10.1634/stemcells.2005-0008.

[75] R. R. Sharma, K. Pollock, A. Hubel, and D. McKenna, "Mesenchymal stem or stromal cells: A review of clinical applications and manufacturing practices," *Transfusion*, vol. 54, no. 5, pp. 1418–1437, 2014, doi: 10.1111/trf.12421.

[76] J. N. M. Ijzermans and R. L. Marquet, "Interferon-gamma: A Review," *Immunobiology*, vol. 179, no. 4–5, pp. 456–473, 1989, doi: 10.1016/S0171-2985(89)80049-X.

[77] Y. Liu *et al.*, "Mesenchymal stem cell-based tissue regeneration is governed by recipient T lymphocytes via IFN-γ and TNF-α," *Nat. Med.*, vol. 17, no. 12, pp. 1594–1601, 2011, doi: 10.1038/nm.2542.

[78] N. P. Group, "The Otogeny of the Neural Crest in Avian."

[79] M. Eddaoudi, H. Li, and O. M. Yaghi, "Highly porous and stable metal-organic frameworks: Structure design and sorption properties," *J. Am. Chem. Soc.*, vol. 122, no. 7, pp. 1391–1397, 2000, doi: 10.1021/ja9933386.

[80] J. Kim *et al.*, "Assembly of metal-organic frameworks from large organic and inorganic secondary building units: New examples and simplifying principles for complex structures," *J. Am. Chem. Soc.*, vol. 123, no. 34, pp. 8239–8247, 2001, doi: 10.1021/ja010825o.

[81] M. Eddaoudi *et al.*, "Modular chemistry: Secondary building units as a basis for the design of highly porous and robust metal-organic carboxylate frameworks," *Acc. Chem. Res.*, vol. 34, no. 4, pp. 319–330, 2001, doi: 10.1021/ar000034b.

[82] H. Kim *et al.*, "Hydrogen Storage in Microporous Metal-Organic Frameworks," *Science (80-.).*, vol. 73, no. 1973, pp. 12–15, 2002.

[83] D. J. Tranchemontagne, J. L. Tranchemontagne, M. O'keeffe, and O. M. Yaghi, "Secondary building units, nets and bonding in the chemistry of metal–organic frameworks," *Chem. Soc. Rev.*, vol. 38, no. 5, pp. 1257–1283, 2009, doi: 10.1039/b817735j.

[84] M. Karagianni *et al.*, "A comparative analysis of the adipogenic potential in human mesenchymal stromal cells from cord blood and other sources," *Cytotherapy*, vol. 15, no. 1, pp. 76-88.e2, 2013, doi: 10.1016/j.jcyt.2012.11.001.

[85] J. R. Long and O. M. Yaghi, “The pervasive chemistry of metal-organic frameworks,” *Chem. Soc. Rev.*, vol. 38, no. 5, pp. 1213–1214, 2009, doi: 10.1039/b903811f.

[86] H. Furukawa, K. E. Cordova, M. O’Keeffe, and O. M. Yaghi, “The chemistry and applications of metal-organic frameworks,” *Science (80-.).*, vol. 341, no. 6149, 2013, doi: 10.1126/science.1230444.

[87] M. Eddaoudi *et al.*, “Systematic design of pore size and functionality in isoreticular MOFs and their application in methane storage,” *Science (80-.).*, vol. 295, no. 5554, pp. 469–472, 2002, doi: 10.1126/science.1067208.

[88] T. Asami *et al.*, “Modulation of murine macrophage TLR7/8-mediated cytokine expression by mesenchymal stem cell-conditioned medium,” *Mediators Inflamm.*, vol. 2013, 2013, doi: 10.1155/2013/264260.

[89] Y. Zhang *et al.*, “Exosomes Derived from Mesenchymal Stromal Cells Promote Axonal Growth of Cortical Neurons,” *Mol. Neurobiol.*, vol. 54, no. 4, pp. 2659–2673, 2017, doi: 10.1007/s12035-016-9851-0.

[90] M. O. Dellacherie, B. R. Seo, and D. J. Mooney, “Macroscale biomaterials strategies for local immunomodulation,” *Nat. Rev. Mater.*, vol. 4, no. 6, pp. 379–397, 2019, doi: 10.1038/s41578-019-0106-3.

[91] R. S. Tuan, G. Boland, and R. Tuli, “Adult mesenchymal stem cells and cell-based tissue engineering,” *Arthritis Res. Ther.*, vol. 5, no. 1, pp. 32–45, 2003, doi: 10.1186/ar614.

[92] R. A. MARKLEIN, M. W. KLINKER, K. A. DRAKE, H. G. POLIKOWSKY, E. C. LESSEY-MORILLON, and S. R. BAUER, “Morphological profiling using machine learning reveals emergent subpopulations of interferon-γ–stimulated mesenchymal stromal cells that predict immunosuppression,” *Cytotherapy*, vol. 21, no. 1, pp. 17–31, 2019, doi: 10.1016/j.jcyt.2018.10.008.

[93] R. A. Marklein, J. Lam, M. Guvendiren, K. E. Sung, and S. R. Bauer, “Functionally-Relevant Morphological Profiling: A Tool to Assess Cellular Heterogeneity,” *Trends Biotechnol.*, vol. 36, no. 1, pp. 105–118, 2018, doi: 10.1016/j.tibtech.2017.10.007.

[94] S. J. Cifuentes, P. Priyadarshani, D. A. Castilla-Casadiego, L. J. Mortensen, J. Almodóvar, and M. Domenech, “Heparin/collagen surface coatings modulate the growth, secretome, and morphology of human mesenchymal stromal cell response to interferon-gamma,” *J. Biomed. Mater. Res. - Part A*, no. March, pp. 1–15, 2020, doi: 10.1002/jbm.a.37085.

[95] D. A. Castilla-Casadiego, L. Pinzon-Herrera, M. Perez-Perez, B. A. Quiñones-Colón, D. Suleiman, and J. Almodovar, “Simultaneous characterization of physical, chemical, and thermal properties of polymeric multilayers using infrared spectroscopic ellipsometry,” *Colloids Surfaces A Physicochem. Eng. Asp.*, vol. 553, pp. 155–168, 2018, doi: 10.1016/j.colsurfa.2018.05.052.

[96] L. Pinzon-Herrera, J. Mendez-Vega, A. Mulero-Russe, D. A. Castilla-Casadiego, and J. Almodovar, “Real-time monitoring of human Schwann cells on heparin-collagen coatings reveals enhanced adhesion and growth factor response,” *J. Mater. Chem. B*, vol. 8, no. 38, pp. 8809–8819, 2020, doi: 10.1039/d0tb01454k.

[97] D. A. Castilla-Casadiego, A. M. Reyes-Ramos, M. Domenech, and J. Almodovar, “Effects of Physical, Chemical, and Biological Stimulus on h-MSC Expansion and Their Functional Characteristics,” *Ann. Biomed. Eng.*, vol. 48, no. 2, pp. 519–535, 2020, doi: 10.1007/s10439-019-02400-3.

[98] D. A. Castilla-casadiego and J. Almodovar, “on heparin-collagen coatings reveals enhanced adhesion and growth factor response †,” 2020, doi: 10.1039/d0tb01454k.

[99] A. Bertolo, D. Pavlicek, A. Gemperli, M. Baur, T. Pötzel, and J. Stoyanov, “Increased motility of mesenchymal stem cells is correlated with inhibition of stimulated peripheral blood mononuclear cells in vitro,” *J. Stem Cells Regen. Med.*, vol. 13, no. 2, pp. P62–P74, 2017, doi: 10.46582/jsrm.1302010.

[100] L. Boland, A. J. Burand, A. J. Brown, D. Boyt, V. A. Lira, and J. A. Ankrum, “IFN-γ and TNF-α Pre-licensing Protects Mesenchymal Stromal Cells from the Pro-inflammatory Effects of Palmitate,” *Mol. Ther.*, vol. 26, no. 3, pp. 860–873, 2018, doi: 10.1016/j.ymthe.2017.12.013.

[101] M. C. Killer *et al.*, “Immunosuppressive capacity of mesenchymal stem cells correlates with metabolic activity and can be enhanced by valproic acid,” *Stem Cell Res. Ther.*, vol. 8, no. 1, pp. 1–8, 2017, doi: 10.1186/s13287-017-0553-y.

[102] K. A. Marx, “Quartz crystal microbalance: A useful tool for studying thin polymer films and complex biomolecular systems at the solution - Surface interface,” *Biomacromolecules*, vol. 4, no. 5, pp. 1099–1120, 2003, doi: 10.1021/bm020116i.

[103] C. D. Easton, A. J. Bullock, G. Gigliobianco, S. L. McArthur, and S. Macneil, “Application of layer-by-layer coatings to tissue scaffolds-development of an angiogenic biomaterial,” *J. Mater. Chem. B*, vol. 2, no. 34, pp. 5558–5568, 2014, doi: 10.1039/c4tb00448e.

[104] Q. Lin, J. Yan, F. Qiu, X. Song, G. Fu, and J. Ji, “Heparin/collagen multilayer as a thromboresistant and endothelial favorable coating for intravascular stent,” *J. Biomed. Mater. Res. - Part A*, vol. 96 A, no. 1, pp. 132–141, 2011, doi: 10.1002/jbm.a.32820.

[105] I. Reviakine, D. Johannsmann, and R. P. Richter, “Hearing what you cannot see and visualizing what you hear: Interpreting quartz crystal microbalance data from solvated interfaces,” *Anal. Chem.*, vol. 83, no. 23, pp. 8838–8848, 2011, doi: 10.1021/ac201778h.

[106] S. Boddohi, J. Almodóvar, H. Zhang, P. A. Johnson, and M. J. Kipper, “Layer-by-layer assembly of polysaccharide-based nanostructured surfaces containing polyelectrolyte complex nanoparticles,” *Colloids Surfaces B Biointerfaces*, vol. 77, no. 1, pp. 60–68, 2010, doi: 10.1016/j.colsurfb.2010.01.006.

[107] Q. Lin, J. Yan, F. Qiu, X. Song, G. Fu, and J. Ji, “Heparin/collagen multilayer as a thromboresistant and endothelial favorable coating for intravascular stent,” *J. Biomed. Mater. Res. - Part A*, vol. 96 A, no. 1, pp. 132–141, 2011, doi: 10.1002/jbm.a.32820.

[108] D. S. Salloum, S. G. Olenych, T. C. S. Keller, and J. B. Schlenoff, “Vascular smooth muscle cells on polyelectrolyte multilayers: Hydrophobicity-directed adhesion and growth,” *Biomacromolecules*, vol. 6, no. 1, pp. 161–167, 2005, doi: 10.1021/bm0497015.

[109] K. Zhang, D. Huang, Z. Yan, and C. Wang, “Heparin/collagen encapsulating nerve growth factor multilayers coated aligned PLLA nanofibrous scaffolds for nerve tissue engineering,” *J. Biomed. Mater. Res. - Part A*, vol. 105, no. 7, pp. 1900–1910, 2017, doi: 10.1002/jbm.a.36053.

[110] A. M. Ferreira, P. Gentile, S. Toumpaniari, G. Ciardelli, and M. A. Birch, “Impact of Collagen/Heparin Multilayers for Regulating Bone Cellular Functions,” *ACS Appl. Mater. Interfaces*, vol. 8, no. 44, pp. 29923–29932, 2016, doi: 10.1021/acsami.6b09241.

[111] D. Li *et al.*, “Chitosan and collagen layer-by-layer assembly modified oriented nanofibers and their biological properties,” *Carbohydr. Polym.*, vol. 254, no. July 2020, p. 117438, 2020, doi: 10.1016/j.carbpol.2020.117438.

[112] J. Almodóvar, S. Bacon, J. Gogolski, J. D. Kisiday, and M. J. Kipper, “Polysaccharide-based polyelectrolyte multilayer surface coatings can enhance mesenchymal stem cell response to adsorbed growth factors,” *Biomacromolecules*, vol. 11, no. 10, pp. 2629–2639, 2010, doi: 10.1021/bm1005799.

[113] H. M. Wobma, M. A. Tamargo, S. Goeta, L. M. Brown, R. Duran-Struuck, and G. Vunjak-Novakovic, *The influence of hypoxia and IFN-γ on the proteome and metabolome of therapeutic mesenchymal stem cells*, vol. 167. Elsevier Ltd, 2018.

[114] J. Du *et al.*, “The different effects of IFN-β and IFN-γ on the tumor-suppressive activity of human amniotic fluid-derived mesenchymal stem cells,” *Stem Cells Int.*, vol. 2019, 2019, doi: 10.1155/2019/4592701.

[115] M. H. Hettiaratchi, T. Miller, J. S. Temenoff, R. E. Guldberg, and T. C. McDevitt, “Heparin microparticle effects on presentation and bioactivity of bone morphogenetic protein-2,” *Biomaterials*, vol. 35, no. 25, pp. 7228–7238, 2014, doi: 10.1016/j.biomaterials.2014.05.011.

[116] S. J. Fritchley, J. A. Kirby, and S. Ali, “The antagonism of interferon-gamma (IFN-γ) by heparin: Examination of the blockade of class II MHC antigen and heat shock protein-70 expression,” *Clin. Exp. Immunol.*, vol. 120, no. 2, pp. 247–252, 2000, doi: 10.1046/j.1365-2249.2000.01178.x.

[117] A. Rezania and K. E. Healy, “Biomimetic peptide surfaces that regulate adhesion, spreading, cytoskeletal organization, and mineralization of the matrix deposited by osteoblast-like cells,” *Biotechnol. Prog.*, vol. 15, no. 1, pp. 19–32, 1999, doi: 10.1021/bp980083b.

[118] V. January, “RTCA DP Instrument Operator’s Manual,” *ACEA Biosci. Inc*, no. January, 2013.

[119] J. J. Montesinos *et al.*, “Human bone marrow mesenchymal stem/stromal cells exposed to an inflammatory environment increase the expression of ICAM-1 and release microvesicles enriched in this adhesive molecule: Analysis of the participation of TNF-α and IFN-γ,” *J. Immunol. Res.*, vol. 2020, 2020, doi: 10.1155/2020/8839625.

[120] O. Takikawa, T. Kuroiwa, F. Yamazaki, and R. Kido, “Mechanism of interferon-γ action. Characterization of indoleamine 2,3-dioxygenase in cultured human cells induced by

interferon -γ and evaluation of the enzyme-mediated tryptophan degradation in its anticellular activity," *J. Biol. Chem.*, vol. 263, no. 4, pp. 2041–2048, 1988.

[121] W. Däubener, N. Wanagat, K. Pilz, S. Seghrouchni, H. G. Fischer, and U. Hadding, "A new, simple, bioassay for human IFN-γ," *J. Immunol. Methods*, vol. 168, no. 1, pp. 39–47, 1994, doi: 10.1016/0022-1759(94)90207-0.

[122] G. Siegel, T. Kluba, U. Hermanutz-Klein, K. Bieback, H. Northoff, and R. Schäfer, "Phenotype, donor age and gender affect function of human bone marrow-derived mesenchymal stromal cells," *BMC Med.*, vol. 11, no. 1, 2013, doi: 10.1186/1741-7015-11-146.

[123] O. Katsara *et al.*, "Effects of donor age, gender, and in vitro cellular aging on the phenotypic, functional, and molecular characteristics of mouse bone marrow-derived mesenchymal stem cells," *Stem Cells Dev.*, vol. 20, no. 9, pp. 1549–1561, 2011, doi: 10.1089/scd.2010.0280.

[124] T. Wang, J. Zhang, J. Liao, F. Zhang, and G. Zhou, "Donor genetic backgrounds contribute to the functional heterogeneity of stem cells and clinical outcomes," *Stem Cells Transl. Med.*, vol. 9, no. 12, pp. 1495–1499, 2020, doi: 10.1002/sctm.20-0155.

[125] M. Science, "Tissue Engineering and Regenerative Medicine T ISSUE E NGINEERING AND R EGENERATIVE M EDICINE MicroRNA-146b , a Sensitive Indicator of Mesenchymal Stem Cell Repair of Acute Renal Injury," pp. 1–10, 2016.

[126] K. E. S. Brian J. Kwee, Johnny Lam, Adovi Akue, Mark A. KuKuruga, K. Zhang, Luo Gu, "Functional heterogeneity of IFN-γ – licensed mesenchymal stromal cell immunosuppressive capacity on biomaterials," pp. 1–12, 2021, doi: 10.1073/pnas.2105972118/-/DCSupplemental.Published.

[127] F. Fallarino and U. Grohmann, "Using an Ancient Tool for Igniting and Propagating Immune Tolerance: IDO as an Inducer and Amplifier of Regulatory T Cell Functions," *Curr. Med. Chem.*, vol. 18, no. 15, pp. 2215–2221, 2012, doi: 10.2174/092986711795656027.

[128] D. S. Kim *et al.*, "Enhanced Immunosuppressive Properties of Human Mesenchymal Stem Cells Primed by Interferon-γ," *EBioMedicine*, vol. 28, pp. 261–273, 2018, doi: 10.1016/j.ebiom.2018.01.002.

[129] W. Juncheng *et al.*, "High glucose inhibits osteogenic differentiation through the BMP signaling pathway in bone mesenchymal stem cells in mice," *EXCLI J.*, vol. 12, no. 2009, pp. 584–597, 2013, doi: 10.17877/DE290R-7335.

[130] A. Zhu, M. Zhang, J. Wu, and J. Shen, "Covalent immobilization of chitosan / heparin complex with a photosensitive hetero-bifunctional crosslinking reagent on PLA surface $," vol. 23, pp. 4657–4665, 2002.

[131] A. M. M. Renata Francielle Bombaldi de Souza, Fernanda Carla Bombaldi de Souza, Andrea Thorpe, Diego Mantovani, Ketul C. Popat, "Phosphorylation of chitosan to improve osteoinduction of chitosan/xanthan-based scaffolds for periosteal tissue engineering," *Int. J. Biol. Macromol.*, 2019, doi: 10.1016/j.ijbiomac.2019.12.004.

[132] R. M. Sabino, G. Mondini, M. J. Kipper, A. F. Martins, and K. C. Popat, “Tanfloc/heparin polyelectrolyte multilayers improve osteogenic differentiation of adipose-derived stem cells on titania nanotube surfaces,” *Carbohydr. Polym.*, vol. 251, no. September 2020, p. 117079, 2021, doi: 10.1016/j.carbpol.2020.117079.

[133] C. Granéli *et al.*, “Novel markers of osteogenic and adipogenic differentiation of human bone marrow stromal cells identified using a quantitative proteomics approach,” *Stem Cell Res.*, vol. 12, no. 1, pp. 153–165, 2014, doi: 10.1016/j.scr.2013.09.009.

[134] V. Michel and M. Bakovic, “The solute carrier 44A1 is a mitochondrial protein and mediates choline transport,” *FASEB J.*, vol. 23, no. 8, pp. 2749–2758, 2009, doi: 10.1096/fj.08-121491.

[135] L. Ding *et al.*, “CD10 expression identifies a subset of human perivascular progenitor cells with high proliferation and calcification potentials,” *Stem Cells*, vol. 38, no. 2, pp. 261–275, 2020, doi: 10.1002/stem.3112.

[136] E. A. Jones *et al.*, “Isolation and characterization of bone marrow multipotential mesenchymal progenitor cells,” *Arthritis Rheum.*, vol. 46, no. 12, pp. 3349–3360, 2002, doi: 10.1002/art.10696.

[137] M. S. Niepel, F. Almouhanna, B. K. Ekambaram, M. Menzel, A. Heilmann, and T. Groth, “Cross-linking multilayers of poly-l-lysine and hyaluronic acid: Effect on mesenchymal stem cell behavior,” *Int. J. Artif. Organs*, vol. 41, no. 4, pp. 223–235, 2018, doi: 10.1177/0391398817752598.

[138] K. Pachmann and W. Leibold, “Insolubilization of protein antigens on polyacrylic plastic beads using poly-l-lysine,” *J. Immunol. Methods*, vol. 12, no. 1–2, pp. 81–89, 1976, doi: 10.1016/0022-1759(76)90098-3.

[139] P. DE KRUIJFF and and P. R. CULLIS, “THE INFLUENCE OF POLY(L-LYSINE) ON PHOSPHOLIPID POLYMORPHISM EVIDENCE,” *Biochim. Biophys. Acta*, vol. 601, pp. 235–240, 1980, doi: 10.1016/0005-2736(80)90528-3.

[140] J. Almodóvar *et al.*, “Spatial patterning of BMP-2 and BMP-7 on biopolymeric films and the guidance of muscle cell fate,” *Biomaterials*, vol. 35, no. 13, pp. 3975–3985, 2014, doi: 10.1016/j.biomaterials.2014.01.012.

[141] A. R. S. L. Michael D. Klein, Robert A. Drongowski, Robert J. Linhardt, “A Colorimetric Assay for Chemical in Plasma,” *Anal. Biochem.*, vol. 64, pp. 59–64, 1982.

[142] L. Richert *et al.*, “Improvement of stability and cell adhesion properties of polyelectrolyte multilayer films by chemical cross-linking,” *Biomacromolecules*, vol. 5, no. 2, pp. 284–294, 2004, doi: 10.1021/bm0342281.

[143] A. Barrantes, O. Santos, J. Sotres, and T. Arnebrant, “Influence of pH on the build-up of poly-L-lysine/heparin multilayers,” *J. Colloid Interface Sci.*, vol. 388, no. 1, pp. 191–200, 2012, doi: 10.1016/j.jcis.2012.08.008.

[144] F. Boulmedais, C. S. Tang, B. Keller, and J. Vörös, “Controlled electrodissolution of polyelectrolyte multilayers: A platform technology towards the surface-initiated delivery of drugs,” *Adv. Funct. Mater.*, vol. 16, no. 1, pp. 63–70, 2006, doi:

10.1002/adfm.200400406.

[145] C. Picart *et al.*, “Molecular basis for the explanation of the exponential growth of polyelectrolyte multilayers,” *Proc. Natl. Acad. Sci. U. S. A.*, vol. 99, no. 20, pp. 12531–12535, 2002, doi: 10.1073/pnas.202486099.

[146] N. Graf *et al.*, “XPS and NEXAFS studies of aliphatic and aromatic amine species on functionalized surfaces,” *Surf. Sci.*, vol. 603, no. 18, pp. 2849–2860, 2009, doi: 10.1016/j.susc.2009.07.029.

[147] O. V. Semenov, A. Malek, A. G. Bittermann, J. Vörös, and A. H. Zisch, “Engineered polyelectrolyte multilayer substrates for adhesion, proliferation, and differentiation of human mesenchymal stem cells,” *Tissue Eng. - Part A*, vol. 15, no. 10, pp. 2977–2990, 2009, doi: 10.1089/ten.tea.2008.0602.

[148] T. Crouzier and C. Picart, “Ion Pairing and Hydration in Polyelectroyte Multilayer Film Containing Polysaccharides,” *Biomacromolecules*, pp. 433–442, 2009.

[149] J. C. Mbongue, D. A. Nicholas, T. W. Torrez, N. S. Kim, A. F. Firek, and W. H. R. Langridge, “The role of indoleamine 2, 3-dioxygenase in immune suppression and autoimmunity,” *Vaccines*, vol. 3, no. 3, pp. 703–729, 2015, doi: 10.3390/vaccines3030703.

Supplementary Information

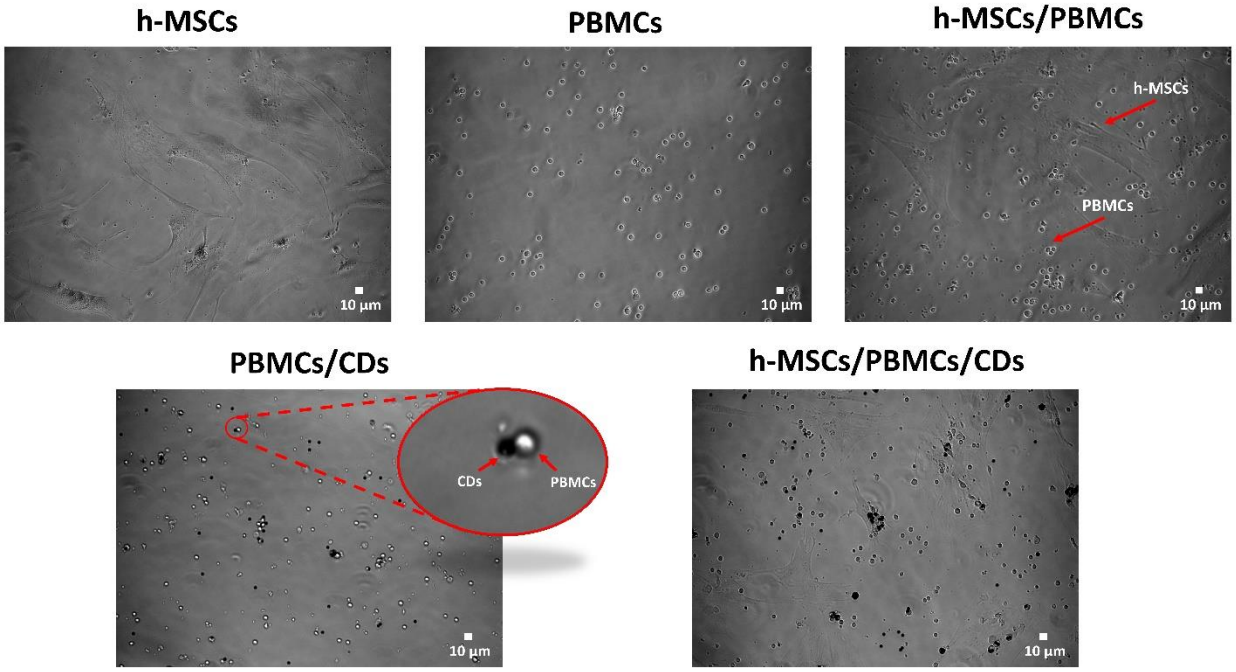

Figure S.2.1. PBMCs with Human T Activator CD3/CD28 Dynabeads (CDs) suspended in hMSCs attached to the surfaces.

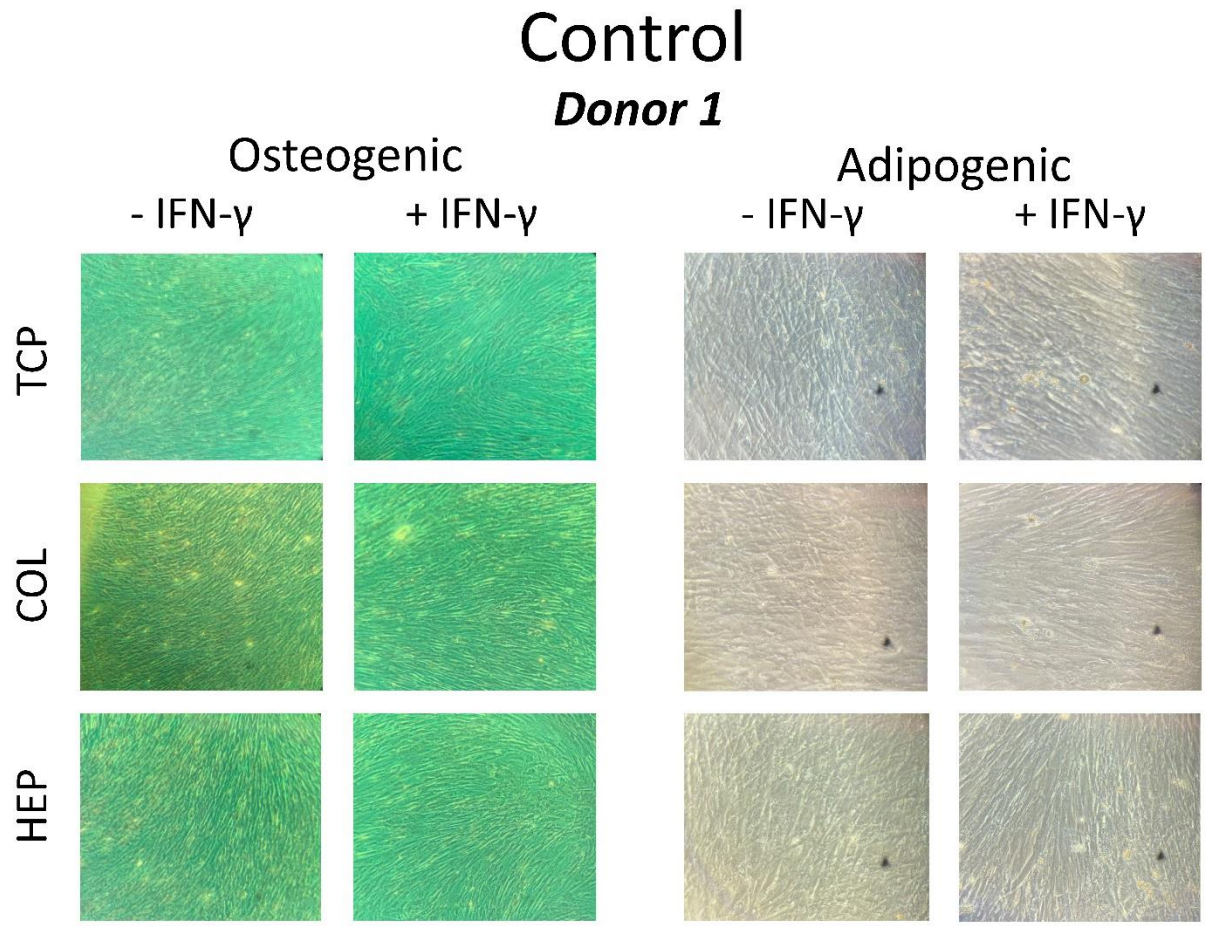

Figure S2.2. hMSCs control for donor#1 cells inducing by normal expansion medium.

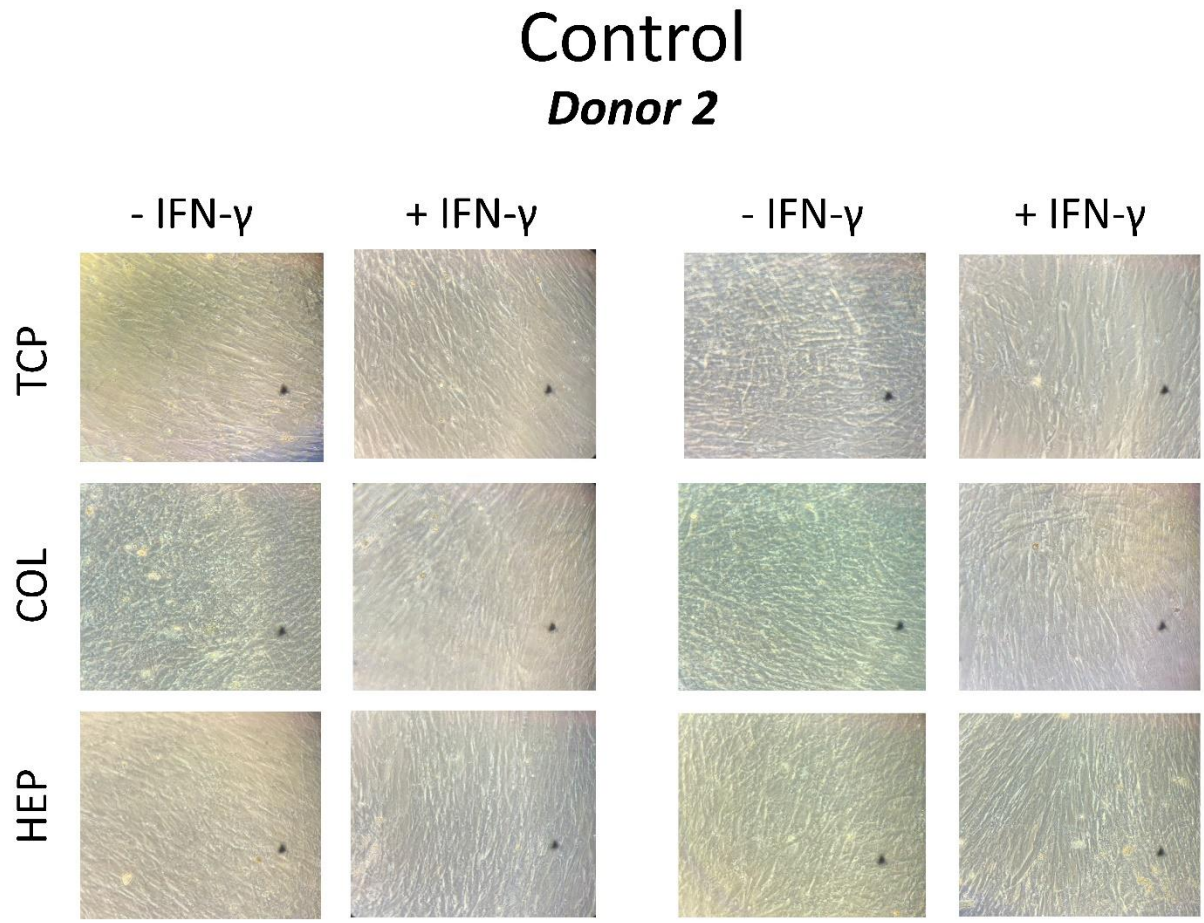

Figure S2.3. hMSCs control for donor#2 cells inducing by normal expansion medium.

3. Crosslinked Layered Surfaces of Heparin and Poly(L-Lysine) Enhance Mesenchymal Stromal Cells Behavior in The Presence of Soluble Interferon Gamma

Mahsa Haseli[1], Luis Pinzon-Herrera[1], and Jorge Almodovar[1*]

[1]Ralph E. Martin Department of Chemical Engineering, University of Arkansas, 3202 Bell Engineering Center, Fayetteville, AR 72701, USA

*The chapter was published and used with permission.

Abstract

Human mesenchymal stromal cells (hMSCs) are multipotent cells that have been proposed for the treatment of immune-mediated diseases. Culturing hMSCs on tissue culture plastic reduces their therapeutic potential in part due to the lack of extracellular matrix components. The aim of this study is to evaluate multilayers of heparin and poly(L-lysine) (HEP/PLL) as a bioactive surface for hMSCs stimulated with soluble interferon gamma (IFN-γ). Multilayers were formed, via layer-by-layer assembly, with HEP as the final layer and supplemented with IFN-γ in the culture medium. Multilayer construction and chemistry were confirmed using Azure A staining, quartz crystal microbalance (QCM), and X-ray photoelectron spectroscopy. hMSCs adhesion, viability, and differentiation, were assessed. Results showed that (HEP/PLL) multilayer coatings were poorly adhesive for hMSCs. However, performing chemical crosslinking using 1-ethyl-3-(3-dimethylaminopropyl) carbodiimide and N-hydroxysuccinimide (EDC/NHS) significantly enhanced hMSCs adhesion and viability. The immunosuppressive properties of hMSCs cultured on crosslinked (HEP/PLL) multilayers were confirmed by measuring the level of indoleamine 2,3-dioxygenase (IDO) secretion. Lastly, hMSCs cultured on crosslinked (HEP/PLL) multilayers in the presence of soluble IFN-γ successfully differentiated towards the osteogenic and adipogenic lineages as confirmed by Alizarin red, and oil-red O staining, as well as alkaline

phosphatase activity. This study suggests that crosslinked (HEP/PLL) films can modulate hMSCs response to soluble factors, which may improve hMSCs-based therapies aimed at treating several immune diseases.

Keywords: Layer-by-layer, Human mesenchymal stromal cells, poly(L-lysine), Heparin, Interferon gamma.

3.1. Introduction

Human mesenchymal stromal cells (hMSCs) are of special interest for cellular therapy programs [59]. This type of cells are pluripotent which are able to differentiate into mesodermal lineage cells, including adipocytes, osteoblasts, and chondrocytes [2][3]. HMSCs therapeutic behavior is affected by the surrounding microenvironment, including growth factors, the extracellular matrix (ECM) and contact with other cells [8][9]. The ECM is a highly complex nanostructure that play vital roles in the determination, differentiation, proliferation, and survival of cells [9]. The ECM structure is filled with the matrix containing glycosaminoglycans [13] and proteins [14], which are known as proteoglycans [9]. The proteoglycans in the ECM contribute to the mechanical properties of the matrix and modulate cell behavior [8][9]. There is a need to learn from cell biology, such as what controls cellular differentiation and growth and how ECM components affect cell function [14].

The layer-by-layer (LbL) deposition of polyelectrolytes has been known as a simple method to generate biologically relevant surfaces by creating nanoscale thin films. The LbL method provides compositional uniqueness of natural or synthetic polymers, such as stimulating a specific signal to cells and enhancing cellular behavior [29]. LbL involves the alternative absorption of polycations and polyanions to produce films with specific and controlled physical-chemical characteristics by adapting the experimental parameters, such as pH, ionic strength, and

polyelectrolyte concentration [30][31][32]. Several studies have recently investigated cell interactions with multilayers. One study by Growth et al. indicated that (hyaluronic acid (HA)/ (poly-L-lysine (PLL) multilayers composed of 24 layers are able to control stem cell response after chemical cross-linking [137].

HMSCs interaction with heparin (HEP/PLL) polymeric multilayer composition in the presence or absence of soluble interferon gamma (IFN-γ) has not been studied yet. It has been shown that the immunosuppressive properties of hMSCs relies on the existence of IFN-γ in the microenvironment [5]. IFN-γ is a potent pro-inflammatory cytokine that is produced by CD4+ lymphocytes, natural killer cells (NKT) cells, and macrophages. IFN-γ plays essential and complex roles in innate and adaptive immune responses against viral infections, bacteria, protozoa, and graft-versus-host disease (GVHD) [76][77]. A study showed that IFN-γ has the ability to modulate the immune properties and differentiation potential of hMSCs which has a significant anti-proliferative effect [6]. Therefore, there is a need to reduce the anti-proliferative effect of IFN-γ on hMSCs.

Heparin is a highly sulfated glycosaminoglycan that contains negatively charged carboxylate or sulfate groups present in the ECM and surface of cells [39][40]. Due to the electrostatic interactions and binding with amino acids, heparin plays a role in cellular functions such as cell adhesion, proliferation, differentiation, migration, and inflammation [41][42]. Furthermore, heparin is well known for its anticoagulant properties, but apart from this ability, heparin has the ability to bind ECM proteins, such as collagen and thus plays an important role in organizing the structure and composition of the ECM. Many studies showed that heparin can prevent proteolytic cleavage of IFN-γ and can improve IFN-γ signaling [39][43]. In addition, PLL is a biocompatible polycation with a large amount of active amino groups. PLL can adopt different secondary

structures (e.g., random coil, b-sheet, or a-helix) depending on the pH of the solution. PLL has been used for many different purposes, such as the study of DNA-Protein interactions, drug delivery, and coating materials to improve cell attachment to plastic and glass surfaces [46]. PLL enhances cell's attachment due to electrostatic interaction between negatively-charged ions of the cell membrane and positively-charged surface ions of attachment factors on the culture surface [138][139].

This research evaluated the (HEP/PLL) multilayer substrates as surfaces for hMSC culture. We evaluated the construction and chemistry of the (HEP/PLL) multilayers, as well as their capacity to support hMSCs. Finally, we investigated hMSC viability, adhesion, proliferation, immunosuppressive properties, and differentiation when cultured on (HEP/PLL) multilayers in the presence of soluble IFN-γ.

3.2. Materials and Methods

3.2.1. Materials

Heparin sodium (HEP) was purchased from Celsus Laboratories, Inc. (Cat. #PH3005). Poly-L-lysine hydrobromide from bovine (Cat. # P2636), poly(ethylenimine) (PEI) (50% solution in Water, Mw ≈ 750 000) (Cat. #P3143), HEPES (Cat. # H3375), 1-ethyl-3-(3-dimethylaminopropyl) carbodiimide hydrochloride (EDC) (Cat. #106627547), and N-Hydroxysulfosuccinimide sodium salt (sulfo-NHS) (Cat. #56485) were purchased from Sigma-Aldrich. Ultrapure water at 18 MΩ·cm was obtained from a Millipore-Sigma™ Direct-Q™ 3 (Cat. #ZRQSVP3US). Tissue culture-treated plates were purchased from Corning Costar (Cat. #07-200- 740). IFN-γ recombinant human protein was purchased from ThermoFisher (Cat. #PHC4031). Human bone-marrow derived mesenchymal stromal cells from two donors purchased from RoosterBio (Cat. #MSC-003), were used between passages 4−6. Donor#1 is a

healthy 25-year-old male (Lot. 00174), and donor#2 is a healthy 22-year-old male (Lot. 00178). MEM Alpha (1X) (Cat. #12561-056) and fetal bovine serum (Cat. #12662029) were obtained from Gibco. Penicillin-streptomycin (Cat. #30002CI), and L-glutamine were purchased from Corning (Cat. #25005CI). Azure A was purchased from Thermo Scientific™ (Cat. #AAJ6134614). PrestoBlue™ cell viability assay was purchased from Invitrogen (Cat. #A13261). Hoechst 33 342 was purchased from Invitrogen (Ref. #H3570). ActinRed 555 Ready Probest was purchased from Invitrogen (Ref. #37112). DMEM (Dulbecco's Modified Eagle Medium) high glucose (Cat. #11965092), and DMEM (Dulbecco's Modified Eagle Medium) low glucose were purchased from ThermoFisher (Cat. #11885084). Ascorbic acid (Cat. #50-81-7), β-glycerophosphate from Sigma (Cat. #154804-51-0), Alizarin Red S (Cat. # 130-22-3), dexamethasone (Cat. #50-02-2), insulin (Cat. # I2643), 3-isobutyl-1-methylxanthine (IBMX) (Cat. #28822-58-4, I5879), indomethacin (Cat. #53-86-1) and Oil Red-O (Cat. #O0625) were purchased from Sigma-Aldrich. Alkaline Phosphatase Colorimetric Assay Kit was purchased from Abcam (ab83369). Micro BCA™ Protein Assay Kit was purchased from Thermofisher (Cat. # 23235).

3.2.2. (HEP/PLL) multilayers fabrication

(HEP/PLL) multilayers were constructed by the layer-by-layer technique. PEI (1 mg/mL), HEP (1 mg/mL), and PLL (0.5 mg/mL) were dissolved in a filtered HEPES-NaCl buffer solution (20 mM HEPES pH 7.4, 0.15 M NaCl), and ultrapure water at 18 MΩ·cm was used to prepare the polymeric and wash solutions. Sequential polymeric layers and rinsing were done using manual pipetting on sterile tissue culture-treated plates. Briefly, the process consisted of creating a positive initial layer by depositing PEI solution for 15 minutes to each well of a sterile tissue culture-treated plate and followed by a 3 minutes washing step with HEPES-NaCl buffer

solution. HEP was added for 5 minutes; then the HEP solution was removed, collected, and rinsed with HEPES-NaCl buffer solution for 3 minutes. Then PLL was added and subsequently rinsed following the same process. This process was followed until obtaining a total of 13 polymeric layers of (HEP/PLL) (layers ending with HEP). Multilayers were crosslinked with EDC at 25 mg/mL and NHS at 11 mg/mL dissolved in NaCl (0.15 M, pH 5.5 in deionized water) and mixed immediately before use, similar to the process described by Almodovar et al. [140]. The multilayers were incubated overnight in a humidified incubator at 37 °C. Then the EDC-NHS solution was removed, followed by extensive rinsing with cold 15 M NaCl buffer solution to hydrolyze unreacted cross-linkers. A final wash was done using Dulbecco's phosphate-buffered saline (DPBS)1X without Ca^{2+} and Mg^{2+} for 3 minutes. Substrates were sterilized using ultraviolet light (UV) for 10 minutes to reduce contamination before seeding the cells.

3.2.3. Experimental design

In this work, the effects on the cellular response of hMSCs of crosslinked multilayers and the presence or absence of IFN-γ in the culture medium were studied. Three surfaces were assessed, these consisted of a control surface of tissue culture plastic labeled as TCP, a bioactive surface of 13 non-crosslinked (HEP/PLL) multilayers, and 13 crosslinked (CL) of (HEP/PLL) multilayers. These multilayers arrangements will be noted as (HEP/ PLL) and (HEP/ PLL) + CL, respectively. IFN-γ supplemented in cell medium was evaluated at a concentration of 50 ng/mL, and conditions with and without IFN-γ were designated as +IFN-γ and −IFN-γ, respectively. A 50 ng/mL concentration for soluble IFN-γ was selected based on our previous study [7][25][26]. Time points and the initial number of cells were selected according to the nature of the specific method used.

3.2.4. Qualitative colorimetric determination of heparin deposited within (HEP/PLL)

The multilayers were coated on 24-well plates from Corning Costar (Cat. #07-200- 740). After multilayers deposition, the plate was dried for 1 day in a laminar flow hood. Once the samples were completely dry, 1 mL of Azure A Blue dye in water (80 µg of Azure A in 1 mL water) was added to each well. The absorbance at 620 nm was read using a BioTek Multi-Mode Microplate Reader (Model Synergyt^{TM} 2).

3.2.5. In-situ deposition of (HEP/PLL) multilayers

Deposition of polycations, polyanions, and crosslinking was measured by quartz crystal microbalance (QCM-D) with dissipation from Biolin Scientific, Sweden. The multilayer buildup process was described in our previous work [33]. Briefly, QCM-D measurements were performed on quartz crystal microbalance. The quartz crystal was cleaned following the manufacturer's protocol. The quartz crystal was immersed in a solution containing 10:2:2 (volume parts) of water, 25% ammonia, and 30% hydrogen peroxide at 75 ℃. The clean quartz crystal was settled in the QCM-D chamber, and the flow rate was set up at 100 mL/min. Then the PEI solution was injected continuously for 15 minutes. Then, the HEPES-NaCl buffer was pumped for 3 minutes at the same speed. The HEP solution was injected at the same rate for 5 minutes, followed by the same HEPES-NaCl buffer injection. After that, the PLL solution was injected for 5 minutes at the same rate, followed by the same HEPES-NaCl buffer injection. HEP and PLL were then alternately injected into the chamber (followed by the same HEPES-NaCl buffer injection after each injection) for 13 multilayers. Then, the crosslinking solution was injected into the chamber for 1 h. The inverse frequency shift ($-\Delta f$) and dissipation (ΔD) vs. time curves were recorded.

3.2.6. X-ray Photoelectron Spectroscopy (XPS).

X-ray Photoelectron Spectroscopy (XPS) (Versaprobe XPS from Physical electronics) was performed at a photoelectron takeoff angle of 458 on a dry glass substrate, and binding energy scales were referenced to the C1s peak (284.7eV).

3.2.7. Cell culture

Human bone-marrow derived mesenchymal stromal cells from two donors were used between passages 4−6. The product specification sheet provided by the vendor shows that these cells demonstrated the ability to undergo adipogenic and osteogenic differentiation and expressed the accepted panel of surface markers (CD45-, CD34-, CD166+, CD90+). hMSCs were grown in MEM Alpha (1X) medium (supplemented with L-glutamine, ribonucleosides, and deoxyribonucleosides) containing 20% fetal bovine serum, 1.2% penicillin-streptomycin, and 1.2% L-glutamine.

3.2.8. Cell viability on (HEP/PLL) multilayers

The PrestoBlue^{TM} cell viability assay reagent was used to measure hMSCs viability after 3 days. HMSCs (10000 cells/cm^2) were seeded on each condition with and without IFN-γ (TCP, (HEP/PLL), and (HEP/PLL)+CL) on a 96 well-plate, and cell viability was measured as described in our previous works [97][94][96]. Briefly, the cell culture medium was removed after 3 days, and 100 µL per well of fresh culture medium containing 10% PrestoBlue reagent. The plate was kept in a humidified incubator with 5% CO_2 and 37℃ for 3 hours (protected from light). The fluorescence intensity measurement was determined using a BioTek Multi-Mode Microplate Reader (Model Synergy^{TM} 2) with excitation/emission of 560/590 nm. Data were summarized per culture conditions.

Fluorescent staining was performed for the detection of the blue fluorescent dye Hoechst 33 342. This dye stains the nucleic acid because it is permeable to the cell. The red-orange fluorescent dye ActinRedt 555 was detected, which is selective to Actin F (a fundamental component of the cellular cytoskeleton). After three days of culture, the cell medium was removed, and the cells were fixed with 4% formaldehyde solution for 15 minutes. The samples were washed several times with PBS following by adding Triton X100 for 10 minutes, then washed with PBS 3 times. ActinRedt 555 was first added and incubated for 30 minutes. Then, Hoechst 33 342 was added for 10 minutes and protected from light by aluminum foil. Both dyes washed 5 times with PBS before and after being added. For cell imaging, Leica inverted fluorescence microscope was used with a standard DAPI filter (excitation/emission of 350/461 nm) for Hoechst 33 342, and a standard TRITC filter (excitation/emission of 540/565 nm) for ActinRedt 55.

3.2.9. Real-time monitoring of hMSCs behavior on (HEP/PLL) multilayers

An xCELLigence Real-Time Cell Analyzer (RTCA S16) instrument from ACEA Biosciences Inc. (Cat. #00380601430) was used to measure real-time cell behavior. (HEP/PLL) multilayers were constructed on the wells of an ACEA^{TM} E-Plate L16 (Cat. #00300600890, cell growth area of 0.32 cm^2 per well), and hMSCs at a concentration of 5000 cells/cm^2 were seeded on each condition (uncovered sensors, non-crosslinked multilayers, and crosslinked multilayers with and without IFN-γ supplemented in the culture medium). The xCELLigence instrument was configured as described in our previous works [96][33]. Briefly, the xCELLigence RTCA S16 was placed inside the incubator to allow the device to warm up for at least 2 hours before use. This step is to avoid any condensation on the station after starting the measurement stage. The RTCA S16 was set up to perform readings every 10 minutes for a period of 72 hours of cell culture.

3.2.10. Immunomodulatory factor expression of hMSCs on (HEP/PLL) multilayers

The hMSCs immunomodulatory factor expression was investigated by indoleamine 2, 3-dioxygenase (IDO) activity. In this regard, hMSCs (5000 cells/cm^2) with and without IFN-γ supplemented in culture medium were seeded on each condition prepared on a 24 well-plate. The IDO activity was measured after 6 days of culture (changing the cells medium each 2 days) as described in our previous works [97][94][33]. Briefly, 100 µL of cell supernatant was mixed with 100 µL standard assay mixture consists of (potassium phosphate buffer (50mM, pH 6.5), ascorbic acid (40 mM, neutralized with NaOH), catalase (200 µg/mL), methylene blue (20 µ M), and L-tryptophan (400 µM)). The mixture was kept at 37°C in a humidified incubator with 5% CO_2 for 30 minutes (in a dark environment to protect solutions from light) to allow IDO to convert L-tryptophan to N-formyl-kynurenine. After that, the reaction was stopped by adding 100 µL trichloroacetic acid 30% (w/vol) and incubated for 30 minutes at 58 °C. Then, 100 µL of mixed cell supernatant/standard transfer into a well of a 96-well microplate, following by adding 100 µL per well of 2% (w/v) p dimethylaminobenzaldehyde in acetic acid. Absorbance was read at 490 nm at the endpoint using a BioTek Synergy™ 2 spectrophotometer (Synergy LX Multi-Mode Reader from BioTek® Model SLXFA).

3.2.11. Cells differentiation assay

hMSCs differentiation was induced by their culture with differentiation media (Osteogenic and Adipogenic media). Control cultures were grown in regular cell expansion medium. Briefly, hMSCs (10000 cells/cm^2) were seeded on each condition prepared on 24 well-plates and grown for 6 days in expansion medium (MEM Alpha (1X) supplemented with L-glutamine, ribonucleosides, and deoxyribonucleosides) containing 20% fetal bovine serum, 1.2% penicillin-streptomycin, and 1.2% L-glutamine) at 37 °C in a humidified incubator with 5% CO_2. After the

cells reached at least 50% confluency, they were exposed to differentiation medium. For osteogenic differentiation, hMSCs were cultured in the differentiation medium (DMEM low glucose, 10% fetal bovine serum,1% penicillin, 1% L-Glutamin, 50 μM ascorbic acid (50mg/10ml), 10 mM β-glycerophosphate, and 100nM dexamethasone). The medium was replaced every 2-3 days. After 8 days of culture, cells were fixed with 10% formaldehyde. For osteogenic differentiation, Alizarin Red S staining solution was prepared by adding 2g Alizarin Red S in 100 mL water, mixed, and the pH was adjusted to 4.1– 4.3 by the addition of Ammonium Hydroxide, as necessary. Alizarin Red S solution was added to the fixed cells, then incubated at room temperature in the dark (cover with aluminum foil) for 15 minutes. The staining solution was removed and rinsed 3 times with PBS. The samples were analyzed immediately under the microscope to detect calcium deposits. For adipogenic differentiation, hMSCs were cultured in the differentiation medium consisting of DMEM high glucose supplemented with 10% fetal bovine serum, 1% penicillin, 1% L-glutamin, 1 μM dexamethasone, 0.01 mg/mL insulin, 0.5 mM 3-isobutyl-1-methylxanthine (IBMX), and 100μM indomethacin. The medium was replaced every 2-3 days. After 8 days of culture, cells were fixed with 10% formaldehyde, stained with 0.5% (w/v) Oil Red O in 100% isopropanol, and incubated at room temperature for 30 minutes and protected from light. The cell monolayer was washed 2 times with PBS. The sample was analyzed under a light microscope to detect lipid vesicles that appeared in bright red color.

3.2.12. Alkaline phosphatase (ALP) assay

To confirm osteogenic differentiation and to determine the level of activity of the differentiated hMSCs, two assays were performed: alkaline phosphatase (ALP) activity and total protein content (micro-BCA assay). Alkaline phosphatase activity was assessed using the Alkaline

Phosphatase Colorimetric Assay Kit. According to standard protocols, after the exposure of cells to osteogenic differentiation medium for 3 days, the samples were washed twice with PBS. Then, 50 μL of the cell lysate with assay buffer was added to a 96 well- plate and 50 μL p-nitrophenyl phosphate (pNPP). The samples incubate at 25°C for 60 minutes, protected from light. In the last step, 20 μL stop solution was added to the wells, then; the plate was read at 405 nm in a microplate reader (Synergy LX Multi-Mode Reader from BioTek® (Model SLXFA). ALP activity was normalized by total protein content (micro-BCA assay). The total protein content was determined according to the protocol of the manufacture 150 μL of the sample was placed in a 96 well-plate with 150 μL of working reagent made from a micro-BCA protein assay kit. The well plate was covered with foil and incubated at 37 °C for 2 hours. Absorbance was read at 562 nm using a BioTek Multi-Mode Microplate Reader (Model Synergy™ 2).

3.2.13. Statistical analysis

The results were presented as mean ± standard error of mean. Comparisons among multiple groups were performed by one-way analysis of variance (ANOVA). A p- value < 0.05 was considered statistically significant. The statistical analysis was done using SigmaPlot 14 software.

3.3. Results and Discussion

3.3.1. Surface characterization

The presence of heparin qualitatively determined by Azure A dye method based on study done by Klein et al. [141]. Figure 3-1 shows the absorbance values obtained for TCP, (HEP/PLL) multilayers, and (HEP/PLL) + CL multilayers samples. The color changed from blue to dark purple due to existence of heparin in the bottom of the TCP and (HEP/PLL) + CL. These changes indicate that amount of heparin on (HEP/PLL) + CL is higher than (HEP/PLL) and TCP

(p-value < 0.05). These findings comply with a study done by Richert et al. which showed that PLL and hyaluronic acid (PLL/HA) multilayers have an exponential growth that occurred by PLL diffusion into the layers. However, Richert et al. showed that in crosslinked (PLL/HA) multilayers, the diffusion of the PLL was vanished [142]. The absorbance shows that (HEP/PLL) + CL have two times higher absorbance than (HEP/PLL) which confirms the changing of colors from light purple to dark purple. This result comply with our previous study done by Pinzon-Herrera et al. which showed the increase in absorbance from 1 to 6 bilayers of heparin/collagen multilayers as measured using Taylor's Blue dye [96].

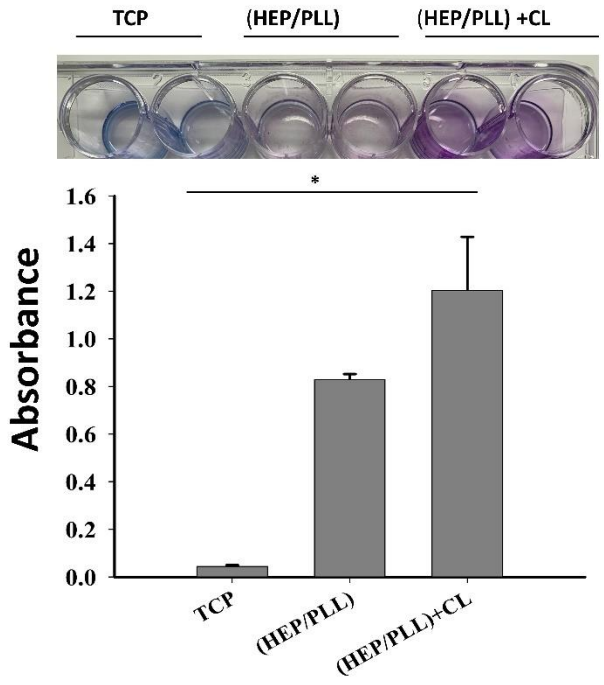

Figure 3-1. Absorbance for Azure A dye solution applied to TCP, (HEP/PLL) multilayers, and (HEP/PLL) + CL multilayers.

The formation of the (HEP/PLL) multilayers was monitored by QCM-D. QCM-D detects the resonant frequency shift (Δf) and measures the dissipation factor (ΔD) [102]. QCM-D was used here to investigate physical structures such as adsorbed mass and viscoelastic properties of

multilayers [102] [143]. Figure 3-2 shows the normalized frequency shift ($-\Delta f_n/n$) and dissipation ($\Delta D/n$) for the 3rd, 4th, and 7th overtones for the (HEP/PLL) and (HEP/PLL) + CL multilayers. The first 15 minutes correspond to a PEI absorption, followed by a 3 minutes rinsing step are shown in Figure 3-2 . The increase in $-\Delta f$ and ΔD of every (HEP/PLL) sequential deposition shows that the multilayers slowly deposit onto the quartz crystal [104]. According to Boulmedais et al. this increase can be considered an exponential increase of thickness for the multilayers [144]. This indicates that at least one of the two components of the multilayers is diffusing within the multilayers as proposed by Picart et al [145]. It is demonstrated that by increasing of $-\Delta f$ the mass of deposited multilayers enhanced, whereas the increase of ΔD enhances the viscoelastic structure of the deposited multilayers [103]. Therefore, adding a rough layer on quartz crystal has a lower $-\Delta f$, whereas a dense layer has a higher ΔD value. When HEP is deposited, $-\Delta f$ and ΔD have a sharp rise with great dispersion between different overtones in both (HEP/PLL) + CL and (HEP/PLL). This indicates that the HEP is a loose and swollen layer. In contrast, the PLL deposited shows not only a slight increase in $-\Delta f$ but also slight decrease in ΔD. This may occur because of the PLL diffused within the multilayers. In addition, the frequency shifts do not overlap for the different overtones not only in the rinse steps but also during the adsorption steps. Consequently, this indicates that the Sauerbrey relation is not valid for determining the film mass during rinse and adsorption steps, which indicates that the multilayers are more viscoelastic. Besides, the ratio of the change during the rinse and the adsorption steps in the dissipation factor to the change in frequency ($\Delta D/(-\Delta f/n)$) remains higher than 4×10^{-7} $Hz^{-}1$; therefore, the film can be considered soft based on study done by Reviakine et al [105]. After adsorption of the crosslinking solution, the frequency shifts no longer overlap. This indicates that adsorbed films are viscoelastic and that the mass does not follow the

Sauerbrey relationship anymore, so a more complex model might be used to determine the adsorbed mass from the frequency shift and dissipation data [106]. Figure 3-2 (A&C) show crosslinking solution absorbed on multilayers by increasing of the frequency shift and dissipation shift. Based on study done by Niepel et al. the increase of the frequency shift and dissipation shift by adding the crosslinking solutions, increase the roughness of the multilayers [137].

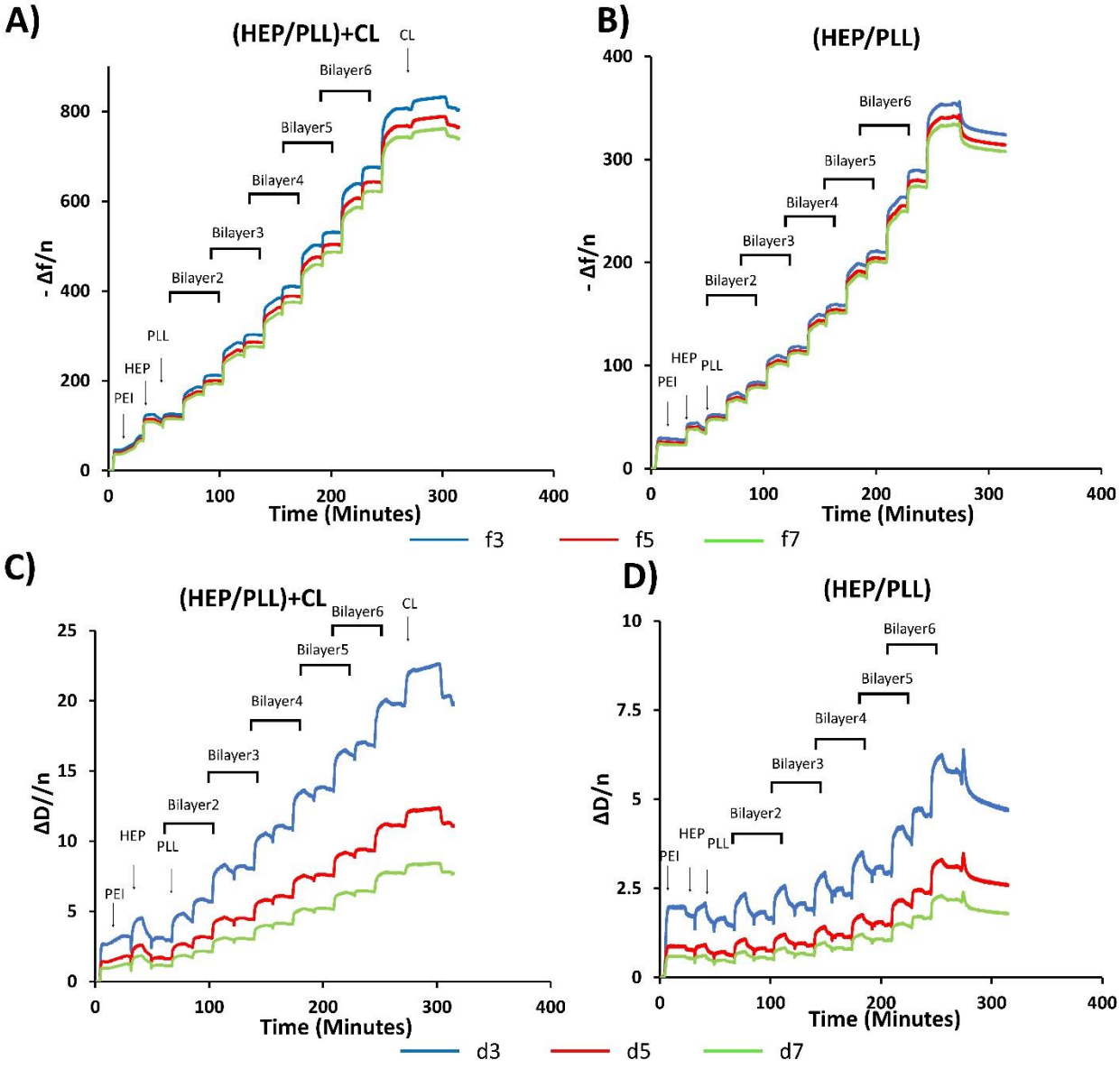

Figure 3-2. QCM-D data showing the normalized frequency shift & dissipation shift as a function of time for the 3rd, 5th, and 7th overtones during the construction of the HEP/PLL

multilayers with IFN-γ, with alternating 3-minute rinse and 5 minutes adsorption intervals. A&B: shows the normalized frequency shift. C&D: shows the normalized dissipation shift. Note that we use -Δf for a clear representation of the results**Error! Reference source not found.**.

The elemental composition obtained by XPS of (HEP/PLL) and (HEP/PLL) + CL are represented in Figure *3-3*. High resolution XPS spectra of C1s (283.4 eV), N1s (398.4 eV), O1s (529.8 eV), and S2P (168.3 eV) are shown in **Error! Reference source not found.**Na and S were mainly the characteristic elements of HEP polysaccharide structure possessing carbonyls (COO^-), sulphate($-SO4^-$), and hydroxyl group (-OH), while PLL contains a large number of various amino (NH_2) group and carboxyl group (-COOH) [109]. The presence of more sulfur was detected on the multilayers revealed the presence of HEP [110]. The increase of sulfur peak due to increasing the number of layers shows a successful deposition of HEP. This finding complies with a previous study by Almodovar et al. [112]. The high-resolution C1s and N1s spectrum indicates the presence of several different chemical species such as amide (288.3 eV and 400.6 eV) [146]. The crosslinking solution reacted with carboxylate groups of HEP and the amino groups of PLL and results in the formation of amide bonds [147]. Moreover, O1s, S2p, C1s, and N1s intensity content decrease in (HEP/PLL) + CL compared to (HEP/PLL), indicating that the presence of the crosslinked multilayers by interacting the amine groups of PLL with the sulfate groups of HEP [148]. These findings confirm the results from colorimetric determination of heparin deposited within (HEP/PLL) multilayers.

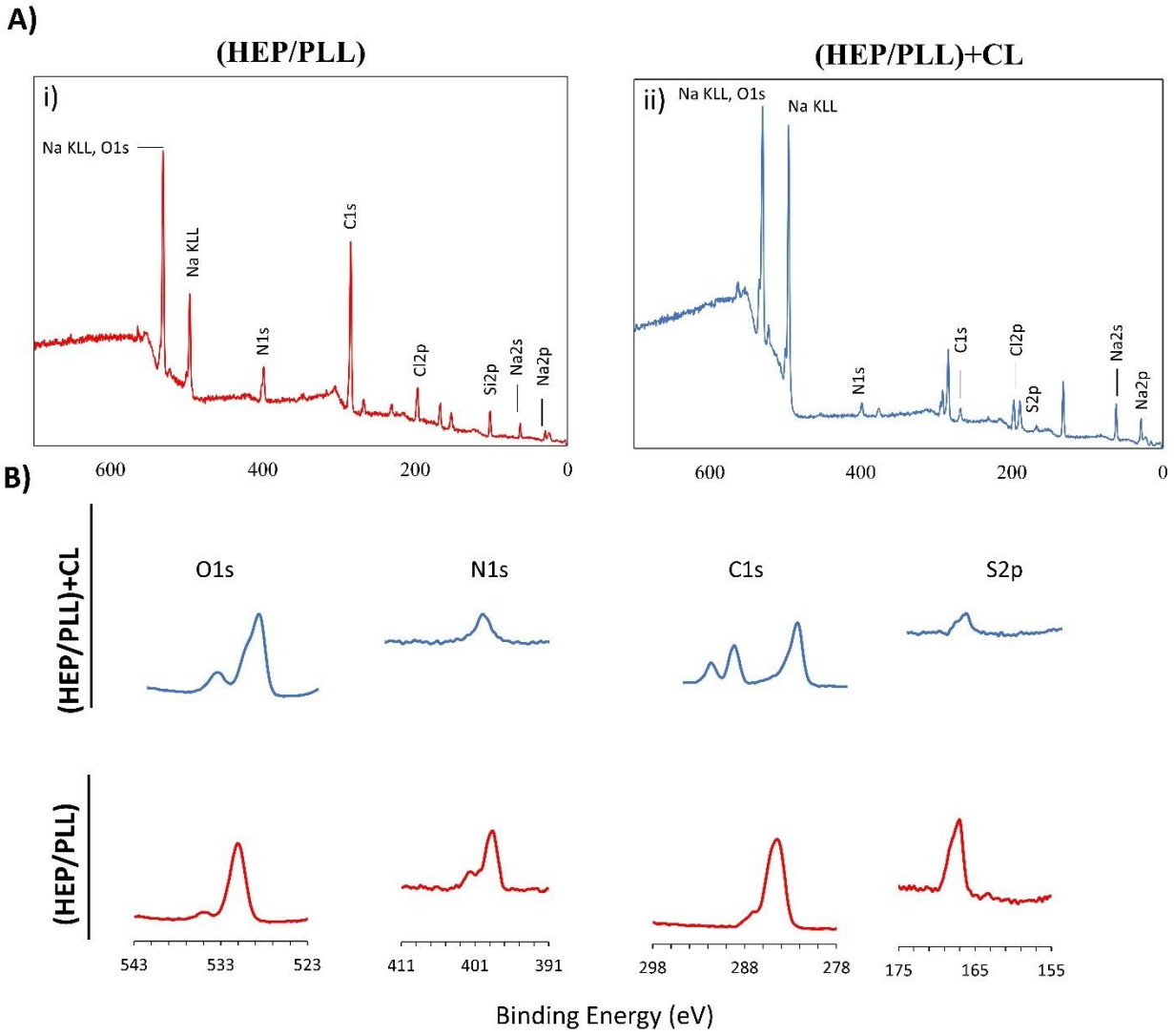

Figure 3-3. Chemical properties of the multilayers of (HEP/PLL) as measured by The XPS broad spectra and high-resolution XPS. (**A)**: XPS survey scan spectrum of (HEP/PLL) and (HEP/PLL) + CL multilayers. **(B):** the corresponding specific spectrum of elemental (HEP/PLL) and (HEP/PLL) + CL multilayers.

3.3.2. PrestoBlue viability assay

The PrestoBlue reagent was used for measuring cell viability after 3 days of culturing hMSCs cells on TCP, (HEP/PLL), and (HEP/PLL) + CL with and without IFN-γ supplemented in the

cell culture medium. In the absence of the IFN-γ in culture medium, TCP were selected as the positive control, and its fluorescence intensity was normalized to 100%. All other conditions were assessed in relation to the positive control. Figure 3-4 (A) shows (HEP/PLL) +CL without IFN-γ has the same viability of the cells compared to TCP, and (HEP/PLL) + CL with IFN-γ has a higher viability about 125% compared to TCP. However, (HEP/PLL) with and without IFN-γ have about 48% (less than half) viability compared to TCP. These findings show that the (HEP/PLL) decrease cell viability. A study done by V. Semenov et al. showed an increase in cell adhesion and growth when using high concentration of crosslinker on (PLL/HA) multilayers [147] which may related to increase in roughness of multilayers. However, (HEP/PLL) + CL have a better ability to increase the cell viability. Figure 3-4 (A) shows significant differences in cell viability on (HEP/PLL) + CL with IFN-γ compared to without IFN-γ (p-value < 0.05) which indicates presence of the IFN-γ supplemented in the culture medium has a considerable impact on the conditions with (HEP/PLL) + CL; suggesting that there is a synergistic action of both components. These findings confirm our previous study done by Cifuentes et al. in which they used collagen instead of PLL as polycation polymer in heparin/collagen multilayers [94].

We performed a similar study using hMSCs from another donor (donor 2). Regarding the cell viability of donor 2, TCP with IFN-γ has a decrease about 20% compared to the TCP without the IFN-γ (p-value<0.001) (Supplementary Information Figure S3.1(A)). Also, Figure S3.1(A) indicates that there are approximately 25% decrease of the cell viability on the surfaces (HEP/PLL) + CL with and without the IFN-γ compared to the TCP. However, donor 1 shows a higher viability when cells supplemented with IFN-γ which can attribute to the different behavior of donors. Also, the cell viability on the (HEP/PLL) for donor 2 decrease below 50%.

Fluorescence microscopy images of hMSCs nuclei labeled with Hoechst of cells attached to the different surfaces after 72 hours validate the findings about cell viability for both donors Figure 3-4.(D) and Supplementary Information Figure S3.1(B)). It is clear that there is less cell attachment on (HEP/PLL) for both donors.

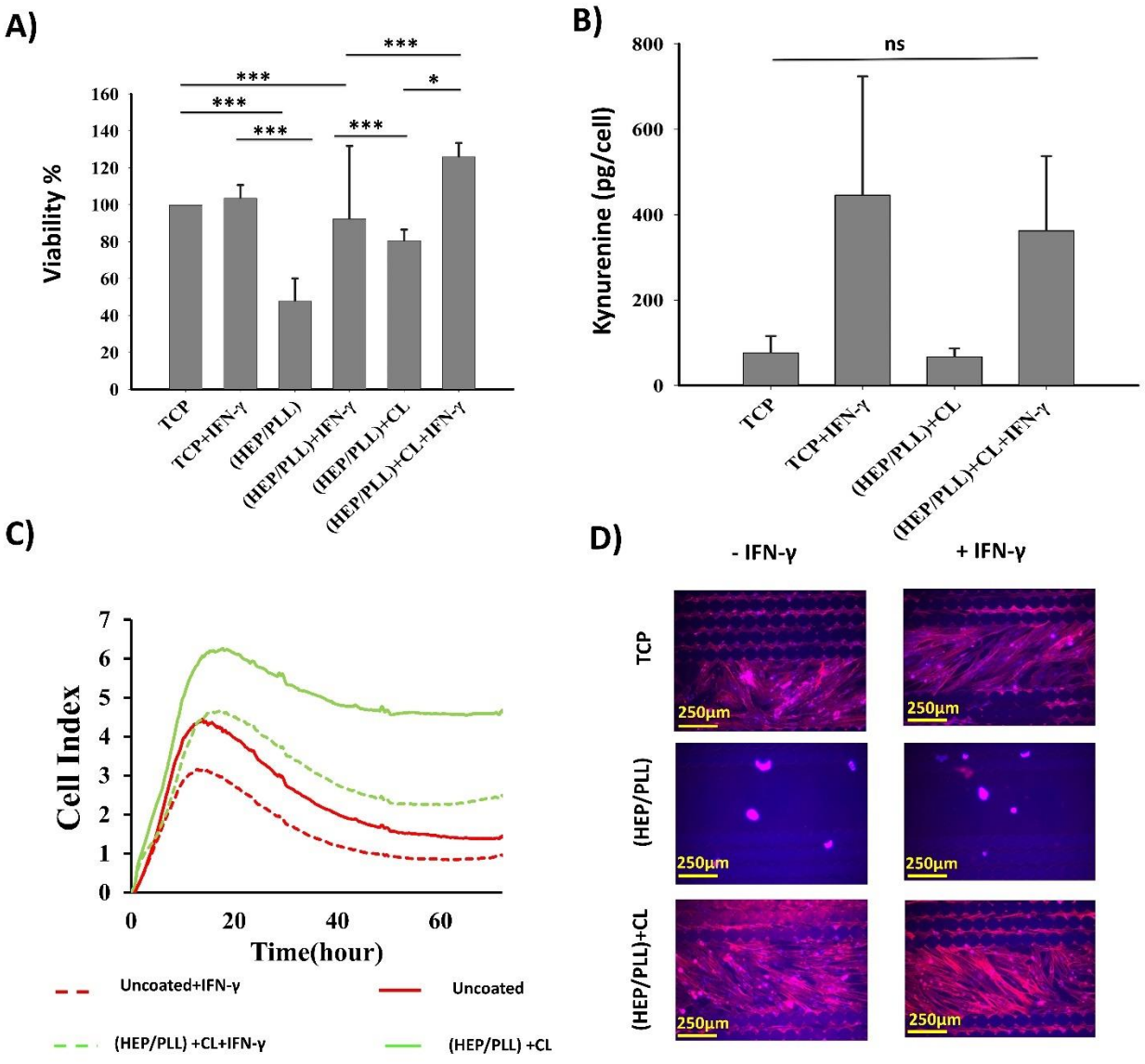

Figure 3-4. **Error! Reference source not found.**

3.3.3. Real-time monitoring of cell behavior and proliferation

In this study, we cultured hMSCs at 25000 cells/cm^2 on TCP, (HEP/PLL), and (HEP/PLL) + CL with and without IFN-γ supplemented in the cell culture medium to evaluate the real-time behavior of the cells during the first 72 hours of culture. The action of presence of the IFN-γ in the cell medium was also evaluated. As a control surface, we evaluated growth on uncoated (TCP) biosensors. An xCELLigence RTCA S16 biosensor system was used, which allows the measurement of cell proliferation and growth. This system constantly measures the impedance difference caused by cells attached to microsensors present in culture plates (E-plates 16) and is monitored by microchips attached under the wells. In this way, the impedance difference is translated into a parameter known as the Cell Index (CI). Therefore, the higher the CI, the greater the number of cells adhered to the bottom of the well [96]. Based on our previous study, the results indicate two phases in the cell behavior: cells adhesion and cell proliferation phases, after 30 hours and between 30-72 hours of culture, respectively [96].

Figure 3-4 (C) shows the CI values as a function of the first 72 hours of culture for the 6 experimental conditions for donor 1. Donor 1 shows a slow cell adhesion stage in the evaluated period, and it reaches a maximum peak around 18 hours. CI values reached a maximum of 6 CI units. Compared to the uncoated sensor without the IFN-γ, cell adhesion has three times higher CI value on (HEP/PLL) + CL without the IFN-γ. In addition, there is no detectable cell adhesion on (HEP/PLL) which confirm our results in cell viability. Regarding the anti-proliferative effect of the IFN-γ on hMSCs, (HEP/PLL) + CL with and without the IFN-γ show to be efficient compared to the uncoated surfaces. This finding indicates that the (HEP/PLL) + CL do not negatively affect hMSCs growth.

3.3.4. Intracellular IDO assay

Indoleamine 2,3-dioxygenase (IDO) is a cytosolic heme protein that is important for immuno-regulatory functions [120][149]. It can be determined by measuring the amino acid kynurenine (pg/cell)), which is known to be a catalyzer to convert L-tryptophan to kynurenine [120] [121]. The ability of IFN-γ to induce IDO expression in hMSCs was compared on TCP, and (HEP/PLL) + CL with and without IFN-γ supplemented in the cell culture medium after 6 days. The results of (HEP/PLL) are not shown because of the cells adhesion limitation (based on the results from cell viability and cells adhesion). Results for IDO activity are summarized in Figure 3-4 (B), which shows that for donor 1, all surfaces with IFN-γ (including TCP, and (HEP/PLL) + CL) have approximately five times a higher level of the IDO activity among surfaces without IFN-γ. Donor 2 shows that the IDO activity on TCP+ IFN-γ increases by adding IFN-γ in cell medium compared to TCP (Supplementary Information Figure S3.1(C)). In addition, the IDO activity on (HEP/PLL) + CL with IFN-γ has a higher activity compared to the (HEP/PLL) + CL without IFN-γ. These results comply with study done by Kwee et al. indicating the IDO activity corelated with amount of IFN-γ [126].

Regarding the (HEP/PLL) + CL (with and without IFN-γ), donor 1 and donor 2 both show a decrease in amount of IDO activity compared to the TCP and TCP + IFN-γ, respectively. These finding may indicate that both donors show that using the (HEP/PLL) +CL does not affect the level of the IDO activity in reference to the same amount of the IDO expression for the TCP and (HEP/PLL) + CL without IFN-γ. These in vitro studies indicate that the level of the IDO depends on not only the different donor's response but also IFN-γ and the multilayers influence the IDO expression. This result is in line with the study done by Cifuentes et al. [94] that showed the IFN-γ is the key regulator of the IDO activity on heparin/collagen multilayers.

3.3.5. Cells differentiation assay

The ability of hMSCs to differentiate into osteogenic and adipogenic lineages cells was induced by supplementing the growth media with differentiation media. The differentiation ability of hMSCs was evaluated to confirm the multipotentiality of hMSCs culturing on TCP, (HEP/PLL), and (HEP/PLL) + CL with and without IFN-γ supplemented in the cell culture medium. After 10 days of incubation, cell functions associated with osteoblast differentiation (ALP activity, calcium deposition) and adipogenic differentiation were evaluated. Mineralization was also characterized from microscope images. The impact of presence of the IFN-γ in the cell medium was also evaluated.

Figure 3-5 (A) shows that there are areas visible with red and purple, indicating the formation of the calcified regions and adipocyte-like cells, respectively. Figure 3-5 (A) shows that cells on (HEP/PLL) expressed no staining due to lack of cells adhesion on (HEP/PLL). However, hMSCs cultured on TCP, and (HEP/PLL) + CL shows an increase in the size of calcium deposits formed by the clustering of cells due to the strong staining with Alizarin red, which indicates osteogenic differentiation of cells. The same results were found for donor 2, as shown in Supplementary Information Figure S3.2 (A). Also, Figure 3-6 shows that the hMSCs on TCP, and (HEP/PLL) + CL has the ability to differentiate to adipogenic cells, which the cells changed from long spindle-shaped to flattened round, or polygonal cells Figure 3-6 (B) and Supplementary Information Figure S3.2 (B). In addition, Figure *3-5* (A) & Figure 3-6 show the treatment with IFN-γ had no inhibitory effect on both the osteogenic and adipogenic differentiation of hMSCs. No staining was observed on cells cultured in regular expansion medium, as shown in Supplementary Information Figure S3.3.

ALP is an enzyme present in bone-related cells and is considered key to mineralization [130]. Its activity is related to the level of inorganic phosphate, a component of the bone mineral phase [131]. Therefore, ALP activity has been considered as an early indicator of osteoblast differentiation. Results for ALP activity are summarized in Figure 3-5 (B) Error! Reference source not found.. Also, ALP activity of undifferentiation cells is considered as controls. Regarding donor 1, (HEP/PLL) + CL with and without IFN-γ showed enhanced intracellular levels of ALP as compared to TCP. Also, the TCP and (HEP/PLL) + CL multilayer surfaces with IFN-γ have a higher ALP activity than the surfaces without IFN-γ. Similarly, donor 2 shows that (HEP/PLL) + CL without IFN-γ has a slightly higher ALP activity compared to TCP. However, (HEP/PLL) + CL with IFN-γ shows the same ALP activity compared to TCP, and less activity compared to the (HEP/PLL) + CL without IFN-γ Supplementary Information Figure S3.2 (C). Also, TCP with IFN-γ supplemented on cells medium shows a higher ALP activity compared to the TCP without IFN-γ. These in vitro studies indicate that IFN-γ can improve the intercellular level of ALP activity. Also, the study done by C. Lamoury et al. indicated that IFN-γ resulted in affecting osteogenic differentiation of both mouse and human MSCs [6]. As well, the study done by V. Semenov et al. [147] show that crosslinking multilayers improve the cells differentiation compared to the non-crosslinked multilayers. Furthermore, these findings show that the differentiation of hMSCs may affected by donor's behavior, so differentiation of hMSCs need more studies.

The undifferentiated hMSCs controls (cultured in hMSCs growth medium) displayed no staining. However, cells show good differentiation on TCP and (HEP/PLL) + CL not only without IFN-γ but also with IFN-γ. These can indicate that the appearance of the IFN-γ and crosslinked multilayers do not suppress cells differentiation.

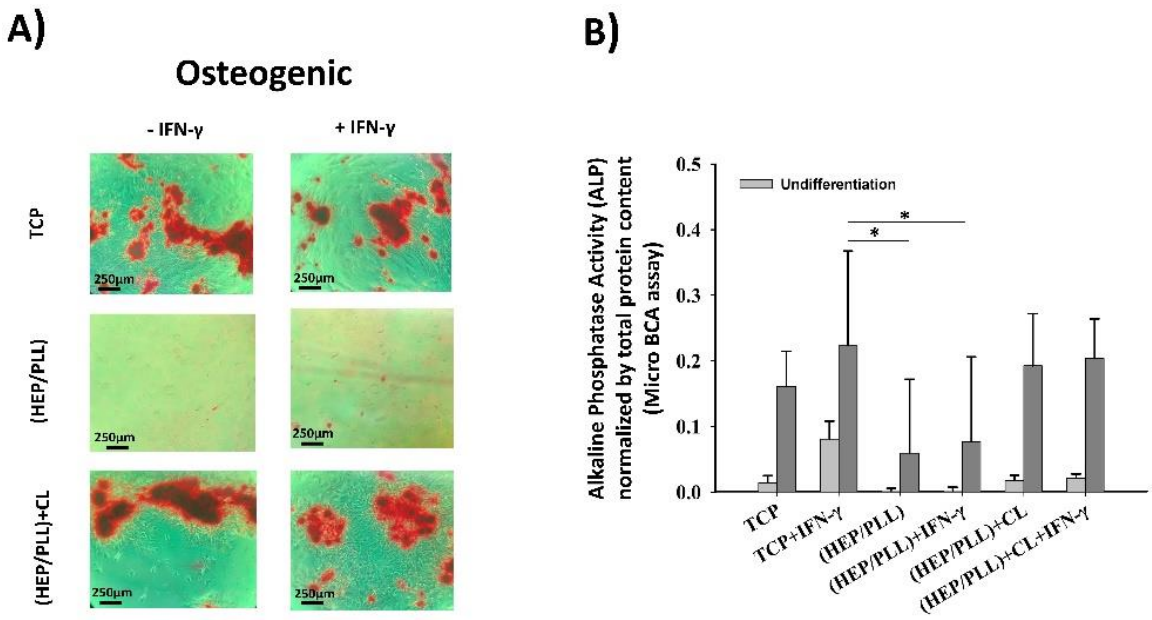

Figure 3-5. hMSCs differentiation donor 1. **(A):** Osteogenic differentiations were stained by Alizarin Red. **(B):** Alkaline phosphatase (ALP) assays were performed after of induced osteogenesis on TCP and (HEP/PLL) + CL multilayers. Data are presented as the mean ± standard deviation of n = 4 samples. The p-values < 0.05 are represented by *, p-values < 0. 01 by **, p-values < 0. 001 by *** and p-values < 0.0001 by ****.**Error! Reference source not found.**

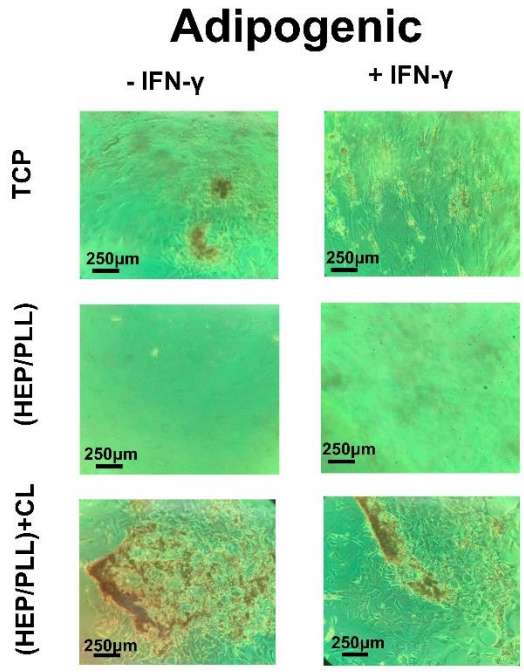

Figure 3-6. hMSCs differentiation donor 1. Adipogenic differentiation were stained by Oil Red.

3.4. Conclusion

This study demonstrates that polyelectrolyte multilayers made of heparin and poly(L-lysine) were successfully built up using the layer-by-layer assembly method. QCM, XPS, and Azure A results demonstrate the construction of the multilayers, and the changes it undergoes after chemical crosslinking. Also, this study evaluated the effect of crosslinked (HEP/PLL) multilayers on the growth and immunosuppressive properties of hMSCs. It shows that (HEP/PLL) + CL have a better cells growth, adhesion, proliferation, differentiation, and immunomodulatory properties compared to the (HEP/PLL). In addition, the (HEP/PLL) + CL show better cell viability compared to the tissue plastic culture even in presence of IFN-γ. However, (HEP/PLL) + CL show less immunomodulatory properties. In contrast to our previous study, we noticed that heparin/collagen multilayers have great stimulation on the protein

expression, immunomodulator factor expression, and adhesion of hMSCs compared to the issue plastic culture. We believe that tissue culture plastic reduces the therapeutic potential of hMSCs due to the lack of extracellular matrix components. Furthermore, ECM components effect the cellular immunomodulator factor, differentiation, and growth. In the future, we need to investigate on (HEP/PLL) + CL to have a better understanding of the modulatory response of hMSCs to soluble factors, which may improve hMSCs-based therapies aimed at treating several immune diseases and the cell manufacturing process.

3.5. Acknowledgement

The authors greatly appreciate the use of the Arkansas Nano & Biomaterials Characterization Facility for use of the XPS. The authors greatly appreciate Dr. Greenlee and Sergio Ivan Perez Bakovic from the University of Arkansas for equipment access and help during quartz crystal microbalance (QCM) measurements. The authors greatly appreciate Frank Omar Aparicio Solis and Trong Nguyen for help in construct the multilayers via LbL method.

Statement of Ethics

This work did not need approval from an ethic committee.

Conflict of Interest

The authors have no conflicts of interest to declare.

Funding Sources

This work was financially supported in part by the National Science Foundation under grant no. 2051582, by the Arkansas Bioscience Institute.

Author Contributions

Mahsa Haseli: The LbL multilayers, XPS, QCM-D, Cell Culture, Cells viability Real-time monitoring of hMSCs, Immunomodulatory factor expression, Differentiation, experiments, Data analyses, Data curation and writing-original draft preparation, Figure preparation.

Luis Pinzon-Herrera: Qualitative colorimetric determination of heparin and data curation.

Jorge Almodovar: Conceptualization, supervision, writing-reviewing and editing, resources, funding acquisition, project administration.

Data Availability Statement

All data generated or analysed during this study are included in this article. Further enquiries can be directed to the corresponding author.

3.6. References

[1] A. Khademhosseini, Y. Du, B. Rajalingam, J. P. Vacanti, and R. S. Langer, "Microscale technologies for tissue engineering," *Adv. Tissue Eng.*, vol. 103, no. 8, pp. 349–369, 2008, doi: 10.1142/9781848161832_0017.

[2] T. Cordonnier, J. Sohier, P. Rosset, and P. Layrolle, "Biomimetic materials for bone tissue engineering - State of the art and future trends," *Adv. Eng. Mater.*, vol. 13, no. 5, pp. 135–150, 2011, doi: 10.1002/adem.201080098.

[3] A. Uccelli, L. Moretta, and V. Pistoia, "Mesenchymal stem cells in health and disease," *Nat. Rev. Immunol.*, vol. 8, no. 9, pp. 726–736, 2008, doi: 10.1038/nri2395.

[4] F. Gao *et al.*, "Mesenchymal stem cells and immunomodulation: Current status and future prospects," *Cell Death Dis.*, vol. 7, no. 1, 2016, doi: 10.1038/cddis.2015.327.

[5] M. W. Klinker, R. A. Marklein, J. L. Lo Surdo, C. H. Wei, and S. R. Bauer, "Morphological features of IFN-γ-stimulated mesenchymal stromal cells predict overall immunosuppressive capacity," *Proc. Natl. Acad. Sci. U. S. A.*, vol. 114, no. 13, pp. E2598–E2607, 2017, doi: 10.1073/pnas.1617933114.

[6] J. Croitoru-Lamoury *et al.*, "Interferon-γ regulates the proliferation and differentiation of mesenchymal stem cells via activation of indoleamine 2,3 dioxygenase (IDO)," *PLoS One*, vol. 6, no. 2, 2011, doi: 10.1371/journal.pone.0014698.

[7] D. A. Castilla-Casadiego, J. R. García, A. J. García, and J. Almodovar, "Heparin/Collagen Coatings Improve Human Mesenchymal Stromal Cell Response to Interferon Gamma," *ACS Biomater. Sci. Eng.*, vol. 5, no. 6, pp. 2793–2803, 2019, doi: 10.1021/acsbiomaterials.9b00008.

[8] F. M. Watt and W. T. S. Huck, "Role of the extracellular matrix in regulating stem cell

fate," *Nat. Rev. Mol. Cell Biol.*, vol. 14, no. 8, pp. 467–473, 2013, doi: 10.1038/nrm3620.

[9] R. O. Hynes, "The extracellular matrix: not just pretty fibrils," *Science (80-.).*, vol. 326, no. 5957, pp. 1216–1219, 2009, doi: 10.1126/science.1176009.

[10] H. Ozcelik *et al.*, "Cell Microenvironment Engineering and Monitoring for Tissue Engineering and Regenerative Medicine : The Citation Accessed Citable Link Cell Microenvironment Engineering and Monitoring for Tissue Engineering and Regenerative Medicine : The Recent Advances," *Biomed Res. Int.*, vol. 2014, no. i, pp. 1–18, 2014.

[11] J. Cuerquis *et al.*, "Human mesenchymal stromal cells transiently increase cytokine production by activated T cells before suppressing T-cell proliferation: Effect of interferon-γ and tumor necrosis factor-α stimulation," *Cytotherapy*, vol. 16, no. 2, pp. 191–202, 2014, doi: 10.1016/j.jcyt.2013.11.008.

[12] T. J. Kean, P. Lin, A. I. Caplan, and J. E. Dennis, "MSCs: Delivery routes and engraftment, cell-targeting strategies, and immune modulation," *Stem Cells Int.*, vol. 2013, 2013, doi: 10.1155/2013/732742.

[13] H. Lortat-Jacob, "The molecular basis and functional implications of chemokine interactions with heparan sulphate," *Curr. Opin. Struct. Biol.*, vol. 19, no. 5, pp. 543–548, 2009, doi: 10.1016/j.sbi.2009.09.003.

[14] M. F. Brizzi, G. Tarone, and P. Defilippi, "Extracellular matrix, integrins, and growth factors as tailors of the stem cell niche," *Curr. Opin. Cell Biol.*, vol. 24, no. 5, pp. 645–651, 2012, doi: 10.1016/j.ceb.2012.07.001.

[15] E. Fuchs, T. Tumbar, and G. Guasch, "Socializing with the neighbors: Stem cells and their niche," *Cell*, vol. 116, no. 6, pp. 769–778, 2004, doi: 10.1016/S0092-8674(04)00255-7.

[16] K. A. Moore and I. R. Lemischka, "Stem cells and their niches," *Science (80-.).*, vol. 311, no. 5769, pp. 1880–1885, 2006, doi: 10.1126/science.1110542.

[17] T. A. Wilgus, "Growth Factor–Extracellular Matrix Interactions Regulate Wound Repair," *Adv. Wound Care*, vol. 1, no. 6, pp. 249–254, 2012, doi: 10.1089/wound.2011.0344.

[18] O. Saksela and M. Laiho, "Growth factors and the extracellular matrix," *Duodecim.*, vol. 106, no. 3, pp. 297–306, 1990, doi: 10.1096/fasebj.11.1.9034166.

[19] M. Khan, "Human mesenchymal stem cells," *Hum. Mesenchymal Stem Cells*, vol. 1416, no. Cmc, pp. 1–127, 2021, doi: 10.1016/s0141-0229(97)83511-9.

[20] V. Poltavets, M. Kochetkova, S. M. Pitson, and M. S. Samuel, "The role of the extracellular matrix and its molecular and cellular regulators in cancer cell plasticity," *Front. Oncol.*, vol. 8, no. OCT, pp. 1–19, 2018, doi: 10.3389/fonc.2018.00431.

[21] A. R. Shelke Roscoe, J. A. , Morrow, G. R. , Colman, L. K. , Banerjee, T. K. , & Kirshner, J. J., "Paracrine and autocrine signals induce and maintain mesenchymal and stem cell states in the breast," *Bone*, vol. 23, no. 1, pp. 1–7, 2008, doi: 10.1016/j.cell.2011.04.029.Paracrine.

[22] P. Zandstra, E. Jervis, D. Kilburn, C. Eaves, and J. Pirel, "Concentration-dependent

internalization of a cytokine/cytokine receptor complex in human hematopoietic cells," *Exp. Hematol.*, vol. 26, no. 8, p. 720, 1998, doi: 10.1002/(sici)1097-0290(19990520)63:4<493::aid-bit13>3.3.co;2-s.

[23] X. Zhao, Q. Li, Z. Guo, and Z. Li, "Constructing a cell microenvironment with biomaterial scaffolds for stem cell therapy," *Stem Cell Res. Ther.*, vol. 12, no. 1, pp. 1–13, 2021, doi: 10.1186/s13287-021-02650-w.

[24] A. Kumari, S. K. Yadav, and S. C. Yadav, "Biodegradable polymeric nanoparticles based drug delivery systems," *Colloids Surfaces B Biointerfaces*, vol. 75, no. 1, pp. 1–18, 2010, doi: 10.1016/j.colsurfb.2009.09.001.

[25] S. Martino, F. D'Angelo, I. Armentano, J. M. Kenny, and A. Orlacchio, "Stem cell-biomaterial interactions for regenerative medicine," *Biotechnol. Adv.*, vol. 30, no. 1, pp. 338–351, 2012, doi: 10.1016/j.biotechadv.2011.06.015.

[26] X. Zhao, K. Cui, and Z. Li, "The role of biomaterials in stem cell-based regenerative medicine," *Future Med. Chem.*, vol. 11, no. 14, pp. 1779–1792, 2019, doi: 10.4155/fmc-2018-0347.

[27] E. For, "Enabling Technologies for Cell-Based Clinical Translation E NABLING T ECHNOLOGIES FOR C ELL -B ASED C LINICAL T RANSLATION Increased Survival and Function of Mesenchymal Stem Cell Spheroids Entrapped in Instructive Alginate Hydrogels," pp. 1–9, 2016.

[28] M. J. Landry, F. G. Rollet, T. E. Kennedy, and C. J. Barrett, "Layers and Multilayers of Self-Assembled Polymers: Tunable Engineered Extracellular Matrix Coatings for Neural Cell Growth," *Langmuir*, vol. 34, no. 30, pp. 8709–8730, 2018, doi: 10.1021/acs.langmuir.7b04108.

[29] V. Gribova, R. Auzely-Velty, and C. Picart, "Polyelectrolyte multilayer assemblies on materials surfaces: From cell adhesion to tissue engineering," *Chem. Mater.*, vol. 24, no. 5, pp. 854–869, 2012, doi: 10.1021/cm2032459.

[30] C. Picart *et al.*, "Primary cell adhesion on RGD-functionalized and covalently crosslinked thin polyelectrolyte multilayer films," *Adv. Funct. Mater.*, vol. 15, no. 1, pp. 83–94, 2005, doi: 10.1002/adfm.200400106.

[31] C. Picart, "Polyelectrolyte Multilayer Films: From Physico-Chemical Properties to the Control of Cellular Processes," *Curr. Med. Chem.*, vol. 15, no. 7, pp. 685–697, 2008, doi: 10.2174/092986708783885219.

[32] P. Gentile, I. Carmagnola, T. Nardo, and V. Chiono, "Layer-by-layer assembly for biomedical applications in the last decade," *Nanotechnology*, vol. 26, no. 42, p. 422001, 2015, doi: 10.1088/0957-4484/26/42/422001.

[33] D. A. Castilla-Casadiego *et al.*, "Methods for the Assembly and Characterization of Polyelectrolyte Multilayers as Microenvironments to Modulate Human Mesenchymal Stromal Cell Response," *ACS Biomater. Sci. Eng.*, vol. 6, no. 12, pp. 6626–6651, 2020, doi: 10.1021/acsbiomaterials.0c01397.

[34] O. Guillaume-Gentil, O. V. Semenov, A. H. Zisch, R. Zimmermann, J. Vörös, and M.

Ehrbar, “PH-controlled recovery of placenta-derived mesenchymal stem cell sheets,” *Biomaterials*, vol. 32, no. 19, pp. 4376–4384, 2011, doi: 10.1016/j.biomaterials.2011.02.058.

[35] J. Chen, C. Chen, Z. Chen, J. Chen, Q. Li, and N. Huang, “Collagen/heparin coating on titanium surface improves the biocompatibility of titanium applied as a blood-contacting biomaterial,” *J. Biomed. Mater. Res. - Part A*, vol. 95 A, no. 2, pp. 341–349, 2010, doi: 10.1002/jbm.a.32847.

[36] A. Tchobanian, H. Van Oosterwyck, and P. Fardim, “Polysaccharides for tissue engineering: Current landscape and future prospects,” *Carbohydr. Polym.*, vol. 205, pp. 601–625, 2019, doi: 10.1016/j.carbpol.2018.10.039.

[37] B. W. Kim, *Clinical regenerative medicine in urology*. 2017.

[38] A. K. Nayak, S. A. Ahmed, M. Tabish, and M. S. Hasnain, *Natural polysaccharides in tissue engineering applications*. Elsevier Inc., 2019.

[39] M. S. Douglas, D. A. Rix, J. H. Dark, D. Talbot, and J. A. Kirby, “Examination of the mechanism by which heparin antagonizes activation of a model endothelium by interferon-gamma (IPN-γ),” *Clin. Exp. Immunol.*, vol. 107, no. 3, pp. 578–584, 1997, doi: 10.1046/j.1365-2249.1997.3141206.x.

[40] S. Sarrazin, D. Bonnaffé, A. Lubineau, and H. Lortat-Jacob, “Heparan sulfate mimicry: A synthetic glycoconjugate that recognizes the heparin domain of interferon-γ inhibits the cytokine activity,” *J. Biol. Chem.*, vol. 280, no. 45, pp. 37558–37564, 2005, doi: 10.1074/jbc.M507729200.

[41] S. J. Paluck, T. H. Nguyen, and H. D. Maynard, “Heparin-Mimicking Polymers: Synthesis and Biological Applications,” *Biomacromolecules*, vol. 17, no. 11, pp. 3417–3440, 2016, doi: 10.1021/acs.biomac.6b01147.

[42] J. Dinoro *et al.*, “Sulfated polysaccharide-based scaffolds for orthopaedic tissue engineering,” *Biomaterials*, vol. 214, no. December 2018, p. 119214, 2019, doi: 10.1016/j.biomaterials.2019.05.025.

[43] H. Lortat-Jacob, F. Baltzer, and J. A. Grimaud, “Heparin decreases the blood clearance of interferon-γ and increases its activity by limiting the processing of its carboxyl-terminal sequence,” *J. Biol. Chem.*, vol. 271, no. 27, pp. 16139–16143, 1996, doi: 10.1074/jbc.271.27.16139.

[44] D. L. Kusindarta and H. Wihadmadyatami, “The Role of Extracellular Matrix in Tissue Regeneration,” *Tissue Regen.*, 2018, doi: 10.5772/intechopen.75728.

[45] G. A. Di Lullo, S. M. Sweeney, J. Körkkö, L. Ala-Kokko, and J. D. San Antonio, “Mapping the ligand-binding sites and disease-associated mutations on the most abundant protein in the human, type I collagen,” *J. Biol. Chem.*, vol. 277, no. 6, pp. 4223–4231, 2002, doi: 10.1074/jbc.M110709200.

[46] S. C. Shukla, A. Singh, A. K. Pandey, and A. Mishra, “Review on production and medical applications of e-polylysine,” *Biochem. Eng. J.*, vol. 65, pp. 70–81, 2012, doi: 10.1016/j.bej.2012.04.001.

[47] O. F. Blood and C. T. O. Connective, “PHYSIOLOGICAL REVIEWS,” vol. IV, no. 4, pp. 533–563, 1924.

[48] A. I. Caplan and The, “Mesenchymal Stem Cells,” *Chem. Phys. Lett.*, vol. 7, no. 6, pp. 581–582, 1970, doi: 10.1016/0009-2614(70)87009-9.

[49] R. K. C. A. K. S. L. A. J. FRIEDENSTEIN, “THE DEVELOPMENT OF FIBROBLAST COLONIES IN MONOLAYER CULTURES OF GUINEA-PIG BONE MARROW AND SPLEEN CELLS,” *Development*, pp. 1–6, 1897.

[50] A. J. Katz, A. Tholpady, S. S. Tholpady, H. Shang, and R. C. Ogle, “Cell Surface and Transcriptional Characterization of Human Adipose-Derived Adherent Stromal (hADAS) Cells,” *Stem Cells*, vol. 23, no. 3, pp. 412–423, 2005, doi: 10.1634/stemcells.2004-0021.

[51] B. M. Seo *et al.*, “Investigation of multipotent postnatal stem cells from human periodontal ligament,” *Lancet*, vol. 364, no. 9429, pp. 149–155, 2004, doi: 10.1016/S0140-6736(04)16627-0.

[52] X. Meng *et al.*, “Endometrial regenerative cells: A novel stem cell population,” *J. Transl. Med.*, vol. 5, pp. 1–10, 2007, doi: 10.1186/1479-5876-5-57.

[53] S. Patki, S. Kadam, V. Chandra, and R. Bhonde, “Human breast milk is a rich source of multipotent mesenchymal stem cells,” *Hum. Cell*, vol. 23, no. 2, pp. 35–40, 2010, doi: 10.1111/j.1749-0774.2010.00083.x.

[54] P. S. in ’t Anker *et al.*, “Isolation of Mesenchymal Stem Cells of Fetal or Maternal Origin from Human Placenta,” *Stem Cells*, vol. 22, no. 7, pp. 1338–1345, 2004, doi: 10.1634/stemcells.2004-0058.

[55] P. S. In ’t Anker *et al.*, “Amniotic fluid as a novel source of mesenchymal stem cells for therapeutic transplantation [1],” *Blood*, vol. 102, no. 4, pp. 1548–1549, 2003, doi: 10.1182/blood-2003-04-1291.

[56] B. M. Deasy *et al.*, “High harvest yield, high expansion, and phenotype stability of CD146 mesenchymal stromal cells from whole primitive human umbilical cord tissue,” *J. Biomed. Biotechnol.*, vol. 2009, 2009, doi: 10.1155/2009/789526.

[57] H. Wang *et al.*, “Mesenchymal Stem Cells in the Wharton’s Jelly of the Human Umbilical Cord,” *Stem Cells*, vol. 22, no. 7, pp. 1330–1337, 2004, doi: 10.1634/stemcells.2004-0013.

[58] M. Dominici *et al.*, “Minimal criteria for defining multipotent mesenchymal stromal cells. The International Society for Cellular Therapy position statement,” *Cytotherapy*, vol. 8, no. 4, pp. 315–317, 2006, doi: 10.1080/14653240600855905.

[59] T. L. Ramos *et al.*, “MSC surface markers (CD44, CD73, and CD90) can identify human MSC-derived extracellular vesicles by conventional flow cytometry,” *Cell Commun. Signal.*, vol. 14, no. 1, pp. 1–14, 2016, doi: 10.1186/s12964-015-0124-8.

[60] G. Brooke *et al.*, “Therapeutic applications of mesenchymal stromal cells,” *Semin. Cell Dev. Biol.*, vol. 18, no. 6, pp. 846–858, 2007, doi: 10.1016/j.semcdb.2007.09.012.

[61] M. F. Pittenger, D. E. Discher, B. M. Péault, D. G. Phinney, J. M. Hare, and A. I. Caplan, "Mesenchymal stem cell perspective: cell biology to clinical progress," *npj Regen. Med.*, vol. 4, no. 1, 2019, doi: 10.1038/s41536-019-0083-6.

[62] E. H. Javazon, K. J. Beggs, and A. W. Flake, "Парадоксы Пассажирования.Pdf," vol. 32, pp. 414–425, 2004.

[63] Y. P. Rubtsov, Y. G. Suzdaltseva, K. V. Goryunov, N. I. Kalinina, V. Y. Sysoeva, and V. A. Tkachuk, "Regulation of Immunity via Multipotent Mesenchymal Stromal Cells," *Acta Naturae*, vol. 4, no. 1, pp. 23–31, 2012, doi: 10.32607/20758251-2012-4-1-23-31.

[64] K. Suzuki, N. Chosa, S. Sawada, N. Takizawa, T. Yaegashi, and A. Ishisaki, "Enhancement of Anti-Inflammatory and Osteogenic Abilities of Mesenchymal Stem Cells via Cell-to-Cell Adhesion to Periodontal Ligament-Derived Fibroblasts," *Stem Cells Int.*, vol. 2017, 2017, doi: 10.1155/2017/3296498.

[65] R. E. Newman, D. Yoo, M. A. LeRoux, and A. Danilkovitch-Miagkova, "Treatment of inflammatory diseases with mesenchymal stem cells," *Inflamm. Allergy - Drug Targets*, vol. 8, no. 2, pp. 110–123, 2009, doi: 10.2174/187152809788462635.

[66] P. S. Frenette, S. Pinho, D. Lucas, and C. Scheiermann, *Mesenchymal stem cell: Keystone of the hematopoietic stem cell niche and a stepping-stone for regenerative medicine*, vol. 31. 2013.

[67] Y. Wang, X. Chen, W. Cao, and Y. Shi, "Plasticity of mesenchymal stem cells in immunomodulation: Pathological and therapeutic implications," *Nat. Immunol.*, vol. 15, no. 11, pp. 1009–1016, 2014, doi: 10.1038/ni.3002.

[68] J. A. Ankrum, J. F. Ong, and J. M. Karp, "Mesenchymal stem cells: Immune evasive, not immune privileged," *Nat. Biotechnol.*, vol. 32, no. 3, pp. 252–260, 2014, doi: 10.1038/nbt.2816.

[69] A. J. Nauta and W. E. Fibbe, "Immunomodulatory properties of mesenchymal stromal cells," *Blood*, vol. 110, no. 10, pp. 3499–3506, 2007, doi: 10.1182/blood-2007-02-069716.

[70] K. English, "Mechanisms of mesenchymal stromal cell immunomodulation," *Immunol. Cell Biol.*, vol. 91, no. 1, pp. 19–26, 2013, doi: 10.1038/icb.2012.56.

[71] P. H. . J. B. M. . S. C. T. et al Gary, "The New England Journal of Medicine Downloaded from nejm.org on April 1, 2015. For personal use only. No other uses without permission. Copyright © 1990 Massachusetts Medical Society. All rights reserved.," *New English J. Med.*, vol. 323, no. 16, pp. 1120–1123, 1990.

[72] A. Gebler, O. Zabel, and B. Seliger, "The immunomodulatory capacity of mesenchymal stem cells," *Trends Mol. Med.*, vol. 18, no. 2, pp. 128–134, 2012, doi: 10.1016/j.molmed.2011.10.004.

[73] G. Ren *et al.*, "Mesenchymal Stem Cell-Mediated Immunosuppression Occurs via Concerted Action of Chemokines and Nitric Oxide," *Cell Stem Cell*, vol. 2, no. 2, pp. 141–150, 2008, doi: 10.1016/j.stem.2007.11.014.

[74] M. Krampera *et al.*, "Role for Interferon-γ in the Immunomodulatory Activity of Human

Bone Marrow Mesenchymal Stem Cells," *Stem Cells*, vol. 24, no. 2, pp. 386–398, 2006, doi: 10.1634/stemcells.2005-0008.

[75] R. R. Sharma, K. Pollock, A. Hubel, and D. McKenna, "Mesenchymal stem or stromal cells: A review of clinical applications and manufacturing practices," *Transfusion*, vol. 54, no. 5, pp. 1418–1437, 2014, doi: 10.1111/trf.12421.

[76] J. N. M. Ijzermans and R. L. Marquet, "Interferon-gamma: A Review," *Immunobiology*, vol. 179, no. 4–5, pp. 456–473, 1989, doi: 10.1016/S0171-2985(89)80049-X.

[77] Y. Liu *et al.*, "Mesenchymal stem cell-based tissue regeneration is governed by recipient T lymphocytes via IFN-γ and TNF-α," *Nat. Med.*, vol. 17, no. 12, pp. 1594–1601, 2011, doi: 10.1038/nm.2542.

[78] N. P. Group, "The Otogeny of the Neural Crest in Avian."

[79] M. Eddaoudi, H. Li, and O. M. Yaghi, "Highly porous and stable metal-organic frameworks: Structure design and sorption properties," *J. Am. Chem. Soc.*, vol. 122, no. 7, pp. 1391–1397, 2000, doi: 10.1021/ja9933386.

[80] J. Kim *et al.*, "Assembly of metal-organic frameworks from large organic and inorganic secondary building units: New examples and simplifying principles for complex structures," *J. Am. Chem. Soc.*, vol. 123, no. 34, pp. 8239–8247, 2001, doi: 10.1021/ja010825o.

[81] M. Eddaoudi *et al.*, "Modular chemistry: Secondary building units as a basis for the design of highly porous and robust metal-organic carboxylate frameworks," *Acc. Chem. Res.*, vol. 34, no. 4, pp. 319–330, 2001, doi: 10.1021/ar000034b.

[82] H. Kim *et al.*, "Hydrogen Storage in Microporous Metal-Organic Frameworks," *Science (80-.).*, vol. 73, no. 1973, pp. 12–15, 2002.

[83] D. J. Tranchemontagne, J. L. Tranchemontagne, M. O'keeffe, and O. M. Yaghi, "Secondary building units, nets and bonding in the chemistry of metal–organic frameworks," *Chem. Soc. Rev.*, vol. 38, no. 5, pp. 1257–1283, 2009, doi: 10.1039/b817735j.

[84] M. Karagianni *et al.*, "A comparative analysis of the adipogenic potential in human mesenchymal stromal cells from cord blood and other sources," *Cytotherapy*, vol. 15, no. 1, pp. 76-88.e2, 2013, doi: 10.1016/j.jcyt.2012.11.001.

[85] J. R. Long and O. M. Yaghi, "The pervasive chemistry of metal-organic frameworks," *Chem. Soc. Rev.*, vol. 38, no. 5, pp. 1213–1214, 2009, doi: 10.1039/b903811f.

[86] H. Furukawa, K. E. Cordova, M. O'Keeffe, and O. M. Yaghi, "The chemistry and applications of metal-organic frameworks," *Science (80-.).*, vol. 341, no. 6149, 2013, doi: 10.1126/science.1230444.

[87] M. Eddaoudi *et al.*, "Systematic design of pore size and functionality in isoreticular MOFs and their application in methane storage," *Science (80-.).*, vol. 295, no. 5554, pp. 469–472, 2002, doi: 10.1126/science.1067208.

[88] T. Asami *et al.*, “Modulation of murine macrophage TLR7/8-mediated cytokine expression by mesenchymal stem cell-conditioned medium,” *Mediators Inflamm.*, vol. 2013, 2013, doi: 10.1155/2013/264260.

[89] Y. Zhang *et al.*, “Exosomes Derived from Mesenchymal Stromal Cells Promote Axonal Growth of Cortical Neurons,” *Mol. Neurobiol.*, vol. 54, no. 4, pp. 2659–2673, 2017, doi: 10.1007/s12035-016-9851-0.

[90] M. O. Dellacherie, B. R. Seo, and D. J. Mooney, “Macroscale biomaterials strategies for local immunomodulation,” *Nat. Rev. Mater.*, vol. 4, no. 6, pp. 379–397, 2019, doi: 10.1038/s41578-019-0106-3.

[91] R. S. Tuan, G. Boland, and R. Tuli, “Adult mesenchymal stem cells and cell-based tissue engineering,” *Arthritis Res. Ther.*, vol. 5, no. 1, pp. 32–45, 2003, doi: 10.1186/ar614.

[92] R. A. MARKLEIN, M. W. KLINKER, K. A. DRAKE, H. G. POLIKOWSKY, E. C. LESSEY-MORILLON, and S. R. BAUER, “Morphological profiling using machine learning reveals emergent subpopulations of interferon-γ–stimulated mesenchymal stromal cells that predict immunosuppression,” *Cytotherapy*, vol. 21, no. 1, pp. 17–31, 2019, doi: 10.1016/j.jcyt.2018.10.008.

[93] R. A. Marklein, J. Lam, M. Guvendiren, K. E. Sung, and S. R. Bauer, “Functionally-Relevant Morphological Profiling: A Tool to Assess Cellular Heterogeneity,” *Trends Biotechnol.*, vol. 36, no. 1, pp. 105–118, 2018, doi: 10.1016/j.tibtech.2017.10.007.

[94] S. J. Cifuentes, P. Priyadarshani, D. A. Castilla-Casadiego, L. J. Mortensen, J. Almodóvar, and M. Domenech, “Heparin/collagen surface coatings modulate the growth, secretome, and morphology of human mesenchymal stromal cell response to interferon-gamma,” *J. Biomed. Mater. Res. - Part A*, no. March, pp. 1–15, 2020, doi: 10.1002/jbm.a.37085.

[95] D. A. Castilla-Casadiego, L. Pinzon-Herrera, M. Perez-Perez, B. A. Quiñones-Colón, D. Suleiman, and J. Almodovar, “Simultaneous characterization of physical, chemical, and thermal properties of polymeric multilayers using infrared spectroscopic ellipsometry,” *Colloids Surfaces A Physicochem. Eng. Asp.*, vol. 553, pp. 155–168, 2018, doi: 10.1016/j.colsurfa.2018.05.052.

[96] L. Pinzon-Herrera, J. Mendez-Vega, A. Mulero-Russe, D. A. Castilla-Casadiego, and J. Almodovar, “Real-time monitoring of human Schwann cells on heparin-collagen coatings reveals enhanced adhesion and growth factor response,” *J. Mater. Chem. B*, vol. 8, no. 38, pp. 8809–8819, 2020, doi: 10.1039/d0tb01454k.

[97] D. A. Castilla-Casadiego, A. M. Reyes-Ramos, M. Domenech, and J. Almodovar, “Effects of Physical, Chemical, and Biological Stimulus on h-MSC Expansion and Their Functional Characteristics,” *Ann. Biomed. Eng.*, vol. 48, no. 2, pp. 519–535, 2020, doi: 10.1007/s10439-019-02400-3.

[98] D. A. Castilla-casadiego and J. Almodovar, “on heparin-collagen coatings reveals enhanced adhesion and growth factor response †,” 2020, doi: 10.1039/d0tb01454k.

[99] A. Bertolo, D. Pavlicek, A. Gemperli, M. Baur, T. Pötzel, and J. Stoyanov, “Increased motility of mesenchymal stem cells is correlated with inhibition of stimulated peripheral

blood mononuclear cells in vitro," *J. Stem Cells Regen. Med.*, vol. 13, no. 2, pp. P62–P74, 2017, doi: 10.46582/jsrm.1302010.

[100] L. Boland, A. J. Burand, A. J. Brown, D. Boyt, V. A. Lira, and J. A. Ankrum, "IFN-γ and TNF-α Pre-licensing Protects Mesenchymal Stromal Cells from the Pro-inflammatory Effects of Palmitate," *Mol. Ther.*, vol. 26, no. 3, pp. 860–873, 2018, doi: 10.1016/j.ymthe.2017.12.013.

[101] M. C. Killer *et al.*, "Immunosuppressive capacity of mesenchymal stem cells correlates with metabolic activity and can be enhanced by valproic acid," *Stem Cell Res. Ther.*, vol. 8, no. 1, pp. 1–8, 2017, doi: 10.1186/s13287-017-0553-y.

[102] K. A. Marx, "Quartz crystal microbalance: A useful tool for studying thin polymer films and complex biomolecular systems at the solution - Surface interface," *Biomacromolecules*, vol. 4, no. 5, pp. 1099–1120, 2003, doi: 10.1021/bm020116i.

[103] C. D. Easton, A. J. Bullock, G. Gigliobianco, S. L. McArthur, and S. Macneil, "Application of layer-by-layer coatings to tissue scaffolds-development of an angiogenic biomaterial," *J. Mater. Chem. B*, vol. 2, no. 34, pp. 5558–5568, 2014, doi: 10.1039/c4tb00448e.

[104] Q. Lin, J. Yan, F. Qiu, X. Song, G. Fu, and J. Ji, "Heparin/collagen multilayer as a thromboresistant and endothelial favorable coating for intravascular stent," *J. Biomed. Mater. Res. - Part A*, vol. 96 A, no. 1, pp. 132–141, 2011, doi: 10.1002/jbm.a.32820.

[105] I. Reviakine, D. Johannsmann, and R. P. Richter, "Hearing what you cannot see and visualizing what you hear: Interpreting quartz crystal microbalance data from solvated interfaces," *Anal. Chem.*, vol. 83, no. 23, pp. 8838–8848, 2011, doi: 10.1021/ac201778h.

[106] S. Boddohi, J. Almodóvar, H. Zhang, P. A. Johnson, and M. J. Kipper, "Layer-by-layer assembly of polysaccharide-based nanostructured surfaces containing polyelectrolyte complex nanoparticles," *Colloids Surfaces B Biointerfaces*, vol. 77, no. 1, pp. 60–68, 2010, doi: 10.1016/j.colsurfb.2010.01.006.

[107] Q. Lin, J. Yan, F. Qiu, X. Song, G. Fu, and J. Ji, "Heparin/collagen multilayer as a thromboresistant and endothelial favorable coating for intravascular stent," *J. Biomed. Mater. Res. - Part A*, vol. 96 A, no. 1, pp. 132–141, 2011, doi: 10.1002/jbm.a.32820.

[108] D. S. Salloum, S. G. Olenych, T. C. S. Keller, and J. B. Schlenoff, "Vascular smooth muscle cells on polyelectrolyte multilayers: Hydrophobicity-directed adhesion and growth," *Biomacromolecules*, vol. 6, no. 1, pp. 161–167, 2005, doi: 10.1021/bm0497015.

[109] K. Zhang, D. Huang, Z. Yan, and C. Wang, "Heparin/collagen encapsulating nerve growth factor multilayers coated aligned PLLA nanofibrous scaffolds for nerve tissue engineering," *J. Biomed. Mater. Res. - Part A*, vol. 105, no. 7, pp. 1900–1910, 2017, doi: 10.1002/jbm.a.36053.

[110] A. M. Ferreira, P. Gentile, S. Toumpaniari, G. Ciardelli, and M. A. Birch, "Impact of Collagen/Heparin Multilayers for Regulating Bone Cellular Functions," *ACS Appl. Mater. Interfaces*, vol. 8, no. 44, pp. 29923–29932, 2016, doi: 10.1021/acsami.6b09241.

[111] D. Li *et al.*, "Chitosan and collagen layer-by-layer assembly modified oriented nanofibers

and their biological properties," *Carbohydr. Polym.*, vol. 254, no. July 2020, p. 117438, 2020, doi: 10.1016/j.carbpol.2020.117438.

[112] J. Almodóvar, S. Bacon, J. Gogolski, J. D. Kisiday, and M. J. Kipper, "Polysaccharide-based polyelectrolyte multilayer surface coatings can enhance mesenchymal stem cell response to adsorbed growth factors," *Biomacromolecules*, vol. 11, no. 10, pp. 2629–2639, 2010, doi: 10.1021/bm1005799.

[113] H. M. Wobma, M. A. Tamargo, S. Goeta, L. M. Brown, R. Duran-Struuck, and G. Vunjak-Novakovic, *The influence of hypoxia and IFN-γ on the proteome and metabolome of therapeutic mesenchymal stem cells*, vol. 167. Elsevier Ltd, 2018.

[114] J. Du *et al.*, "The different effects of IFN-β and IFN-γ on the tumor-suppressive activity of human amniotic fluid-derived mesenchymal stem cells," *Stem Cells Int.*, vol. 2019, 2019, doi: 10.1155/2019/4592701.

[115] M. H. Hettiaratchi, T. Miller, J. S. Temenoff, R. E. Guldberg, and T. C. McDevitt, "Heparin microparticle effects on presentation and bioactivity of bone morphogenetic protein-2," *Biomaterials*, vol. 35, no. 25, pp. 7228–7238, 2014, doi: 10.1016/j.biomaterials.2014.05.011.

[116] S. J. Fritchley, J. A. Kirby, and S. Ali, "The antagonism of interferon-gamma (IFN-γ) by heparin: Examination of the blockade of class II MHC antigen and heat shock protein-70 expression," *Clin. Exp. Immunol.*, vol. 120, no. 2, pp. 247–252, 2000, doi: 10.1046/j.1365-2249.2000.01178.x.

[117] A. Rezania and K. E. Healy, "Biomimetic peptide surfaces that regulate adhesion, spreading, cytoskeletal organization, and mineralization of the matrix deposited by osteoblast-like cells," *Biotechnol. Prog.*, vol. 15, no. 1, pp. 19–32, 1999, doi: 10.1021/bp980083b.

[118] V. January, "RTCA DP Instrument Operator's Manual," *ACEA Biosci. Inc*, no. January, 2013.

[119] J. J. Montesinos *et al.*, "Human bone marrow mesenchymal stem/stromal cells exposed to an inflammatory environment increase the expression of ICAM-1 and release microvesicles enriched in this adhesive molecule: Analysis of the participation of TNF-α and IFN-γ," *J. Immunol. Res.*, vol. 2020, 2020, doi: 10.1155/2020/8839625.

[120] O. Takikawa, T. Kuroiwa, F. Yamazaki, and R. Kido, "Mechanism of interferon-γ action. Characterization of indoleamine 2,3-dioxygenase in cultured human cells induced by interferon -γ and evaluation of the enzyme-mediated tryptophan degradation in its anticellular activity," *J. Biol. Chem.*, vol. 263, no. 4, pp. 2041–2048, 1988.

[121] W. Däubener, N. Wanagat, K. Pilz, S. Seghrouchni, H. G. Fischer, and U. Hadding, "A new, simple, bioassay for human IFN-γ," *J. Immunol. Methods*, vol. 168, no. 1, pp. 39–47, 1994, doi: 10.1016/0022-1759(94)90207-0.

[122] G. Siegel, T. Kluba, U. Hermanutz-Klein, K. Bieback, H. Northoff, and R. Schäfer, "Phenotype, donor age and gender affect function of human bone marrow-derived mesenchymal stromal cells," *BMC Med.*, vol. 11, no. 1, 2013, doi: 10.1186/1741-7015-11-

146.

[123] O. Katsara *et al.*, “Effects of donor age, gender, and in vitro cellular aging on the phenotypic, functional, and molecular characteristics of mouse bone marrow-derived mesenchymal stem cells,” *Stem Cells Dev.*, vol. 20, no. 9, pp. 1549–1561, 2011, doi: 10.1089/scd.2010.0280.

[124] T. Wang, J. Zhang, J. Liao, F. Zhang, and G. Zhou, “Donor genetic backgrounds contribute to the functional heterogeneity of stem cells and clinical outcomes,” *Stem Cells Transl. Med.*, vol. 9, no. 12, pp. 1495–1499, 2020, doi: 10.1002/sctm.20-0155.

[125] M. Science, “Tissue Engineering and Regenerative Medicine T ISSUE E NGINEERING AND R EGENERATIVE M EDICINE MicroRNA-146b , a Sensitive Indicator of Mesenchymal Stem Cell Repair of Acute Renal Injury,” pp. 1–10, 2016.

[126] K. E. S. Brian J. Kwee, Johnny Lam, Adovi Akue, Mark A. KuKuruga, K. Zhang, Luo Gu, “Functional heterogeneity of IFN-γ – licensed mesenchymal stromal cell immunosuppressive capacity on biomaterials,” pp. 1–12, 2021, doi: 10.1073/pnas.2105972118/-/DCSupplemental.Published.

[127] F. Fallarino and U. Grohmann, “Using an Ancient Tool for Igniting and Propagating Immune Tolerance: IDO as an Inducer and Amplifier of Regulatory T Cell Functions,” *Curr. Med. Chem.*, vol. 18, no. 15, pp. 2215–2221, 2012, doi: 10.2174/092986711795656027.

[128] D. S. Kim *et al.*, “Enhanced Immunosuppressive Properties of Human Mesenchymal Stem Cells Primed by Interferon-γ,” *EBioMedicine*, vol. 28, pp. 261–273, 2018, doi: 10.1016/j.ebiom.2018.01.002.

[129] W. Juncheng *et al.*, “High glucose inhibits osteogenic differentiation through the BMP signaling pathway in bone mesenchymal stem cells in mice,” *EXCLI J.*, vol. 12, no. 2009, pp. 584–597, 2013, doi: 10.17877/DE290R-7335.

[130] A. Zhu, M. Zhang, J. Wu, and J. Shen, “Covalent immobilization of chitosan / heparin complex with a photosensitive hetero-bifunctional crosslinking reagent on PLA surface $,” vol. 23, pp. 4657–4665, 2002.

[131] A. M. M. Renata Francielle Bombaldi de Souza, Fernanda Carla Bombaldi de Souza, Andrea Thorpe, Diego Mantovani, Ketul C. Popat, “Phosphorylation of chitosan to improve osteoinduction of chitosan/xanthan-based scaffolds for periosteal tissue engineering,” *Int. J. Biol. Macromol.*, 2019, doi: 10.1016/j.ijbiomac.2019.12.004.

[132] R. M. Sabino, G. Mondini, M. J. Kipper, A. F. Martins, and K. C. Popat, “Tanfloc/heparin polyelectrolyte multilayers improve osteogenic differentiation of adipose-derived stem cells on titania nanotube surfaces,” *Carbohydr. Polym.*, vol. 251, no. September 2020, p. 117079, 2021, doi: 10.1016/j.carbpol.2020.117079.

[133] C. Granéli *et al.*, “Novel markers of osteogenic and adipogenic differentiation of human bone marrow stromal cells identified using a quantitative proteomics approach,” *Stem Cell Res.*, vol. 12, no. 1, pp. 153–165, 2014, doi: 10.1016/j.scr.2013.09.009.

[134] V. Michel and M. Bakovic, “The solute carrier 44A1 is a mitochondrial protein and

mediates choline transport," *FASEB J.*, vol. 23, no. 8, pp. 2749–2758, 2009, doi: 10.1096/fj.08-121491.

[135] L. Ding *et al.*, "CD10 expression identifies a subset of human perivascular progenitor cells with high proliferation and calcification potentials," *Stem Cells*, vol. 38, no. 2, pp. 261–275, 2020, doi: 10.1002/stem.3112.

[136] E. A. Jones *et al.*, "Isolation and characterization of bone marrow multipotential mesenchymal progenitor cells," *Arthritis Rheum.*, vol. 46, no. 12, pp. 3349–3360, 2002, doi: 10.1002/art.10696.

[137] M. S. Niepel, F. Almouhanna, B. K. Ekambaram, M. Menzel, A. Heilmann, and T. Groth, "Cross-linking multilayers of poly-l-lysine and hyaluronic acid: Effect on mesenchymal stem cell behavior," *Int. J. Artif. Organs*, vol. 41, no. 4, pp. 223–235, 2018, doi: 10.1177/0391398817752598.

[138] K. Pachmann and W. Leibold, "Insolubilization of protein antigens on polyacrylic plastic beads using poly-l-lysine," *J. Immunol. Methods*, vol. 12, no. 1–2, pp. 81–89, 1976, doi: 10.1016/0022-1759(76)90098-3.

[139] P. DE KRUIJFF and and P. R. CULLIS, "THE INFLUENCE OF POLY(L-LYSINE) ON PHOSPHOLIPID POLYMORPHISM EVIDENCE," *Biochim. Biophys. Acta*, vol. 601, pp. 235–240, 1980, doi: 10.1016/0005-2736(80)90528-3.

[140] J. Almodóvar *et al.*, "Spatial patterning of BMP-2 and BMP-7 on biopolymeric films and the guidance of muscle cell fate," *Biomaterials*, vol. 35, no. 13, pp. 3975–3985, 2014, doi: 10.1016/j.biomaterials.2014.01.012.

[141] A. R. S. L. Michael D. Klein, Robert A. Drongowski, Robert J. Linhardt, "A Colorimetric Assay for Chemical in Plasma," *Anal. Biochem.*, vol. 64, pp. 59–64, 1982.

[142] L. Richert *et al.*, "Improvement of stability and cell adhesion properties of polyelectrolyte multilayer films by chemical cross-linking," *Biomacromolecules*, vol. 5, no. 2, pp. 284–294, 2004, doi: 10.1021/bm0342281.

[143] A. Barrantes, O. Santos, J. Sotres, and T. Arnebrant, "Influence of pH on the build-up of poly-L-lysine/heparin multilayers," *J. Colloid Interface Sci.*, vol. 388, no. 1, pp. 191–200, 2012, doi: 10.1016/j.jcis.2012.08.008.

[144] F. Boulmedais, C. S. Tang, B. Keller, and J. Vörös, "Controlled electrodissolution of polyelectrolyte multilayers: A platform technology towards the surface-initiated delivery of drugs," *Adv. Funct. Mater.*, vol. 16, no. 1, pp. 63–70, 2006, doi: 10.1002/adfm.200400406.

[145] C. Picart *et al.*, "Molecular basis for the explanation of the exponential growth of polyelectrolyte multilayers," *Proc. Natl. Acad. Sci. U. S. A.*, vol. 99, no. 20, pp. 12531–12535, 2002, doi: 10.1073/pnas.202486099.

[146] N. Graf *et al.*, "XPS and NEXAFS studies of aliphatic and aromatic amine species on functionalized surfaces," *Surf. Sci.*, vol. 603, no. 18, pp. 2849–2860, 2009, doi: 10.1016/j.susc.2009.07.029.

[147] O. V. Semenov, A. Malek, A. G. Bittermann, J. Vörös, and A. H. Zisch, “Engineered polyelectrolyte multilayer substrates for adhesion, proliferation, and differentiation of human mesenchymal stem cells,” *Tissue Eng. - Part A*, vol. 15, no. 10, pp. 2977–2990, 2009, doi: 10.1089/ten.tea.2008.0602.

[148] T. Crouzier and C. Picart, “Ion Pairing and Hydration in Polyelectroyte Multilayer Film Containing Polysaccharides,” *Biomacromolecules*, pp. 433–442, 2009.

[149] J. C. Mbongue, D. A. Nicholas, T. W. Torrez, N. S. Kim, A. F. Firek, and W. H. R. Langridge, “The role of indoleamine 2, 3-dioxygenase in immune suppression and autoimmunity,” *Vaccines*, vol. 3, no. 3, pp. 703–729, 2015, doi: 10.3390/vaccines3030703.

Supplementary Information

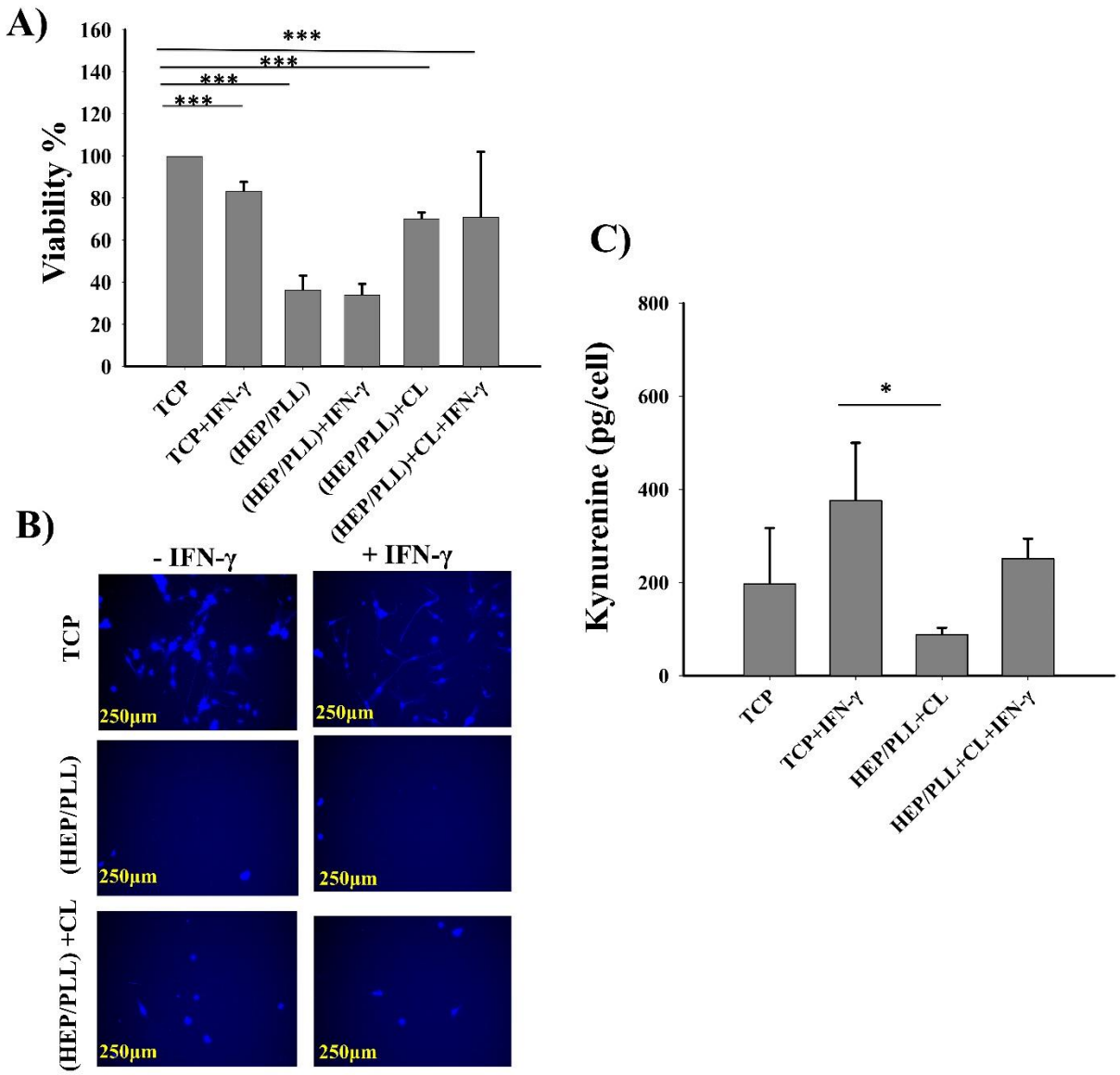

Figure S3.1. (A): PrestoBlue Viability assay for cultured hMSCs donor 1. Cellular behavior in cell cultures on TCP, (HEP/PLL), and (HEP/PLL) +CL multilayers with and without IFN-γ. (B): Fluorescence microscopy images of hMSCs nuclei labeled with Hoechst of cells attached to the TCP, (HEP/PLL), and (HEP/PLL) + CL multilayers with and without IFN-γ. (C): Cells immunomodulatory potential by IDO activity for hMSCs as a measure of picograms of kynurenine produced by cells cultured on TCP, (HEP/PLL), and (HEP/PLL)+CL multilayers

with and without IFN-γ. Data are presented as the mean ± standard deviation of n = 4 samples. The p-values < 0.05 are represented by *, p-values < 0. 01 by **, p-values < 0. 001 by *** and p-values < 0.0001 by ****.

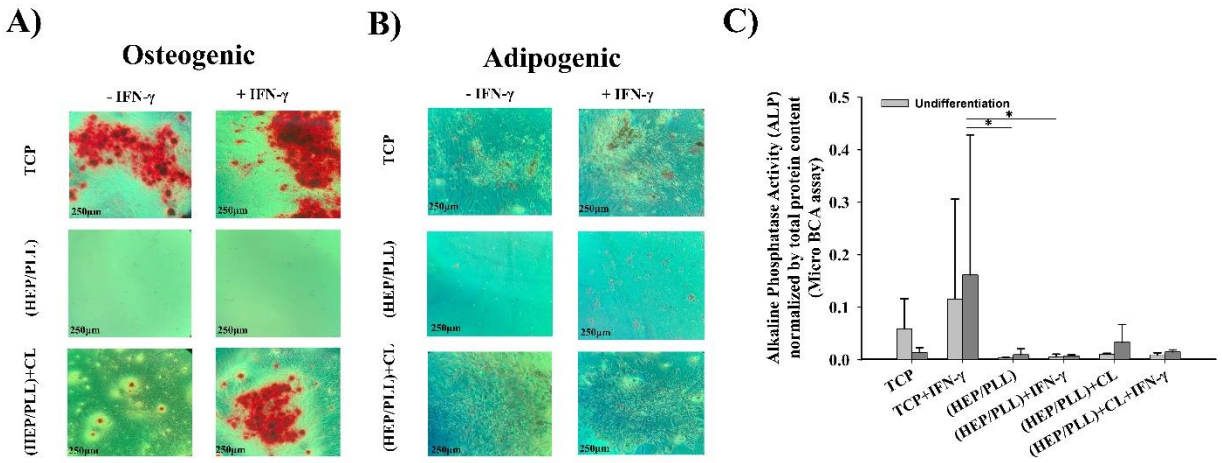

Figure S3.2. hMSCs differentiation donor2. (A): Osteogenic differentiations were stained by Alizarin Red. (B): Adipogenic differentiation were stained by Oil Red. (C): Alkaline phosphatase (ALP) assays were performed after of induced osteogenesis on TCP and (HEP/PLL) + CL multilayers. Data are presented as the mean ± standard deviation of n = 4 samples. The p-values < 0.05 are represented by *, p-values < 0. 01 by **, p-values < 0. 001 by *** and p-values < 0.0001 by ****.

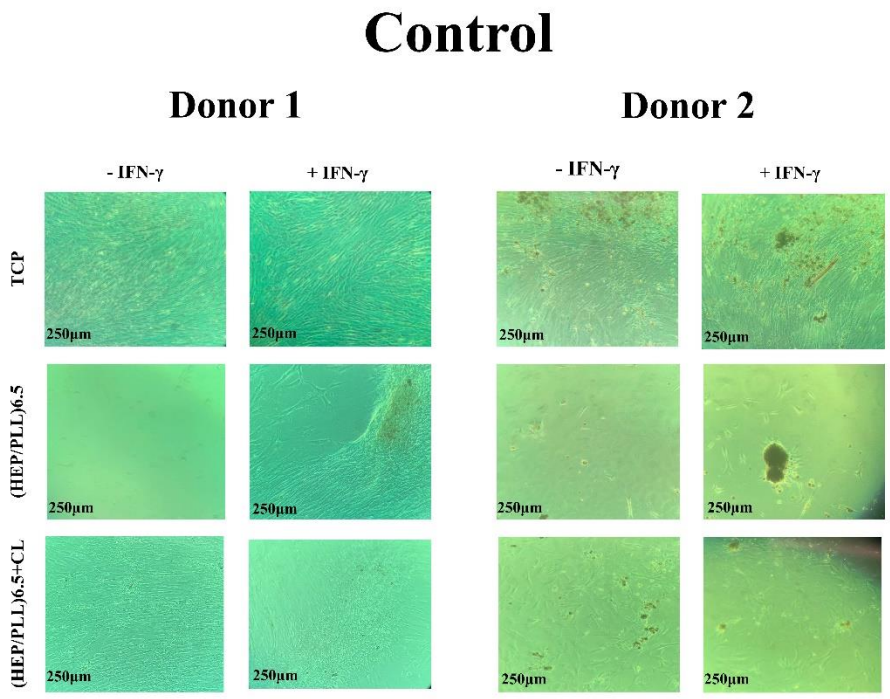

Figure S3.3. hMSCs control cells inducing by normal expansion medium

4. Delivery of Immobilized IFN-γ with PCN-333 and its Effect on Human Mesenchymal Stem Cells

Josh Phipps[†], Mahsa Haseli[‡], Luis C. Pinzon-Herrera[‡], Ben Wilson[‡], Joshua Corbitt[‡], Shannon Servoss[‡], and Jorge Almodóvar[†‡]

†Cell and Molecular Biology Graduate Program, University of Arkansas, Fayetteville, AR 72701, United States

‡Ralph E. Martin Department of Chemical Engineering, University of Arkansas, Fayetteville, AR 72701, United States

*The chapter was published and used with permission.

Abstract

Interferon-gamma (IFN-γ) plays a vital role in modulating the immunosuppressive properties of human mesenchymal stem/stromal cells (hMSCs) used in cell therapies. However, IFN-γ suffers from low bioavailability and degrades in media creating a challenge when using IFN-γ during the manufacturing of hMSCs. Metal-organic frameworks (MOFs), with their porous interiors, biocompatibility, high loading capacity, and ability to be functionalized for targeting, have become an increasingly suitable platform for protein delivery. In this work, we synthesize the MOF PCN-333(Fe) and show that it can be utilized to immobilize and deliver IFN-γ to the local extracellular environment of hMSCs. In doing so, the cells proliferate and differentiate appropriately with no observed side effects. We demonstrate that PCN-333(Fe) MOFs containing IFN-γ are not cytotoxic to hMSCs, can promote the expression of proteins that play a role in immune response, and are capable of inducing indoleamine 2,3-dioxygenase (IDO) production similar to that of soluble IFN-γ at lower concentrations. Overall, using MOFs to deliver IFN-γ may be leveraged in the future in the manufacturing of therapeutically relevant hMSCs.

4.1. Introduction

Recent years have seen a significant increase in the study of metal-organic frameworks (MOFs) since their foundational introduction by Omar Yagi and coworkers [1]–[7]. These porous crystalline particles are often produced on the nanoscale and due to their interchangeable parts, are vastly customizable [7]. This ability to selectively choose components and synthesize tailor-made MOF allows these particles to be functionalized as well as have their three-dimensional size and shape manipulated [3][8]. This is further promoted by the open pores and large surface areas of MOF which allow materials to move into the particles providing a high loading capacity and surface area [8]. This effect is excellent for reactions, allowing the free flow of reactants and products to reaction sites. This trait has also been exploited to encapsulate or trap objects, which can be as big as proteins or as small as gas particles making MOF prominent devices for gas storage, drug delivery, and protein immobilization and/or encapsulation [7].

Protein immobilization and encapsulation is made possible by the fluid nature of proteins with their ability to fold and unfold as well as the inherent interactions arising between the chemical groups on MOF particles and the proteins. Immobilization is a relatively simple process where the charged portions of proteins interact with the positively charged bare node sites on the framework and become coordinated to that site [9][10]. Encapsulation is a more complicated process where the protein either moves into the framework via diffusion or is placed in solution with MOF reactants and the framework is built up around it. The former is called post-synthetic encapsulation (PSE) and the latter is known as De-novo encapsulation or DNE [11]. In both PSE and DNE, proteins are held in place physically by the surrounding framework, but they are also held in place by intermolecular forces such as London dispersion forces (LDFs), dipole-dipole interactions, and hydrogen bonding between the framework and the protein [10][12].

Protein immobilization and encapsulation using MOF has been shown to allow improved reaction kinetics while protecting the housed protein from extreme conditions that would otherwise cause the protein to denature and become inactive [13]–[15]. This includes reactions taking place at temperatures above 60°C, in organic solvents, and at both high and low Ph [16]. We demonstrate this effect in a recent publication encapsulating and monitoring the loading and reaction kinetics of alcohol dehydrogenase in the MOF PCN-333(Fe) [11]. While catalytic reactions are a major interest in MOF-protein immobilization using biocompatible MOFs, another key use of is in drug and protein delivery [17][18]. An excellent example is provided in a recent work by Luzuriaga et. al. where it is shown that proteinaceous vaccines can be both protected/insulated from the outside environment as well as carried by site-directed delivery to a given location even inside the cell [19].

The delivery of proteins is a very promising area of study with the ability to have a dramatic impact. Human mesenchymal stem/stromal cells (hMSCs) are an excellent model cell and are particularly interesting to cellular therapy programs due to their function as an immunosuppressant [20]. During tissue damage, hMSCs have the ability to secrete paracrine and anti-inflammatory factors to repair tissue [21]–[23]. In addition, hMSCs contribute not only to the repair of damaged tissues but also possess remarkable immunomodulatory activity by producing anti-inflammatory and immunosuppressive factors [24]–[30]. This has led to hMSCs to becomee a promising tool for new medical applications and therapies in the treatment of diverse diseases and disorders, such as graft-versus-host disease (GVHD), inflammatory diseases, and autoimmune disorders [31]–[34].

It has been shown that the immunosuppressive properties of hMSCs rely on the existence of IFN-γ in the microenvironment [27]. This signaling protein is a potent pro-inflammatory

cytokine produced by CD4+ lymphocytes, natural killer cells (NKT) cells, and macrophages. Because of this function, IFN-γ plays an essential and complex role in innate and adaptive immune responses toward viral infections, bacteria, protozoa, and GVHD [28][29]. A recent study by Croitoru-Lamoury et. al. showed that IFN-γ has the ability to modulate the immune properties and differentiation potential of hMSCs [31]. While this presence of IFN-γ increases the immunosuppressive properties of hMSCs, the transient effects of IFN-γ may limit the potential of hMSCs to modulate immune responses for more than a few days in cell environments that do not expose the cells to adequate concentrations of IFN-γ, such as in chronic inflammatory states [35]. Therefore, providing a means of locally concentrating and sustaining the presentation of IFN-γ to hMSCs may significantly enhance the immunomodulatory potential of the cells. A recent study by Zimmerman et. al. illustrated this effect and showed that heparin based nanoparticles could be used to deliver IFN-γ and demonstrated increased IDO expression and improved immune suppressive properties [35]. MOF having proven themselves as an effective and biocompatible tool for drug delivery may aid this process through its own unique characteristics. In this paper we seek to show that the immobilization, protection from degradation, and delivery of factors, specifically IFN-γ with PCN-333(Fe) to the local extracellular environment is an effective means for delivery to potentiate hMSCs immunomodulatory activity.

4.2. Experimental Section

4.2.1. Synthesis of PCN-333(Fe)

The precursor 4,4′,4″-s-triazine-2,4,6-triyl-tribenzoic acid (H_3TATB) and MOF PCN-333(Fe) were synthesized according to the method described in the work by Park et. al. 2015 [36]. In a 15 mL reaction vessel, we combined 60 mg H_3TATB, 60 mg anhydrous $FeCl_3$ (III), 0.6 mL TFA,

and 10 mL dimethylformamide. The vessel was then sealed and placed in an oven at 150°C for 12 hours. Brown precipitate formed and was collected by centrifugation. The product was washed several times each by dimethylformamide, acetone, and water with centrifugation after each step to collect. Water was then exchanged with acetone three times before activation in an oven at 70°C overnight. The product was then confirmed via X-ray diffraction using a Rigaku® MiniFlex II. Size and shape were also determined via the use of a Horiba LA-950 particle size analyzer and scanning electron microscope (SEM), respectively.

4.2.2. Immobilization of IFN-γ with PCN-333(Fe)

A loading solution of PCN-333 and IFN-γ was combined with a final concentration 0.1 mg/mL IFN-γ and either 0.5 or 1 mg/mL PCN-333 depending on the test. This solution was vortexed and allowed to sit at 4°C for 24 hours. The solution was then removed after gentle centrifugation leaving the immobilized IFN-γ and PCN-333. Percent immobilization was determined using Ultraviolet-Visible (UV-Vis) absorption of an aliquot of the supernatant at 395nm.

4.2.3. Experimental design

In this work, the effects of MOF concentration and presence or absence of recombinant human IFN-γ (ThermoFisher, Cat. #PHC4031) immobilized with the MOF in culture medium were studied and their effect on the hMSCs are reported. Six test conditions were examined including a negative control group lacking IFN-γ (-IFN-γ), a positive control group (+IFN-γ) (50 ng/mL), and test groups containing either 0.5 mg/mL or 1 mg/mL MOF with and without IFN-γ immobilized. The choice in concentration of our control was selected based on our previous works [32][37]. Cell media containing MOF was created by placing MOF (either loaded with IFN-γ or bare) in 15 mL of media 15 mL centrifuge tube and subsequently vortexed before addition to cells soon after and had a final concentration of 14.2 ng/mL for the 0.5 mg/mL MOF

sample and 14.4 ng/mL for the 1 mg/mL sample. Conditions will hereafter be referred to as "control groups" containing media with and without IFN-γ (+/-) and "test groups" containing MOF at a concentration of either 0.5 mg/mL or 1 mg/mL with or without IFN-γ loaded.

4.2.4. HMSC viability

For hMSCs viability, PrestoBlueTM cell viability assay from Invitrogen (Cat. #A13261) was used. hMSCs (10,000 cells/cm^2) were seeded on a 96 well-plate, and cell viability was measured after 3 and 6 days of culture with control groups and test groups containing. This viability testing was conducted as we have described in our previous works [37]–[40]. Following propagation, the cell culture medium was removed, and 100 µL of solution was added per well containing 90% fresh cell medium and 10% PrestoBlue reagent. The plate was then incubated for 3 hours, and the fluorescence intensity was measured using a BioTek Multi-Mode Microplate Reader (Model SynergyTM 2) with excitation/emission of 560/590 nm. Data was reported as the average with standard deviation shown from experiments with 4 wells per condition.

Cell nuclei and actin cytoskeleton were stained using the fluorescent dyes Hoechst 33342 which was purchased from Invitrogen (Ref. #H3570) and ActinRed 555 Ready Probest (Invitrogen, Ref. #37112). After three days of culture, the cell medium was removed, and the cells were fixed with 4% formaldehyde solution for 15 minutes. The samples were washed several times with PBS followed by the addition of Triton X100 for 10 minutes before being washed 3 times with PBS. ActinRed 555 was first added and incubated for 30 minutes. Then, Hoechst 33342 was added for 10 minutes and protected from light using aluminum foil. Both dyes were washed 5 times with PBS before and after being added. For cell imaging, a Leica inverted fluorescence microscope was used with a standard DAPI filter (excitation/emission of 350/461 nm) for

Hoechst 33342, and a standard TRITC filter (excitation/emission of 540/565 nm) for ActinRed 555.

4.2.5. Real-time monitoring of hMSCs behavior

An xCELLigence Real-Time Cell Analyzer (RTCA S16) instrument from ACEA Biosciences Inc. (Cat. #00380601430) was used to measure real-time cell behavior. hMSCs at a concentration of 5,000 cells/cm^2 were seeded on the wells of an ACEATM E-Plate L16 (Cat. #00300600890, cell growth area of 0.32 cm^2 per well), on both control groups and test groups. The xCELLigence instrument was configured as described in our previous works [37][38]. Briefly, the xCELLigence RTCA S16 was placed inside the incubator to allow the device to warm up for at least 2 hours before use. The RTCA S16 was set up to perform readings every 10 minutes for a period of 72 hours of cell culture.

4.2.6. Immunomodulatory factor expression of hMSCs

For the hMSCs immunomodulatory factor expression, hMSCs (5000 cells/cm^2) were seeded on each well of a 24 well-plate using the previously mentioned control and test conditions, and the IDO activity was measured after 3 and 6 days of culture as described in our previous works [37][39][41]. Briefly, cell supernatant 100 µL was mixed with 100 µL standard assay mixture consisting of (potassium phosphate buffer (50mM, pH 6.5), ascorbic acid (40 mM, neutralized with NaOH), catalase (200 µg/ml), methylene blue (20 µ M), L-tryptophan (400 µM)). The mixture was kept at 37°C in a humidified incubator with 5% CO_2 for 30 min (in a dark environment to protect solutions from light) to allow IDO to convert L-tryptophan to N-formyl-kynurenine. After that, the reaction was stopped by adding 100 µL trichloroacetic acid 30% (wt./vol.) and incubating for 30 min at 58 °C. After hydrolysis of N-formyl-kynurenine to kynurenine, 100 µL of mixed cell supernatant/standard transfer into a well of a 96-well

microplate, followed by adding 100 μL per well of 2% (w/v) p- dimethylaminobenzaldehyde in acetic acid. Absorbance was read at 490 nm at the endpoint using a BioTek® Synergy 2 spectrophotometer (Synergy LX Multi-Mode Reader from BioTek® Model SLXFA).

4.2.7. HMSC differentiation

hMSCs differentiation was induced by exchange of culture with differentiation media (Osteogenic and Adipogenic media). Control cultures were grown in a regular cell expansion medium. Briefly, hMSCs (10,000 cells/cm^2) were seeded with each testing condition prepared on 24 well-plates and grown for 6 days in expansion medium (MEM Alpha (1X) supplemented with L-glutamine, ribonucleosides, and deoxyribonucleosides) containing 20% fetal bovine serum, 1.2% penicillin-streptomycin, and 1.2% L-glutamine at 37 °C in a humidified incubator with 5% CO_2. After the cells reached at least 50% confluency, they were exposed to a differentiation medium. For osteogenic differentiation, hMSCs were cultured in the differentiation medium (DMEM low glucose, 10% fetal bovine serum,1% penicillin, 1% L-Glutamin, 50 μM ascorbic acid (50mg/10ml)) (Sigma, Cas Number: 50-81-7), 10 mM β-glycerophosphate (Sigma, CAS Number: 154804-51-0, G9422), and 100nM dexamethasone (Sigma, CAS Number 50-02-2). The medium was replaced every 2-3 days. After 8 days of culture, cells were fixed with 10% formaldehyde. For osteogenic differentiation, Alizarin Red S (Sigma, CAS Number 130-22-3) staining solution was prepared by adding 2g Alizarin Red S in 100 mL water mixed. The pH was adjusted to 4.1– 4.3 by the addition of Ammonium Hydroxide, as necessary. Alizarin Red S solution was added to the fixed cells, then incubated at room temperature in the dark (cover with aluminum foil) for 15 minutes. The staining solution was removed and rinsed 3 times with PBS. The samples were analyzed immediately under the microscope to detect calcium deposits. For adipogenic differentiation, hMSCs were cultured in the differentiation medium consisting of

DMEM high glucose supplemented with 10% fetal bovine serum, 1% penicillin, 1% L-glutamine, 1 μM dexamethasone (Sigma, CAS Number 50-02-2), 0.01 mg/mL insulin (Sigma-Aldrich, Catalog No. I2643), 0.5 mM 3-isobutyl-1-methylxanthine (IBMX) (Sigma, CAS Number: 28822-58-4, I5879), and 100μM indomethacin (Sigma, CAS Number: 53-86-1). The medium was replaced every 2-3 days. After 8 days of culture, cells were fixed with 10% formaldehyde, stained with 0.5% (w/v) Oil Red O (Sigma-Aldrich, Catalog Number: O0625) in 100% isopropanol, and incubated at room temperature for 30 minutes and protected from light. The cell monolayer was washed 2 times with PBS. The sample was analyzed under a light microscope to detect lipid vesicles that appeared in bright red.

4.2.8. Effect of IFN-γ and PCN-333 on hMSCs protein expression

Protein expression was determined using a Luminex MAGPIX® and the Invitrogen Th1/Th2 Cytokine 11-Plex Human Kit (Assay ID: EPX110108010). The cells tested were seeded at a density of 5,000 cells/cm^2 in a 24-well plate. After 3 days of culture, 500 μL of supernatant from culture medium of each test and control group was collected. The samples were stored in a freezer at -80°C. On the day of reading, the samples were slowly thawed on ice, vortexed for 30 seconds, and then centrifuged at 2000g for 1 minute. Following this, 50 μL of each sample was analyzed according to the kit protocol. A total of 11 analytes were determined in this study. A one-way analysis of variance (ANOVA) performed comparisons among multiple groups. A p-value < 0.05 was considered statistically significant. The statistical analysis was done using SigmaPlot software version 14.

4.3. Results And Discussion

4.3.1. Characterization of PCN-333(Fe)

The successful synthesis of PCN-333(Fe) was confirmed via powder X-ray Diffraction, showing a pattern consistent with previous works (Figure 4-1 (A)) [11][36]. The product was then observed under SEM (Figure 4-1 (B)), which shows that the product is roughly spherical in nature. Upon size analysis using the Horiba LA-950, it was determined that the average particle size was 17.8 µm while the mode was 18.6 µm. The standard deviation was determined to be 2.7.

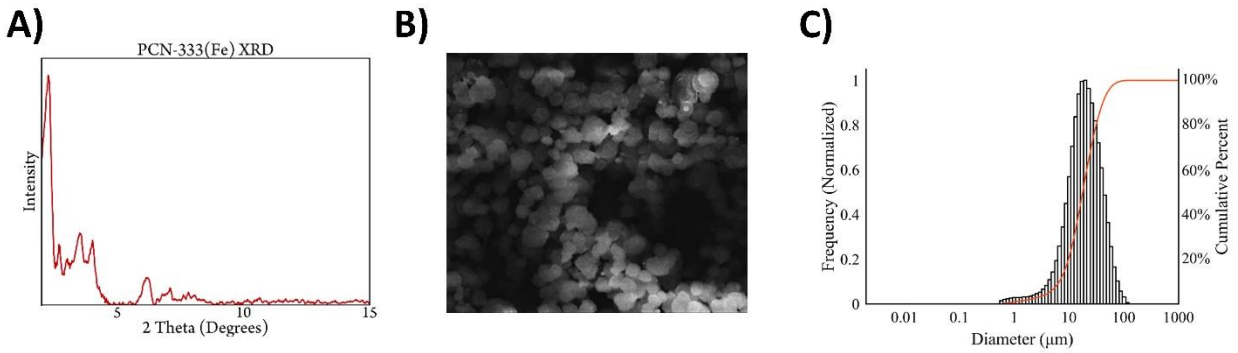

Figure 4-1. A) pXRD of synthesized PCN-333 (Fe) B) SEM image of synthesized PCN-333(Fe) with scale bar representing 40 µm. C) Size distribution of synthesized PCN-333(Fe)(black) and cumulative percentage of product (red).

4.3.2. Immobilization of IFN-γ with PCN-333(Fe)

To immobilize IFN-γ, a solution of 0.1 mg/ml IFN-γ and either 0.5 or 1 mg/ml PCN-333 in 20mM pH 7 HEPES buffer was prepared. The solution was lightly vortexed and allowed to sit at 4°C for 24 hours. The solution was then lightly vortexed and subsequently centrifuged at 1000 g for 1 minute. The supernatant was removed, and the sample was ready for incorporation into the cell media. Percent immobilization was then determined by absorbance of the supernatant at 280 nm against controls via Bradford Assay using UV-Vis spectrometry. This showed the percent immobilization to be 63.9% for the 0.5 mg/mL loading and 65.0% for the 1.0 mg/mL sample

4.3.3. PrestoBlue viability assay

Cytotoxicity was evaluated by monitoring the activity of the reagent Presto Blue after all conditions reached full confluency (Figure 4-2(A)). Using this reagent, cell viability was measured after 3 and 6 days of culturing hMSCs cells under each condition as described in the experimental design. Those conditions being with and without IFN-γ supplemented in the culture medium, MOF (0.5mg/mL), MOF (0.5mg/mL) + IFN-γ, MOF (1mg/mL), and MOF (1mg/mL) + IFN-γ. The negative control group selected contained cell medium lacking IFN-γ. The fluorescence intensity of this control was normalized to 100% and all other conditions were assessed in relation to this control group at 3 days and 6 days, respectively. Figure 4-2 (B) shows that the presence of IFN-γ in cell medium yields an increase cell viability of 5% and 11% compared to the control at 3 and 6 days, respectively. This 3 day result was not statistically different from the control ($P>0.05$) and show that IFN-γ itself does not significantly affect cell viability in the short term; however, over a longer period it appears to have a promoting effect. In contrast to this, the addition of MOF at both concentrations after 3 days showed a statistically significant increase in cell viability with the 0.5 mg/mL sample yielding a 14.5% increase and 6.7% increase for the 1 mg/mL sample ($P<0.05$). Thus, suggesting that MOF alone when present in media may improve cell viability. The reason for this is presently not clear. Apart from these results, all other data points did not statistically deviate from the control group and although there appears to be a decrease in the 1 mg/mL MOF sample at 6 days, this can be attributed to a slower growth rate as the value is in relation to the control group which slightly surpassed it in cell number. In regard to the MOF samples, this data indicates that they do not present a cytotoxic threat to hMSCs, making them suitable carriers.

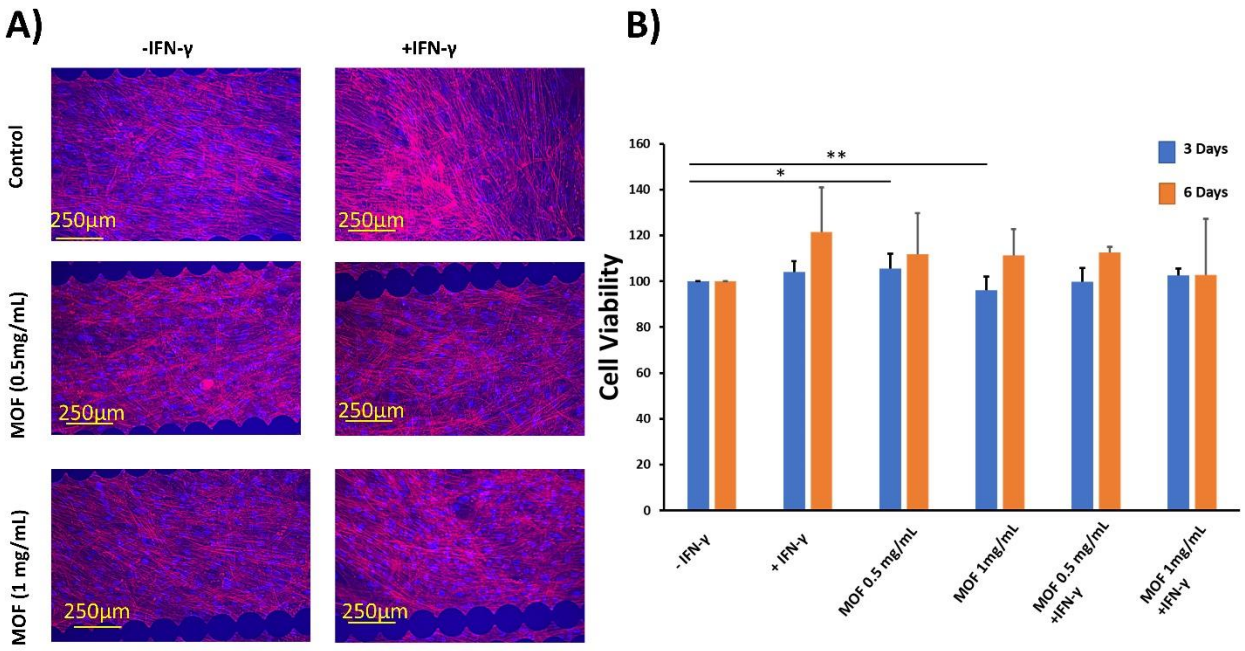

Figure 4-2. A) Fluorescence microscopy images of hMSCs nuclei and actin cytoskeleton, labeled with Hoechst and Actin Red. B) PrestoBlue Viability assay for cultured hMSCs after 3 and 6 days with each group normalized against their respective control (-IFN-γ) and with significant differences ($P<0.05$) compared to that control denoted with an asterisk.

4.3.4. Real-time monitoring of cell behavior and proliferation

In this study, hMSCs at 25,000 cells/cm^2 were cultured on E-Plate 16 to evaluate the real-time behavior of the cells during the first 72 hours of culture. The effect of control and test group media on these cells was evaluated. An xCELLigence RTCA S16 biosensor system was used to measure cell proliferation and growth. This system constantly measures the impedance difference caused by cells attached to microsensors present in culture plates (E-plates 16) and is monitored by microchips attached under the wells. In this way, the impedance difference is translated into a parameter known as the Cell Index (CI). Therefore, the higher the CI, the greater the number of cells are adhered and present on the bottom of the well [38]. Based on our

previous study, our results indicate two cell behavior phases: a cell adhesion (hours 0 – 20) and a cell growth phase (hours 20 – 50) [42]. In this test we used a similar cell density to our previous work which is also recommended by the manufacturer [38].

Figure 4-3 shows the CI values as a function of the first 50 hours of culture for the test and control groups. The figure shows a cell adhesion stage in the evaluated period, reaching a maximum peak at approximately 9 hours. CI values reached a maximum of 8 CI units. Compared to the samples with IFN-γ present, those lacking IFN-γ showed a slightly lower CI value which may correspond to slightly fewer cells adhering which is consistent with a recent study which showed that IFN-γ can lead to improved cell adhesion [43]. The decrease in CI between hours 9 – 20 corresponds to possible cell detachment and rearranging. Beyond hour 20, the CI index begins to increase slightly corresponding to a slow growth phase. These results indicate that the hMSCs have a similar adhesion and growth behavior in all of the conditions evaluated. This is in agreement with our PrestoBlue data, that MOF at both concentrations and with or without IFN-γ does not negatively affect cell adhesion. Regarding cell growth, there was almost no growth measured between hours 20 – 50. This performance could be because of the rapid increase in cell adherence observed in the first 10 hours leading to a confluence close to 100% in a short period [38].

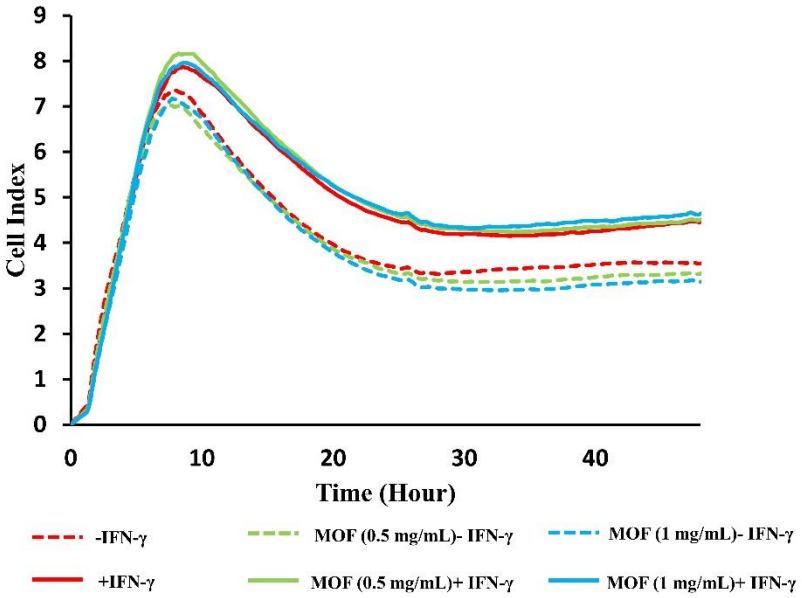

Figure 4-3. Real-time monitoring of hMSCs after 72 hours using xCELLigence

4.3.5. IDO assay

Indoleamine 2,3-dioxygenase (IDO) is a cytosolic heme protein important for immuno-regulatory functions [42][44]. Its presence can be evaluated by measuring the concentration of kynurenine, which is a known catalyzer that helps convert L-tryptophan to kynurenine [44][45]. The ability of IFN-γ to induce IDO expression in hMSCs was compared using the control and test groups and results were gathered after 3 days and 6 days. These results for IDO activity are summarized in Figure 4-4 which shows that IFN-γ supplemented in cell medium increases the IDO activity by roughly 3 times when compared to the cell medium without IFN-γ. These results are in line with the study done by Kwee et. al., indicating the IDO activity was correlated with the amount of IFN-γ present [46].

With regard to the bare MOF (0.5 mg/mL and 1 mg/mL) in cells medium, the results show no statistical differences when compared to the negative IFN-γ control. This indicates that MOF alone does not induce IDO activity. Also, both of the loaded MOF samples showed an increase

in IDO activity that was consistent to that of the positive IFN-γ control ($P<0.05$). This supports our claim that IFN-γ was successfully incorporated with the MOF particles in agreement with our Bradford Assay results. It also shows that, although a smaller portion of IFN-γ was loaded into the framework and provided to the cells in media compared to the control (50 ng/mL in the control vs. ~14 ng/mL loaded into MOF), there was an equivalent production of IDO. This result suggests that the immobilization of IFN-γ and its localized delivery to hMSCs provides a more bioavailable and active source than that of free IFN-γ in solution. In addition, the MOF (0.5mg/mL) + IFN-γ sample shows consistent IDO activity between both the 3 day and 6 day results. The same is true for the test using MOF (1 mg/mL) + IFN-γ at 3 days. These results indicate that the MOF at these concentrations and time period do not inhibit the release of IFN-γ. There was, however, a minor contrast in the test using MOF (1 mg/mL) + IFN-γ at 6 days. Although there was no statistical difference, a decrease in the average amount of IDO was present when compared to the positive control. This difference may be related to the amount of IFN-γ encapsulated in MOF when compared to the actual MOF concentration and can be expected when there are more potential binders in solution, given that there are twice the amount of MOF particles. Meaning that some IFN-γ released by the particles could have been immobilized again on another particle, thus, leading to this decreased affect. Together, these results indicate that MOF have the ability to release IFN-γ through passage of time and can provide excellent bioavailability of loaded IFN-γ to the localized cellular environment significantly surpassing the efficiency of free IFN-γ in solution.

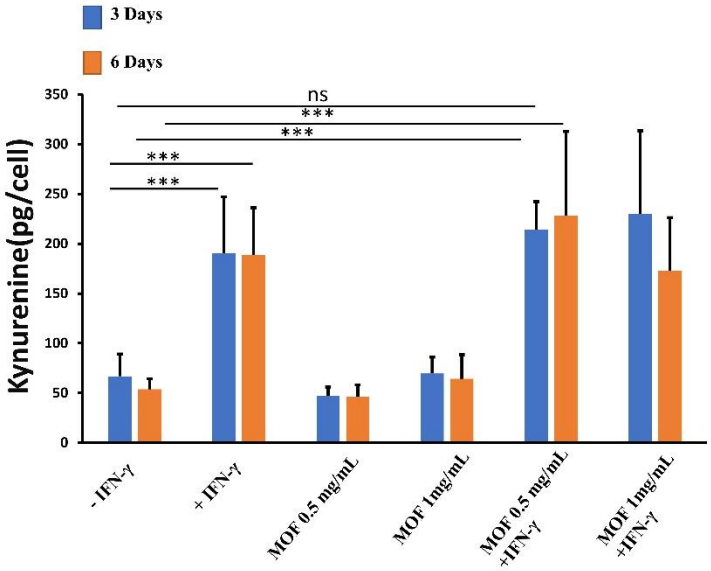

Figure 4-4. Cells immunomodulatory potential by IDO activity for hMSCs as a measure of picograms of kynurenine produced by cells cultured after 3 and 6 days with significant differences from respective controls marked accordingly (*P<0.05 & ***P<0.005).

4.3.6. Cell differentiation assay

The ability of hMSCs to differentiate into osteogenic and adipogenic lineages cells was induced by replacing the growth medium with the differentiation medium. The differentiation ability of hMSCs was evaluated to confirm the multipotentiality of hMSCs. After 10 days of incubation, cell functions associated with osteoblast differentiation (calcium deposition) and adipogenic differentiation were evaluated. Mineralization was also characterized from microscope images. Figure 4-5 shows that there are areas visible with red and purple, indicating the formation of the calcified regions and adipocyte-like cells, respectively. Figure 4-5 also shows that control cells show a calcium deposit formed by the clustering of cells due to the strong staining with Alizarin red even with and without IFN-γ, which indicates osteogenic differentiation of cells. The same results were found for MOF (0.5 and 1mg/mL) and MOF (0.5 and 1mg/mL) + IFN-γ, as shown

in Figure 4-5. This figure also shows that control cells, even with and without IFN-γ, have the ability to differentiate into adipogenic cells, which the cells changed from long spindle-shaped to flattened round or polygonal cells. In addition, the treatment with IFN-γ encapsulated in MOFs shows no inhibitory effect on the osteogenic and adipogenic differentiation of hMSCs and no staining was observed on cells cultured in regular expansion medium.

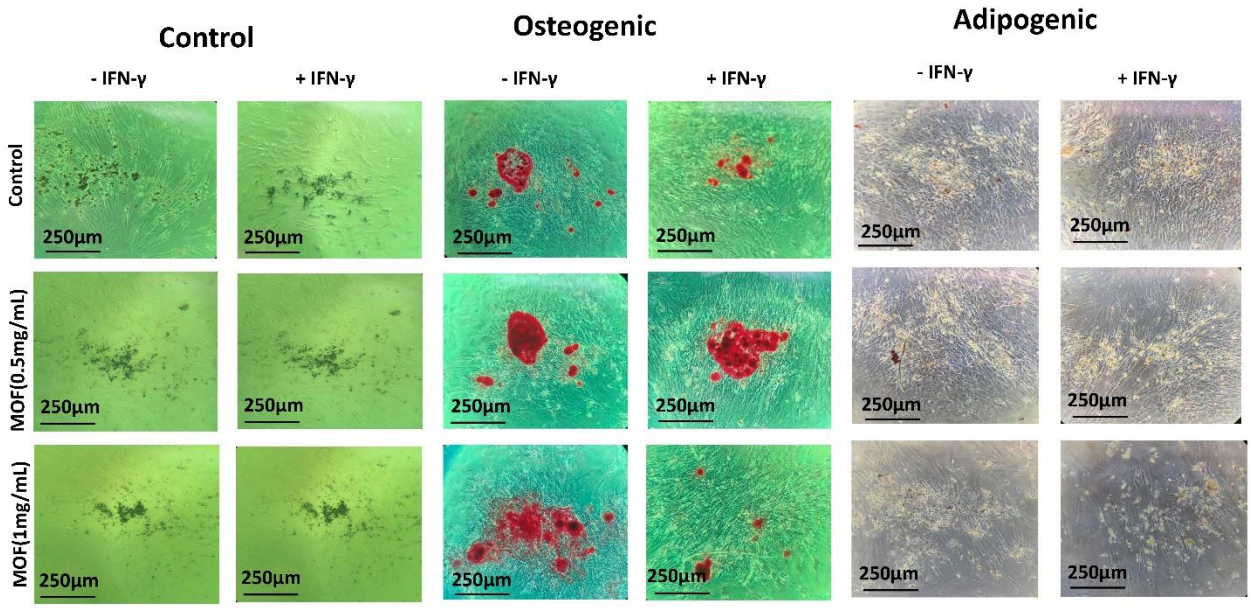

Figure 4-5. hMSCs differentiation. control cells inducing by normal expansion medium (left). Osteogenic differentiations were stained by Alizarin Red (center). Adipogenic differentiation were stained by Oil Red (right).

4.3.7. Effect of IFN-γ and PCN-333 on hMSCs protein expression

To determine whether the effect of the introduction of IFN-γ and MOF particles on the expected protein expression of hMSCs, we conducted a protein expression test. In doing so, a total of 11 cytokines were monitored for this assay. The five test conditions including the presence and/or absence of IFN-γ and MOF were analyzed, and the resulting concentration of the cytokines was

obtained in pg/ml. A Z-score for each analyte can be observed in a heat map provided in Figure 4-6 and an accompanying table of values has been provided in Table 1.

Table 1 Raw data results monitoring the effect of IFN-γ and PCN-333 on hMSCs protein expression using Invitrogen Th1/Th2 Cytokine 11-Plex Human Kit (Assay ID: EPX110108010) after 3-days of culture. Results are in pg/mL.

	CONTROL		MOF (0.5 mg/ml)		MOF (1 mg/ml)	
	(-) IFN-γ	(+) IFN-γ	(-) IFN-γ	(+) IFN-γ	(-) IFN-γ	(+) IFN-γ
IL-1 beta	303.18	654.04	215.92	768.79	277.00	805.67
IL-2	611.69	625.91	501.39	826.98	473.29	983.37
IL-4	547.57	1078.16	369.11	1245.27	369.11	1352.63
IL-5	110.73	505.55	110.73	834.63	110.73	1059.27
IL-6	39613.62	40363.60	29714.15	30582.78	30512.57	30484.39
IL-12p70	488.46	1015.03	418.70	1180.27	418.70	1212.23
IL-13	507.42	967.90	320.39	1108.24	320.39	1132.38
IL-18	676.91	3218.57	455.52	3580.66	486.73	3786.53
GM-CSF	1255.28	1298.82	1002.44	1920.01	1160.46	2208.34
TNF alpha	1099.78	1325.68	1066.55	1365.82	1040.70	1415.52
IFN gamma	ND	19059.37	ND	23411.19	ND	25433.80

After 3 days of cell culture, the control group containing IFN-γ showed a considerable increase in the concentration of all the analytes except for IL-6 compared to the negative control. These results demonstrate, in agreement with recent work by Garcia et. al., that the presence of IFN-γ produces a favorable effect on hMSCs protein expression [40]. This increase in Z-value by the control group was surpassed by the test groups containing IFN-γ immobilized with PCN-333 and showed a direct correlation between the concentration of MOF and resulting Z-value indicating that the presence of MOF in this process was contributing to amplified expression. Specifically, the IFN-γ immobilized on MOF resulted in increased expression of IL-2, GM-CSF, and TNF alpha in a ratio of about 1.5 times higher than that of the positive control, increases in IL-1 beta, IL-4, IL-12p70, and IL-13 were slightly more than doubled, and expression of IL-5 and IL-18 was over five times greater. In contrast to this, IL-6 expression decreased with the addition of

MOF and was not affected as IFN-γ was introduced indicating that its expression was independent from IFN-γ.

Although IL-6 acts dually as a pro- or anti-inflammatory cytokine, hMSCs have been shown to activate its immunosuppressive role [47]. Therefore, a decrease in the expression of IL-6 can be attributed as a favorable result for the immune response of hMSCs. This decrease in expression as MOF was introduced was not unique to IL-6 as the presence of bare MOF resulted in a decrease across the board to all proteins. This can be attributed to the extensive sink created with the addition of MOF as its presence introduces a severe depression in the distribution of extracellular components owing to its large inner pores.

Finally, IFN-γ concentration was also determined for all culture conditions. Samples containing IFN-γ showed approximately 19,000, 23,400, and 25,400 pg/ml for positive control, MOF 0.5 mg/mL, and MOF 1 mg/mL, respectively after these 3 days period. For this condition, an initial concentration of 50,000 pg/ml was dissolved in the cell media for the control group; therefore, our results indicate that the amount of IFN-γ decreases over time due to transient effects in the presence of hMSCs [35]. These can include protein degradation or consumption by cells. Alternatively, this sharp decrease in concentration is not observed in the presence of MOF particle.

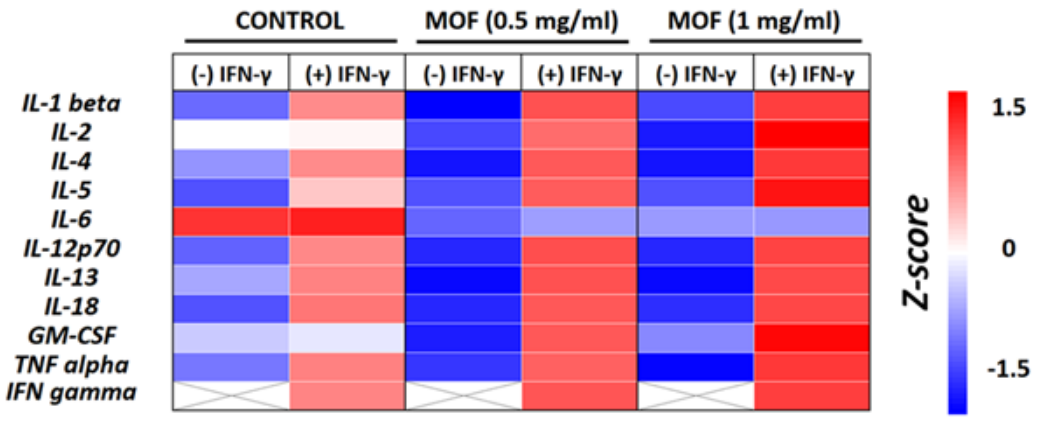

Figure 4-6. hMSC protein expression potential as a response of 3 days of cell culture under various conditions. Heatmap shows the Z-score val-ues of 11 human cytokines. Data is presented as the mean of n = 5 samples.

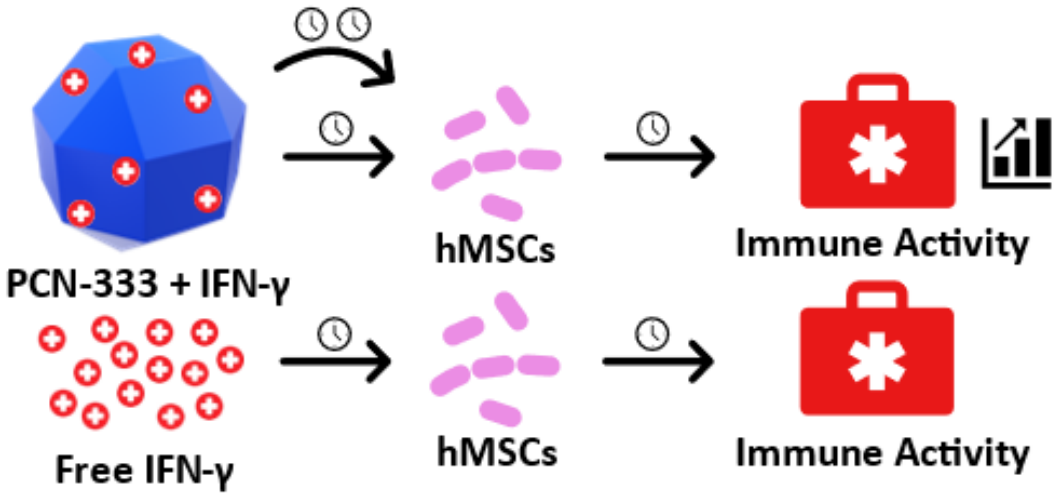

Figure 4-7. Experimental overview depicting the proposed sustained release and improved immunological activity of IFN-γ immobilized using PCN-333.

These results agree with recent studies showing that IFN-γ immobilization can lead to an increased immunological response [35][48]. They also indicate that MOFs can be applied to locally concentrate and provide sustained release of bioactive IFN-γ to potentiate hMSC immunomodulatory activity [35]. Additionally, the proteins selected for this panel were specifically chosen due to their role in the immune response. Thus, providing evidence that this

proposed synergistic effect using MOF to promote downstream proteins could be utilized as an instigator in applications to promote more efficient wound healing. A schematic overview of this process has been provided in Figure 4-7 where it shows the increased concentration of IFN-γ in solution compared to that loaded into the MOF, the release over time from the MOF (where the clock represents a time unit), and the improved immune activity promoted as a result of the immobilization of IFN-γ on PCN-333.

4.4. Conclusions

In this work, we tested the viability of the metal-organic framework PCN-333(Fe) as a carrier device for the local extracellular delivery of IFN-γ to hMSCs and monitored their immunomodulatory activity to determine efficacy. From our results, we show that, likewise to other publications, the PCN-333(Fe) has little to no effect on cell viability and the particle does not present signs of cytotoxicity. Additionally, when introduced to the cell differentiation assay, the experimental group containing the MOF particles showed no variance and continued to differentiate appropriately. When measuring the efficiency of IFN-γ to induce IDO, in the presence of MOF, the controls containing only the particle had no effect showing it to be an ideal carrier, not interfering with the biological pathways and, in fact, showed a slight promoting effect on cell viability at 3-days. When the immobilized IFN-γ with MOF was examined, although it had a lower IFN-γ content relative to the control group (~14 ng/mL vs. 50 ng/mL, respectively), it did not have a significant decrease in IDO activity and yielded an increase in the expression of proteins related to immune response exceeding that of the free IFN-γ control. This successful action of immobilized IFN-γ compared to the control group over the course of 3 and 6 days shows that PCN-333(Fe) (and likely other MOFs) is a suitable delivery device for small proteins and drugs to the localized cellular environment with no significant side effects on the

surrounding environment or the cellular ability to reproduce/differentiate and has the added benefit of providing a sustained release of loaded materials to nearby cells. Future studies will be needed to further understand the viability of this delivery method, but the results from this work suggest that the use of MOFs as a delivery device is a reasonable alternative to conventional methods of drug delivery.

ASSOCIATED CONTENT

Supporting Information

AUTHOR INFORMATION

Corresponding Author

*Dr. Jorge Almodovar, jlalmodo@uark.edu

Author Contributions

The manuscript was written through contributions of all authors. All authors have given approval to the final version of the manuscript.

4.5. ACKNOWLEDGMENT

This work was financially supported in part by the National Science Foundation under grant no. 2051582, and by the University of Arkansas Cell and Molecular Biology Graduate Program by providing JP with a scholarship. The authors thank the Arkansas Nano & Biomaterials Characterization Facility for their assistance with SEM. The authors thank the University of Arkansas Chemistry Department for access to the XRD.

ABBREVIATIONS

DNE, de-novo encapsulation; PSE, post-synthetic encapsulation; IFN-γ, interferon gamma; hMSCs, human mesenchymal stem cell

4.6. References

[1] M. Eddaoudi, H. Li, and O. M. Yaghi, “Highly Porous and Stable Metal−Organic Frameworks: Structure Design and Sorption Properties,” *J. Am. Chem. Soc.*, vol. 122, no. 7, pp. 1391–1397, Feb. 2000, doi: 10.1021/ja9933386.

[2] J. Kim *et al.*, “Assembly of Metal−Organic Frameworks from Large Organic and Inorganic Secondary Building Units: New Examples and Simplifying Principles for Complex Structures,” *J. Am. Chem. Soc.*, vol. 123, no. 34, pp. 8239–8247, Aug. 2001, doi: 10.1021/ja010825o.

[3] M. Eddaoudi *et al.*, “Modular Chemistry: Secondary Building Units as a Basis for the Design of Highly Porous and Robust Metal−Organic Carboxylate Frameworks,” *Acc. Chem. Res.*, vol. 34, no. 4, pp. 319–330, Apr. 2001, doi: 10.1021/ar000034b.

[4] N. L. Rosi *et al.*, “Hydrogen Storage in Microporous Metal-Organic Frameworks,” *Science*, vol. 300, no. 5622, pp. 1127–1129, May 2003, doi: 10.1126/science.1083440.

[5] D. J. Tranchemontagne, J. L. Mendoza-Cortés, M. O’Keeffe, and O. M. Yaghi, “Secondary building units, nets and bonding in the chemistry of metal–organic frameworks,” *Chem. Soc. Rev.*, vol. 38, no. 5, pp. 1257–1283, Apr. 2009, doi: 10.1039/B817735J.

[6] J. R. Long and O. M. Yaghi, “The pervasive chemistry of metal–organic frameworks,” *Chem. Soc. Rev.*, vol. 38, no. 5, pp. 1213–1214, Apr. 2009, doi: 10.1039/B903811F.

[7] H. Furukawa, K. E. Cordova, M. O’Keeffe, and O. M. Yaghi, “The Chemistry and Applications of Metal-Organic Frameworks,” *Science*, vol. 341, no. 6149, p. 1230444, Aug. 2013, doi: 10.1126/science.1230444.

[8] M. Eddaoudi *et al.*, “Systematic Design of Pore Size and Functionality in Isoreticular MOFs and Their Application in Methane Storage,” *Science*, vol. 295, no. 5554, pp. 469–472, Jan. 2002, doi: 10.1126/science.1067208.

[9] P. Li *et al.*, “Hierarchically Engineered Mesoporous Metal-Organic Frameworks toward Cell-free Immobilized Enzyme Systems,” *Chem*, vol. 4, no. 5, pp. 1022–1034, May 2018, doi: 10.1016/j.chempr.2018.03.001.

[10] Y. Pan *et al.*, “How Do Enzymes Orient When Trapped on Metal–Organic Framework (MOF) Surfaces?,” *J. Am. Chem. Soc.*, vol. 140, no. 47, pp. 16032–16036, Nov. 2018, doi: 10.1021/jacs.8b09257.

[11] J. Phipps *et al.*, “Catalytic Activity, Stability, and Loading Trends of Alcohol Dehydrogenase Enzyme Encapsulated in a Metal–Organic Framework,” *ACS Appl. Mater. Interfaces*, vol. 12, no. 23, pp. 26084–26094, Jun. 2020, doi: 10.1021/acsami.0c06964.

[12] Y. Chen, S. Han, X. Li, Z. Zhang, and S. Ma, “Why Does Enzyme Not Leach from Metal–Organic Frameworks (MOFs)? Unveiling the Interactions between an Enzyme Molecule and a MOF,” *Inorg. Chem.*, vol. 53, no. 19, pp. 10006–10008, Oct. 2014, doi: 10.1021/ic501062r.

[13] X. Lian, Y.-P. Chen, T.-F. Liu, and H.-C. Zhou, “Coupling two enzymes into a tandem nanoreactor utilizing a hierarchically structured MOF,” *Chem. Sci.*, vol. 7, no. 12, pp. 6969–6973, Nov. 2016, doi: 10.1039/C6SC01438K.

[14] M. B. Majewski, A. J. Howarth, P. Li, M. R. Wasielewski, J. T. Hupp, and O. K. Farha, “Enzyme encapsulation in metal–organic frameworks for applications in catalysis,” *CrystEngComm*, vol. 19, no. 29, pp. 4082–4091, Jul. 2017, doi: 10.1039/C7CE00022G.

[15] X. Lian *et al.*, “Enzyme–MOF (metal–organic framework) composites,” *Chem. Soc. Rev.*, vol. 46, no. 11, pp. 3386–3401, Jun. 2017, doi: 10.1039/C7CS00058H.

[16] Y. Zhang, J. Ge, and Z. Liu, “Enhanced Activity of Immobilized or Chemically Modified Enzymes,” *ACS Catal.*, vol. 5, no. 8, pp. 4503–4513, Aug. 2015, doi: 10.1021/acscatal.5b00996.

[17] X. Lian, A. Erazo-Oliveras, J.-P. Pellois, and H.-C. Zhou, “High efficiency and long-term intracellular activity of an enzymatic nanofactory based on metal-organic frameworks,” *Nat. Commun.*, vol. 8, no. 1, Art. no. 1, Dec. 2017, doi: 10.1038/s41467-017-02103-0.

[18] À. Ruyra *et al.*, “Synthesis, Culture Medium Stability, and In Vitro and In Vivo Zebrafish Embryo Toxicity of Metal–Organic Framework Nanoparticles,” *Chem. – Eur. J.*, vol. 21, no. 6, pp. 2508–2518, 2015, doi: 10.1002/chem.201405380.

[19] M. A. Luzuriaga *et al.*, “Enhanced Stability and Controlled Delivery of MOF-Encapsulated Vaccines and Their Immunogenic Response In Vivo,” *ACS Appl. Mater. Interfaces*, vol. 11, no. 10, pp. 9740–9746, Mar. 2019, doi: 10.1021/acsami.8b20504.

[20] T. L. Ramos *et al.*, “MSC surface markers (CD44, CD73, and CD90) can identify human MSC-derived extracellular vesicles by conventional flow cytometry,” *Cell Commun. Signal.*, vol. 14, no. 1, p. 2, Jan. 2016, doi: 10.1186/s12964-015-0124-8.

[21] G. Brooke *et al.*, “Therapeutic applications of mesenchymal stromal cells,” *Semin. Cell Dev. Biol.*, vol. 18, no. 6, pp. 846–858, Dec. 2007, doi: 10.1016/j.semcdb.2007.09.012.

[22] M. F. Pittenger, D. E. Discher, B. M. Péault, D. G. Phinney, J. M. Hare, and A. I. Caplan, “Mesenchymal stem cell perspective: cell biology to clinical progress,” *Npj Regen. Med.*, vol. 4, no. 1, pp. 1–15, Dec. 2019, doi: 10.1038/s41536-019-0083-6.

[23] F. M. Watt and W. T. S. Huck, “Role of the extracellular matrix in regulating stem cell fate,” *Nat. Rev. Mol. Cell Biol.*, vol. 14, no. 8, pp. 467–473, Aug. 2013, doi: 10.1038/nrm3620.

[24] R. O. Hynes, “The extracellular matrix: not just pretty fibrils,” *Science*, vol. 326, no. 5957, pp. 1216–1219, Nov. 2009, doi: 10.1126/science.1176009.

[25] H. Lortat-Jacob, “The molecular basis and functional implications of chemokine interactions with heparan sulphate,” *Curr. Opin. Struct. Biol.*, vol. 19, no. 5, pp. 543–548, Oct. 2009, doi: 10.1016/j.sbi.2009.09.003.

[26] M. F. Brizzi, G. Tarone, and P. Defilippi, “Extracellular matrix, integrins, and growth factors as tailors of the stem cell niche,” *Curr. Opin. Cell Biol.*, vol. 24, no. 5, pp. 645–651, Oct. 2012, doi: 10.1016/j.ceb.2012.07.001.

[27] M. W. Klinker, R. A. Marklein, J. L. Lo Surdo, C.-H. Wei, and S. R. Bauer, "Morphological features of IFN-γ-stimulated mesenchymal stromal cells predict overall immunosuppressive capacity," *Proc. Natl. Acad. Sci. U. S. A.*, vol. 114, no. 13, pp. E2598–E2607, Mar. 2017, doi: 10.1073/pnas.1617933114.

[28] J. N. Ijzermans and R. L. Marquet, "Interferon-gamma: a review," *Immunobiology*, vol. 179, no. 4–5, pp. 456–473, Oct. 1989, doi: 10.1016/S0171-2985(89)80049-X.

[29] Y. Liu *et al.*, "Mesenchymal stem cell–based tissue regeneration is governed by recipient T lymphocytes via IFN-γ and TNF-α," *Nat. Med.*, vol. 17, no. 12, pp. 1594–1601, Dec. 2011, doi: 10.1038/nm.2542.

[30] R. Prakash, R. K. Mishra, A. Ahmad, M. A. Khan, R. Khan, and S. S. Raza, "Sivelestat-loaded nanostructured lipid carriers modulate oxidative and inflammatory stress in human dental pulp and mesenchymal stem cells subjected to oxygen-glucose deprivation," *Mater. Sci. Eng. C*, vol. 120, p. 111700, Jan. 2021, doi: 10.1016/j.msec.2020.111700.

[31] J. Croitoru-Lamoury *et al.*, "Interferon-γ regulates the proliferation and differentiation of mesenchymal stem cells via activation of indoleamine 2,3 dioxygenase (IDO)," *PloS One*, vol. 6, no. 2, p. e14698, Feb. 2011, doi: 10.1371/journal.pone.0014698.

[32] D. A. Castilla-Casadiego, J. R. García, A. J. García, and J. Almodovar, "Heparin/Collagen Coatings Improve Human Mesenchymal Stromal Cell Response to Interferon Gamma," *ACS Biomater. Sci. Eng.*, vol. 5, no. 6, pp. 2793–2803, Jun. 2019, doi: 10.1021/acsbiomaterials.9b00008.

[33] J. K. Leach and J. Whitehead, "Materials-Directed Differentiation of Mesenchymal Stem Cells for Tissue Engineering and Regeneration," *ACS Biomater. Sci. Eng.*, vol. 4, no. 4, pp. 1115–1127, Apr. 2018, doi: 10.1021/acsbiomaterials.6b00741.

[34] A. Ahmad *et al.*, "Gelatin-Coated Polycaprolactone Nanoparticle-Mediated Naringenin Delivery Rescue Human Mesenchymal Stem Cells from Oxygen Glucose Deprivation-Induced Inflammatory Stress," *ACS Biomater. Sci. Eng.*, vol. 5, no. 2, pp. 683–695, Feb. 2019, doi: 10.1021/acsbiomaterials.8b01081.

[35] J. A. Zimmermann, M. H. Hettiaratchi, and T. C. McDevitt, "Enhanced Immunosuppression of T Cells by Sustained Presentation of Bioactive Interferon-γ Within Three-Dimensional Mesenchymal Stem Cell Constructs," *Stem Cells Transl. Med.*, vol. 6, no. 1, pp. 223–237, Jan. 2017, doi: 10.5966/sctm.2016-0044.

[36] J. Park, D. Feng, and H.-C. Zhou, "Dual Exchange in PCN-333: A Facile Strategy to Chemically Robust Mesoporous Chromium Metal–Organic Framework with Functional Groups," *J. Am. Chem. Soc.*, vol. 137, no. 36, pp. 11801–11809, Sep. 2015, doi: 10.1021/jacs.5b07373.

[37] D. A. Castilla-Casadiego, A. M. Reyes-Ramos, M. Domenech, and J. Almodovar, "Effects of Physical, Chemical, and Biological Stimulus on h-MSC Expansion and Their Functional Characteristics," *Ann. Biomed. Eng.*, vol. 48, no. 2, pp. 519–535, Feb. 2020, doi: 10.1007/s10439-019-02400-3.

[38] L. Pinzon-Herrera, J. Mendez-Vega, A. Mulero-Russe, D. A. Castilla-Casadiego, and J. Almodovar, “Real-time monitoring of human Schwann cells on heparin-collagen coatings reveals enhanced adhesion and growth factor response,” *J. Mater. Chem. B*, vol. 8, no. 38, pp. 8809–8819, Oct. 2020, doi: 10.1039/D0TB01454K.

[39] S. J. Cifuentes, P. Priyadarshani, D. A. Castilla-Casadiego, L. J. Mortensen, J. Almodóvar, and M. Domenech, “Heparin/collagen surface coatings modulate the growth, secretome, and morphology of human mesenchymal stromal cell response to interferon-gamma,” *J. Biomed. Mater. Res. A*, vol. 109, no. 6, pp. 951–965, Jun. 2021, doi: 10.1002/jbm.a.37085.

[40] M. Haseli *et al.*, “Immunomodulatory functions of human mesenchymal stromal cells are enhanced when cultured on HEP/COL multilayers supplemented with interferon-gamma,” *Mater. Today Bio*, vol. 13, p. 100194, Jan. 2022, doi: 10.1016/j.mtbio.2021.100194.

[41] D. A. Castilla-Casadiego *et al.*, “Methods for the Assembly and Characterization of Polyelectrolyte Multilayers as Microenvironments to Modulate Human Mesenchymal Stromal Cell Response,” *ACS Biomater. Sci. Eng.*, vol. 6, no. 12, pp. 6626–6651, Dec. 2020, doi: 10.1021/acsbiomaterials.0c01397.

[42] J. C. Mbongue, D. A. Nicholas, T. W. Torrez, N.-S. Kim, A. F. Firek, and W. H. R. Langridge, “The Role of Indoleamine 2, 3-Dioxygenase in Immune Suppression and Autoimmunity,” *Vaccines*, vol. 3, no. 3, pp. 703–729, Sep. 2015, doi: 10.3390/vaccines3030703.

[43] J. J. Montesinos *et al.*, “Human Bone Marrow Mesenchymal Stem/Stromal Cells Exposed to an Inflammatory Environment Increase the Expression of ICAM-1 and Release Microvesicles Enriched in This Adhesive Molecule: Analysis of the Participation of TNF-α and IFN-γ,” *J. Immunol. Res.*, vol. 2020, p. 8839625, Nov. 2020, doi: 10.1155/2020/8839625.

[44] O. Takikawa, T. Kuroiwa, F. Yamazaki, and R. Kido, “Mechanism of interferon-gamma action. Characterization of indoleamine 2,3-dioxygenase in cultured human cells induced by interferon-gamma and evaluation of the enzyme-mediated tryptophan degradation in its anticellular activity.,” *J. Biol. Chem.*, vol. 263, no. 4, pp. 2041–2048, Feb. 1988, doi: 10.1016/S0021-9258(19)77982-4.

[45] W. Däubener, N. Wanagat, K. Pilz, S. Seghrouchni, H. G. Fischer, and U. Hadding, “A new, simple, bioassay for human IFN-gamma,” *J. Immunol. Methods*, vol. 168, no. 1, pp. 39–47, Jan. 1994, doi: 10.1016/0022-1759(94)90207-0.

[46] B. J. Kwee *et al.*, “Functional heterogeneity of IFN-γ–licensed mesenchymal stromal cell immunosuppressive capacity on biomaterials,” *Proc. Natl. Acad. Sci.*, vol. 118, no. 35, pp. 1–12, Aug. 2021, doi: 10.1073/pnas.2105972118.

[47] A. Dorronsoro *et al.*, “Intracellular role of IL-6 in mesenchymal stromal cell immunosuppression and proliferation,” *Sci. Rep.*, vol. 10, no. 1, Art. no. 1, Dec. 2020, doi: 10.1038/s41598-020-78864-4.

[48] J. R. García *et al.*, “IFN-γ-tethered hydrogels enhance mesenchymal stem cell-based immunomodulation and promote tissue repair,” *Biomaterials*, vol. 220, p. 119403, Nov. 2019, doi: 10.1016/j.biomaterials.2019.119403.

5. Enhanced Immunosuppression of Human Mesenchymal Stem/Stromal Cells by Sustained Presentation of Interferon-Gamma (IFN-Γ) within Metal-Organic Frameworks (MOFs) Embedded on Heparin/Collagen Multilayers

Mahsa Haseli[1], Xiaolei Hao[2], S. Ranil Wickramasinghe[1], and Jorge Almodovar[1*]

[1]Ralph E. Martin Department of Chemical Engineering, University of Arkansas, 3202 Bell Engineering Center, Fayetteville, AR 72701, USA

[2]Department of Biomedical Engineering, John A. White, Jr. Engineering Hall, 790 W. Dickson St. Suite 120, Fayetteville, AR 72701

Abstract

The immunomodulatory activity of human mesenchymal stem/stromal cells (hMSCs) can be enhanced in the presence of interferon-gamma (IFN-γ). Although pretreatment with IFN-γ is commonly used to potentiate hMSCs immunomodulatory activity, sustaining the presentation of IFN-γ in cell environments is limited. Therefore, in this study, we investigate the sustainable presence of IFN-γ in the cell culture medium by immobilizing it in a water-stable metal-organic frameworks (MOFs) [PCN-333(Fe)]. The immobilized IFN-γ in MOFs is coated on top of multilayers of heparin (HEP), and collagen (COL) (HEP/COL) that were used as a bioactive surface. Multilayers were formed, via layer-by-layer assembly, varying the final layer between COL and HEP. We evaluated the viability, differentiation, and immunomodulatory activity of hMSCs cultured on (HEP/COL) multilayers coated with immobilized IFN-γ in MOFs after 3 and 6 days. Cell viability was not affected by the presence of immobilized IFN-γ in MOFs when coated on (HEP/COL) multilayers compared to tissue culture plastic. We also confirmed that hMSCs osteogenic and adipogenic differentiation remained unaffected. We measured the immunomodulatory activity of hMSCs by measuring the level of indoleamine 2,3-dioxygenase (IDO) expression. IDO expression was higher in (HEP/COL) multilayers coated with immobilized IFN-γ in MOFs after 6 days of culture. Altogether, (HEP/COL) multilayers coated

with immobilized IFN-γ in MOFs provide a sustained presentation of cytokines to potentiate hMSCs immunomodulatory activity.

Keywords: Metal-organic framework, layer-by-layer assembly, immunomodulatory activity, collagen, heparin, mesenchymal stromal cells

5.1. Introduction

Human mesenchymal stromal cells (hMSCs) are of particular interest for cellular therapy programs [1]. They can differentiate into mesodermal lineage cells, including adipocytes, osteoblasts, and chondrocytes [2][3]. During tissue damage, hMSCs also have the ability to secrete paracrine and anti-inflammatory factors to repair tissue [4][5][6]. In addition, hMSCs possess remarkable immunomodulatory activity by producing anti-inflammatory and immunosuppressive factors [7][8][9][10][11][12]. By producing immunosuppressive factors, hMSCs inhibit the activation, proliferation, and function of both adaptive immune and innate immune cells, such as B cells and T cells [8][13][14]. Immune suppression by hMSCs appears as a multifactorial process that relies on cell-cell contact working in collaboration with the secretion of soluble immune factors [15][16]. These specific immune factors, including IFN-γ initiate the hMSCs immunosuppression program, by inducing the synthesis of protein factors, in particular indolamine-2,3-dioxygenase (IDO) and inducible nitric oxide synthase [17][18][19]. However, the expression of IDO is critically necessary for hMSCs suppression of T-cell proliferation; IDO is not constitutively expressed by resting hMSCs, and its expression is strongly induced by exposure of hMSCs to IFN-γ [20]. A study showed that IFN-γ has the ability to modulate the immune properties and differentiation potential of hMSCs, which has a significant antiproliferative effect [21]. Therefore, there is a need to reduce the antiproliferative effect of IFN-γ on hMSCs. To overcome the antiproliferative effect of IFN-γ on hMSCs, we designed polyelectrolyte multilayers via the layer-by-layer (LbL) technique. We have previously

demonstrated the construction of polyelectrolyte multilayers composed of heparin and collagen (HEP/COL), terminating in COL (12 layers HEP/COL) or HEP (13 layers HEP/COL) [22]. We confirmed that (HEP/COL) multilayers with IFN-γ supplemented in a cell medium increase the immunomodulatory activity of hMSCs [23]. However, pretreatment of hMSCs may limit the potential of hMSCs to modulate immune responses for more than a few days in environments due to transient effects [24]. With the purpose of enhancing the sustainable presence of IFN-γ in the cell medium, we hypothesized that metal-organic frameworks (MOFs) loaded with IFN-γ may provide sustaining presentation of bioactive IFN-γ to potentiate hMSCs immunomodulatory activity. MOFs are porous crystalline materials synthesized with metal-containing nodes and organic ligands [48][49]. MOFs have many advantages, such as tunable but uniform pore sizes, ultrahigh surface area, and easy modification, that make for the immobilization of many molecules, such as metal complexes, nanoparticles, and proteins [25][26]. Among different types of MOFs PCN-333(Fe) shows a high stability in aqueous solution, higher surface area and ultra-high porosity, which can lead to high protein loading [27].

Here, we expand on our previous work by evaluating the behavior of hMSCs-derived from bone marrow on polymeric multilayers coated with immobilized IFN-γ in MOFs PCN-333(Fe). Polymeric multilayers composed of collagen (COL) and heparin (HEP) that are either terminated in COL (12 layers of HEP/COL) or HEP (13 layers of HEP/COL) were investigated. We evaluated 12 and 13 layers of HEP/COL because we showed no differences in cell function as a function of the number of layers after 12 layers [29]. We also have previously demonstrated that 12 layers are the minimum number of layers to provide complete surface coverage [38]. These heparin/collagen arrangements will be noted as COL and HEP, respectively. The experiments were conducted for cases with and without IFN-γ supplemented in the culture medium as

control. The immobilized IFN-γ in MOFs arrangement will be noted as MOFs. Also, the cell behavior was evaluated for immobilized IFN-γ in MOFs supplemented in the culture medium and coated on top of COL and HEP multilayers after 3 and 6 days after cell culture. The ability of MOFs coated on polymeric multilayers to induce sustained immunomodulatory activity was evaluated by measuring IDO expression. This study evaluated hMSCs viability and differentiation as a function of MOFs coated on polymeric multilayers composition. This study demonstrates that the MOFs coating did not negatively influence the viability and differentiation of hMSCs. Moreover, this study shows that hMSCs cultured on HEP multilayers coated with MOFs have a greater capacity to provide sustaining presentation of bioactive IFN-γ to potentiate hMSCs immunomodulatory activity. Altogether, this study shows that MOFs PCN-333(Fe) can successfully be coated on (HEP/COL) multilayers to provide a sustainable presentation of IFN-γ to potentiate hMSCs immunomodulatory activity.

5.2. Experimental

5.2.1. Synthesis of PCN-333(Fe)

The precursor 4,4′,4″-s-triazine-2,4,6-triyl-tribenzoic acid (H_3TATB) and MOFs PCN-333(Fe) were synthesized according to the method described in work done by Park et al. 2015 [28]. In a 15 mL reaction vessel, we combined 60 mg H_3TATB, 60 mg anhydrous $FeCl_3$ (III), 0.6 mL TFA, and 10 mL dimethylformamide. The vessel was then sealed and placed in an oven at 150°C for 12 hours. Brown precipitate formed and was collected by centrifugation. The product was washed several times each by dimethylformamide, acetone, and water with centrifugation after each step to collect. Water was then exchanged with acetone three times before activation in an oven at 70°C overnight. The product was then confirmed via X-ray diffraction (XRD) PW1830

using a Panalytical MPD system equipped with a Cu sealed tube (λ = 1.54178) at 40 kV and 40 mA at 25 °C **Error! Reference source not found.**.

5.2.2. Encapsulation of IFN-γ on MOFs

A loading solution of MOFs and IFN-γ was combined with a final concentration 0.5 mg/mL MOFs and 5mg/mL of IFN-γ, diluted in Dulbecco's phosphate-buffered saline (DPBS)1X without Ca2+ and Mg2+ with final volume 50µL. This solution was vortexed and allowed to sit at 4°C for 24 hours. The supernatant was then removed after gentle centrifugation at 1000 g for 1 minute leaving the immobilized IFN-γ and MOFs. The supernatant was re-moved, and the sample was ready for incorporation into the cell medium.

The encapsulation efficiency of immobilized IFN-γ in MOFs was determined from the supernatant of two different batches after storing at 4°C for 24 hours. The standard curve was determined from the four samples containing 0, 0.05,0.1, and 0.2 mg/mL IFN-γ in DPBS. Encapsulation was determined by 214 nm High-Performance Liquid Chromatography (HPLC) (Waters HPLC with Empower 3 software, 2695 separations module with inline 2998 photodiode array detector C18 column is a Cogent Bidentate C18 2.1 x 150mm, particle size 4um). The injection volume for the sample was 20 µL.

In addition, protein quantification was determined micro-BCA protein assay kit (Thermo Scientific). According to the manufacturer's protocol, 150 µL of the sample's supernatant (was placed in a 96 well-plate with 150 µL of working reagent made from a micro-BCA protein assay kit (Thermo Scientific). The well plate was covered with foil and incubated at 37 °C for 2 hours. Absorbance was read at 562 nm using a BioTek Multi-Mode Microplate Reader (Model SynergyTM 2).

5.2.3. (HEP/COL) Multilayers Fabrication

(HEP/COL) multilayers were constructed by the LbL technique as described in our previous works [22][29][30][31]. Heparin sodium (HEP) was purchased from Celsus Laboratories, Inc. (Cat. #PH3005) and lyophilized type I collagen sponges (COL) derived from bovine tendon (generously donated by Integra Lifesciences Holdings Corporation, Añasco, PR) were used to construct polymeric multilayers by the LbL technique on sterile tissue culture-treated plates from Corning Costar (Cat. #07-200- 740). Poly(ethylenimine) (PEI) (50% solution in Water, Mw ≈ 750 000) from Sigma-Aldrich (Cat. #P3143) was used to produce a strong anchoring layer prior to (HEP/COL) multilayers fabrication. PEI (1 mg/mL), HEP (1 mg/mL) and COL (1 mg/mL) were dissolved in sodium acetate buffer (0.1 M sodium acetate anhydrous, 0.1 M acetic acid, at pH 5 for HEP and PEI, and pH 4 for COL). Sodium acetate buffer at pH 5 was used as washing solution, ultrapure water at 18 MΩ·cm used to prepare polymeric and wash solutions was obtained from a Millipore-SigmaTM Direct-QTM 3 (Cat. #ZRQSVP3US). Sequential polymeric layers and rinsing were done using manual pipetting on sterile tissue culture-treated plates. Briefly, the process consisted of creating a positive initial layer by depositing PEI solution for 15 minutes to each well of a sterile tissue culture-treated plate and followed by a 3 minute washing step with sodium acetate buffer at pH 5. HEP was added for 5 minutes; then the HEP solution was removed, collected, and rinsed with sodium acetate buffer at pH 5 solution for 3 minutes. Then COL was added and subsequently rinsed following the same process. This process was followed until obtaining a total of 12 polymeric layers of (HEP/COL) (layers ending with COL) and 13 polymeric layers of (HEP/COL) (layers ending with HEP). Then, immobilized IFN-γ in MOFs which was dissolved in 15 mL DPBS were coated on top of the last layer of each multilayers for at least 1 hour. Then, the solution was removed after 1 hour, a final wash was

done using DPBS for 3 minutes. Substrates were sterilized using ultraviolet light (UV) for 10 minutes to reduce contamination before seeding the cells.

5.2.4. Experimental Design

In this work, the effects on the cellular response of hMSCs of the presence of IFN-γ recombinant human protein (ThermoFisher, Cat. #PHC4031) encapsulated inside MOFs in the culture medium and coated at the last layer of (HEP/COL) multilayers were studied. Six test conditions were examined including a negative control group lacking IFN-γ (-IFN-γ), a positive control group (+IFN-γ) (50 ng/mL), and test groups containing either 0.5 mg/mL MOFs with immobilized IFN-γ either supplemented in the cell culture medium or coated at top of the last layer of (HEP/COL) multilayers. Cell medium containing MOFs was created by placing MOFs (loaded with IFN-γ) in 15 mL of medium in 15 mL centrifuge tube and subsequently vortexed before addition to cells soon after and had a final concentration of 14.2 ng/mL for the 0.5 mg/mL MOFs sample. Conditions will hereafter be referred to as “control groups” containing media with and without IFN-γ (+/-) and “test groups” containing MOFs at a concentration of 0.5 mg/mL with IFN-γ loaded. IFN-γ supplemented in cell medium was evaluated at a concentration of 50 ng/mL, and conditions with and without IFN-γ were designated as +IFN-γ and −IFN-γ, respectively. A 50 ng/mL concentration for soluble IFN-γ was selected based on our previous study [25][26]. Time points and the initial number of cells were selected according to the nature of the specific method used.

5.2.5. Characterizations

(HEP/COL) multilayers coated with MOFs were coated on glass with size 10*10 um to be used for future characterization. An Agilent Atomic Force Microscope (AFM), Dimension Icon with ScanAsyst, Bruke was used to characterize the topography properties of coating. Contact in air

mode was used to analyze the topography. The scanning speed used was 512 data points per scan line. Scan frequency was 1.0 Hz, and size was 10*10 um.

Surface morphology images were obtained using a scanning electron microscope (SEM) (FEI Nova Nanolab 200 workstation fitted with Bruker Quantax EDX). Before imaging, each sample was coated with 10 nm of gold/palladium.

The multilayers growth and MOFs interaction with the (HEP/COL) multilayers were followed by quartz crystal microbalance (QCM-D) with dissipation measurements. QCM-D measurements were performed on quartz crystal microbalance with dissipation from Biolin Scientific, Sweden. The multilayers build-up process was described in our previous work [39]. Briefly, the quartz crystal was immersed in 5:1:1 (volume parts) at 75 °C of water, 25% ammonia, and 30% hydrogen peroxide. The clean quartz crystal was placed in the QCM-D chamber. Then the PEI solution was injected at a flow rate of 100 mL/min continuously for 15 minutes. After PEI, sodium acetate buffer at pH 5 was performed for 3 minutes at the same flow rate. The HEP solution was injected at the same rate for 5 minutes, followed by the same sodium acetate buffer at pH 5 injection. After that, the COL solution was injected for 5 minutes at the same rate, followed by the same sodium acetate buffer at pH 5 injection. HEP and COL were then alternately injected into the chamber (followed by the same sodium acetate buffer at pH 5 buffer injection after each injection). After 12 and 13 multilayers were built up on quartz crystal microbalance, the MOFs solved in DPBS at pH 7.4 were injected into the chamber for 1 hour. the frequency shift (-ΔF) and dissipation (ΔD) vs. time curves were recorded.

5.2.6. Cell culture

hMSCs derived from bone marrow purchased from RoosterBio (Cat. #MSC-003) were used between passages 4−6. The donor is a healthy 25-year-old male (Lot. #00174). The product

specification sheet provided by the vendor shows that these cells were positive for CD90 and CD166 hMSCs identity markers (as tested by flow cytometry), negative for CD45 and CD34 (as tested by flow cytometry) and could differentiate into osteogenic and adipogenic cells. hMSCs were grown in alpha-minimum essential media MEM Alpha (1×) from Gibco (supplemented with L-glutamine, ribonucleosides, and deoxyribonucleosides) (Cat. #12561-056) containing 20% fetal bovine serum from Gibco (Cat. #12662029), 1.2% penicillin-streptomycin from Corning (Cat. #30002CI), and 1.2% L-glutamine from Corning (Cat. #25005CI).

5.2.7. Cell viability

For the hMSCs viability, PrestoBlueTM cell viability assay from Invitrogen (Cat. #A13261) was used. hMSCs (10000 cells/cm2) were seeded on all surfaces in 96 well-plate, and cell viability was measured after 3 and 6 days of culture as described in our previous works [32][33][31]. Briefly, the cell culture medium was removed, and 100 µL per well containing 90% fresh cell medium and 10% PrestoBlue reagent were added. The plate was incubated for 3 hours, and the fluorescence intensity measurement was determined using a BioTek Multi-Mode Microplate Reader (Model SynergyTM 2) with excitation/emission of 560/590 nm. Data were summarized per culture conditions.

5.2.8. Fluorescent staining

Cell nuclei and actin cytoskeleton were stained using the fluorescent dyes Hoechst 33342 which was purchased from Invitrogen (Ref. #H3570) and ActinRed 555 Ready Probest (Invitrogen, Ref. #37112). After 3 days of cell culture, the cell medium was removed, and the cells were fixed with 4% formaldehyde solution for 15 minutes. The samples were washed several times with DPBS followed by the addition of Triton X100 for 10 minutes. Then, the Triton X100 solution was removed and washed 3 times with DPBS. ActinRed 555 was first added and

incubated for 30 minutes. After removing the ActinRed 555 and washed 5 times with DPBS, Hoechst 33342 was added for 10 minutes and protected from light using aluminum foil. After 10 minutes, Hoechst 33342 was removed, and fixed cells were washed 5 times with DPBS. For cell imaging, a Leica inverted fluorescence microscope was used with a standard DAPI filter (excitation/emission of 350/461 nm) for Hoechst 33342, and a standard TRITC filter (excitation/emission of 540/565 nm) for ActinRed 555.

5.2.9. Immunomodulatory factor expression of hMSCs

For the hMSCs immunomodulatory factor expression, hMSCs (5000 cells/cm2) were seeded on each surface on a 24 well-plate, and the intracellular IDO activity was measured after 3 and 6 days of culture (without changing the cells medium) as described in our previous works [32][31][30]. Briefly, cell supernatant 100 µL was mixed with 100 µL standard assay mixture consisting of (potassium phosphate buffer (50mM, pH 6.5), ascorbic acid (40 mM, neutralized with NaOH), catalase (200 µg/ml), methylene blue (20 µ M), L-tryptophan (400 µM)). The mixture was kept at 37°C in a humidified incubator with 5% CO2 for 30 min (in a dark environment to protect solutions from light) to allow IDO to convert L-tryptophan to N-formyl-kynurenine. After that, the reaction was stopped by adding 100 µL trichloroacetic acid 30% (wt/vol) and incubating for 30 min at 58 °C. After hydrolysis of N-formyl-kynurenine to kynurenine, 100µL of mixed cell supernatant/standard transfer into a well of a 96-well microplate, followed by adding 100 µL per well of 2% (w/v) p-dimethylaminobenzaldehyde in acetic acid. Absorbance was read at 490 nm at the endpoint using a BioTek Synergy 2 spectrophotometer (Synergy LX Multi-Mode Reader from BioTek® Model SLXFA).

5.2.10. Cells differentiation assay

hMSCs differentiation was induced by their culture with differentiation media (Osteogenic and Adipogenic media). Control cultures were grown in a regular cell expansion medium. Briefly, hMSCs (10000 cells/cm^2) were seeded on each surface prepared on 24 well-plates and grown for 6 days in expansion medium (MEM Alpha (1X) supplemented with L-glutamine, ribonucleosides, and deoxyribonucleosides) containing 20% fetal bovine serum, 1.2% penicillin-streptomycin, and 1.2% L-glutamine) at 37 °C in a humidified incubator with 5% CO2. After the cells reached at least 50% confluency, they were exposed to differentiation medium. For osteogenic differentiation, hMSCs were cultured in the differentiation medium (DMEM low glucose, 10% fetal bovine serum,1% penicillin, 1% L-Glutamin, 50 μM ascorbic acid (50mg/10ml) (Sigma, Cas Number: 50-81-7), 10 mM β-glycerophosphate (e.g., Sigma, CAS Number: 154804-51-0, G9422), and 100nM dexamethasone (e.g., Sigma, CAS Number 50-02-2)). The medium was replaced every 2-3 days. After 8 days of culture, cells were fixed with 10% formaldehyde. For osteogenic differentiation, Alizarin Red S (Sigma, CAS Number 130-22-3) staining solution was prepared by adding 2 g Alizarin Red S in 100 mL water mixed. The pH was adjusted to 4.1– 4.3 by the addition of Ammonium Hydroxide, as necessary. Alizarin Red S solution was added to the fixed cells, then incubated at room temperature in the dark (cover with aluminum foil) for 15 minutes. The staining solution was removed and rinsed 3 times with PBS. The samples were analyzed immediately under the microscope to detect calcium deposits. For adipogenic differentiation, hMSCs were cultured in the differentiation medium consisting of DMEM high glucose supplemented with 10% fetal bovine serum, 1% penicillin, 1% L-glutamin, 1 μM dexamethasone (e.g., Sigma, CAS Number 50-02-2), 0.01 mg/mL insulin (Sigma-Aldrich, Catalog No. I2643), 0.5 mM 3-isobutyl-1-methylxanthine (IBMX) (e.g., Sigma, CAS Number:

28822-58-4, I5879), and 100μM indomethacin (Sigma, CAS Number: 53-86-1). The medium was replaced every 2-3 days. After 8 days of culture, cells were fixed with 10% formaldehyde, stained with 0.5% (w/v) Oil Red O (Sigma-Aldrich, Catalog Number: O0625) in 100% isopropanol, and incubated at room temperature for 30 minutes and protected from light. The cell monolayer was washed 2 times with PBS. The sample was analyzed under a light microscope to detect lipid vesicles that appeared in bright red.

5.2.11. Statistical Analysis

The results were presented as mean ± standard error of the mean. A one-way analysis of variance (ANOVA) performed comparisons among multiple groups. A p-value < 0.05 was considered statistically significant.

5.2.12. Results and Discussion

5.2.13. Characterization of MOFs and polyelectrolyte multilayers

The successful synthesis of PCN-333(Fe) was confirmed via XRD at 25 °C, **Error! Reference source not found.**, showing a pattern consistent with previous works by Phipps et al. [34]. The enlarged SEM image with EDX mapping is shown in the Figure *2-1*, and MOFs with good crystal morphology can be seen. The presence of a large amount of Fe and C implies the successful assembly of MOFs on (HEP/COL) multilayers, which complies with a study done by Zhe Zhao et al. [22].

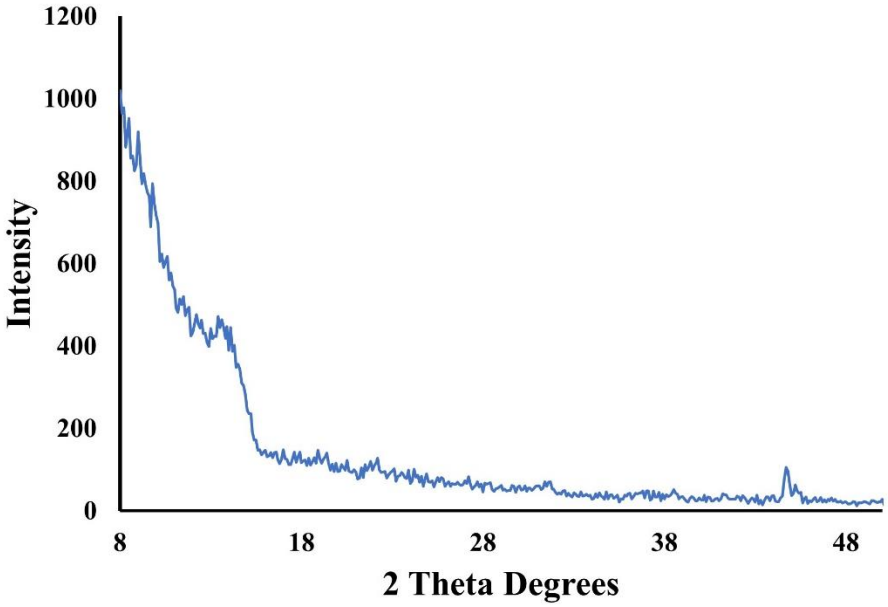

Figure 5-1. XRD of synthesized PCN-333 (Fe) (λ = 1.54178) at 25 °C.

8

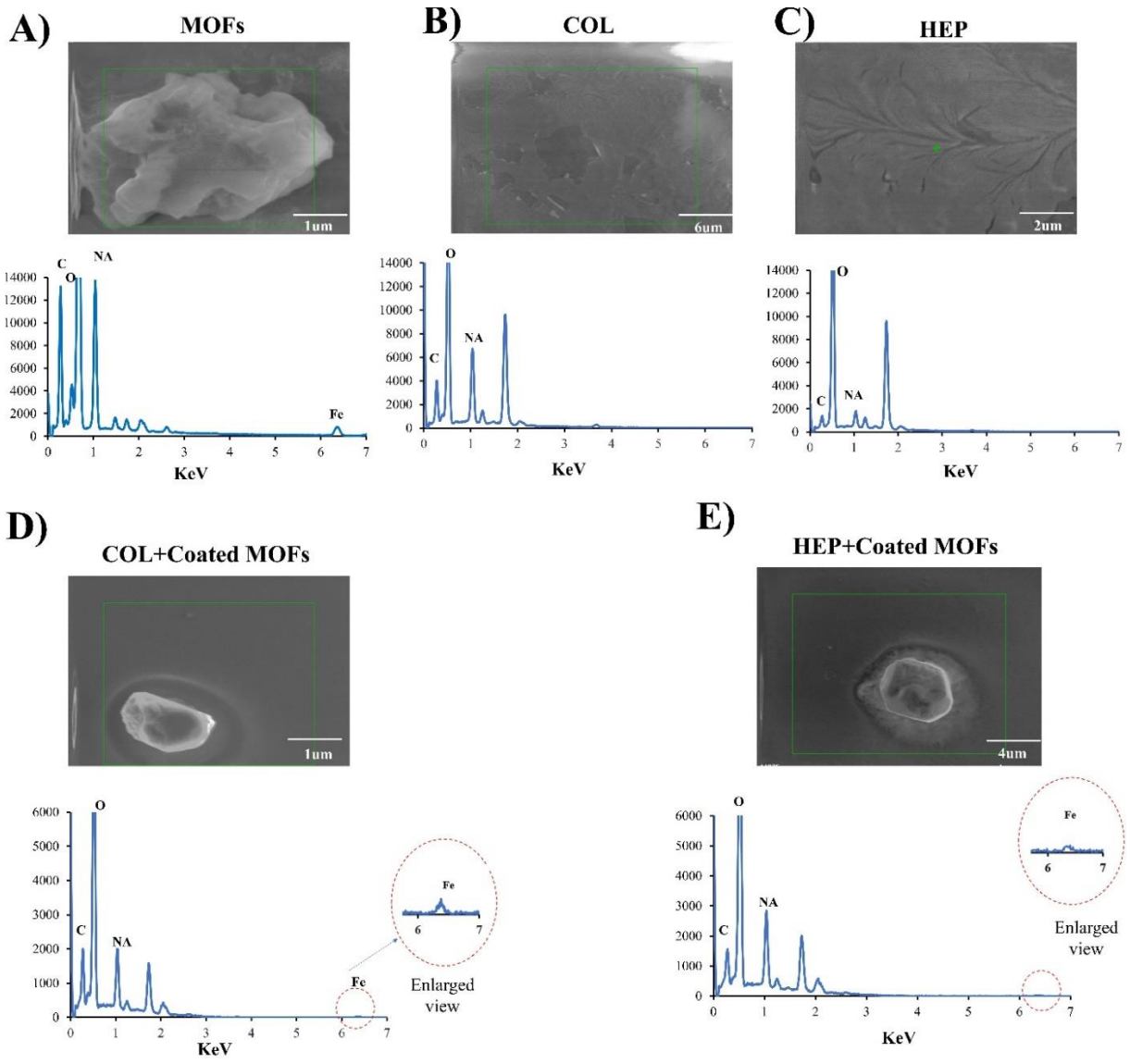

Figure 5-2. SEM image with EDX mapping.

The topography of (HEP/COL) multilayers coated and non-coated with MOFs was investigated by AFM. Analyzing the topographic images in Figure 5-9 shows HEP has a larger cluster on the surface compared to COL, which demonstrates considerable accumulation associated with surface deposition [35], which complies with our previous study done by Haseli et al. [23]. Regarding surfaces coated with MOFs, Figure 5-9 shows COL and HEP coated with MOFs have a higher roughness after MOFs coating, from 141nm to 210 nm and 210 nm to 270 nm,

respectively. Also, the deposition of MOFs on (HEP/COL) multilayers lead to a rougher surface, demonstrating that the MOFs successfully attached to the surface may increase the roughness of surfaces [28]. These results confirm the conclusions drawn from the QCM-D results, in which a rough layer was obtained after the deposition of MOFs.

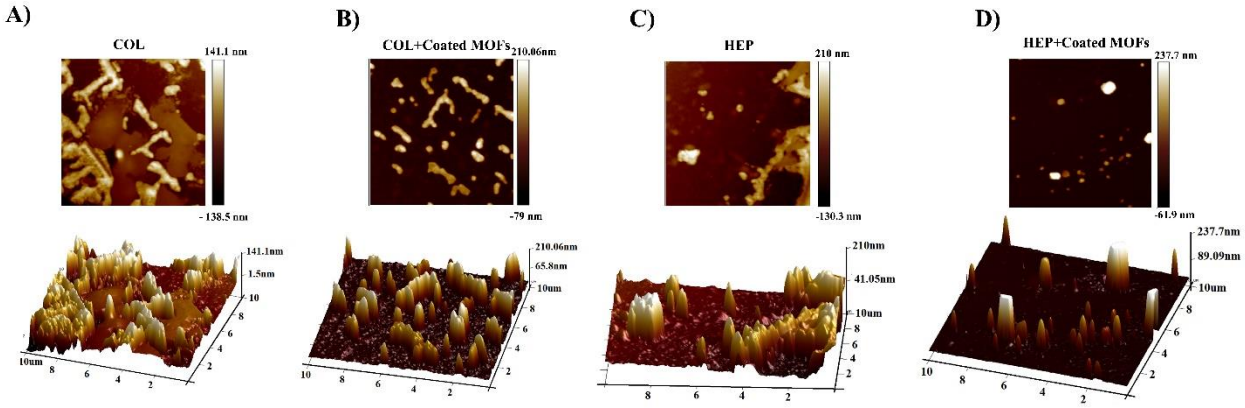

Figure 5-9. Surface morphology as measured by AFM. A) . Surface morphology COL, B) COL+Coated (MOF+IFN-γ), C) HEP, D) HEP+Coated (MOF+IFN-γ).

QCM-D monitored the formation of the multilayers. QCM-D detects the resonant frequency shift (ΔF and measures the dissipation factor (ΔD) [36]. QCM-D was used here to investigate physical structures such as adsorbed mass and viscoelastic properties of multilayers [36][37]. Figure 5-10 shows the normalized frequency shift ($-\Delta F_n/n$) and dissipation (ΔD/n) for the 3rd, 4th, and 7th overtones for the (HEP/COL) multilayers coated with MOFs. The first 15 minutes correspond to a PEI absorption, followed by a 3-minute rinsing step as shown in Figure 5-10. The increase in -ΔF and ΔD of every (HEP/COL) sequential deposition shows that the multilayers slowly deposit onto the quartz crystal [23][38]. It is demonstrated that by increasing of -ΔF the mass of deposited multilayers increases, whereas the increase of ΔD enhances the viscoelastic structure of the deposited multilayers [39]. Therefore, adding a rough layer on quartz crystal has a lower -ΔF, whereas a dense layer has a higher ΔD value. We previously reported that the Sauerbrey

equation (relationship between the frequency change and mass uptake) is not valid for (HEP/COL) multilayers which indicates the film is more viscoelastic with a linear mass increase over time [23]. When MOFs are deposited, -ΔF and ΔD have a slight decrease in both HEP and COL ending multilayers, resulting in negligible adsorption of the MOFs. MOFs absorption shows a lower -ΔF, confirming the AFM results, which show MOFs assembly increase the roughness of layers. Following adsorption of the MOFs, a quick decrease of the frequency shifts are found for both COL and HEP-ending multilayers due to the buffer effect [40]. These results indicate that the (HEP/ COL) multilayers present good stability in the presence of the MOFs.

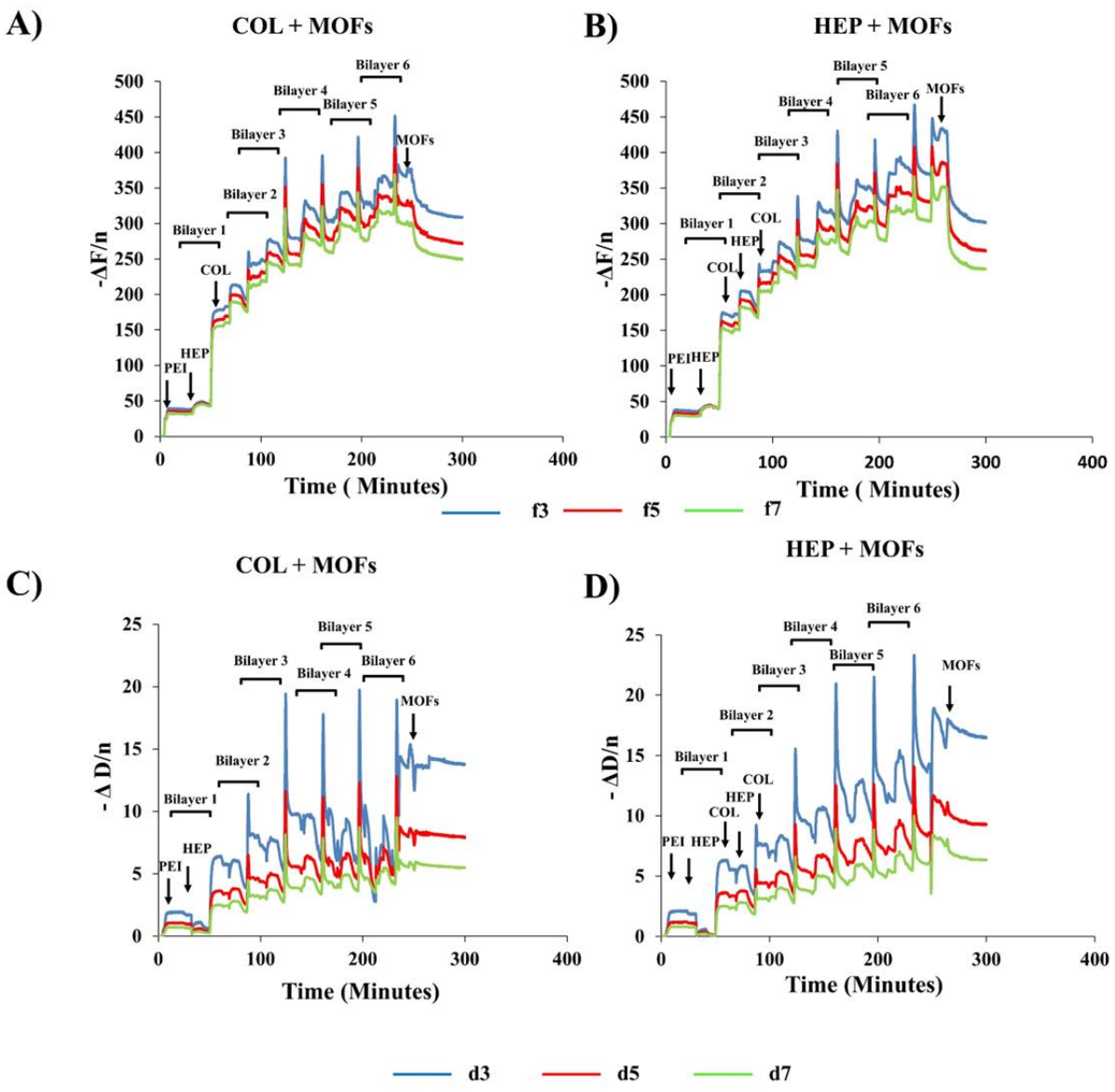

Figure 5-10. QCM-D data showing the normalized frequency shift& dissipation shift as a function of time for the 3rd, 5th, and 7th overtones during the construction of the COL and HEP ending multilayers coated with MOFs, with alternating three-minute rinse and five-minutes adsorption intervals. A&B: showing the normalized frequency shift for the COL and HEP ending multilayers. C&D: showing the normalized frequency dissipation shift for the Col and Hep ending multilayers.

5.2.14. Encapsulation efficiency of IFN-γ with PCN-333(Fe)

The encapsulation efficiency of IFN-γ loaded in PCN-333(Fe) was determined by micro-BCA assay and HPLC. Encapsulation efficiency was calculated using the difference between theoretical and experimental values, taken at three separate concentrations (0.2 mg/mL, 0.1 mg/mL and 0.05 mg/mL) to generate calibration curve [41]. The encapsulation efficiency was calculated by Equation [42]:

$$Encapsulation\ efficiency\% = \frac{(True\ Value - measured\ value)}{True\ Value} \times 100 \qquad \textit{Equation 5-1}$$

The average percentage of encapsulation IFN-γ loaded in PCN-333(Fe) was 60% by HPLC and 76% by micro-BCA assay. This result indicates that the PCN-333(Fe) has a highly efficient loading capacity for IFN-γ, which comply with a study by Chen et al. [25].

5.2.15. PrestoBlue viability assay

Cytotoxicity was evaluated using Presto Blue assay. PrestoBlue was used for measuring cell viability after 3 and 6 days of culturing hMSCs cells per each condition. TPC with the absence of IFN-γ in the culture medium was selected as the positive control. The fluorescence intensity of the positive control was normalized to 100%. All other conditions were normalized against the positive control. Cell viability results shows a higher viability of about 15% in COL and HEP surfaces after 3 and 6 days compared to the control. However, cell viability decreases in COL+Coated MOFs and HEP+Coated MOFs compared to COL and HEP after both 3 and 6 days Figure 5-11. PrestoBlue Viability assay for cultured hMSCs. Data are presented as the mean ± standard deviation of n = 4 samples. The p-values < 0.05 are represented by *, p-values < 0. 01 by **, p-values < 0. 001 by *** and p-values < 0.0001 by ****.. However, cell viability percentage does not decrease in COL+Coated MOFs and HEP+Coated MOFs compared to control. Figure 5-11 shows significant differences in the cell viability of TCP compared to COL,

HEP, COL+Coated MOFs, and HEP+Coated MOFs in 3 days, respectively ($p < 0.01$, $p < 0.001$, p-values < 0.0001, p-values < 0.05 and p-values < 0.001, respectively). In addition, **Error! R eference source not found.**-5 shows there is no significant differences in cell viability of COL+Coated MOFs and HEP+Coated MOFs after 6 days compared to control. These cell viability results show that (HEP/COL) multilayers may have the ability to increase cell viability up to 15% compared to control, while the presence of MOFs do not negatively affect the viability compared to the control. However, there is a little decrease in cell viability in the presence of MOFs coated in (HEP/COL) multilayers compared to (HEP/COL) multilayers without MOFs. These results show that MOFs alone do not have any cytotoxicity effect on hMSC.

Fluorescence microscopy images of hMSCs nuclei labeled with Hoechst of cells attached to the different surfaces after 72 hours validate the findings of cell viability of hMSCs in each condition (Figure S5-1).

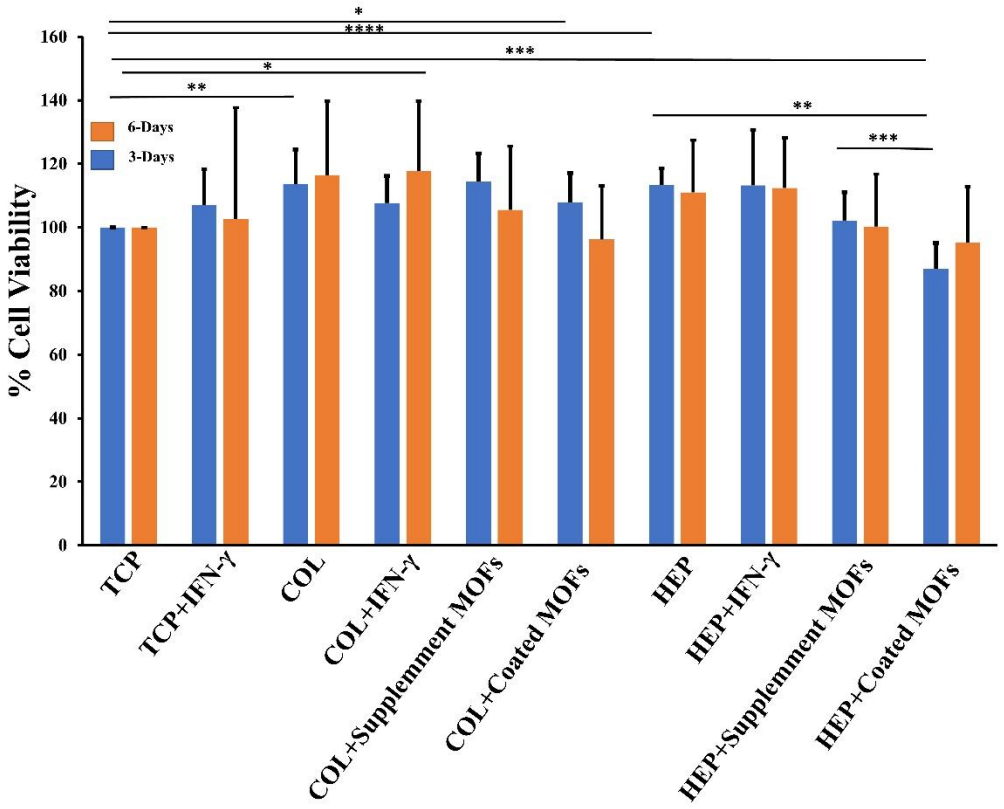

Figure 5-11. PrestoBlue Viability assay for cultured hMSCs. Data are presented as the mean ± standard deviation of n = 4 samples. The p-values < 0.05 are represented by *, p-values < 0. 01 by **, p-values < 0. 001 by *** and p-values < 0.0001 by ****.

5.2.16. Intracellular IDO assay

Indoleamine 2,3-dioxygenase (IDO) is a cytosolic heme protein that is important for immuno-regulatory functions [43][44]. It can be determined by measuring the level of kynurenine (pg/cell) produced by cells in the presence of IFN-γ given that IFN-γ is known to be a catalyzer to convert L-tryptophan to kynurenine [43] [45]. The ability of IFN-γ to induce IDO expression in hMSCs was compared with all samples after 3 days and 6 days. Results for IDO activity are summarized in Figure 5-12,which shows that IFN-γ supplemented in cells medium increase the

IDO activity compared to the cell medium without IFN-γ. These results align with the study by Kwee et al., indicating the IDO activity correlated with the amount of IFN-γ [46]. However, The IDO activity decreases after 6 days in comparison with 3 days for both TCP and TCP+IFN-γ (8-fold decrease in IDO expression, $p < 0.01$). Also, COL and HEP with and without IFN-γ follow the same trend in IDO activity after 6 days except HEP+IFN-γ which shows the same level of IDO expression after 3 days and 6 days.

Regarding (HEP/COL) multilayers coated with MOFs, the results show a higher IDO activity after 3 and 6 days in comparison with TCP with and without IFN-γ; in particular, HEP+Coated MOFs has a higher IDO expression 500 pg/cell after 6 days ($p < 0.0001$). These results indicate that IFN-γ was loaded successfully into the MOFs; it was revealed that loaded IFN-γ prolonged existence at 6 days in comparison to soluble IFN-γ. In addition, These results indicate that MOFs may have better coating ability in HEP as the last layer of the (HEP/COL) multilayers because of their catalytic activities [47]. Therefore, HEP ending multilayers coated with MOFs is a better candidate for the presentation of IFN-γ.

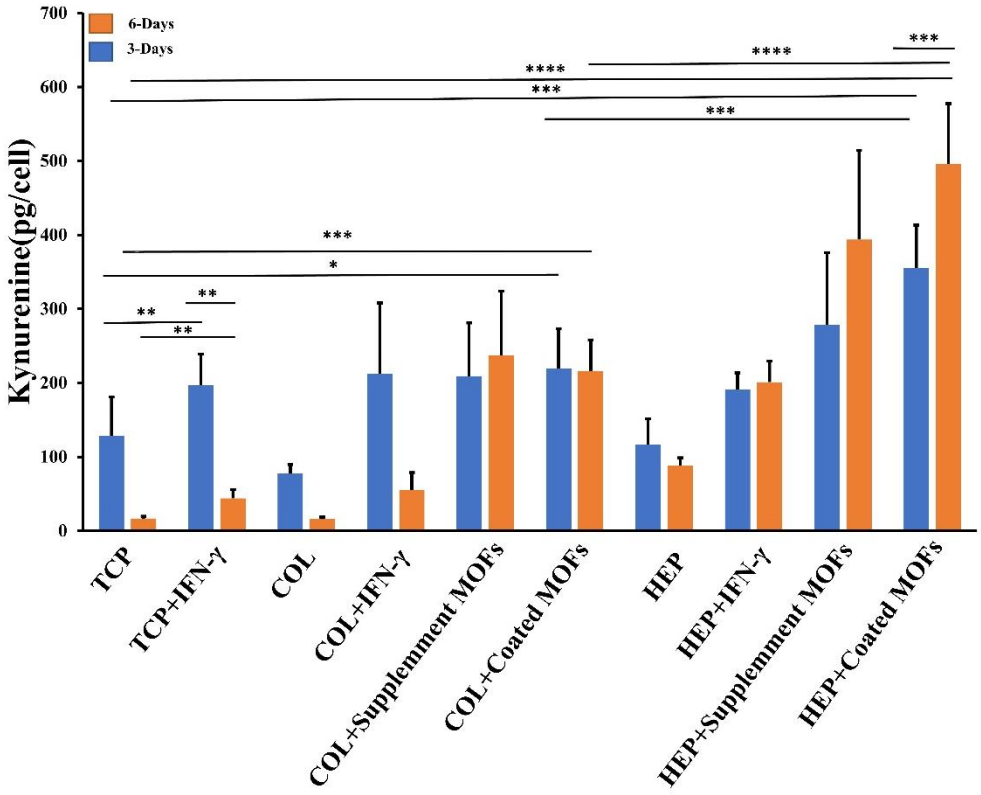

Figure 5-12. Cells immunomodulatory potential by IDO activity for hMSCs as a measure of picograms of kynurenine produced by cells cultured Data are presented as the mean ± standard deviation of n = 4 samples. The p-values < 0.05 are represented by *, p-values < 0. 01 by **, p-values < 0. 001 by *** and p-values < 0.0001 by ****.

5.2.17. Cells differentiation assay

The ability of hMSCs to differentiate into osteogenic and adipogenic lineages cells was induced by replacing the growth medium with the differentiation medium. The differentiation ability of hMSCs was evaluated to confirm the multipotentiality of hMSCs. After 10 days of incubation, cell functions associated with osteoblast differentiation (calcium deposition) and adipogenic differentiation were evaluated. Mineralization was also characterized from microscope images.

Figure 5-13 shows that there are areas visible with red and purple, indicating the formation of the calcified regions and adipocyte-like cells, respectively. Figure 5-13 (A) shows a calcium deposit formed by the clustering of cells due to the strong staining with Alizarin red for all samples, which indicates osteogenic differentiation of cells. Also, Figure 5-13 (B) shows cells can differentiate into adipogenic cells, which changed from long spindle-shaped to flattened round or polygonal cells. In addition, Figure 5-13 shows that MOFs had no inhibitory effect on the osteogenic and adipogenic differentiation of hMSCs even supplemented in the cells medium or coated on (HEP/COL) multilayers.

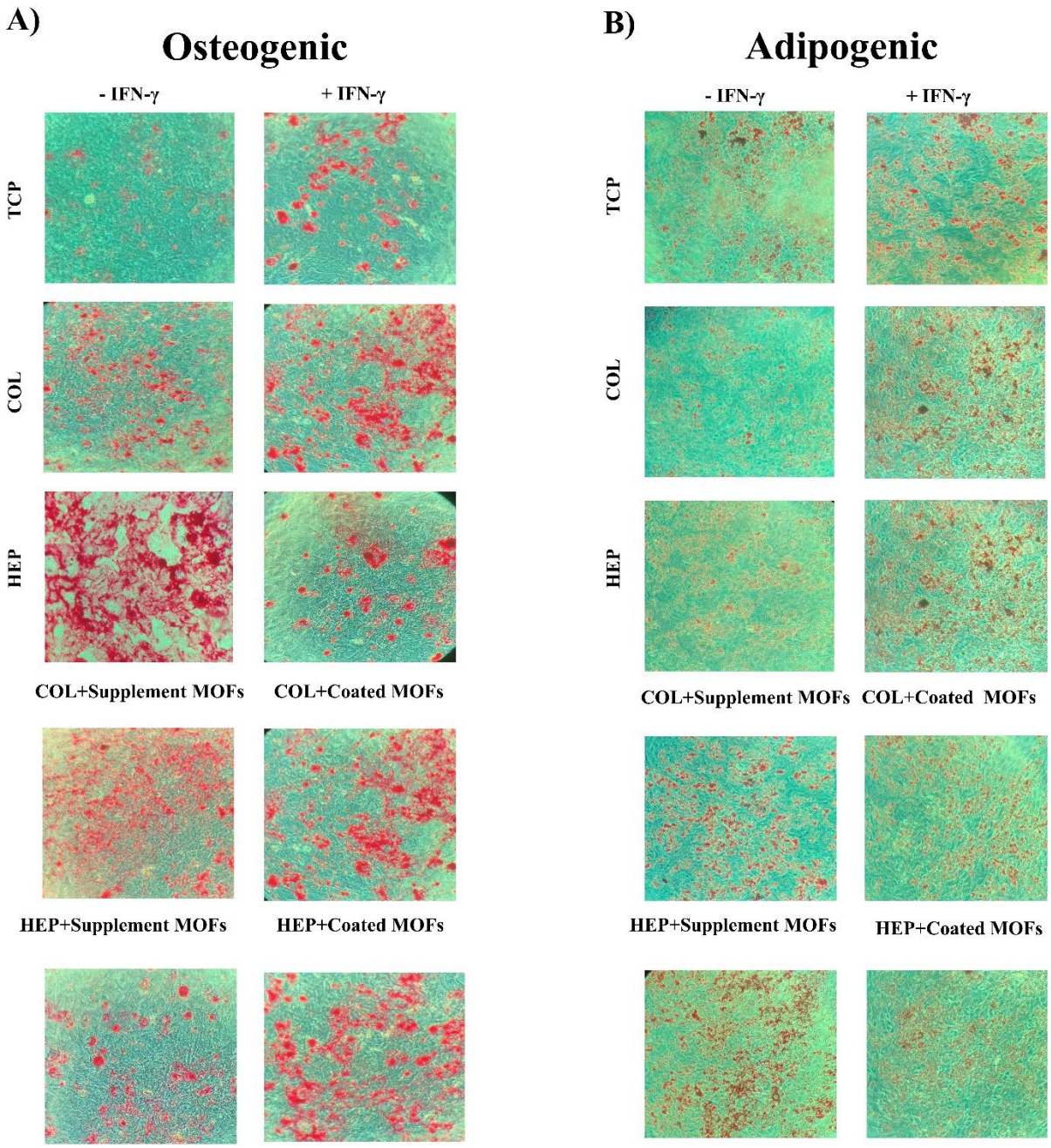

Figure 5-13. hMSCs differentiation. A) Osteogenic differentiations were stained by Alizarin Red. B) Adipogenic differentiation were stained by Oil R

In this study, we designed and evaluated a strategy for locally presenting IFN-γ within hMSCs constructs to potentiate sustained hMSCs immunomodulatory activity. To do so, we took

advantage of a metal-organic frameworks approach previously developed to encapsulate enzymes [34]. MOFs were chosen to deliver IFN-γ to exploit the high native affinity of IFN-γ, the ability of MOFs to maintain protein bioactivity. These MOFs have previously demonstrated excellent recyclability, stability, and increased loading for MOF-encapsulated enzymes [34][25]. Consistent with previous studies, MOFs show good stability and efficient loading capacity for IFN-γ, which comply with a study by Chen et al. [2] which concluded that MOFs could encapsulate cytokine. IFN-γ loaded in MOFs could still induce hMSCs IDO expression even after 6 days of incubation at physiologic conditions compared with soluble IFN-γ. These results contrast with a previous study investigating the IFN-γ immobilization to biomimetic hydrogel in which immobilized IFN-γ did not prolong expected signaling at 7 days compared to soluble IFN-γ [48]. These results suggest that MOFs are a good candidate for encapsulating cytokine.

5.3. Conclusion

The results of this study demonstrate that MOFs were successfully deposited on (HEP/COL) multilayers. QCM-D results demonstrate that MOFs absorbed of each layer. Also, (HEP/ COL) multilayers present good stability in the presence of the MOFs. This approach shows that (HEP/COL) multilayers did not negatively influence the viability and differentiation of hMSCs in the presence of MOFs. In addition, this study shows that (HEP/COL) multilayers coated with MOFs provide a sustained presentation of cytokines to potentiate hMSCs immunomodulatory activity. Also, this study shows that HEP-ending multilayers may be a good candidate for MOFs coating to increase IFN-γ presentation in the cell microenvironment. Overall, this approach could overcome the limitations of pretreatment of hMSCs by continuously presenting IFN-γ within the cell microenvironment, which induces a sustained hMSCs immunosuppression.

■ AUTHOR INFORMATION

Corresponding Author

*E-mail: jlalmodo@uark.edu

ORCID

Jorge Almodovar: 0000-0002-1151-3878

Present Address

§M.H.: Ralph E. Martin Department of Chemical

Engineering, University of Arkansas, 3202 Bell Engineering

Center, Fayetteville, AR 72701, Phone: +1 479-575-3924, Fax:

+1 479-575-7926.

Notes

The authors declare no competing financial interest.

5.4. Acknowledgement

The authors greatly appreciate the use of the Arkansas Nano & Biomaterials Characterization Facility for use of the SEM and XRD. The authors greatly appreciate Dr. Walters from the University of Arkansas for equipment access and help during quartz crystal microbalance (QCM) measurements.

Conflict of Interest

The authors have no conflicts of interest to declare.

Funding Sources

This work was financially supported in part by the National Science Foundation

under grant no. 2051582.

5.5. References

[1] T. L. Ramos *et al.*, "MSC surface markers (CD44, CD73, and CD90) can identify human MSC-derived extracellular vesicles by conventional flow cytometry," *Cell Commun. Signal.*, vol. 14, no. 1, pp. 1–14, 2016, doi: 10.1186/s12964-015-0124-8.

[2] G. Brooke *et al.*, "Therapeutic applications of mesenchymal stromal cells," *Semin. Cell Dev. Biol.*, vol. 18, no. 6, pp. 846–858, 2007, doi: 10.1016/j.semcdb.2007.09.012.

[3] M. F. Pittenger, D. E. Discher, B. M. Péault, D. G. Phinney, J. M. Hare, and A. I. Caplan, "Mesenchymal stem cell perspective: cell biology to clinical progress," *npj Regen. Med.*, vol. 4, no. 1, 2019, doi: 10.1038/s41536-019-0083-6.

[4] E. H. Javazon, K. J. Beggs, and A. W. Flake, “Парадоксы Пассажирования.Pdf,” vol. 32, pp. 414–425, 2004.

[5] Y. P. Rubtsov, Y. G. Suzdaltseva, K. V. Goryunov, N. I. Kalinina, V. Y. Sysoeva, and V. A. Tkachuk, “Regulation of Immunity via Multipotent Mesenchymal Stromal Cells,” *Acta Naturae*, vol. 4, no. 1, pp. 23–31, 2012, doi: 10.32607/20758251-2012-4-1-23-31.

[6] K. Suzuki, N. Chosa, S. Sawada, N. Takizawa, T. Yaegashi, and A. Ishisaki, “Enhancement of Anti-Inflammatory and Osteogenic Abilities of Mesenchymal Stem Cells via Cell-to-Cell Adhesion to Periodontal Ligament-Derived Fibroblasts,” *Stem Cells Int.*, vol. 2017, 2017, doi: 10.1155/2017/3296498.

[7] R. E. Newman, D. Yoo, M. A. LeRoux, and A. Danilkovitch-Miagkova, “Treatment of inflammatory diseases with mesenchymal stem cells,” *Inflamm. Allergy - Drug Targets*, vol. 8, no. 2, pp. 110–123, 2009, doi: 10.2174/187152809788462635.

[8] A. Uccelli, L. Moretta, and V. Pistoia, “Mesenchymal stem cells in health and disease,” *Nat. Rev. Immunol.*, vol. 8, no. 9, pp. 726–736, 2008, doi: 10.1038/nri2395.

[9] F. Gao *et al.*, “Mesenchymal stem cells and immunomodulation: Current status and future prospects,” *Cell Death Dis.*, vol. 7, no. 1, 2016, doi: 10.1038/cddis.2015.327.

[10] P. S. Frenette, S. Pinho, D. Lucas, and C. Scheiermann, *Mesenchymal stem cell: Keystone of the hematopoietic stem cell niche and a stepping-stone for regenerative medicine*, vol. 31. 2013.

[11] Y. Wang, X. Chen, W. Cao, and Y. Shi, “Plasticity of mesenchymal stem cells in immunomodulation: Pathological and therapeutic implications,” *Nat. Immunol.*, vol. 15, no. 11, pp. 1009–1016, 2014, doi: 10.1038/ni.3002.

[12] J. A. Ankrum, J. F. Ong, and J. M. Karp, “Mesenchymal stem cells: Immune evasive, not immune privileged,” *Nat. Biotechnol.*, vol. 32, no. 3, pp. 252–260, 2014, doi: 10.1038/nbt.2816.

[13] A. J. Nauta and W. E. Fibbe, “Immunomodulatory properties of mesenchymal stromal cells,” *Blood*, vol. 110, no. 10, pp. 3499–3506, 2007, doi: 10.1182/blood-2007-02-069716.

[14] K. English, “Mechanisms of mesenchymal stromal cell immunomodulation,” *Immunol. Cell Biol.*, vol. 91, no. 1, pp. 19–26, 2013, doi: 10.1038/icb.2012.56.

[15] J. Cuerquis *et al.*, “Human mesenchymal stromal cells transiently increase cytokine production by activated T cells before suppressing T-cell proliferation: Effect of interferon-γ and tumor necrosis factor-α stimulation,” *Cytotherapy*, vol. 16, no. 2, pp. 191–202, 2014, doi: 10.1016/j.jcyt.2013.11.008.

[16] T. J. Kean, P. Lin, A. I. Caplan, and J. E. Dennis, “MSCs: Delivery routes and engraftment, cell-targeting strategies, and immune modulation,” *Stem Cells Int.*, vol. 2013, 2013, doi: 10.1155/2013/732742.

[17] A. Gebler, O. Zabel, and B. Seliger, “The immunomodulatory capacity of mesenchymal stem cells,” *Trends Mol. Med.*, vol. 18, no. 2, pp. 128–134, 2012, doi: 10.1016/j.molmed.2011.10.004.

[18] G. Ren *et al.*, “Mesenchymal Stem Cell-Mediated Immunosuppression Occurs via Concerted Action of Chemokines and Nitric Oxide,” *Cell Stem Cell*, vol. 2, no. 2, pp. 141–150, 2008, doi: 10.1016/j.stem.2007.11.014.

[19] M. Krampera *et al.*, “Role for Interferon-γ in the Immunomodulatory Activity of Human Bone Marrow Mesenchymal Stem Cells,” *Stem Cells*, vol. 24, no. 2, pp. 386–398, 2006, doi: 10.1634/stemcells.2005-0008.

[20] M. W. Klinker, R. A. Marklein, J. L. Lo Surdo, C. H. Wei, and S. R. Bauer, “Morphological features of IFN-γ-stimulated mesenchymal stromal cells predict overall immunosuppressive capacity,” *Proc. Natl. Acad. Sci. U. S. A.*, vol. 114, no. 13, pp. E2598–E2607, 2017, doi: 10.1073/pnas.1617933114.

[21] J. Croitoru-Lamoury *et al.*, “Interferon-γ regulates the proliferation and differentiation of mesenchymal stem cells via activation of indoleamine 2,3 dioxygenase (IDO),” *PLoS One*, vol. 6, no. 2, 2011, doi: 10.1371/journal.pone.0014698.

[22] D. A. Castilla-Casadiego, J. R. García, A. J. García, and J. Almodovar, “Heparin/Collagen Coatings Improve Human Mesenchymal Stromal Cell Response to Interferon Gamma,” *ACS Biomater. Sci. Eng.*, vol. 5, no. 6, pp. 2793–2803, 2019, doi: 10.1021/acsbiomaterials.9b00008.

[23] M. Haseli *et al.*, “Immunomodulatory functions of human mesenchymal stromal cells are enhanced when cultured on HEP/COL multilayers supplemented with interferon-gamma,” *Mater. Today Bio*, vol. 13, no. November 2021, p. 100194, 2022, doi: 10.1016/j.mtbio.2021.100194.

[24] J. A. ZIMMERMANN, b M. H. H. A, and C. a TODD C. MCDEVITTb, “Enhanced Immunosuppression of T Cells by Sustained Presentation of Bioactive Interferon-g Within Three_Dimensional Mesenchymal Stem Cell Construct,” *Stem Cells Transl. Med.*, no. Il, pp. 523–531, 2015, doi: http://dx.doi.org/ 10.5966/sctm.2016-0044.

[25] W. Chen, W. Yang, Y. Lu, W. Zhu, and X. Chen, “Encapsulation of enzyme into mesoporous cages of metal-organic frameworks for the development of highly stable electrochemical biosensors,” *Anal. Methods*, vol. 9, no. 21, pp. 3213–3220, 2017, doi: 10.1039/c7ay00710h.

[26] Z. Liang *et al.*, “A protein@metal-organic framework nanocomposite for pH-triggered anticancer drug delivery,” *Dalt. Trans.*, vol. 47, no. 30, pp. 10223–10228, 2018, doi: 10.1039/c8dt01789a.

[27] D. Feng *et al.*, “Stable metal-organic frameworks containing single-molecule traps for enzyme encapsulation,” *Nat. Commun.*, vol. 6, pp. 1–8, 2015, doi: 10.1038/ncomms6979.

[28] J. Park, D. Feng, and H. C. Zhou, “Dual Exchange in PCN-333: A Facile Strategy to Chemically Robust Mesoporous Chromium Metal-Organic Framework with Functional Groups,” *J. Am. Chem. Soc.*, vol. 137, no. 36, pp. 11801–11809, 2015, doi: 10.1021/jacs.5b07373.

[29] L. Pinzon-Herrera, J. Mendez-Vega, A. Mulero-Russe, D. A. Castilla-Casadiego, and J. Almodovar, “Real-time monitoring of human Schwann cells on heparin-collagen coatings

reveals enhanced adhesion and growth factor response," *J. Mater. Chem. B*, vol. 8, no. 38, pp. 8809–8819, 2020, doi: 10.1039/d0tb01454k.

[30] D. A. Castilla-Casadiego *et al.*, "Methods for the Assembly and Characterization of Polyelectrolyte Multilayers as Microenvironments to Modulate Human Mesenchymal Stromal Cell Response," *ACS Biomater. Sci. Eng.*, vol. 6, no. 12, pp. 6626–6651, 2020, doi: 10.1021/acsbiomaterials.0c01397.

[31] S. J. Cifuentes, P. Priyadarshani, D. A. Castilla-Casadiego, L. J. Mortensen, J. Almodóvar, and M. Domenech, "Heparin/collagen surface coatings modulate the growth, secretome, and morphology of human mesenchymal stromal cell response to interferon-gamma," *J. Biomed. Mater. Res. - Part A*, no. March, pp. 1–15, 2020, doi: 10.1002/jbm.a.37085.

[32] D. A. Castilla-Casadiego, A. M. Reyes-Ramos, M. Domenech, and J. Almodovar, "Effects of Physical, Chemical, and Biological Stimulus on h-MSC Expansion and Their Functional Characteristics," *Ann. Biomed. Eng.*, vol. 48, no. 2, pp. 519–535, 2020, doi: 10.1007/s10439-019-02400-3.

[33] D. A. Castilla-casadiego and J. Almodovar, "on heparin-collagen coatings reveals enhanced adhesion and growth factor response †," 2020, doi: 10.1039/d0tb01454k.

[34] J. Phipps *et al.*, "Catalytic Activity, Stability, and Loading Trends of Alcohol Dehydrogenase Enzyme Encapsulated in a Metal-Organic Framework," *ACS Appl. Mater. Interfaces*, vol. 12, no. 23, pp. 26084–26094, 2020, doi: 10.1021/acsami.0c06964.

[35] S. Boddohi, J. Almodóvar, H. Zhang, P. A. Johnson, and M. J. Kipper, "Layer-by-layer assembly of polysaccharide-based nanostructured surfaces containing polyelectrolyte complex nanoparticles," *Colloids Surfaces B Biointerfaces*, vol. 77, no. 1, pp. 60–68, 2010, doi: 10.1016/j.colsurfb.2010.01.006.

[36] K. A. Marx, "Quartz crystal microbalance: A useful tool for studying thin polymer films and complex biomolecular systems at the solution - Surface interface," *Biomacromolecules*, vol. 4, no. 5, pp. 1099–1120, 2003, doi: 10.1021/bm020116i.

[37] A. Barrantes, O. Santos, J. Sotres, and T. Arnebrant, "Influence of pH on the build-up of poly-L-lysine/heparin multilayers," *J. Colloid Interface Sci.*, vol. 388, no. 1, pp. 191–200, 2012, doi: 10.1016/j.jcis.2012.08.008.

[38] Q. Lin, J. Yan, F. Qiu, X. Song, G. Fu, and J. Ji, "Heparin/collagen multilayer as a thromboresistant and endothelial favorable coating for intravascular stent," *J. Biomed. Mater. Res. - Part A*, vol. 96 A, no. 1, pp. 132–141, 2011, doi: 10.1002/jbm.a.32820.

[39] C. D. Easton, A. J. Bullock, G. Gigliobianco, S. L. McArthur, and S. Macneil, "Application of layer-by-layer coatings to tissue scaffolds-development of an angiogenic biomaterial," *J. Mater. Chem. B*, vol. 2, no. 34, pp. 5558–5568, 2014, doi: 10.1039/c4tb00448e.

[40] Q. Lin, J. Yan, F. Qiu, X. Song, G. Fu, and J. Ji, "Heparin/collagen multilayer as a thromboresistant and endothelial favorable coating for intravascular stent," *J. Biomed. Mater. Res. - Part A*, vol. 96 A, no. 1, pp. 132–141, 2011, doi: 10.1002/jbm.a.32820.

[41] M. Umrethia, V. L. Kett, G. P. Andrews, R. K. Malcolm, and A. D. Woolfson, "Selection of an analytical method for evaluating bovine serum albumin concentrations in pharmaceutical

polymeric formulations," *J. Pharm. Biomed. Anal.*, vol. 51, no. 5, pp. 1175–1179, 2010, doi: 10.1016/j.jpba.2009.12.004.

[42] B. C. Garms *et al.*, "Evaluating the effect of synthesis, isolation, and characterisation variables on reported particle size and dispersity of drug loaded PLGA nanoparticles," *Mater. Adv.*, vol. 2, no. 17, pp. 5657–5671, 2021, doi: 10.1039/d1ma00410g.

[43] O. Takikawa, T. Kuroiwa, F. Yamazaki, and R. Kido, "Mechanism of interferon-γ action. Characterization of indoleamine 2,3-dioxygenase in cultured human cells induced by interferon -γ and evaluation of the enzyme-mediated tryptophan degradation in its anticellular activity," *J. Biol. Chem.*, vol. 263, no. 4, pp. 2041–2048, 1988.

[44] J. C. Mbongue, D. A. Nicholas, T. W. Torrez, N. S. Kim, A. F. Firek, and W. H. R. Langridge, "The role of indoleamine 2, 3-dioxygenase in immune suppression and autoimmunity," *Vaccines*, vol. 3, no. 3, pp. 703–729, 2015, doi: 10.3390/vaccines3030703.

[45] W. Däubener, N. Wanagat, K. Pilz, S. Seghrouchni, H. G. Fischer, and U. Hadding, "A new, simple, bioassay for human IFN-γ," *J. Immunol. Methods*, vol. 168, no. 1, pp. 39–47, 1994, doi: 10.1016/0022-1759(94)90207-0.

[46] K. E. S. Brian J. Kwee, Johnny Lam, Adovi Akue, Mark A. KuKuruga, K. Zhang, Luo Gu, "Functional heterogeneity of IFN-γ – licensed mesenchymal stromal cell immunosuppressive capacity on biomaterials," pp. 1–12, 2021, doi: 10.1073/pnas.2105972118/-/DCSupplemental.Published.

[47] D. Feng *et al.*, "Stable metal-organic frameworks containing single-molecule traps for enzyme encapsulation," *Nat. Commun.*, vol. 6, pp. 1–8, 2015, doi: 10.1038/ncomms6979.

[48] H. J. Baumann, P. Betonio, C. S. Abeywickrama, L. P. Shriver, and N. D. Leipzig, "Metabolomic and Signaling Programs Induced by Immobilized versus Soluble IFN γin Neural Stem Cells," *Bioconjug. Chem.*, vol. 31, no. 9, pp. 2125–2135, 2020, doi: 10.1021/acs.bioconjchem.0c00338.

Supplementary Information

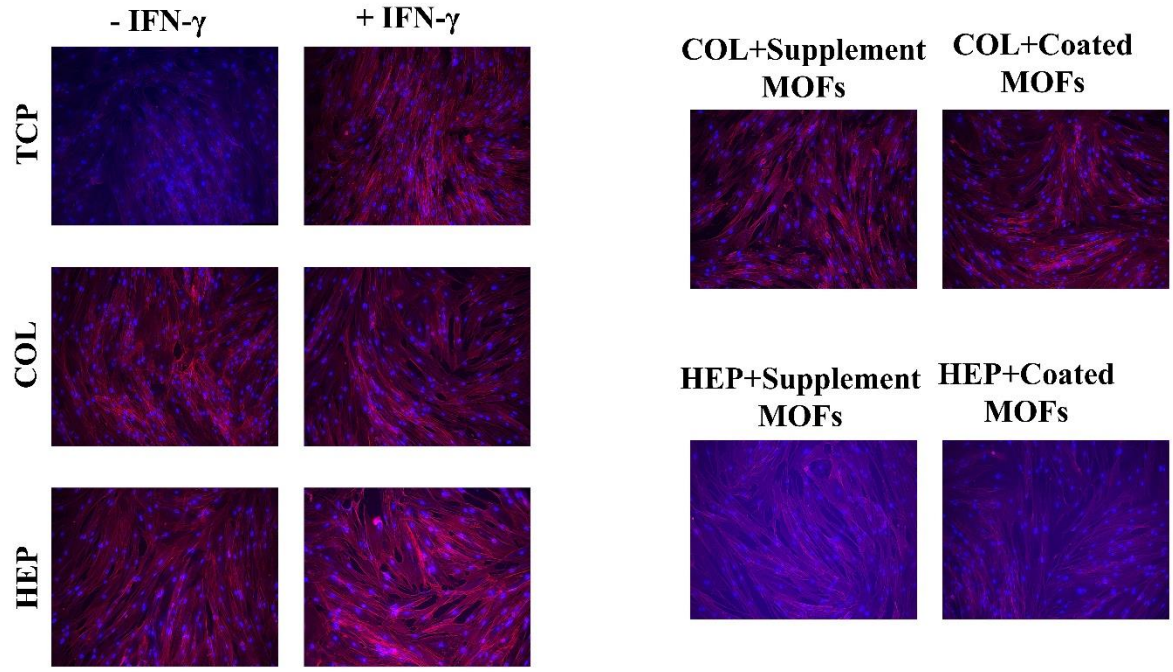

Figure S5-1. Fluorescent staining was performed to detect the blue fluorescent dye Hoechst 33 342.

6. Engineer Novel Oxygen-Releasing Cellular Microenvironments for Human Mesenchymal Stromal Cells (HMSCs)

6.1. Introduction

Cell-based therapy aims to repair and regenerate organs and tissues [1], but a major problem for successful cell therapy is the poor survival of transplanted cells. For the transplanted cells to remain alive, they should contain proper oxygenation [2]. Oxygen is a crucial element for the repopulation of damaged tissue and cellular process. Once the tissue is engineered, constructs are transplanted, its survival depends on the oxygen diffusion until vascular formation occurs [3][4][5]. Thus, by providing oxygen to transplants, the number of live cells increases and improves regeneration capacity [5][6]. To tackle this problem, the generation of oxygen-releasing biomaterials as transplantable constructs have been considered in many studies [7][8]. Oxygen regulation in cell culture is typically achieved either by controlling oxygen content inside an incubation chamber or by introducing oxygen generating species to the culture medium [9]. Application of oxygen generating species has largely been limited to in vitro studies since they exhibit toxicity to cells within certain concentration ranges. Alternatively, biomaterials have been developed integrating oxygen generators to overcome some toxicity effects [7].Various materials have been explored as a source of oxygen. Perfluorocarbons (PFCs) showed significant advantages and oxygen-releasing ability among all oxygen carriers due to their higher oxygen solubility in comparison with water alone [10]. One of the advantages of using PFCs is the high oxygen delivery with lower oxygen concentrations [11][12]. The downside of PFCs is that they are not soluble in water due to their hydrophobicity structure [11]. Using the emulsion system can tackle this obstacle. However, long-term stability and cytotoxic effects due to the lipophilic nature of PFCs, have been challenging. Thus, PFCs covalently immobilized to biomaterials have

been developed, integrating oxygen generators to overcome toxicity effects. Collagen is one of the biomaterials used in tissue engineering applications [13]. In 1986, Weinberg and Bell generated scaffold-based tissue consisting of a cell populated in collagen gel [14]. However, it has weak mechanical properties. To respond to this limitation, multiple modification methods have been investigated. Methacrylamide modification is a method to improve the mechanical properties of collagen [15]. In addition, many experiments showed that methacrylamide modification is a method for holding great promise for tissue engineering research [15][16]. Methacrylamide modification is practicable for preparing photo-crosslinked hydrogels by intermolecular covalent bonding has been one of the most popular methods of modification. This study investigates the cell function on ECM components and oxygen-releasing hydrogels to provide sufficient oxygen in cells' microenvironment. Collagen was modified with methylacrylamide according to the study done by Ke Yang et. Al. [15], then the oxygen carriers (PFCs) was encapsulated into the modified collagen.

6.2. Experimental

6.2.1. Synthesize Fluorinated Methacrylate Type-I Collagen (CMAF) and Methacrylate type-I Collagen (CMA)

To prepare CMA and CMAF, collagen (2 mg/mL) was initially dissolved in acetic acid 2N. Next, Fluorinated groups in three different concentration (0.1,0.5 and 1%w/v) will be added to collagen solution, to create CMAF the resulting polymer was modified with methacrylicanhydride to add methacrylate groups (0.05,0.1, and 0.5 %v/v). for creating CMA, methacrylate groups (0.05,0.1, and 0.5 %v/v) were added to the collagen solution. For purification, CMAF or CMA solutions was placed in dialysis membranes and dialyzed against deionized water for 3 days with 3 changes of water each day followed by lyophilizing to yield

dry CMAF or CMA polymer and keep them for further use at −80 °C. HNMR was used to find percent methacrylation and percent fluorination.

6.2.2. Characterization of CMAF / CMA functionalization

The degree of functionalization was determined by Fluoraldehyde o-phthaldialdehyde reagent solution (Life Technologies, cat. no. 26025; store it at 4 °C). Then, CMAF / CMA was mixed in solution with Fluor aldehyde reagent. The solutions were placed in 96 well-plate and read at 360 nm by BioTek Multi-Mode Microplate Reader plate reader.

6.2.3. CMAF / CMA Hydrogel Preparation

The prepared CMAF/CMA was dissolved in water and neutralized to a concentration of 7 mg/ mL, then exposed to UV light (8 W cm^2 /365nm) for 30 seconds to form the CMA hydrogel. The native collagen solution (COL, 7 mg/ mL) was assembled at 37 $^{\circ}$C to form the hydrogel. Photoinitiator crosslink solution (0.05%, w/v, final concentration) was introduced into both CMAF / CMA solutions before gelation. Hydrogels were formed by transferring 300 µL solution to a 24 well-plate (Corning Inc., Corning, NY, USA) followed by exposing UV light (365 nm) for 30 seconds. Next, hydrogels were washed thoroughly with phosphate buffered saline (PBS) with 3 changes per day for 3 days to remove all the unreacted polymer and photo-initiator solution shown in Figure 6-1.

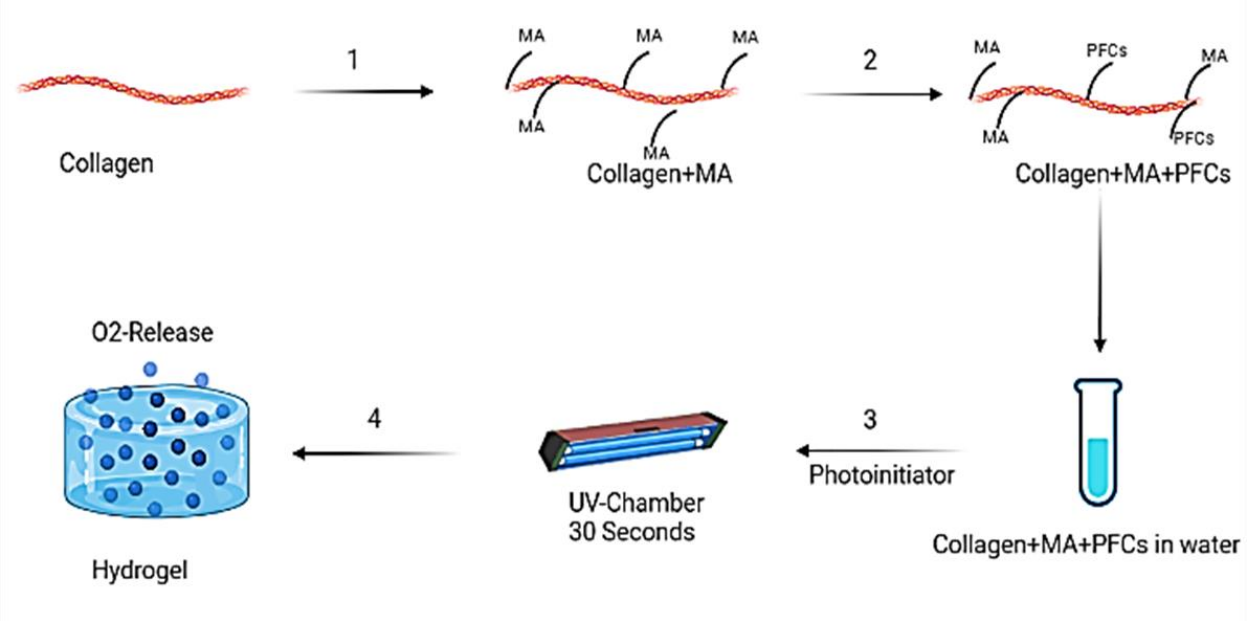

Figure 6-1. Schematic of collagen modification hydrogel.

6.2.3.1. Procedure

6.2.3.1.1. CMA functionalization, dialysis and lyophilization:

1. For a large reaction volume, we have tested reaction volumes of up to 500 ml, corresponding to 10 g of collagen in 100 mL 0.2N acetic acid.

2. While stirring moderately, heat the mixture to (and keep at) 50 °C in a water bath until the collagen is fully dissolved and the solution becomes clear. Then, increase PH to 8-9 by adding NaHCO3.

3. While stirring vigorously, slowly add 0.6 g of methacrylic anhydride (very viscous liquid for 100ml of collagen we need to 24.5mL of methacrylic anhydride) per 1 g of dissolved collagen for a high degree of methacryloyl functionalization.

CRITICAL STEP. Use a glass pipette when handling methacrylic anhydride, as organic solvents may dissolve plastic pipette tips.

CRITICAL STEP. Use nitrogen gas to degas the solution for 15mins and try to control the air intake into the solution during the reaction.

4. Stir vigorously for 4 hours. If mixing is sufficient, the solution will turn homogeneously white color solution owing to the dispersion of methacrylic anhydride.

CRITICAL STEP. Ensure adequate stirring during functionalization while minimizing air uptake. Insufficient stirring will lead to visible phase separation.

5. After the reaction period, transfer the solution into 50-ml plastic tubes , and remove unreacted methacrylic anhydride by centrifugation at 3,500g for 3 min at RT. Decant the CMA-containing supernatant (clear solution and separated from the ‘pellet’) into a large (200–500 ml) glass beaker, and discard the unreacted methacrylic anhydride deposited at the bottom of the 50-ml tubes. Then, pour waste in dark glass container.

6. Transfer the solution via plastic pipettes to a dialysis membrane with a 12-kDa MWCO and dialyze at 40 °C against a large volume of demineralized or UltraPure water for 5–7 d in a chemical safety fume hood. Change water at least once daily. Alternatively, dialysis can be performed at 4 °C in the cold room to minimize degradation. However, this may require extended dialysis time owing to reduced diffusion at lower temperatures.

7. Adjust the pH of the solution to 7.4 using 1 M $NaHCO_3$.

8. In a class II biological safety cabinet, filter-sterilize the solution using 0.2-µm syringe filter units or disposable vacuum filtration units with a PES membrane.

9. Transfer all aliquots to the freeze-dryer without allowing the solutions to thaw, and lyophilize them until the CMA is fully dehydrated (typically 4–7 d).

To maintain a sterile barrier during lyophilization, the 50-ml tubes need to be sealed with vented screw-top caps or press-fitted with 0.2-µm syringe filter units before lyophilization. Exchange

vented caps or filters with standard screw-top caps after lyophilization is completed to avoid hygroscopic absorption of water during storage.

10. Store lyophilized CMA protected from light and moisture at −20 °C until use.

6.2.3.1.2. CMAF functionalization, dialysis and lyophilization:

1. A three-glass neck flask was used. For a large reaction volume, we have tested reaction volumes of up to 500 ml, corresponding to 10 g of collagen in100 mL 0.2N acetic acid.

2. While stirring moderately, heat the mixture to (and keep at) 50 °C in a water bath until the collagen is fully dissolved and the solution becomes clear.

3. After the solution was purged with N2 for 15 min.

4. Add a solution of perfluorooctanoyl chloride (5.73 mL, 23.0 mmol) dropwise for 1 h.

5. Filter the solution.

6. The solution was then dialyzed against deionized water for 3 days with three changes per day, then lyophilized. This lyophilized fluorine-containing chitosan was further modified with methacrylic anhydride, as described above.

6.3. Result and Discussion

The conformations of collagen (COL) and collagen methacrylamide (CMA), before crosslinking are presented in Figure 6- , new proton peaks (methylene, d = 5.28 and 5.55 ppm and a methyl peak, d = 1.85 ppm) appeared in CMA compared with COL, indicating that methacrylate moieties were introduced on collagen chains. Besides, as shown in the FTIR spectra Figure 6- , the positions of the feature amide bands, thought to be related to the triple helical structure of collagen did not shift upon modification.

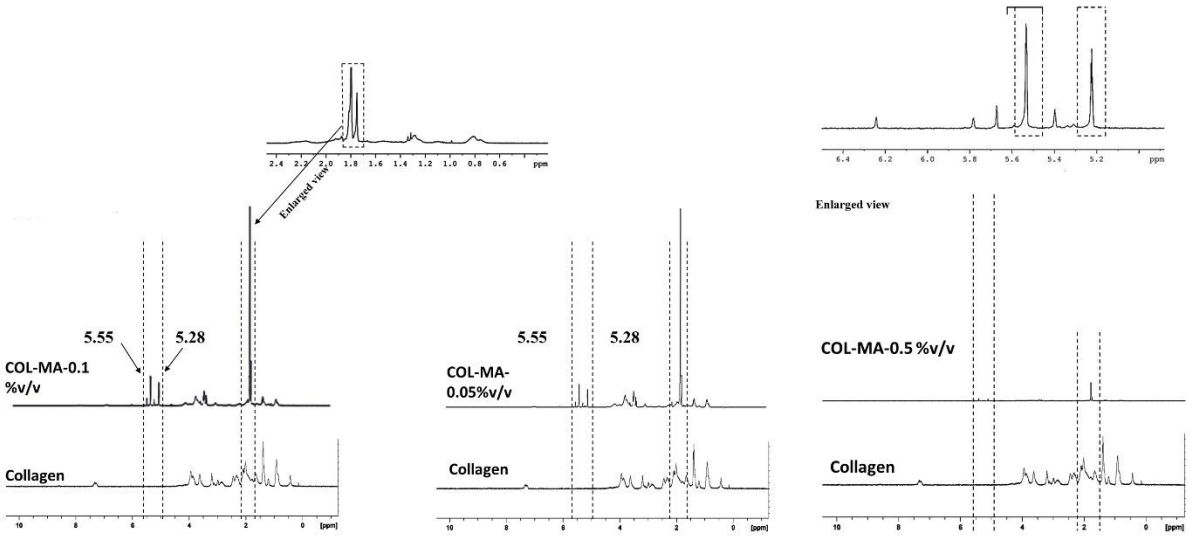

Figure 6- 2. Physicochemical properties of CMA and COL. HNMR spectra and characterized proton peaks are displayed in higher-magnification images.

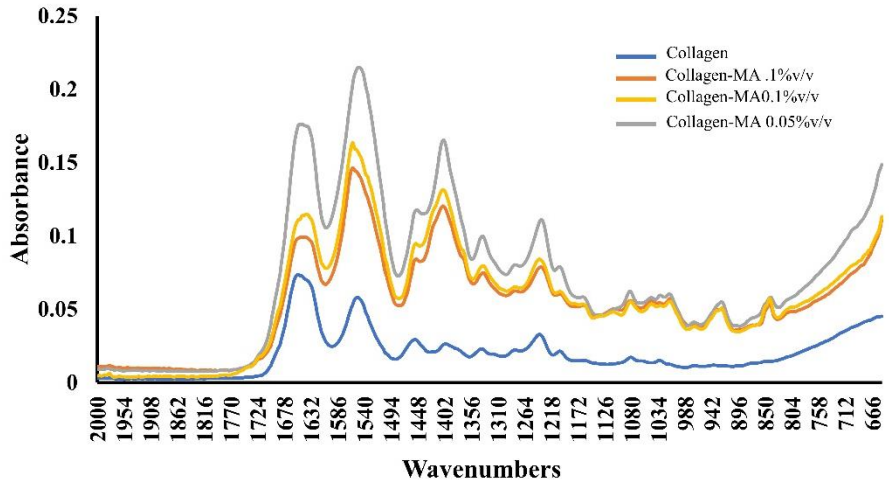

Figure 6- 3. FTIR spectra.

High resolution 19F NMR spectroscopy (Figure 6-) revealed that the degree of PFC substitution lies in the range 37–43% for CMAF. During PFC conjugation each CMAF reaction mixture remained homogeneously mixed at low viscosity throughout the period of the reaction. Thus, it is assumed that the PFC ligands were uniformly distributed throughout the polymer network. This was confirmed by the 19F NMR spectrum, that indicated the absence of additional peaks (Figure 6-). Also, the results were confirmed by Fluor aldehyde reagent.

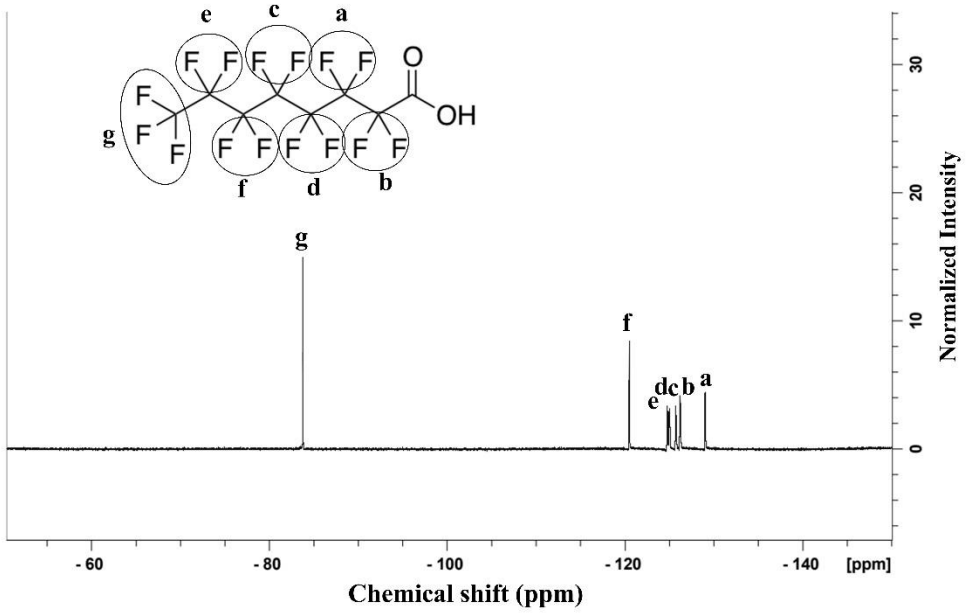

Figure 6- 4. High resolution 19F NMR spectra.

6.4. Discussion and Conclusion

Previously reported in vitro results indicate that chitosan modified with methacrylic anhydride can uptake and deliver oxygen to enhance fibroblast cell proliferation and metabolism [17]. Long aliphatic PFC chains immobilized to chitosan provide maximal oxygen affinity and biological benefit, which has also been reported in colloidal suspensions. This foundational work also studied varied PFC modifications (aromatic and aliphatic). The study done by Ke Yang

at.al. shows that collagen can successfully modified with methacrylic anhydride with well-preserved triple helical conformation [18]. In the present study, the most promising formulation was used, integrating 15 fluorines per PFC substitution (Ali15F), to create the MACF hydrogel. The results show that we can modify collagen with preserved the triple helical conformation. Also, we can immobilize PFC into the collagen modified. This study still needs more experimental design to find the optimized immobilization and oxygen delivery capability. The, we can evaluate the new hydrogel characterization and in vitro experiment. If that works, collagen modified with PFC can be used in many applications such as tissue engineering and cell culture techniques.

6.5. References

[1] A. Khademhosseini, Y. Du, B. Rajalingam, J. P. Vacanti, and R. S. Langer, "Microscale technologies for tissue engineering," *Adv. Tissue Eng.*, vol. 103, no. 8, pp. 349–369, 2008, doi: 10.1142/9781848161832_0017.

[2] M. Csete, "Oxygen in the cultivation of stem cells," *Ann. N. Y. Acad. Sci.*, vol. 1049, pp. 1–8, 2005, doi: 10.1196/annals.1334.001.

[3] A. Amirsadeghi, A. Jafari, L. J. Eggermont, S. S. Hashemi, S. A. Bencherif, and M. Khorram, "Vascularization strategies for skin tissue engineering," *Biomater. Sci.*, vol. 8, no. 15, pp. 4052–4073, 2020, doi: 10.1039/d0bm00266f.

[4] J. Rouwkema, N. C. Rivron, and C. A. van Blitterswijk, "Vascularization in tissue engineering," *Trends Biotechnol.*, vol. 26, no. 8, pp. 434–441, 2008, doi: 10.1016/j.tibtech.2008.04.009.

[5] S. H. Oh, C. L. Ward, A. Atala, J. J. Yoo, and B. S. Harrison, "Oxygen generating scaffolds for enhancing engineered tissue survival," *Biomaterials*, vol. 30, no. 5, pp. 757–762, 2009, doi: 10.1016/j.biomaterials.2008.09.065.

[6] B. S. Harrison, D. Eberli, S. J. Lee, A. Atala, and J. J. Yoo, "Oxygen producing biomaterials for tissue regeneration," *Biomaterials*, vol. 28, no. 31, pp. 4628–4634, 2007, doi: 10.1016/j.biomaterials.2007.07.003.

[7] H. Li, A. Wijekoon, and N. D. Leipzig, "Encapsulated neural stem cell neuronal differentiation in fluorinated methacrylamide chitosan hydrogels," *Ann. Biomed. Eng.*, vol. 42, no. 7, pp. 1456–1469, 2014, doi: 10.1007/s10439-013-0925-0.

[8] P. S. Patil, M. Mansouri, and N. D. Leipzig, "Fluorinated Chitosan Microgels to Overcome Internal Oxygen Transport Deficiencies in Microtissue Culture Systems," *Adv.*

Biosyst., vol. 1900250, pp. 1–10, 2020, doi: 10.1002/adbi.201900250.

[9] T. Abudula *et al.*, “Sca ff olds for Tissue Engineering Applications,” 2020.

[10] K. C. Lowe, M. R. Davey, and J. B. Power, “Perfluorochemicals: Their applications and benefits to cell culture,” *Trends Biotechnol.*, vol. 16, no. 6, pp. 272–277, 1998, doi: 10.1016/S0167-7799(98)01205-0.

[11] K. Chin, S. F. Khattak, S. R. Bhatia, and S. C. Roberts, “Hydrogel-perfluorocarbon composite scaffold promotes oxygen transport to immobilized cells,” *Biotechnol. Prog.*, vol. 24, no. 2, pp. 358–366, 2008, doi: 10.1021/bp070160f.

[12] S. F. Khattak, S. R. Bhatia, and S. C. Roberts, “Pluronic F127 as a cell encapsulation material: Utilization of membrane-stabilizing agents,” *Tissue Eng.*, vol. 11, no. 5–6, pp. 974–983, 2005, doi: 10.1089/ten.2005.11.974.

[13] S. Chattopadhyay and R. T. Raines, “Review collagen-based biomaterials for wound healing,” *Biopolymers*, vol. 101, no. 8, pp. 821–833, 2014, doi: 10.1002/bip.22486.

[14] C. B. Weinberg and E. Bell, “A blood vessel model constructed from collagen and cultured vascular cells,” *Science (80-.).*, vol. 231, no. 4736, pp. 397–400, 1986, doi: 10.1126/science.2934816.

[15] K. Yang *et al.*, “Methacrylamide-modified collagen hydrogel with improved anti-actin-mediated matrix contraction behavior,” *J. Mater. Chem. B*, vol. 6, no. 45, pp. 7543–7555, 2018, doi: 10.1039/C8TB02314J.

[16] L. Chen *et al.*, “Biomineralized Hydrogel with Enhanced Toughness by Chemical Bonding of Alkaline Phosphatase and Vinylphosphonic Acid in Collagen Framework,” *ACS Biomater. Sci. Eng.*, vol. 5, no. 3, pp. 1405–1415, 2019, doi: 10.1021/acsbiomaterials.8b01197.

[17] P. S. Patil et al., “Fluorinated methacrylamide chitosan hydrogels enhance collagen synthesis in wound healing through increased oxygen availability,” Acta Biomater., vol. 36, pp. 164–174, 2016, doi: 10.1016/j.actbio.2016.03.022.

[18] K. Yang et al., “Photo-crosslinked mono-component type II collagen hydrogel as a matrix to induce chondrogenic differentiation of bone marrow mesenchymal stem cells,” J. Mater. Chem. B, vol. 5, no. 44, pp. 8707–8718, 2017, doi: 10.1039/c7tb02348k.

7. Entrepreneurship and Commercialization Approaches

7.1. Introduction

In 1981, there was an 18-year-old boy whose dream was to be a doctor. He was determined to work hard to go to the medical school, indeed he did. He was admitted to the medical school in one of the top universities in Iran, but he could not afford it and therefore, did not go. Since then, he decided to start his own business and not think more about his dream (being a doctor) due to financial issues. He was smart and had a successful business. However, he always thought there is a missing puzzle piece in his life. He always encouraged my brother and me to pursue higher educations. He is my father. I was born and raised in a business-oriented family and know what the pros and cons are of running a business. So, I decided to start my business by having a higher education. My father's story makes me motivated to work hard and listen carefully to my mentors and put all my puzzles pieces carefully.

7.2. Commercialization

In 2020, when the Covid-19 pandemic occurred, the university was shut down. During that time, I got familiar with the OEI workshop at the university of Arkansas, where I heard about the Entrepreneurship program at the university of Arkansas. The Entrepreneurship program helped me to learn about the commercialization and bringing technology from the lab to the market. I started my journey to have a business by learning how to find your customers and market value. I realized that our customer will be scientists and engineers who are working in cell and gene therapy manufacturers and struggling with cell culture. I also did regional NSF-I Corps in summer 2021 and interviewed 12 scientists and researchers who are struggling with the cell culture. In addition to that, I participated to Empower program which is a program for women who want to start a business. In this program, I had several mentors who were helping me to

understand our first potential customers and business plan. Finally, I was awarded the National NSF I-Corps for $50K in summer 2022. I interviewed over 130 customers and learnt about the beachhead market, pricing tactics, and some federal funding available for startup companies such as NSF SBIR/STTR. After the national I-Corps program, I founded the Vitruvian Matrix LLC company. I felt I needed to have a team and strong business plan to be successful. Finding your potential customer is just the beginning. So, I took the Entrepreneurship program for the second time for those purposes. Also, Vitruvian Matrix raised 150K in 2022 to do more research and development by getting The Gap and Commercialization Fund at the University of Arkansas. In addition, I participated in some business plan competitions to raise more money and practice how explain the technology in front of investors.

7.3. Market Analysis

Overall, the global cell culture market is projected to reach USD $67.34 billion by 2030 from USD $22.8 billion in 2021, at a CAGR of 12.6% [5]. Our product addresses 7% of this total market for those cells requiring an adhesive to grow and is aligned to North American standards (largest market share at 39.6%) expandable worldwide. Our serviceable obtainable market is cell therapy applications, which holds the largest market share in 2021 in North America and is expected to continue during the forecast period owing to the wide scope of applications the segment offers. Within this growing market, our product has many applications in a wide range of

Our Sector:
Pre-Coated Consumable Cell Growth Environments

Our Sector Size:
$800M

Cell Culture Market Value:
$22.8b, CAGR +12.6%

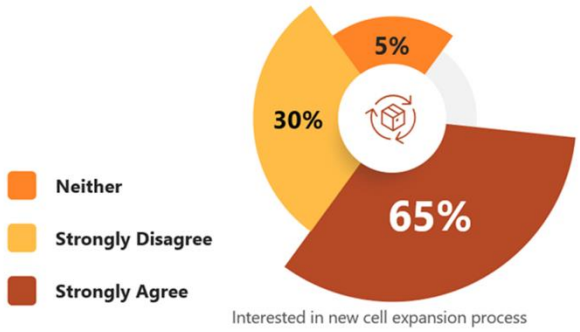

industries, including drug discovery, biopharmaceuticals (monoclonal antibodies, vaccines production, and other therapeutic proteins), tissue engineering & regenerative medicine (cell therapy, gene therapy), and vaccine production. This flexibility offers Vitruvian Matrix the capacity to quickly introduce additional variants to our products and customers and rapidly expand market share. Currently, we are focused on developing solutions more specifically for R&D scientists in early-stage cell therapy manufacturers, for three key reasons: 1) high growth potential, 2) relative lack of competitors, and 3) short time to market.

We interviewed 130+ scientists and engineers, struggling with cell culture, working at cell and gene therapy manufacturers. Based on our customer discovery interviews, cell therapy manufacturers currently pay $65 to $100 per unit, a single unit being a single T-flask coated with a cell adherent matrix. Over 65% of them showed the same need to enhance cell therapy manufacturers' cell expansion process, thus improving cell therapeutic potency.

7.4. Future Plan

Vitruvian Matrix has a strong team to continue the commercialization and path to the market. We plan to raise more money to support our research and development of the technology. To date, Vitruvian Matrix has raised a total of $165k towards advancing the business. $50k – From the National NSF I-Corps program (Summer 2022), received as non-dilutive funding to advance customer discovery $115k – From the University of Arkansas (Fall 2022), commercialization grant In future, we plan to submit for: A non-dilutive NSF SBIR Phase I grant, to support technology development, prototype optimization, and product efficacy A non-dilutive NSF SBIR Phase II grant, to support product scaling into 2024 We are currently working towards: A seed-stage investment of $250-$500k to complement our non-dilutive funding to assist in accelerating product development and securing key business relationships.

8. Conclusion and Future Directions

The increased existence of biomimetic materials for biomedical applications has led to the development of more complex technologies. Specifically, there is a need for a biomaterial that is low cost, bioavailable, and reproducible manner for various applications. This dissertation demonstrates the potential of biopolymers such as collagen, heparin, and poly-l-lysine for the development of biomaterials could be used to control a cell's environment for adherent cells. In addition, the ability of the Metal-Organic-Frameworks (MOFs) nanocarriers as a carrier for delivering essential cytokines such as interferon-gamma (IFN-γ) to cells to overcome the limitations of pretreatment of cells. Polymeric biomaterials will tackle mimicking the microenvironment extracellular matrix (ECM) limitations in cell-based therapy and manufacturing process. This dissertation studied (1) the physical and chemical properties of the polyelectrolytes multilayers along with their robustness in biological environments (Chapter 2&3), (2) the ability of MOFs to utilize to immobilize and deliver IFN-γ to the local extracellular environment (Chapter 4), (3) the tunability of the MOFs coatings added to PEM films (chapter 5), and (4) the ability of collagen can be modified with methylacrylamide to be used as oxygen carriers (PFCs) in cell culturing applications (Chapter 6). Our results indicated that heparin/collagen coating containing which provides an extracellular matrix (ECM) mimetic surface for adherent cells to improve the cell manufacturing process. It has also been proven that LbL technologies can be used to create a more biocompatible and novel interface for cell culturing. These new materials have been proven to be non-toxic and effective in cell adhesion, proliferation, and viability. Our results showed that HEP/COL multilayers are promising tools to improve the cell’s viability, proliferation, differentiation, and immunosuppression properties of the cells particularly with presence of IFN-γ. HEP/PLL multilayers also showed good results to

improve the cell viability of the cells. However, it did not showed good immunosuppression properties compared to the HEP/COL multilayers. Our study also showed that MOFs are promising tolls be to used as a delivery system for cytokine for the cells microenvironment.

Future studies for the cell manufacturing topic will focus on elucidating the mechanisms by which HEP/COL films enhance cell's behavior such as attachment, viability, proliferation and immunomodulatory properties of cells. Moreover, we will perform experiments to evaluate the translational potential of this technology toward manufacturing by coating bioreactors and evaluating Xenon free/Serum free media. Also, HEP/COL multilayers will be evaluated by animal free collagen and heparin to provide animal free coatings for cell therapy manufacturers. For the MOFs topic, future work includes evaluating the growth factors delivery in the cell's microenvironment. Regarding the collagen modified for oxygen-delivery, The optimized modified collagen hydrogel can be used for oxygen delivered in the cell culture. The collagen hydrogel will be used to control the viability of cells under hypoxic conditions by controlling the three-dimensional properties of hydrogels and oxygen delivery.